COMPATIBILISATION AND STABILISATION OF IMMISCIBLE POLYMER BLENDS BY REACTIVE PROCESSING

SURANI BUNIRAN

Doctor of Philosophy

THE UNIVERSITY OF ASTON IN BIRMINGHAM

JUNE 1998

THE UNIVERSITY OF ASTON IN BIRMINGHAM

COMPATIBILISATION AND STABILISATION
OF IMMISCIBLE POLYMER BLENDS BY REACTIVE PROCESSING

SURANI BUNIRAN
Doctor of Philosophy

SUMMARY

The main objectives of this research were to develop optimised chemical compositions and reactive processing conditions for grafting a functional monomer maleic anhydride (MA) in Polypropylene (PP), ethylene propylene diene monomer (EPDM) and mixtures of PP-EPDM, and to optimise synthetic routes for production of PP/EPDM copolymers for the purpose of compatibilisation of PP/EPDM blends. The MA-functionalisation was achieved using an internal mixer in the presence of low concentrations (less than 0.01 molar ratio) of a free radical initiator. Various methods were used to purify MA-functionalised PP and the grafting yield was determined using either FTIR or titrametry. The grafting yield of MA alone which due to its low free-radical reactivity towards polymer macroradicals was accompanied by severe degradation in the case of PP and crosslinking for EPDM. In the case of MA-functionalised PP/EPDM, both degradation and crosslinking occured though not to a great extent. The use of a tri-functional coagent e.g. trimethylolpropane triacrylates (TRIS) with MA led to high improvement of the grafting yield of MA on the polymers. This is almost certainly due to high free-radical activity of TRIS leading to copolymerisation of MA and TRIS which was followed by grafting of the copolymer onto the polymer backbone. In the case of PP, the use of coagent was also found to reduce the polymer degradation.

PP/EPDM copolymers with optimum tensile properties were synthesised using a 'one-step' continues reactive processing procedure. This was achieved firstly by functionalisation of a mixture of PP (higher w/w ratio) and EPDM (low w/w ratio) with MA, in the presence of the coagent TRIS and a small concentration of a free radical initiator. This was then followed by an imidisation reaction with the interlinking agent hexamethylene diamine (HEMDA).

Small amount of copolymers, up to 5 phr, which were interlinked with up to 15 phr of HEMDA, were sufficient to compatibilise PP/EPDM75/25 blends resulting in excellent tensile properties compared to binary PP/EPDM 75/25 blend. Improvement in blend's compatibility and phases-stabilisation (observed through tensile and SEM analysis) was shown in all cases with significant interphases adhesion improvement between PP and EPDM, and reduction in domain size across the fractured surface indicating efficient distribution of the compatibiliser.

Keywords: Polymer blends, Reactive processing, Polypropylene, EPDM, Maleic anhydride, Interlinking agent, Compatibilisation.

2

ACKNOWLEDGEMENTS

In the name of ALLAH, Most Gracious, Most Merciful

LIST OF CONTENT *page*

CHAPTER 1

GENERAL INTRODUCTION

4

LIST OF CONTENT *page*

CHAPTER 2

EXPERIMENTAL AND ANALYTICAL TECHNIQUES

LIST OF CONTENT

CHAPTER 3

FUNCTIONALISATION OF POLYPROPYLENE, EPDM AND
POLYPROPYLENE BLEND WITH MALEIC ANHYDRIDE BY
REACTIVE PROCESSING

CHAPTER 4

IN-SITU SYNTHESIS, USING REACTIVE PROCESSING METHODS, OF FUNCTIONALISED PP/EPDM COPOLYMERS FOR USE AS SOLID PHASE DISPERSANTS

CHAPTER 5

COMPATIBILISATION OF PP/EPDM BLENDS USING PP/EPDM COPOLYMERS

CHAPTER 6
CONCLUSIONS AND RECOMMENDATIONS
FOR FURHER WORKS

List of Tables

11

List of Figures

14

at 8 to 2. Purification of all samples via Soxhlet extraction in DCM. MA grafting yields were determined by titration.

16

ABBREVIATIONS AND SYMBOLS

AA	acrylic acid
ABS	acrylonitrile- butadiene-styrene terpolymer
AC	Ethylene acrylate copolymer
BP	benzoyl peroxide
BR	butyl rubber
CTC	charge transfer complex
CPE	chlorinated polyethylene
CSTR	continuous slurry tank reactor
CPB	compatibilised polymer blend
CM	closed mixing
DMF	dimethyl formamide
DMAC	dimethyl acetamide
DCP	dicumyl peroxide
DTBPIB	1,3-bis(t-butyl peroxyisopropyl) benzene
DCM	dichloromethane
DSC	differential scanning calorimetry
EPR	ethylyne propylene rubber copolymer
EPM	ethylene propylene monomer
EPDM	ethylene propylene diene terpolymer
EP-g-PP	ethylene propylene rubber graft polypropylene
EPDM-g-MMA	ethylene propylene diene terpolymer graft methylmetharylate
EPDM-g-MA	ethylene propylene diene terpolymer graft maleic anhydride adduct
EPM-g-MA	ethylene propylene monomer graft maleic anhydride adduct
EVAc	ethylene vinyl acetate copolymer
FRI	free radical initiator
FTIR	Fourier Transform Infrared
GMA	glycidyl methacrylate
HEMDA	hexamethylene diamine
HCl	hydrochloric acid
H_2O	water
Hg	mercury
HDPE	high density polyethylene
KOH	potassium hydroxide
LLDPE	low linear density polyethylene
MFI	melt flow index
MA	maleic anhydride
MAA	methacrylic acid
MAT	maleated EPDM
MB	maleated blend
NR	natural rubber
NBR	nitrile butadiene rubber
PA-6	polyamide-6 (nylon-6)
PA-6,6	polyamide-6,6
PAA	polyacrylic acid
PBT	poly(butylene terephthalate)
PB	polybutylene

PE	polyethylene
PEO	polyethylene oxide
PET	polyethylene terephthalate
PF	phenol-formaldehyde
PF-g-MMA	phenol-formaldehyde graft methyl methacrylate adduct
phr	part per hundred
PMA	maleated PP
PMAc	polymethacrylic acid
PMMA	poly(methyl methacrylate)
PP	polypropylene
PP-g-AA	polypropylene graft acrylic acid adduct
PP-g-MA	polypropylene graft maleic anhydride adduct
PPE	Poly(2,6-dimethyl-1,4-phenylene ether)
PS	polystyrene
PVC	polyvinyl chloride
PVDF	polyvinylidene fluoride
PVME	poly(vinyl methyl ether)
R*	macroradical
SA	succinic acid
SAn	succinic anhydride
SAN	styrene acrylonitrile
S-B	styrene-butadiene copolymer
SBR	styrene butadiene rubber
S-B-S	styrene-butadiene-styrene terpolymer
S-EB-S	styrene-ethylene/butylene-styrene triblock copolymer
S-EP	styrene-ethylene propylene copolymer
S-I-S	styrene-isoprene-styrene terpolymer
S-I-HDB	styrene-isoprene-hydrogenated butylene
SMA	styrene maleic acid copolymer
SPD	solid phase dispersant
SPDx	extracted solid phase dispersant
St	styrene monomer
T101	2,5-dimethyl-2,5-bis-tertiarybutyl peroxy-hexane
TRIS	Trimethylolpropane triacrylate
ε_b	extension to break point
ε_y	extension to yield point
ΔG_{mix}	Gibbs free energy of mixing
ΔH_{mix}	enthalphy of mixing
MW	molecular weight
m.r	molar ratio
M	molarity
N	normality
ϕ_1	volume fraction of component one
ϕ_2	volume fraction of component two

CHAPTER ONE

GENERAL INTRODUCTION

1.1   INTRODUCTION

The increasing use of plastics materials as substitute for conventional materials like wood, glass and metal, led to the development and introduction of specially designed polymer materials. In time, material requirements became more demanding and diverse, and were increasingly difficult to be satisfied with a single polymer resin [1]. Although synthesis of new polymers from new monomers to develop new engineering materials is still a possibility , combination of different polymers with complementary properties has become more attractive. Polymer blends have become a versatile and economically viable solution to the need of industry for improving the performance of commodity and engineering plastics. By blending there are potential opportunities for combining the attractive features of several materials into one or to improve deficient characteristics of a particular materials.

Polyolefins find many useful commercial applications, but suffer a major deficiency due to their poor interactions with other materials. The inert nature of polyolefins significantly limits diversity of end uses, particularly, those in which adhesion, dyeability, paintability or compatibility with other polymers are important. It has been clearly demonstrated [2,3,4,5,6,7] that the addition of polar group to polyolefins can improve the above properties.

22

1.2 POLYMER BLENDS

The terms blends and alloys are often used interchangeably. In this work a terminology as employed by Utracki [8] has been adopted. Polymer blends are mixtures at least of two macromolecular species, polymers and/or copolymers. Ideally, two or more polymers may be blended together to form a wide variety of random or structured morphologies to obtain products that potentially offer desirable combinations of characteristics. Figure 1.1 shows two widely useful types of polymer blends; that are miscible and immiscible. The
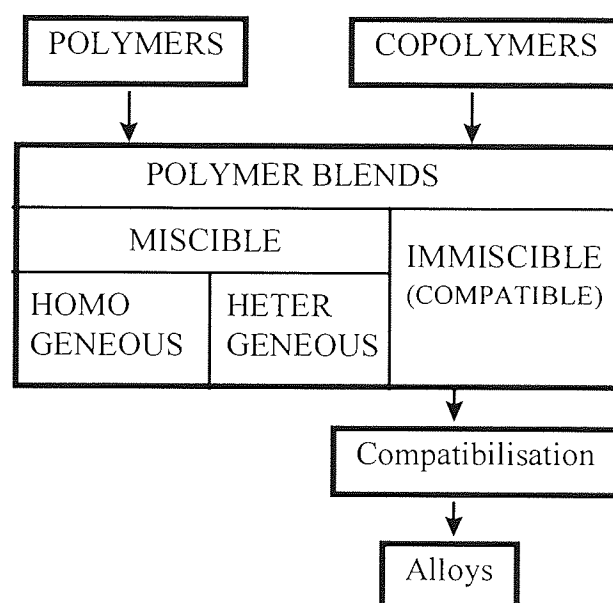
Figure 1.1 :Interrelation in polymer blend nomenclature [8]

term miscibility is used for polymer blends where the Gibbs free energy of mixing is smaller than 0 ($\Delta G_{mix} < 0$), and compatible blends stand for immiscible polymer blends that have been modified (compatibilised) to produce blends which posses commercially attractive properties. A polymer alloy refers to a polymer combination with a modified

interface and/or morphology. In order to avoid confusion, the term **blend** will be used throughout for all combinations of two (or more) polymers in this work.

There are more than 1600 of miscible blends have been identified, however most physical blends of different high molecular weight polymers prove to be immiscible [19]. That is when mixed together, the blend components are likely to separate into phases containing predominantly their own kind. Phase separated immiscible blends, exhibiting glass transition temperatures and/or melting temperatures of each blend component, is due to the low entropy of mixing of long polymer chains. This phenomenon however provides the advantage of maintaining some of the individual properties of the blend's components. Their overall performance depends not only upon the properties of the individual components but also depends significantly upon the morphology of the blends and the interfacial properties between the blend component phases.

The main property improvement sought through polymer blending/alloying include impact strength, heat distortion temperature, permeability characteristics, and processibility in addition to cost 'dilution'. These properties are governed by the morphology of the blend.

In the case of amorphous blends the morphology (e.g. domain size and shape) and interfacial interaction are influenced by the miscibility, relative polarity, and melt viscosity of the component polymers, as well as compounding process parameters such as temperature and shear rate. For crystalline polymer blends, in which at least one of the component polymers is semicrystalline, crystallisability and rate of crystallisation of polymers in the multicomponent system also affect the phase morphology. Even if the

polymers are thermodynamically miscible, crystallisation results in phase segregation unless the polymers can form isomorphic blends [10].

1.3 THERMODYNAMIC CONCEPT OF POLYMER BLENDS

The primary consideration for determining miscibility of two polymers is a thermodynamic issue that is governed by Gibbs free energy of mixing ΔG_{mix} (eq. 1) [8]. The state of miscibility of any mixture is define as :

$$\Delta G_{mix} = \Delta H_{mix} - T\Delta S_{mix} \qquad \text{(eq. 1)}$$

where ΔH_{mix} and ΔS_{mix} are enthalpy and entropy of mixing, respectively, and T is temperature. Figure 1.2 shows three possible ways in which the free energy of mixing may vary with the composition of the overall mixture ($\varnothing_i$ is volume fraction of component i) [1]. In Case A the free energy of mixing is always positive, and thus the two components are not miscible with each other to any extent. In Case B the components are completely miscible in all proportions. Here, miscibility refers to the existence of an equilibrium state in which the component of a mixture are mutually soluble. This implies that $\Delta G_{mix} \leq 0$. However, a negative free energy of mixing does not assure complete miscibility as in Case C. Here the free energy of mixing shows a reverse curvature in the mid-composition range by splitting into two phases with compositions given by the two minima. This results in partial miscibility.
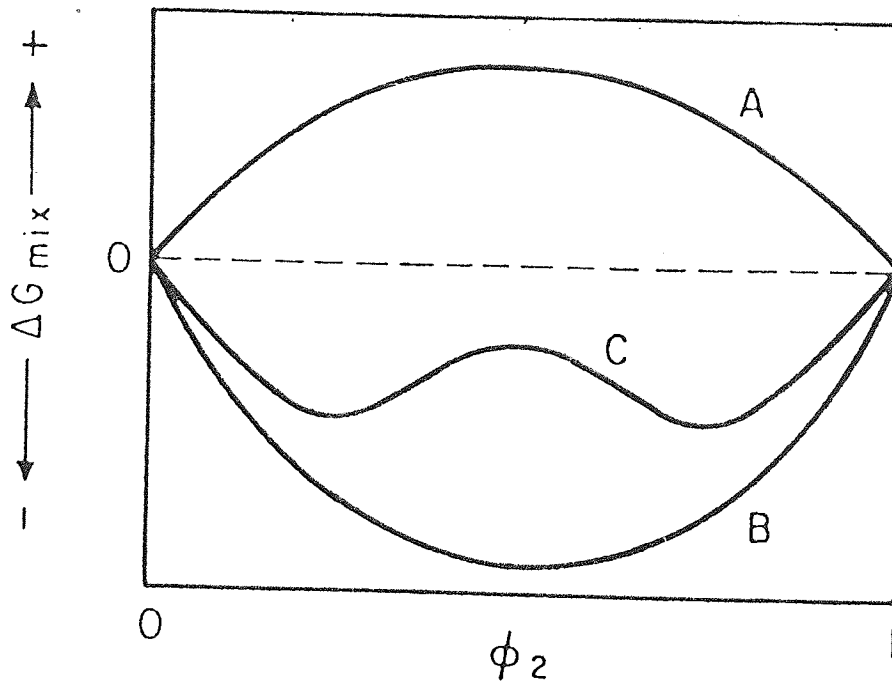
Figure 1.2: Free energy of mixing for binary mixtures which are completely immiscible (A), completely miscible (B), and partially miscible (C) [1]

A negative ΔG_{mix} is a necessary but not sufficient condition for complete miscibility. The second derivative of ΔG_{mix} with respect to the volume fraction of component 2 ($\varnothing_2$) must be greater than zero over the whole composition range.

$$\frac{\partial^2 \Delta G_{mix}}{\partial(\varnothing_2)^2} > 0 \qquad \text{(eq.2)}$$

If $\Delta G_{mix} < 0$, but Eq.2 is not satisfied (i.e., the appearance of local minima in the free energy curve as shown in Fig 1.2), the mixture will separate at equilibrium into two mixed-composition phases [11,12]. This means that each phase (i.e., the dispersed and continuous phase) will contain some of each component.

In order for $\Delta G_{mix} < 0$ (Eq.1) as a necessary condition of miscibility, the enthalpic contribution to mixing, ΔH_{mix} must be either negative or zero, or have a small value. This implies that blend miscibility requires favourable interactions such as hydrogen bonding, dipolar interactions, phenyl group coupling, charge transfer complex formation, Lewis acid-base or ionic interactions. They all contribute to the negative heat of mixing [8,12]. Table 1.1 shows polymers pairs that show complete miscibility [12].

Blends do not have to be miscible to be useful. Most commercially important polymer blends are immiscible but are compatibilised through interfacial modification. Immiscibility in these blends is related to the disparity between the polarities of the component and the existence of finite interfacial tension resulting in a low adhesion [8,13]. The interfacial tension together with high viscosity of blend components, contributes to the inherent difficulty of imparting the desired degree of dispersion to random mixtures and to their subsequent lack of stability to gross separation or stratification during later processing or use [14].

Satisfactory overall physical and mechanical properties of an immiscible but compatibilised blends should be related to low interfacial tension and strong adhesion between the phases. Blends of this type are termed 'compatible' even though in a thermodynamic sense they are not miscible. Compatible blends are characterised by the presence of a finely dispersed phase, good adhesion between blend phases, strong resistance to phase coalescence resulting in technologically desireable properties.

Table1.1: Examples of Miscible Polymer Pairs

Polymer 1	Polymer 2
I. Polystyrene, PS $-CH_2-CH-$ (benzene ring)	1. Poly(vinyl methyl ether), PVME $-CH_2-CH-$ $O-CH$
II. Poly(vinyl chloride), PVC $-CH_2-CH$ Cl	1. Polyester $-O-C-(CH_2)_n$ $\parallel$ O
	2. Poly(butylene terephthalate), PBT O O $\parallel$ $\parallel$ $-O-C$(benzene ring)$-C-O-(CH_2)$
III. Polyethylene oxide, PEO $-CH_2-CH_2-O$	1. Polyacrylic acid, PAA $-CH_2-CH-$ $C=$ OH 2. Polymethacrylic acid, PMAc CH_3 $-CH_2-C-$ $HO-C=$
IV. Poly(sodium styrene sulfonate) $-CH_2-CH-$ (benzene ring) $SO_3Na^\ominus$	1. Poly(vinylbenzyltrimethyl amonium chloride) $-CH_2-CH-$ (benzene ring) $N(CH_3)_3^\oplus Cl^\ominus$
V. Polybutylene - 1, PB $-CH_2-CH-$ CH_2-CH	1. Polypropylene, PP $-CH_2-CH-$ CH

1.4   COMPATIBILISATION IN POLYMER BLENDS

For improved performance, the immiscible blends usually need compatibilisation which is a process of modification of the interphase and/or morphology by either physical or chemical means. Compatibilisation is carried out in order to achieve [1,11,12].

1. reduction in the interfacial tension that facilitate dispersion of the phases,

2. stabilisation of morphology against high stress and strain processes,

3. enhanced adhesion between the phases in the solid state.

They are several approaches for compatibilising immiscible blends [8, 12-15]:

1.4.1   Addition of non-reactive Block or Graft Copolymers

Block and graft copolymers can be used as compatibilisers for polymer blends. A suitable block or graft copolymer contains a segment miscible with one blend component and another segment with the other blend component. Interfacial active graft or block copolymer of types **A-B** or **A-C** may compatibilise the immiscible polymers **A** and **B** provided that **C** is also miscible or capable of strong interactions with **B**. Significant amounts of the copolymer are expected to locate at the interface between the immiscible blend phases as classically shown in Fig. 1.3.

The copolymer location will reduce interfacial tension between components, reducing the resistance to minor breakup during melt mixing thus reducing the size of the dispersed phase, and stabilising the dispersion against coalescance.
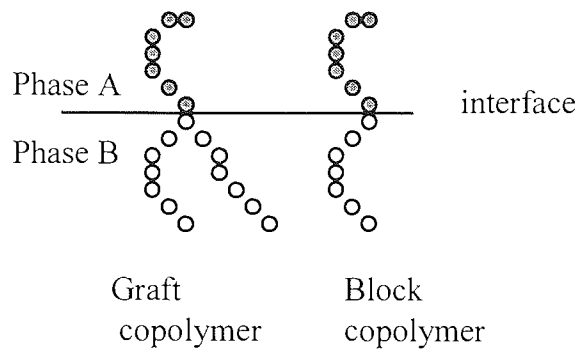
Figure 1.3: Ideal location of block or graft copolymer at the interface
between phase A and phase B of a polymer blend

The finer morphology and the increased interfacial adhesion usually result in improved

physical properties [16]. Table 1.2 lists various compatibilised systems that have been

studied. Examples from such systems include styrene/butadiene or styrene/isoprene

diblock and triblock copolymers in blends of PS with polyolefins, EPM or EPDM in PE/PP

blends, and PS/PMMA block copolymers in PVDF/PS-PMMA mixtures [18]. Generally

only about 1-2 wt% of the copolymer was required to produced stable dispersion in the

blends studied [19].

1.4.2 Addition of Reactive Block or Graft Copolymers

Reactive copolymers or functionalised polymers of the type **A-C** (where **C** is a long

reactive segment or a functional group attached to the main chain) may compatibilise a

polymer pair **A** and **B** provided that **C** is capable of chemically reacting with **B** [15]. The

nonreactive segment of the polymeric compatibiliser often has different chemical and

structural identity from component **A**, but is still capable of specific interactions leading to

a certain degree of miscibility. Table 1.3 contains examples of systems that are compatibilised through reactive copolymers [18].

Table 1.2 : Compatibilisation through non-reactive copolymers [17,18]

Main Component	Minor Component	Compatibiliser
PE or PS	PS or PE	S-B, S-EP, S-I-S, S-I-HDB, S-EB-S, S-B-S, PS/PE graft copolymers
PP	PS or PMMA	S-EB-S
PE or PP	PP or PE	EPM, EPDM
EPDM	PMMA	EPDM-g-MMA
PS	PA-6, EPDM or PPE	PS/PA-6 block copolymers, or S-EB-S
PET	HDPE	S-EB-S
PF	PMMA or PS	PF-g-MMA or PF-g-S
PVDF	PS/PPE	PS/PMMA block copolymers
PVC	PS or PE or PP	PCL/PS block copolymer or CPE
SAN	SBR	BR/PMMA block copolymer

The majority of blends in this category have compositions containing polyamide as the constituent that may react with compatibilisers containing anhydride or carboxyl functionalities. Examples of reactions involved are depicted in Fig. 1.4 whereby amide or imide linkages are formed from terminal $-NH_2$ and the carboxyl functionality. Other compatibilising copolymers may contain the highly reactive oxazolin, epoxy, isocyanate, or carbidiimide groups

31

Table 1.3 : Compatibilisation via reactive copolymers [18]

No.	Main Component	Minor Component	Compatibiliser
1	ABS	PA-6/PA-6,6 copolymer	SAN/MA copolymer
2	PP or PA-6	PA-6 or PP	EPM/MA copolymer
3	PE	PA-6 or PA-6,6	Ionomers, carboxyl functional PE
4	PA-6,6	Acrylate rubber or EPM	SMA or EPM-g-MA
5	PP or PE	PET	PP-g-AA, carboxyl functional PE
6	PPE/PS	Sulfonated EPDM (zinc salt), or phosphonate ester of EPM or EPDM	Sulfonated PS (zinc salt) plus zinc stearate

1.4.3 In situ Formed Copolymers

Graft or block copolymers acting as compatibilisers for polymer blends can be formed in situ through covalent or ionic bonding during the melt blending of a suitably functionalised polymer [16,20]. During melt blending of a pair of suitably functionalised polymers **A** and **B**, interchain block or graft copolymers may be formed at various concentrations through covalent or ionic bonding. The in situ formed compatibilisers have segments that are chemically identical to those in the respective unreacted homopolymers and are thought to be located preferably at the interface. This will lower interfacial tension and promote mechanical interlocking through interpenetration and entanglements. Table 1.4 shows examples of some important compatibilising reactions that could take place easily across polymer phase boundaries [17]. Such reactions can occur rapidly at elevated processing temperatures and are frequently used in reactive compatibilisation.

32

1. **PP-g-MA with PA-6**

PP
+ H$_2$N--PA-6 $\longrightarrow$ CH-CO-NH--PA-6
CH$_2$-COOH

2. **EPDM-g-MA with PA-6,6**

EPDM
+ H$_2$N--PA-6,6--NH$_2$ $\longrightarrow$ CH-CO-NH--PA-6
CH$_2$-CONH--PA-6,6--NH
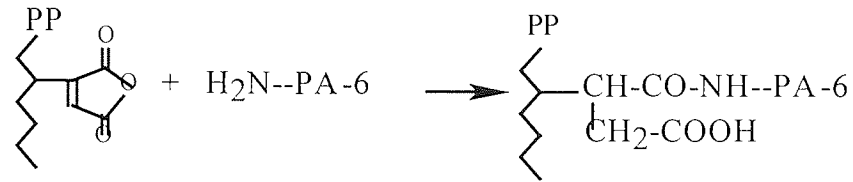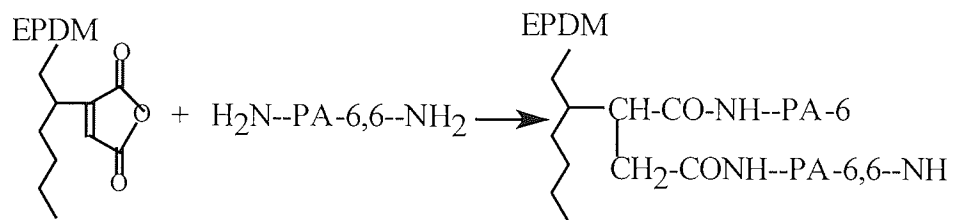
3. **Oxazoline functionalised PS with Ethene-acrylic acid copolymers**

PS
+
PE
HOOC
HOOC
$\longrightarrow$
HOOC
CO-NH-(CH$_2$)$_2$-OCO
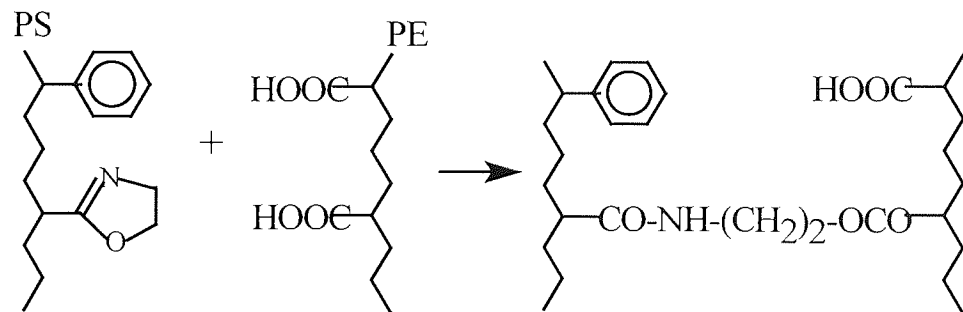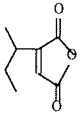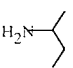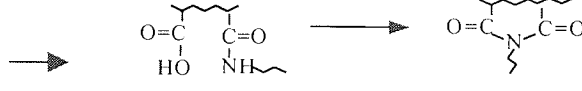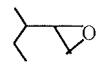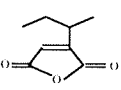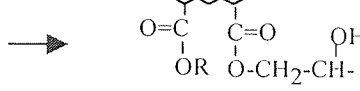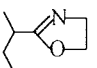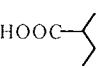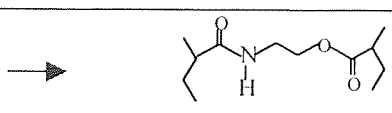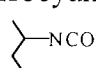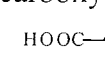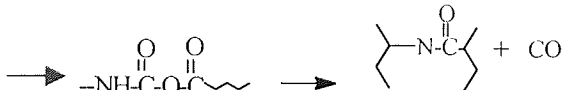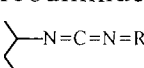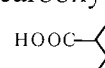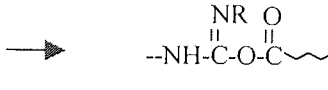
Fig. 1.4 : Reactions between various functionalised polymers that may lead to the formation of compatibilised copolymers

Generally one component of a blend contains functional groups inherited in the polymer while the other has no inherent functionality. Functional groups could be incorporated into the second component by chemically adding to it a functionalised polymer which is

33

miscible with it. In some cases, both components may have to be functionalised. Examples includes blending of polypropylene containing grafted maleic anhydride residue with polyamide through a chemical linkage between maleic anhydride in PP and terminal amino group in polyamide [21]

Table 1.4 : Common compatibilising reactions between functionalised
blend constituents [17]

Functional Groups		Copolymer
--anhydride	amine	
--epoxy	anhydride	
--oxazolin	carboxylic acid HOOC–⟨	
--isocyanate ⟩–NCO	carboxylic acid HOOC–⟨	
-carbodiimide ⟩–N=C=N=R	carboxylic acid HOOC–⟨	
radical **A·** +	radical **B·**	⟶ **A-B**

34

1.4.4 Addition of low-molecular weight coupling agent

Addition of low molecular weight (MW) functional compounds in polymer blends may promote compatibility through the formation of copolymers (random, block, graft) or through the combined effects of copolymer formation and crosslinking. Low MW compounds are usually added at relatively low concentrations typically 0.1 to 3 %. Examples of copolymer formation include the compatibilisation of poly(styrene-co-maleic anhydride) - brominated butyl rubber blends by dimethylaminomethanol, polyamide and polyester blends by compounds such as p-toluene sulfonic acid or phosphites via transamidation melt reactions in the blends containing polyamides and polyesters have been mentioned [21,22]. Peroxides (often in combination with co-agents) were also applied to promote compatibilisation through the recombination of polyolefin macroradicals [23,24,25], and crosslinking in 'dynamically vulcanized' thermoplastic elastomers of PP-EPDM [26].

1.5 REACTIVE PROCESSING

Polyolefin backbones contain no active site. A required reactive group can be inserted into the polymer backbone by (a) incorporating into the backbone, side chains, and at chain ends as a natural result of polymerisation (b) copolymerisation of monomers containing the desired reactive groups, and (c) chemical modification of a preformed polymer through a variety of chemical reactions [16]. Table 1.5 lists a number of examples of reactive polymers obtained by different preparation methods . Chemical reactions on polymers have been carried out in dilute systems, to avoid the problem of high viscosity encountered

in the polymer melts. As melt processing technology has improved such chemical reactions are now being performed in the conventional processing equipment such as internal mixers, extruders and mills [25,27-30]. In this case the processing device is used as a chemical reactor instead of a processing aid only. This process is termed reactive processing. An extruder is used as a chemical reactor in which

Table 1.5 : Example of different preparation methods for reactive polymers [16]

Preparation Method	Examples		Remark
Polymerisation a.Terminal group	-COOH -OH -NH$_2$	on polyamides, polyesters on polyester, polycarbonates on polyamides	inherent in condensation polymers
b.Backbone structure	in polyester, polycarbonate in polyamides		inherent in condensation polymers
c. Side chain reaction	in polyacrylate, polymethacrylate poly(vinyl acetate)		mainly for addition polymers
Copolymerisation	MA with PS, PE, SAN, AC; AA with PE, PS, NBR, AC; MAA with PE; Maleate with PPE; Methacrylate with PE; acrylate and vinyl oxazoline with SAN, PS GMA with PS, PE; Vinyl pyridine with PS		for addition and condensation polymer
Modification a. Grafting	MA on EPR, EPDM, PE, PP, PPE, ABS; AA on PP; Acrylate and maleate on PE; Epoxide on NR, EPDM, PP: lactam and amine on EPR, hydroxyl on EPR, PP		addition and condensation polymers
b. Concerted addition	MA on EPDM and PB		
c. Substitution	Bromide on PPE; hydroxyl on EVAc; sulfonic acid on PS and EPDM; ethylphosphonate on EPDM		for addition and condensation polymers
d. Terminal substitution	Isocyanate on polyamide; epoxide and carbidiimide on PPe; hydroxyl and amine on NBR		for condensation polymers
e. Photooxidation	Carbonyl on PE		

chemical reaction may take place in the polymer melt phase or less commonly , in the liquid phase, as when bulk polymerisation of monomers is performed in the extruder, or in the solid phase when the polymer is conveyed through the extruder in a solvent slurry. Advantages and disadvantages of some devices commonly used in reactive processing are described in Table 1.6 [31].

There is a considerable interest in reactive processing at present largely in industrial laboratories [32,33]. Reasons for this include first, strong move away from organic solvent based polymerisation reaction - the process offers the prospect of carrying out solventless polymerisation reactions. Secondly, the development of new polymers from the bench scale through to full scale production is very expensive compared with making new polymers from existing, readily available polymers. Thirdly, the chemical modification of low cost polymers for specific speciality markets can be very cost effective.

The technical importance of extruders and the versatility of chemical reactions that can take place during reactive processing have been reviewed recently [32,34]. In a twin screw extruder, the two screws can be organised in a variety of ways, for example co-rotating or counter rotating screws, with various degrees of intermashing, and a considerable range of screw elements for feeding, fixing the output rate and mean residence time. Because the screws run only partially full, it is relatively easy to

Table 1.6 . Advantages and disadvantages of some devices for polymer reactive processing [31]

Machine	Advantages	Disadvantages
Twin-screw extruder	Uniform high shear stress flow, short residence time, self-cleaning, flexibility and ease of cleaning	Capital cost high
Single-screw extruder	Cost, availability, flexibility for modification of screws and add-ons	Poor control, low rate of shearing, long residence time,
Multi-stage system	Flexibility, control, uniformity	Capital cost (for large diameter machine the uniformity of temperature can be poor)
Internal mixer	Uniform stress history, control	Capital and operating cost, long cycle, batch to batch variation

incorporate any desired additives at points along the extruder barrel. A range of processes occur inside the extruder during reactive processing. In the case of polymer modification, the polymer is normally fed into the extruder in the form of pellets or powder which require melting. Additives such as organic free radicals and chemical modifiers have to be incorporated, typically involving the addition of solids or liquids in small, controlled amounts. Mixing with the viscoelastic polymer melt has to be achieved to obtain the desired reaction in the residence time available. Non-reacted reagents or volatile by-

products have to be removed, as has heat generated by the reaction. Sufficient pressure must also be developed in the polymer to achieve flow through a die. Screw geometry, temperature control along the barrel and die geometry are all important factors to be considered if the complete conversion of reagents to a product is to be achieved.

The advantages of the extruder as a chemical reactor against the use of solvents or diluents, is the absence of solvent as the reaction medium [35]. No solvent stripping or recovery process is required, and product contamination by solvent or solvent impurity is avoided. Furthermore there will be no, or, minimum solvent emissions to the environment. Since the solvent/diluent usually comprises 5 to 20 times the weight of the desired polymer, most of the plant equipment and the space it occupies can be saved when replaced by reactive processing using the conventional processing devices. Fig.1.5 illustrates the commonalities and differences of reactive processing done in an extruder and in a Polymer Slurry done in hydrocarbon solution [35]. Operations unique to the solution process are shown inside the solid circle while the dashed circle shows equipment unique to the extruder process.

The absence of a liquid phase in most reactive processing may make heat transfer inefficient and difficult to control in exothermic chemical reactions. Since a common characteristic of extruder reactors is a very high surface-to-volume ratio of reactant mixture, problem involving heat transfer are overcome by varying screw geometry. For any new chemical reaction, a new specific screw geometry has to be design/developed but this is relatively easy due to the developments of modular extruders [36].
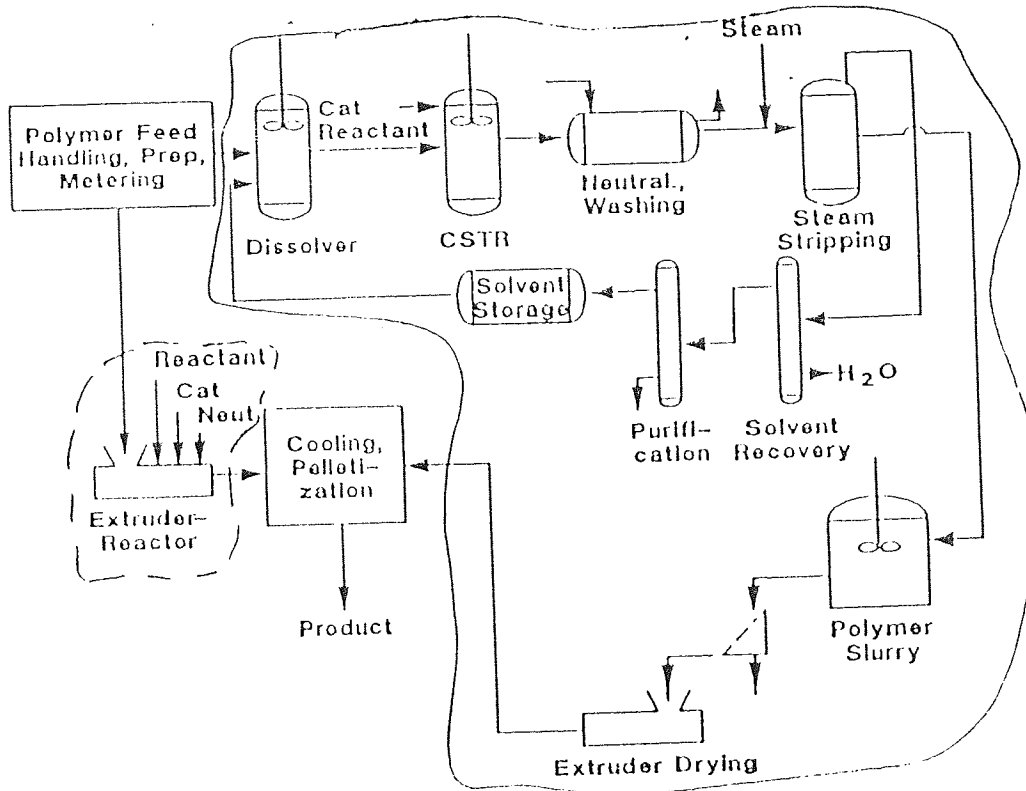
Fig. 1.5 General polymer modification process comparison [35]

1.6 APPLICATIONS OF REACTIVE PROCESSING

Chemical reactions may take place in the polymer melt phase or, less commonly, in the liquid phase, as when bulk polymerisation of monomers is performed in an extruder, or in the solid phase when the polymer is conveyed through the extruders in a solvent slurry. The types of reactions commonly carried out in the extruders have been reviewed [16,17,22,23,34,37] and could be broadly classified as follows:

a. **Bulk polymerisation** in which monomer or a mixture of monomers is converted to high molecular weight polymers with little or no solvent dilution. The polymerisation is either free radical, anionic, condensation, addition or coordination polymerisation.

b. **Controlled degradation and crosslinking of polymers** (usually polyolefins) by means of free radical initiator for the purpose of producing a product with controlled molecular weight distribution and a higher concentration of reactive sites for grafting.

c. **Functionalisation of commodity polymers** to introduce functional groups into polymer backbone, end group, or side chain, or modification of existing functional groups.

d. **Polymer modification by grafting** of monomers or mixture of monomers onto the backbone of existing polymers for the purpose of improving various properties of the starting materials. Free radical initiators and ionising radiation can be used to initiate the grafting reactions.

e. **Interchange copolymer formation.** Usually this type of reaction involves combination of reactive groups from several polymers to form random or block copolymer through ionic or covalent bonds.

f. **Coupling or branching reactions** which involve reaction of a homopolymer with a polyfunctional coupling agent or a condensing agent to build molecular weight by chain extension or branching.

Reactive processing techniques clearly involve molecular organisation in the polymer chain, as part of the processing operation, which can lead to a wide variety of product properties by judicious choice of reactants. They also allow the possibility of incorporation of reinforcing agents to enhance mechanical properties simultaneously with the reactions occuring.

1.7 FREE RADICAL GRAFTING REACTION

Free radical grafting is a widely practised chemical modification of polymers [38,39,40]. It involves reaction of a polymer with vinyl-containing monomer or a mixture of monomers capable of forming grafts onto the polymer backbone. If the grafts are long, the modified polymer becomes a true graft copolymer, of which the properties will be very different from those of the original polymer substrate. When the grafts are short, most of the physical and/or mechanical properties of the modified polymer substrate will be retained. However, the chemical properties of the modified polymer may become quite different. Free-radical grafting has been used to promote functional and/or mechanical properties of various types of polymers, but most frequently to promote those of polyolefins such as polyethylene (PE), polypropylene (PP), ethylene-propylene copolymer rubber, EPDM and ABS. This is due to the lack of reactive groups in their polymer structure that limits many of their end-uses, particularly those in which adhesion, dyeability, paintability or reactivity with other polymer is needed. .

A free-radical grafting system normally involves three types of reactants: polymer, unsaturated molecule such as vinyl monomer, and a free radical initiator. Irrespective of their nature, a typical free-radical grafting scheme can be represented by Fig. 1.6 [41]. Primary free radical ($R^{\bullet}$) are generated by initiator decomposition in the presence of monomer (M) and polymer. The primary free radical may follow two completely different reaction pathways; one leading to undesired homopolymerisation (reaction b) and the other one desired grafting (reaction d). When it reacts with a monomer molecule (reaction b), the undesired homopolymerisation is initiated forming a monomer radical ($RM^{\bullet}$). If this

monomer radical continues to react with more monomer molecules (reaction c) an oligomer or polymer will be formed. The grafting of this oligomer or polymer onto the desired polymer backbone rarely occurs because a propagating monomer radical usually has a limited hydrogen abstracting capacity unless it is very reactive, such as the vinyl acetate radical. When the primary free radical undergoes transfer with the polymer upon abstracting a hydrogen from the polymer backbone (reaction d) a macroradical is then formed. This macroradical faces one of the three important route, the probability of which depends on its structure: chain scission (reaction e), crosslinking (reaction f) and grafting (reaction g). When the macroradical reacts with a monomer molecule, this monomer molecule is then grafted onto the polymer backbone forming a branched macroradical (reaction h). This branched macroradical may continue to react with more monomer molecules forming longer graft . It may also undergo transfer with a hydrogen atom of the same or the another polymer backbone forming a new macroradical (reaction j). The macroradical transfer can be an important step for grafting as a newly formed macroradical is expected to repeat the grafting cycle described above, yielding more grafts. The above scheme clearly shows that free-radical grafting competes against homopolymerisation of the monomer.

1.8 GRAFTING OF MALEIC ANHYDRIDE ONTO POLYOLEFINS

Various functional monomers have been grafted onto polyolefins backbone: maleic acid, itaconic acid, crotonic acid, and related anhydride and esters, alkenyl succinic anhydride, fumaric acid, acrylic acid, methacrolic acid, glycidyl methacrylate , oxazoline and with
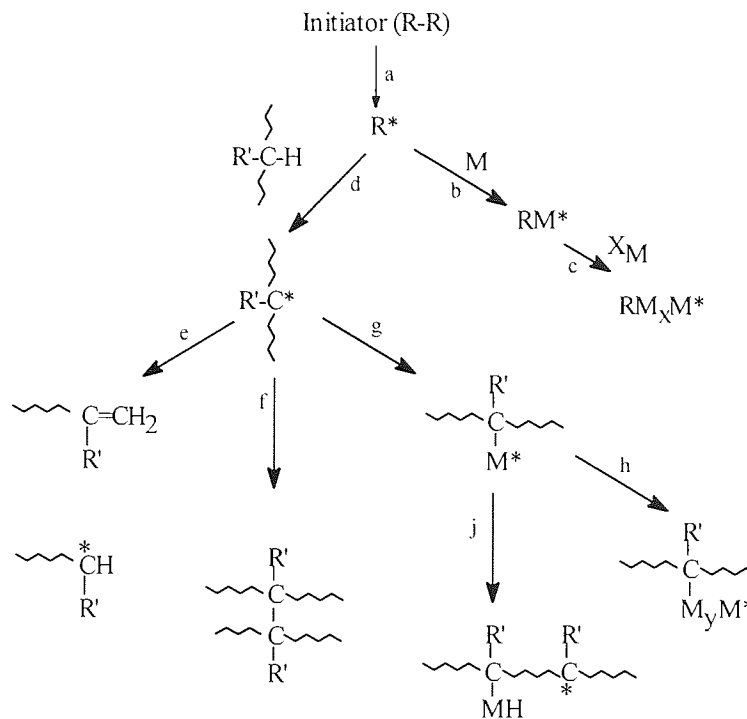
Fig. 1.6 : Overall Scheme of free-radical grafting onto a polymer backbone [41]

vinyl silanes such vinyltrimethoxysilane, vinyltriethoxysilane and 3-methacroloxy-propyltrimethylsilane [16,23,27,42-45]. Such modifications are generally aimed at modifying the chemical properties but not the mechanical properties.

Maleic anhydride (MA) has been found to be an extremely useful compound for the modification of polymers. MA (see Fig. 1.7) possesses a double reactivity: free radical reactivity (unsaturation of the C=C double bond) and functional reactivity (cyclic anhydride), that enable the MA to be used in both addition and condensation polymerisation systems. In fact, one of the largest uses of MA is in unsaturated polyester resins in which both carbon-carbon double bond and cyclic anhydride functions are involved in producing the final product [46].
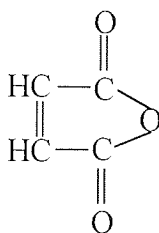
Fig. 1.7   Chemical structure of maleic anhydride (MA)

Once grafted onto a polymer backbone in the form of a substituted succinic anhydride (SA), it provides the polymer with high reactivity toward various nucleophilic groups such as amines, alcohols, thiols, or electrophilic groups (epoxies) in the presence of a catalyst. This high reactivity of SA has been explored for numerous industrial applications, including adhesion, painting, coating [46]. MA modified polymers has been increasingly used as in situ compatibiliser precursors for compatibilising polymer blends (47).

MA has been grafted to saturated polymers such as PE, PP, PVC, PS, EPR, EPDM by mechanochemical , mechanochemical with free-radical initiators, free radical, ionic, and radiation-initiation techniques [48]. Generally reported functionalisation procedures consist of grafting MA in the presence of organic peroxide either in the melt [49], in the solid state [50], or in solution [51]. In any case, the most widespread method is melt reactive processing [52-54]

A comprehensive review on the free-radical grafting of monomers onto polymers has been written recently by Hu, Flat and Lambla [41]. These workers pointed out that one of the most important challenges facing melt free radical grafting was to obtain a sufficient

45

amount of grafted MA onto polymer backbones while retaining the mechanical properties and thus the molecular weight of the virgin polymer.

Ide et. al. [55] carried out the melt grafting of MA onto PP in a Brabender batch mixer at 185 °C using benzoyl peroxide (BP) or dicumyl peroxide (DCP) as a free radical. In order to reach sufficient conversion (30% - 40%), the peroxide concentration had to be high (0.4 - 1.8 phr) causing PP degradation. Temperature had a negative effect on MA grafting yield owing, at least in part, to the fact that MA tends to sublime (the boiling point of MA is 202°C at 760 mm Hg). The authors also showed that MA melt free-radical grafting was very rapid process because grafting yield and viscosity of modified PP started levelling off after one minute of reaction.

Hogt [48] performed the melt free-radical grafting of MA onto PP in a co-rotating twin screw extruder (screw speed 200 rpm; barrel temperature 200°C - 240°C) in the presence of 1,3-bis(t-butyl peroxyisopropyl) benzene (DTBPIB). It was found that although an increase in the peroxide concentration increased the MA grafting yield (the magnitude of increase reduced with increasing peroxide concentration) it caused further PP degradation. When 2 phr Ma and 1 phr DTBPIB were added, only 0.4 phr or 20% of the total MA was grafted, and the PP thus modified was highly degraded with an melt flow index (MFI) greater than 1600 per 10 min (230°C and 2.16 kg).

The above two and many others studies [49,50,51,55,56] reveal a common problem facing the melt free-radical grafting of MA onto PP: there is serious competition between the

desired grafting and the undesired PP degradation by β-scission. The higher the MA grafting yield needed, the greater the peroxide concentration should be and the more severe the chain degradation of the resulting PP becomes. In the case of PE, EPR and EPDM, most studies reported in the literature reveal the difficulty of getting a high monomer grafting yield along with an acceptable degree of cross-linking.

Gaylord et. al. have conducted many studies [49,57-62] as an attempt to minimise PP degradation or PE cross-linking. They tested many 'electron-donating' organic additives such as dimethylformamide (DMF) and dimethylacetamide (DMAC), and found that the additives were capable of reducing PP degradation or PE cross-linking but also reduced MA grafting yield. Recently, Lambla et.al. [41] reported that addition of styrene (St) as a comonomer not only allowed to increase greatly the grafting yield of MA but also to reduce PP degradation.

Several studies have shown that only one unit of SA and MA were appended to one bonding site [63-65]. The principle reason to this was supposed to be the steric hindrance imposed by the 1,2-disubstitution of the double bond of the MA species [41]. The resonance and polar characteristics of MA were also mentioned as contributing to the sterically inherent non-homopolymerisable character. However many works have shown that MA could be homopolymerised [57,66-70]. Gaylord et. al. proposed the mechanism of homopolymerisation of MA and grafting of the poly(maleic anhydride) during the functionalisation of PP, PE [49,57,58]. Current work conducted by Roover et. al. [71] also

indicated that poly(maleic anhydride) could be grafted onto PP. These authors mentioned homopolymerisation of MA without grafting is also possible.

On the other hand, Russell [72] invokes a thermodynamic argument based on ceiling temperature of poly(maleic anhydride) which would preclude any homopolymerisation of MA at temperature higher than 160°C. The formation and consequently the grafting of poly(maleic anhydride) during maleation of polyolefins in the melt would therefore be impossible. If the major prevention of formation of long side-chain grafts is ceiling temperature, an increase in monomer concentration and a drop in reaction temperature should cause a significant change in the microstructure of the grafts. Russell and co-workers [56,73] have studied reactions of MA onto n-eicosane and squalane at low temperature (60-80°C) in 1,2-dichlorobenzene using BP as the free radical. They found that in the absence of the hydrocarbon and with monomer concentrations of the order of 1 M, low molecular weight PMA was formed. On addition of the hydrocarbon, the main product was grafted material, and very little homopolymer was formed. The grafts consisted primarily of single SA units but some of them were short poly(maleic anhydride) chains. They concluded that ceiling temperature controlled the formation of homopolymer in the absence of hydrocarbon substrate, whereas in the presence of a hydrocarbon the main factor controlling the graft length was the ratio between the rate of intramolecular and/or intermolecular macroradical transfer and that of monomer addition to SA radicals. If this ratio is high, the graft length should be short, and vice versa.

All possible mechanisms reported in the literature for grafting MA onto polyolefins or maleation of polyolefins in the presence of organic peroxide could be summarised as

48

shown in the reaction scheme represented in Fig. 1.8 [71]. Different pathways can correspond to different conditions. The first step of the grafting mechanism involves homolytic scission of each organic peroxide producing two radicals. The decomposition rate (or half-life time of the peroxide) depends mainly on the temperature. PP pending hydrogens, normally of the tertiary carbon (for radical stability consideration) is abstracted by a radical attack which results in a new radical onto PP.

Different possibilities exist for the second steps. These can be described as follows: the radical onto a PP chain can lead to β-scission (reaction A) or to MA grafting (Fig 1.8, reaction B). The β-scission (reaction A) is a fast intramolecular reaction and seems predominant in the melt state in the present of an organic peroxide [74,75]. Nevertheless, reaction B, i.e. MA grafting on the primary radicals which occurs before β-scission, has been suggested [75]. However, it seems that grafting in solution, or in the solid state could favour this mechanism. Reaction C seems unlikely as a consequent of the stability of the anhydride radical but sequence B+C is, in fact, undistinguishable from sequence A + H. Reaction D which could lead to the grafting of MA by ene-reaction needs very severe condition : very low PP molecular mass (high concentration of double bond chain ends) very high concentration of MA, high temperature and pressure and long reaction time. Depolymerisation (reaction E) seems very unlikely at 190°C. Indeed, depolymerisation of PP becomes only significant at temperature above 300°C. MA end chain grafting (reaction H) has been suggested [71]. Recombinations (reactions I and J) and mainly the grafting of poly(maleic anhydride) (reaction K) remain the subjects of controversy [39,49,59,62].

As has been mentioned earlier, because of the stability of PP tertiary macroradicals

associated with their tertiary character, the degradation process of PP is extremely fast and

important at elevated temperatures. Therefore normally low grafting yields of MA   (less
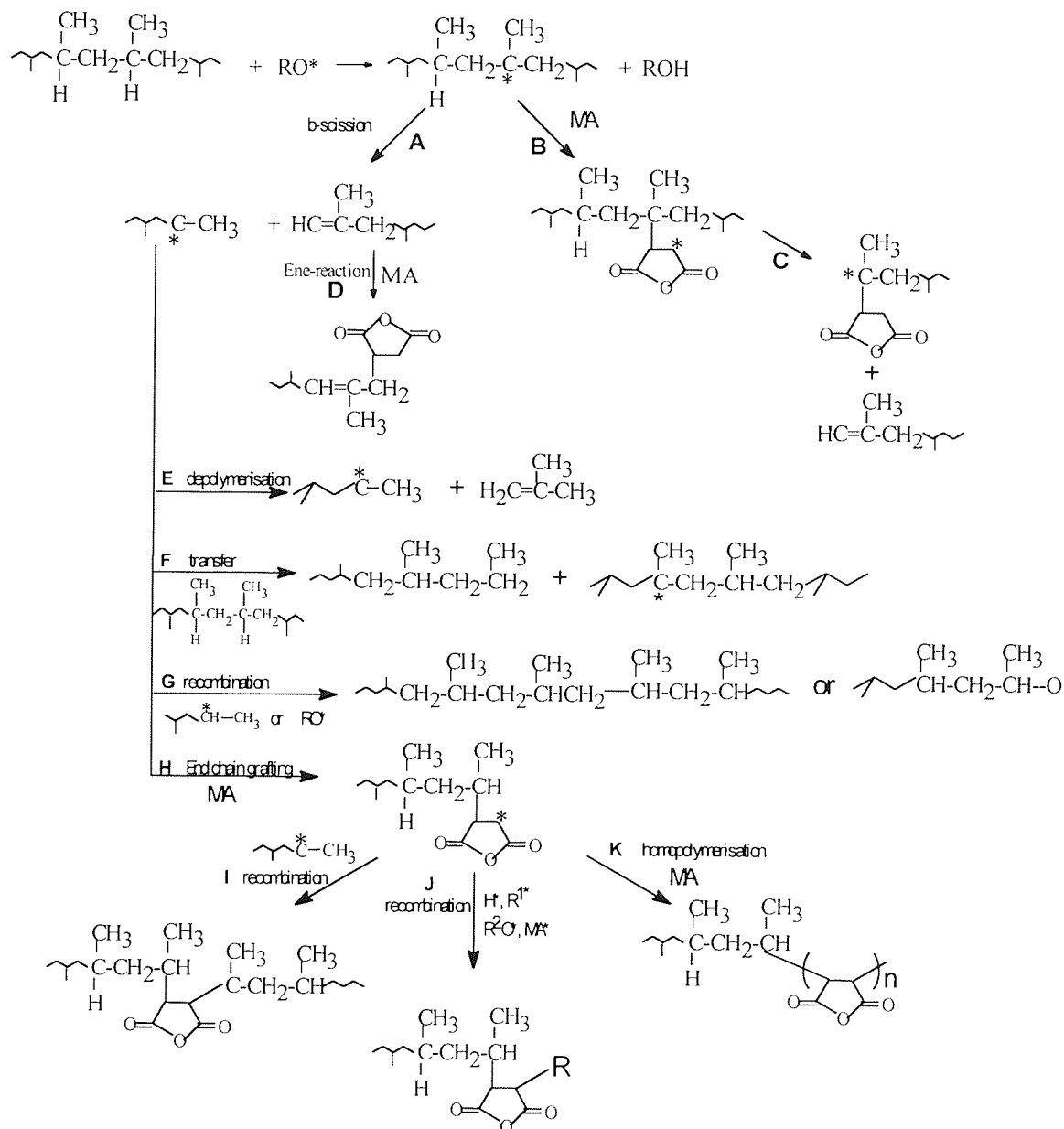
Fig: 1.8   Possible reaction mechanism for the grafting of maleic anhydride (MA)

onto polypropylene in the melt state in the presence of organic   peroxide.

than 0.7 phr) [62] together with severe PP degradation must be attributed to the weak free-radical reactivity of MA. Lambla et.al. [41] explained that it results from the inherent structural characteristics of MA: a strong steric hindrance arising from di-substitution of the two adjacent carbonyl groups at positions 1 and 2 of the double bond, a deficiency of electron-attracting nature of the carbonyl groups, and the symmetry of the double bond and the corresponding electron cloud. As a result, MA is reluctant to be grafted onto PP backbones. These authors also explained that an improved MA grafting yield and reduced PP chain degradation can be possible by promoting the free-radical reactivity of the double bond of MA. This was achieved [41] by 'activating' the double bond of MA such that the occurrence of the desired grafting between MA and PP macroradical precedes the PP chain degradation at these macroradical points by β-scission. One of the methods suggested [41] is addition of an electron-donating monomer such as styrene that is capable of forming a charge transfer complex (CTC) with accepting monomer MA. A mixture of an electron-donating monomer (D) and an electron-accepting monomer (A) will allow monoelectronic transfer from the D to the A. As a result, the symmetric character of the
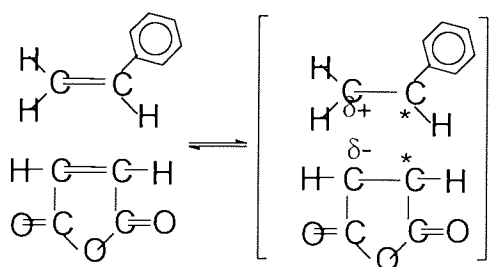
Figure 1.9 : Formation of charge transfer complex (CTC); example MA with styrene [77].

double bond of MA will be modified with the formation of a radical anion. This is called charge transfer complex (CTC), as depicted in Fig. 1.9 in which the mixture of MA-St is taken as an example [77,78]. It is hoped that smaller amount of peroxide will be enough to obtain sufficient MA grafting yields with reduced PP chain degradation

1.9 POLYPROPYLENE BLENDS

Blends of PP and ethylene-propylene rubber (EPM), ethylene-propylene diene monomer (EPDM), styrene-butadiene-styrene copolymer (SBS), polyisoprene have beeen commercialised for automotive applications such as bumper and dashboards [79,80]

Useful materials are obtained from blends over nearly the whole range of composition [79,81]. Blends with a small percentage of rubber are a toughened version of PP, while those with majority of EP are thermoplastic elastomers. In between, a wide variety of stiffness, toughness and other physical properties can be obtained by choosing the proper composition. PP has also been toughened by blending with HDPE or LLDPE, especially with a view to improving low temperature impact performance [82,83].

It has been reported [10,85-87] that the blending of PP with elastomers such as EPDM, EPM, SBS, SIS, PIB and polyisoprene affects both the morphology and the crystallisation behaviour of PP. EPDM and EPM were found chemically more compatible with PP than other elastomers. Generally elastomers reduce both the degree of the crystallinity of PP and the average spherulite size which contribute to an improvement in the impact strength.

Impact properties of such blends are strongly dependent on rubber particle size and size distribution. These particle parameters reflect, in part, shear developed during melt compounding and therefore are dependent on the melt viscosity of the PP. An optimum enhancement is achieved as the rubber particle size approaches 0.5 μm with a narrow particle size distribution [88,89].

It has been suggested that some degree of crosslinking of the rubber modifier phase is necessary to improve the toughening effect of the rubber . Elliot [90] in his work on PP/NR (natural rubber) blend, found substantial improvement in impact strength for slightly crosslinked NR compared to the uncrosslinked NR phase. Similarly Dao [91] found that a slightly crosslinked EPDM rubber is more effective in toughening PP.

EP copolymer could serve as compatibilising agents for PP/PE blends [90,92-94]. Those copolymers, which displayed residual crytallinity because of longer ethylene sequences, were more effective than purely amorphous copolymer. Addition of 5% EPR is necessary to ensure a linear relationship between tensile strength and composition for HDPE/PP blends. Addition of EP block copolymers to LLDPE/PP blends, and resulted in improved modulus and strength (especially at low temperature) and reduced elongation; however, the effects were fairly marginal [95]. Replacing up to 20% HDPE (in a 20/80 HDPE/PP blend) by EPDM led to improved impact and tensile properties [96]. In this case the EPDM appeared to act both as impact modifier and as compatibiliser.

As has been mentioned in Section 4.1, a block copolymer can compatibilise mixtures of the 'parent' homopolymers. The block copolymers act as macromolecular surfactants to

promote and stabilise the emulsion of the molten homopolymers. Lohse et. al. [3,97] have reported useful compatibilisation of EP/PP blends by addition of up to 10% by weight EP-g-PP graft copolymers, leading to four-fold reduction in phase size and doubling of low temperature impact strength. The EP-g-PP graft copolymer was synthesised by growing pendent PP grafts from the unreacted double bonds in EPDM, using a two-stage polymerisation process.   In another work, Lohse et. al. [98] have reported similar result. These authors have synthesised the EP-g-PP by reacting a succinic anhydride grafted PP (maleated PP) with EPR containing primary amine groups, either in solution or in the melt state.

Blend of PP and nitrile butadiene rubber (NBR) has been technologically compatibilised by dimethylol phenolic compound [88]. This compatibilisation could be the result of the formation of a block copolymer which could be formed by the reaction as shown in Fig. 1.10. Maleic modified PP has been used to form block-polymeric compatibilising agent by reaction with amine terminated liquid NBR.   If part of the PP in a NBR/PP mixture is maleic-modified PP, and if part of the NBR is amine-terminated, then a compatibilising amount of NBR/PP block copolymer forms in situ during melt-mixing.

polypropylene   R   nitrile butadiene rubber (NBR)
                            dimethylolphenol
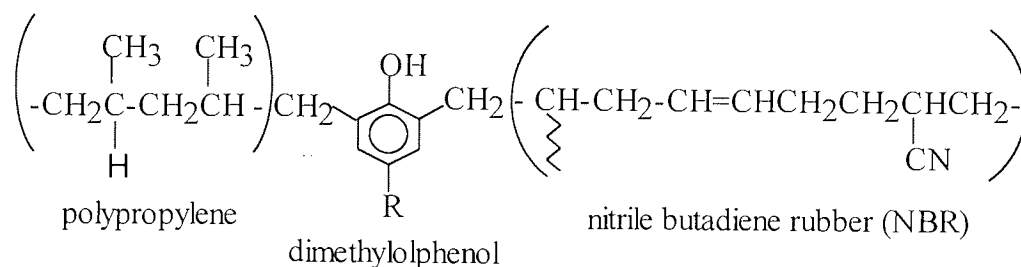
Figure 1.10: Compatibilisation of NBR/PP with dimethylolphenol

Polyolefin has also been blended with polyamide [99-102]. A commonly used method of inducing compatibility is by chemical modification of the polyolefin to contain pendant carboxyl group, often by grafting with MA or similar compounds, which form chemical linkages to polyamide via the terminal amino group. An early example is work by Ide and Hasegawa [99], who added various levels of MA-g-PP to extrusion compounded blends of PP with nylon 6. Addition of MA-g-PP caused a dramatic reduction in the phase size of blends containing 20% (w/w) of nylon-6. Cimmino et.al. [103] have demonstrated the effectiveness of MA-g-EPDM in producing a stable and more uniform phase dispersion in EPDM/nylon-6 blends. Recently Chen et. al. [104] investigated the effects of adding PP-g-MA compatibiliser on the phase morphology of blends of HDPE and LDPE with nylon 6 and nylon 11. In all cases addition of 5% by weight PP-g-MA resulted in a substantial reduction in the size of the dispersed phase, but in addition caused a reduction in the phase growth seen in the binary blends. The compatibilising effect of PE-g-MA in PE/Nylon 6 blends has also been reported by Kim et. al. [105]

Ide and Hasegawa [99] have also investigated compatibilisation of nylon 6/polystyrene blends by addition of styrene-methacrylate acid (MAA) copolymer. The authors claim improved dispersibility for the compatibilised blend, caused by the same reaction, between terminal amino groups in nylon 6 and the MAA in the copolymer. More recent work on nylon 6/polysrtyrene blends [106] shows that addition of polystyrene functionalised with MA into nylon 6/polystyrene blends has significantly change the morphology, and rheological and tensile properties of the blends.

1.10 OBJECTIVE OF THE STUDY

From the literature review on the technology of grafting of maleic anhydride (MA) onto polyolefins, it is revealed that the low grafting yield of MA, along with severe PP chain degradation is attributed to the weak free-radical reactivity of MA towards polyolefin macroradicals. A novel approach which has been developed at Aston's University which is based on classical copolymerisation principles could be used to enhance the MA grafting yield. A key feature in this approach is the use of an enhancing agent (co-monomer) in addition to a vinyl containing modifiers [107].

In this research work, functionalisation of polyolefins will be conducted during reactive processing by co-grafting the functional modifier, MA (Fig.1.7), to the polyolefins in the presence of a second multifunctional monomer (co-agent) and a trace amount of a free radical initiator. The object is to develop optimised chemical compositions and reactive processing conditions for grafting MA onto PP, EPDM and blends of PP and EPDM. It is expected that, instead of grafting MA directly onto polyolefin chains, the co-monomer will act as an interlinking agent between the polyolefin and the MA. The research work will also evaluate the efficiency of various methods of purification of maleated polyolefins and analysis of MA grafting yield.

The functionalisation research will be extended to research on compatibilisation of polymer blends. In-situ synthesis of block copolymers of PP and EPDM will be achieved by promoting reactions between the MA moiety introduced in the components of the blends in the presence of an interlinking agent. The synthesised block copolymers will

56

then be used to compatibilise blends of PP and EPDM. The physical properties and surface morphology of the compatibilised blends will be assessed as a criteria to measure the effectiveness of the block copolymers as compatibilisers for the PP and EPDM blends.
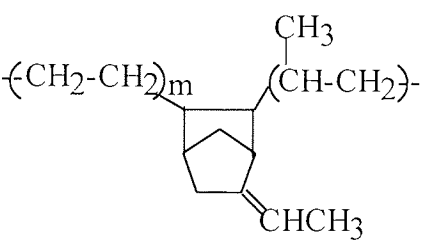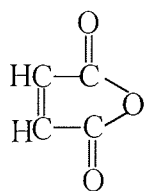
CHAPTER TWO
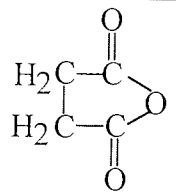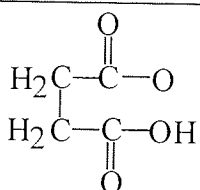
EXPERIMENTAL AND ANALYTICAL TECHNIQUE

2.1   MATERIALS

(i)   Polypropylene (PP)   :   Commercial grade unstabilised PP (Propathene ICI, HF-26), powder white, supplied by ICI Plastics Division Ltd. (**I**). The melt flow index (MFI) is 0.65 g/10 min. (using small die with diameter 0.06656 cm).

(ii)   Ethylene Propylene Diene Terpolymer (EPDM) :   Commercial grade EPDM (Vistalon 2504 supplied by Exxon), composed of 50 % ethylene and 4-7 % 5-ethylidene-2-norbonene (**II**).

(iii)   Maleic Anhydride (MA), Ex-Aldrich, solid white, MW=98 and 98 % purity. It was recrystallised from chloroform and kept in air tight container (**III**). The MA is referred to as the reactive agent.

(iv)   Trimethylolpropane Triacrylate (TRIS), Ex-Ancomer, viscous liquid, MW 296 (**IV**). TRIS is referred to as co-agent.

(v)   2,5-dimethyl-2,5-bis-tertiarybutyl peroxy-hexane commercially known as Trigonox 101 (T101), Ex-Akzo Chemie, liquid colourless, MW=290 (**V**).

(vi)   Hexamethylene diamine (HEMDA), Ex-Aldrich, solid crystal white, MW=116 (**VI**).

(vii)   Succinic anhydride (SAn), Ex-Aldrich, solid white, MW=100 and 98 % purity.

(viii) Succinic acid, (SA) Ex-Aldrich, solid white, MW=118 and 99% purity.

Table 2.1:   Chemical structurs of polymers, reactive agents, co-agent and free radical initiator

No	Chemical structure and name	Origin	Abbreviation	FTIR spectra
I	$CH_3 \quad CH_3$ $-CH_2CHCH_2CH-$ Polypropylene	ICI	**PP** white powder (HF-26)	Fig. 2.1a
II	CH_3 $-(CH_2-CH_2)_m \quad (CH-CH_2)-$ $CHCH_3$ Ethylene Propylene Diene Terpolymer	Exxon	**EPDM** Soft solid (Vistalon 2504)	Fig. 2.1b
III	$HC-C$ $\quad \quad \quad O$ $HC-C$ Maleic Anhydride	Aldrich	**MA** white solid crystall 98% pure	Fig.2.2
IV	$O \quad\quad CH_2CH_3 \quad O$ $CH_2=CHC-O-CH_2-C-CH_2-O-C-CH=CH_2$ $CH_2-O-C-CH=CH_2$ O Trimethyolpropane triacrylate	Ancomer	**TRIS** clear viscous liquid	Fig 2.3
V	$CH_3 \quad CH_3 \quad\quad CH_3 \quad CH_3$ $CH_3-C-O-O-C-CH_2-CH_2-C-O-O-C-CH_3$ $CH_3 \quad CH_3 \quad\quad CH_3 \quad CH_3$ 2,5-dimethyl 2,5-ditertiary butylperoxy hexane	Akzo	**T101** clear liquid	Fig 2.4

No	Chemical structure and name	Origin	Abbreviation	FTIR spectra
VI	$H_2N\text{-}(CH_2)_6\text{-}NH_2$ Hexamethylene diamine	Aldrich	**HEMDA** white solid crystal	Fig. 2.5
VII	Succinic anhydride	Aldrich	**SAn** solid white	Fig. 2.6
VIII	Succinic acid	Aldrich	**SA** solid white	Fig. 2.7

(ix)   Solvents : Dichloromethane, hexane, acetone, methanol, xylene, benzene, petrolium ether, methanol were standard laboratory reagent grades, used as supplied from Fissions or BDH Chemicals. 1,2-dimethoxyethane known as glyme (liquid, 99.5% purity) was supplied by Aldrich.

2.2   REACTIVE PROCESSING AND BLENDING OF POLYMERS

An internal mixer, Hampden-RAPRA Torque Rheometer, consisting of a pair of counter rotating rotors in a mixing chamber heated by oil and run with a Brabender motor drive, having a digital torque recording unit, was used for the reactive processing methods employed in polymer modification (Chap.3 and Chap.4), as well as for blending PP and EPDM in the presence and absence of compatibilisers (Chap.

5). Unstabilised PP was dried at ambient temperature before used. EPDM elastomer supplied as a large rubbery slab was cut into wafers, then strips and finally cut into small cubes about 3 mm^3.

Unless otherwise stated, compounds for reactive processing were prepared by pre-weighing exact amount of polymer(s), reactive agent(s), co-agent TRIS and free radical initiator (FRI) (total weight 35 g.) in a paper cup, tumble mixed to homogenise the mixing prior to processing in an internal mixer. Weight of polymer (or polymers in blends), reactive agent and co-agent in a sample batch were expressed as a percentage. Amount of FRI used was expressed as a molar ratio (m.r.) which is a mole ratio of FRI to a total mole of reactive agent and co-agent. An example of the calculation is shown below for a PP sample containing 8 phr TRIS, 2 phr MA and 0.002 m.r. T101:

Total sample weight is 35 g containing 2.8 g TRIS and 0.7 g MA .

$$\text{Molar ratio of FRI (T101)} = \frac{\text{mole of T101}}{(\text{mole of TRIS}) + (\text{mole of MA})}$$

Mole of T101 $= \{\text{Molar ratio of T101}\}\{[\text{mole of TRIS}] + [\text{mole of MA}]\}$

$= \{0.002\}\{[2.8/296] + [0.7/98]\}$ mole

Weight of T101 $= (\text{mole of T101})(\text{molecular weight T101})$

$= 0.0096$ g

All polymer processing were carried out in the internal mixer under restricted oxygen excess achieved by sealing the chamber via a pneumatic ram (closed mixing, CM).

61

The processing of all samples was carried-out at an oil temperature of 180°C, rotor speed of **60 rotations per minute**, and processing time was varied from **10 to 20 minutes**; all samples were processed using 35 g of polymer(s). Torque values were recorded every 15 seconds. The processing commenced after the compound was charged into the internal mixer and the ram was in a closed position, CM. At the end of the processing, the polymer was removed and immediately immersed in cold water to retard any further reaction. For water sensitive materials i.e. maleated polymers, solid phase dispersants and blends containing maleated polymers, they were sheeted and immediately cut into small pieces to facilitate cooling at ambient temperature. The polymer sample was kept in air tight polyethylene bags before storing in a dry and dark place. The internal mixer was cleaned after each sample preparation by processing a mixture of polystyrene with a small amount of PP.

2.3   PREPARATION OF POLYMER FILMS AND PLAQUES

Thin films (0.1-0.2 mm) for infrared analysis and plaques (1 mm) for tensile measurements were prepared by compression moulding using a Daniel Press equipped with electrically heated platens. The polymer (ca. 5 g) was placed in the middle of a spacer which was laminated across both surfaces with a folded sheet of special heat resistant grade cellophane, and was preheated at 180°C for 1.5 minutes. The pressure was increased gradually over a period of 1.5 minutes up to a maximum value (85 kg/cm^2) which was maintained for another 1 minute. Heating was then isolated and cold water was circulated through the platens, whilst maintaining full pressure. The

sample was taken out once the temperature has reached to below 100°C. Plaques with obvious flaws (crease, unfilled templates) were discarded and fresh samples prepared.

2.4 REMOVAL OF NON-GRAFTED MALEIC ANHYDRIDE

Functionalised PP, functionalised EPDM, and functionalised PP-EPDM blends were expected to contain non-grafted and grafted reactive agent, maleic anhydride (MA). Three procedures were used to purify the functionalised samples from non-grafted MA.

2.4.1 Soxhlet Extraction

Film samples (2 x 3 cm²) or small granules were exhaustively Soxhlet extracted to remove any free reactive agent, MA and other low molecular mass materials, by using a suitable solvent e.g. dichloromethane. The optimum time for extraction was obtained by following the rate of increment of extracted reactive agent concentration in the solvent at time intervals, until no further change was observed. Fig. 2.6 shows that for MA, 40 hr. extraction was sufficient. However 48 hr was taken as standard extraction time. The extracted samples were dried-up overnight at 60°C under vacuum before being kept in air tight container for analysis. The concentration of MA in the sample films before and after extraction was determined by IR spectroscopy.

2.4.2 Heating in Vacuum Oven

Maleated PP (PMA) and maleated EPDM (MAT) films samples (2 x 3 cm^2) were heated at 120^{0}C in a vacuum oven for 72 hr, to remove residual free maleic anhydride (MA) and to reconvert grafted hydrolysed maleic anhydride (i.e acid functions) to anhydride function [48]. The samples were then kept in air tight container for further analysis.

2.4.3 Precipitation in Xylene-Acetone Solvent

Xylene is a good solvent for PP and EPDM, and acetone is a good solvent for MA (solubility of MA in acetone is 227 g/100 g acetone at 25 ^{0}C [46]). Granules of maleated polymers were dissolved (some of maleated EPDM was only swelled) in 100 ml hot xylene at 120 ^{0}C. Once the sample dissolved, the polymer was precipitated by adding slowly to the hot xylene solution, excess acetone followed by vacuum filtration, rinsing with acetone and drying at 60^{0}C in vacuum oven overnight [60,108 - 100].

2.5   GRAFTING EFFICIENCY OF MALEIC ANHYDRIDE

The concentration of MA in the non-extracted and extracted samples was calculated using FTIR spectroscopy and/or by titration .

2.5.1 FTIR Method Using Calibration Curves [109]

Fig 2.7 shows a typical infrared spectra of a maleated PP (PMA) processed in the presence of peroxide only. The spectrum indicates that in the maleated sample, maleic anhydride (MA) is present in part in the anhydride form as indicated by absorption peak at 1789 cm^{-1} , and is also present partly in the hydrolysed form i.e. as acid form as indicated by absorption peak at 1729 cm^{-1}. The concentration of MA in the polymer is therefore the sum of concentrations of both the anhydride and acid moities.

An IR calibration curve for MA was developed using succinic anhydride (SAn) (Fig. 2.8) and succinic acid (SA) (Fig. 2.9); for quantitative measurement of MA concentration in the polymer samples . Solution of SAn and SA in 1,2 - dimethoxyethane (glyme, Fig. 2.10) at several different concentrations were prepared and IR spectra were scanned [24]. It was observed that SAn and SA were difficult to dissolve in glyme; hence solubilisation was achieved by sonicating the mixture using a sonicator bath at 35 ^{0}C for at least 1 h. Area ratio of anhydride (area 2780 cm^{-1}/ area 2725 cm^{-1}), and area ratio of acid (area 1720 cm^{-1} / area 2725 cm^{-1}) were plotted against concentration of succinic anhydride and succunic acid, respectively. (Fig. 2.11). Eq. 2.1 and Eq. 2.2 were derived from the calibration curves.

$$y = 1.70 \, x \; + 0.05 \qquad \text{for anhydride} \qquad \text{Eq. 2.1}$$

$$y = 1.23x \; + 0.08 \qquad \text{for acid} \qquad \text{Eq.2.2}$$

where y is area ratio and x is concentration. The general procedure is as shown in Scheme 2.1.

The concentration of MA in a sample was examined by measuring each of the carbonyl and acid area ratios: individual area of carbonyl and acid peaks with reference to a 'constant' PP absorption ($>CH_2$) at 2725 cm^{-1}. The absorption areas of the carbonyl group and acid group were calculated using application software (M1700) in Data Station of the Perkin Elmer FTIR machine. With reference to Fig. 2.7, the carbonyl and acid area ratios are defined as:

Anhydride peak: Anhydride area ratio $= \dfrac{(\text{area } 1767\text{cm}^{-1} - 1808\text{cm}^{-1})}{(\text{area } 2695\text{cm}^{-1} - 2750\text{cm}^{-1})}$

i.e. $\dfrac{(\text{peak maximum at } 1789 \text{ cm}^{-1})}{(\text{peak maximum at } 2725 \text{ cm}^{-1})}$

Acid peak: Acid area ratio $= \dfrac{(\text{area } 1688\text{cm}^{-1} - 1763 \text{ cm}^{-1})}{(\text{area } 2695\text{cm}^{-1} - 2750 \text{ cm}^{-1})}$

i.e. $\dfrac{(\text{peak maximum at } 1729 \text{ cm}^{-1})}{(\text{peak maximum at } 2725 \text{ cm}^{-1})}$

The concentration of the anhydride and acid functions were calculated by fitting the area ratios into Eq. 2.1 and Eq. 2.2. The concentration of MA in the sample was the sum of the concentration of anhydride and acid moities. The overall reproducibility of this method was found to be within ± 6 % which was determined from replicate analysis of a series of samples.

2.5.2 Titration

A known weight (about 1 g) of non-extracted or extracted sample was dissolved in 100 ml of hot xylene at about 120^{0}C. After addition of 5 ml water the heating was

anhydride + H$_2$O (excess) →(heat) carboxylic acid →(KOH) (indicator yellow, excess KOH indicator blue HCl)
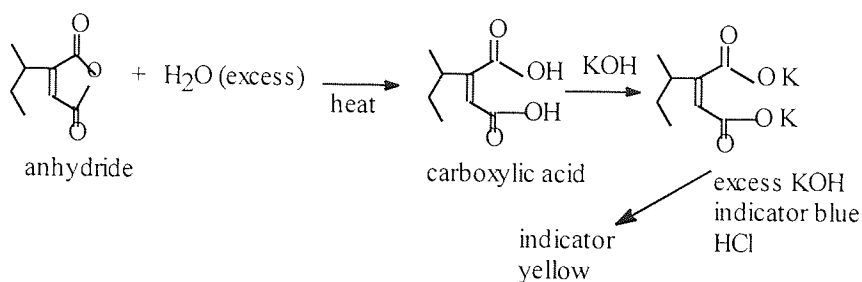
continued at 90 °C for 1 hr. The hot solution, placed on a hot heating mantle to maintain temperature at 90°C and magnetically stirred, was titrated (while hot at about 90°C) with 0.02N pottasium hydroxide (KOH) solution in ethanol. Phenopthalene was added as an indicator. The KOH solution was added in about 1 ml excess and the dark blue colouration was back titrated to yellow end-point with 0.05 N HCl in ethanol [100-102]. For each sample, titration was carried out in. The percent reproducibility of titration procedure in determining the MA grafting level was found to be around ±7%.

2.6   MEASUREMENTS OF INSOLUBLE GEL

Insoluble gel, or gel content, is a measure of the insoluble fraction caused by crosslinking of a modified polymer after being exhaustively extracted with a solvent that dissolves the virgin polymer. A known weight of finely cut processed polymer sample was placed in a known weight paper thimble and was Soxhlet extracted using xylene as a solvent for 48 h. The extractor was covered with aluminium foil to maintain hot xylene temperature at 135°C. After that the thimble was dried in vacuum

67

oven at 50°C, cooled down to room temperature and reweighted. The net weight of the residue was calculated and gel content was computed as follows:

$$\text{Gel content \%} = \frac{(W_1)}{(W_2)} \times 100$$

where W_1 is the residual weight of the extracted polymer (insoluble in the thimble) and W_2 is the original weight of the polymer before extraction. The gel content analysis was done in duplicates. The percent reproducibility of the gel content determination was found to be around $\pm 5 \%$.

2.7   MEASUREMENT OF MELT FLOW INDEX

Melt flow index (MFI) is a measure of melt viscosity and is related to the molecular weight of the polymer. It is defined as the mass (g) of the molten polymer extruded under a given weight (2.16 kg) through a standard die (0.1180 cm diameter) in a given time (normally 10 minutes). The MFI was determined by using a Devonport Melt Flow Indexer at constant extrusion temperature of 230 ± 2 °C and 2.16 kg load. 5 g of small cut polymer sample was charged into the barrel using a charging tool in such a ways to exclude air, within one minute. The sample was preheated for 4 minutes before putting the load to drive the molten polymer through the standard die. For maleated samples, small die (0.06656 cm diameter) was used. The time interval for the first extrudate or cut-offs was 30 seconds and discarded, then from 5 to 10 successive cut-off's were taken every interval of 30 seconds. The MFI was calculated using the following equation:

$$\text{MFI (g/10 min.)} \quad = \quad \frac{\text{Average weight of each cut (g)}}{\text{Cutting time interval (sec)}} \times 100$$

Every sample was carried out in triplicate. The percent reproducibility of MFI measurement was found to be about ± 3 %.

2.8 FOURIER TRANSFORM INFRA-RED SPECTROSCOPY

A Perkin Elmer FTIR Spectrophotometer model 1700 equipped with Perkin Elmer Data Station Applications Software (M1700), and a Perkin Elmer FTIR Spectrophotometer Model interfaced with Gram Analyst Software were used to evaluate the grafting efficiency of MA onto the polymers during reactive processing. A film specimen inserted into a metal holder having a 10 x 20 mm^2 aperture was presented to the sample beam in the usual position. Spectra were obtained over the range 4000 to 600 cm^{-1} from 5 scans at a resolution of 4 cm^{-1} and saved using the above software for subsequent analysis and manipulation.

2.9 SCANNING ELECTRON MICROSCOPY

Scanning electron microscopy (SEM) was used to view fracture surfaces from tensile testing for comparative assessment of blend morphology. A thin specimen cut from one of the broken ends of the test piece was attached to a metal stub using a double sided sticky carbon pad, with the fractured face over the edge of the stub. Before viewing, sample was coated with a conducting layer of gold using an Emscope SM300

Coater. Fractures were then viewed end-on at appropriate magnification in a Cambridge Instruments Stereoscan 90 Scanning Electron Microscope.

2.10 TENSILE TESTING

Tensile test was carried out on Testometric MACRO Tensile Tester, using a crosshead speed of 5 cm/min. The machine was equipped with a dedicated routine programme to collect the data and report a statistical analysis of the selected tensile parameters from five replicates per samples. Dumb-bell shaped test pieces used have the dimensions indicated in Fig 2.12

Total sample length   : 50 mm

Gauge length   : 30 mm

Width at gauge length   : 4 mm

Thickness   : 0.5 - 1.0 mm

The tensile properties measured were as follows, and explained with reference to the idealised stress strain curves shown in Fig. 2. 13.

Tensile Strength (TS), Mpa - the maximum stress (tensile load per unit cross-sectional area) sustanined by the sample during test; typically occurred at the point of repture (points C and E in Fig. 2.13) due to the characteristics of the blends tested.

Young's Modulus (YM, Mpa - the ratio of stress to corresponding strain below the yield or break point, shown by the slope of the initial straight line of the tensile curve (ab/bc in Fig. 2.13), and was used to give an index of the stiffness of the material.

Extension - %- the gain in length caused by a tensile load expressed as a percentage of original length, to both yield ($\in_y$) and break ($\in_b$) points. The yield point was detected as the point at which an increase in strain first occurred without an increase in stress (position B in Fig.2.13). Some of the cells tested broke without yielding (line AE) which means the material is brittle.

Toughness Factor (TF) - Mpa - this was obtained by normalising the energy to break under the tensile curve (area ABCD - Fig. 2.13) to specimen volume (cross-section area multiplied by gauge length) and is termed the tensile energy to break (TEB) in the ASTM D 882-83 [103]. This is quite different from measurement of toughness from impact testing (Charpy or Izod), but was useful in that it provided an integrated measure of tensile characteristics.

Five specimen were examined for the tensile test of each sample The percent reproducibility of tensile measurement was about ± 5 .
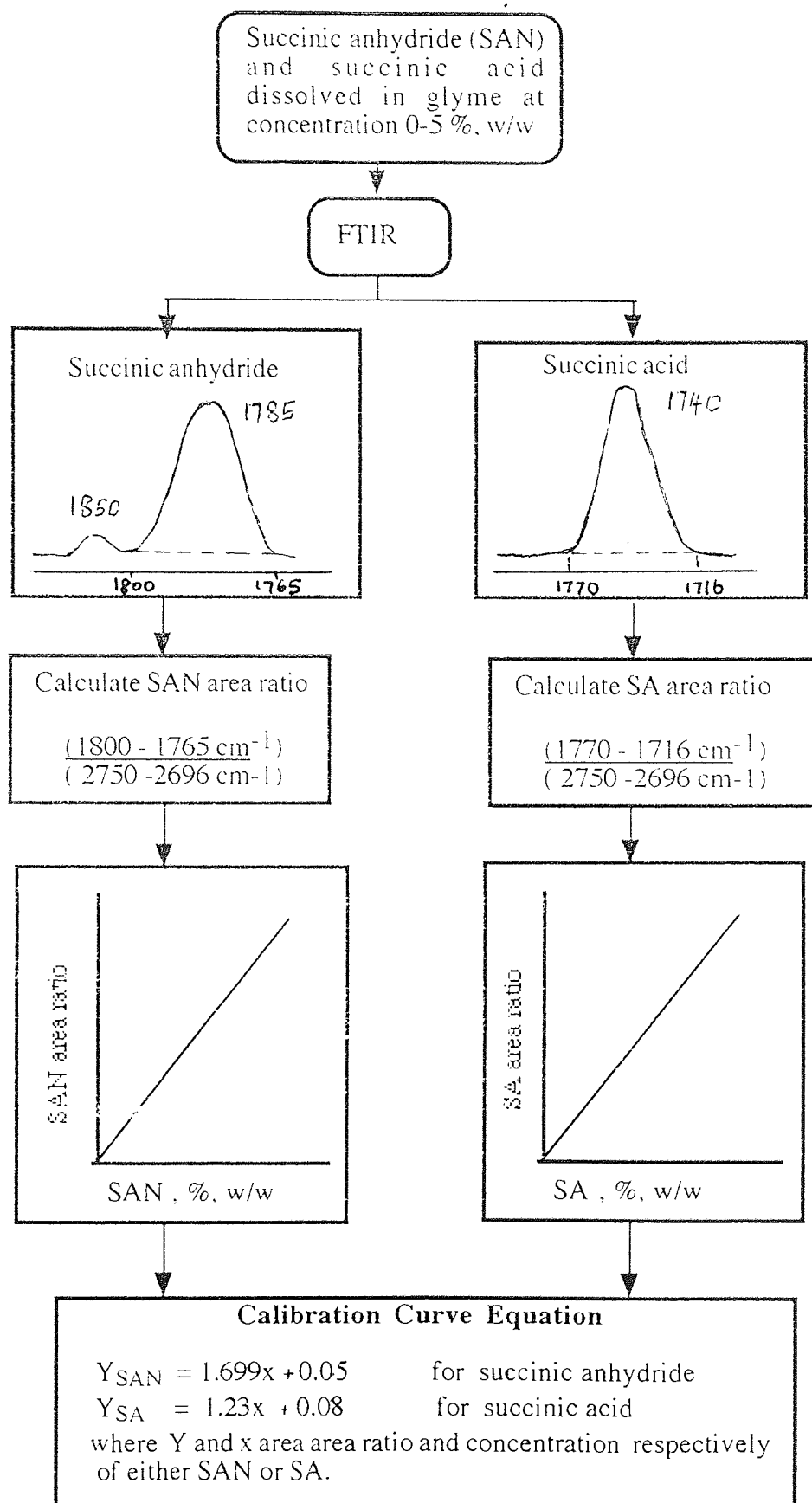
Scheme 2.1 : Flow chart for derivation of Calibration Curve Equation to calculate succinic anhydride (SAN) and succinic acid concentrations in maleated polymer from FTIR spectra.

Figure 2.1 : Infrared spectra of unstabilised polypropylene and EPDM films

(processed at 180°C, 10 min., closed mixing)
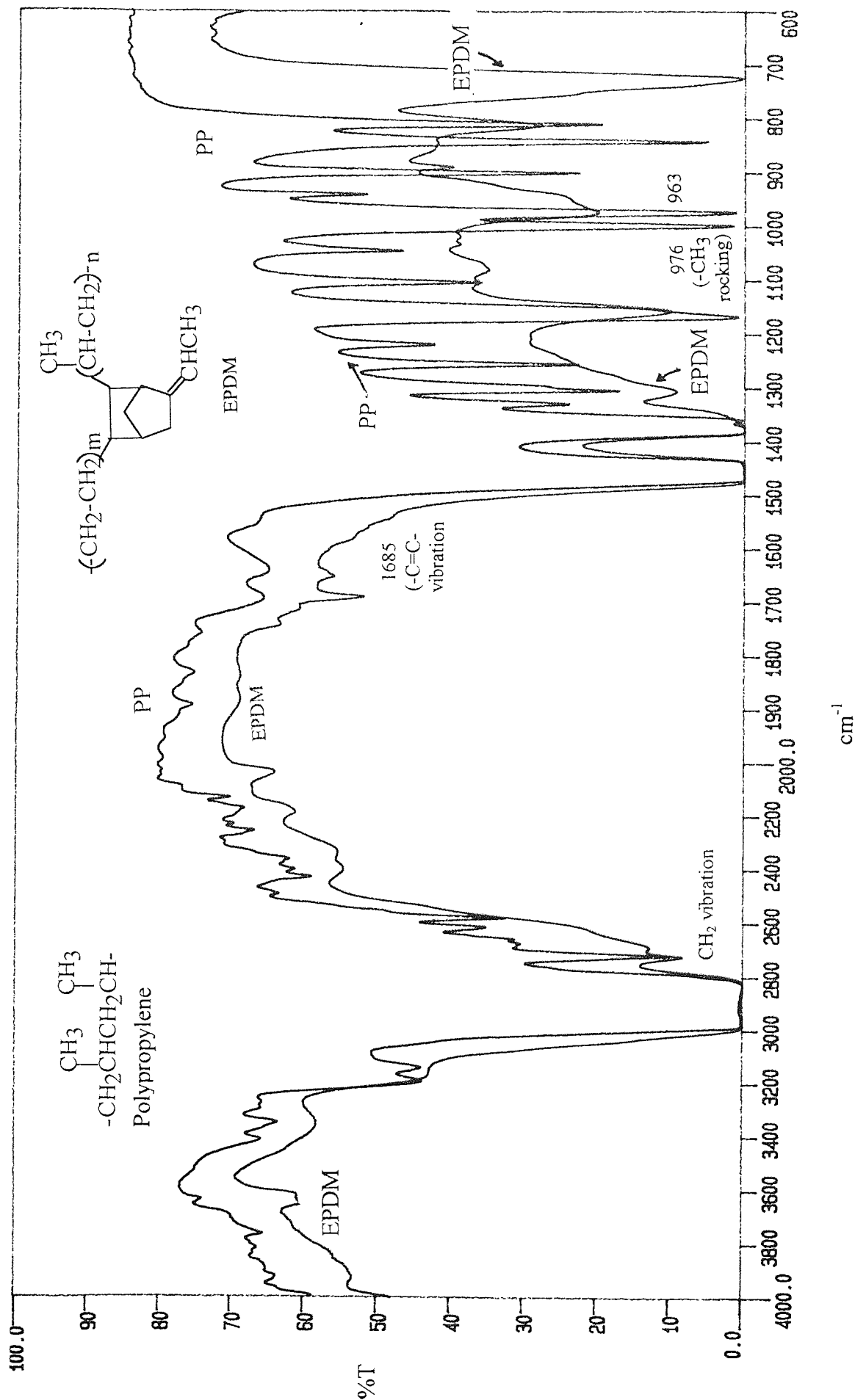
Fig. 2.2 : Infrared spectra of maleic anhydride in dichloromethane

74
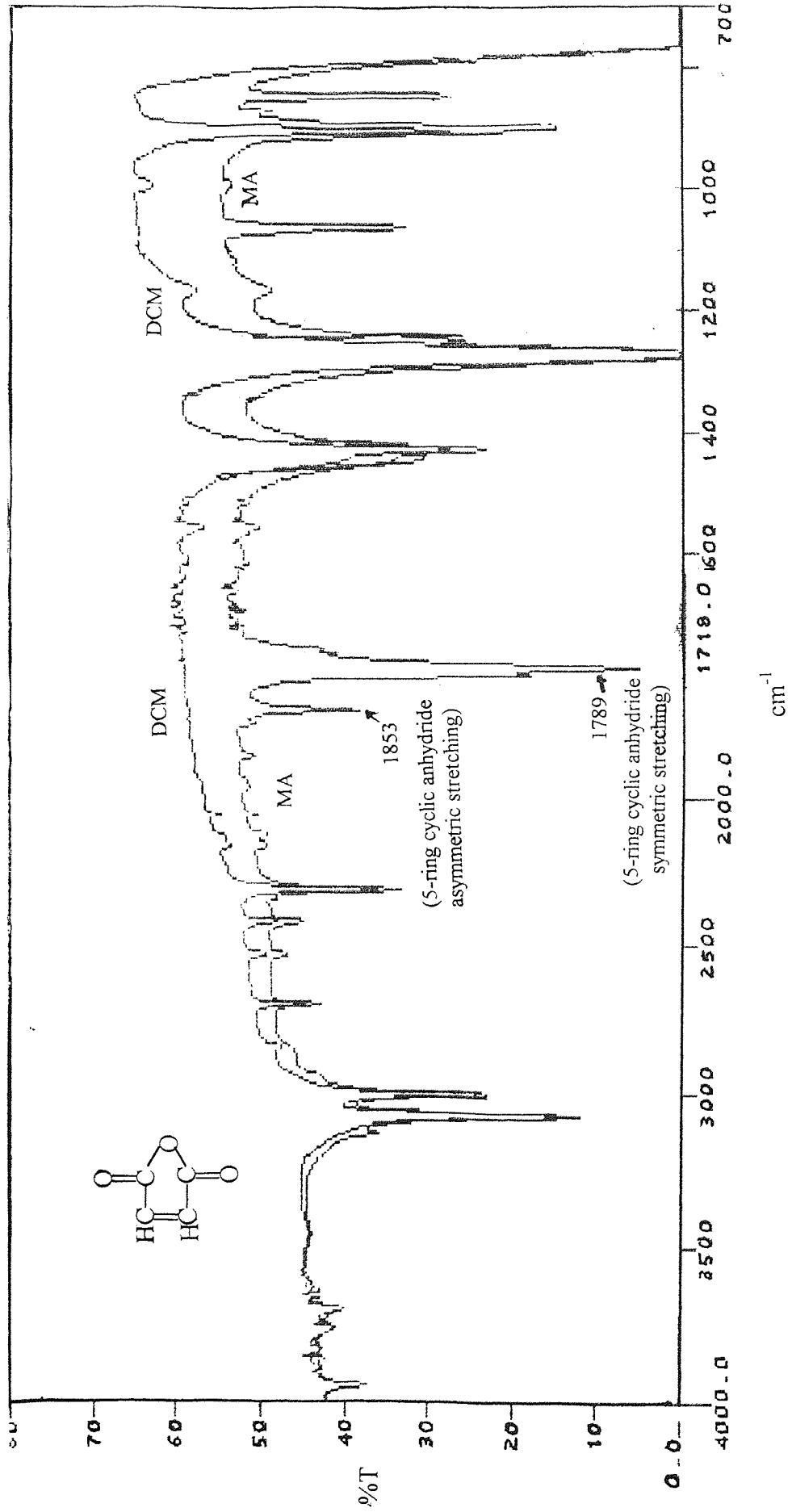
Fig. 2.3: Infrared spectra of pure trimethyolpropane triacrylate (TRIS) (between KBr disk)

$$CH_2=CHC-O-CH_2-\overset{\overset{\displaystyle CH_2CH_3}{|}}{\underset{|}{C}}-CH_2-O-C-CH=CH_2$$

$$CH_2-O-C-CH=CH_2$$

1647
(-C=C-
stretching)

(-C=O stretching)
1738

cm^{-1}

%T

100.0

80

60

40

20

0

-7.0

4000.0   3500   3000   2500   2000.0   1800   1600   1400   1200   1000   800   500.0

75
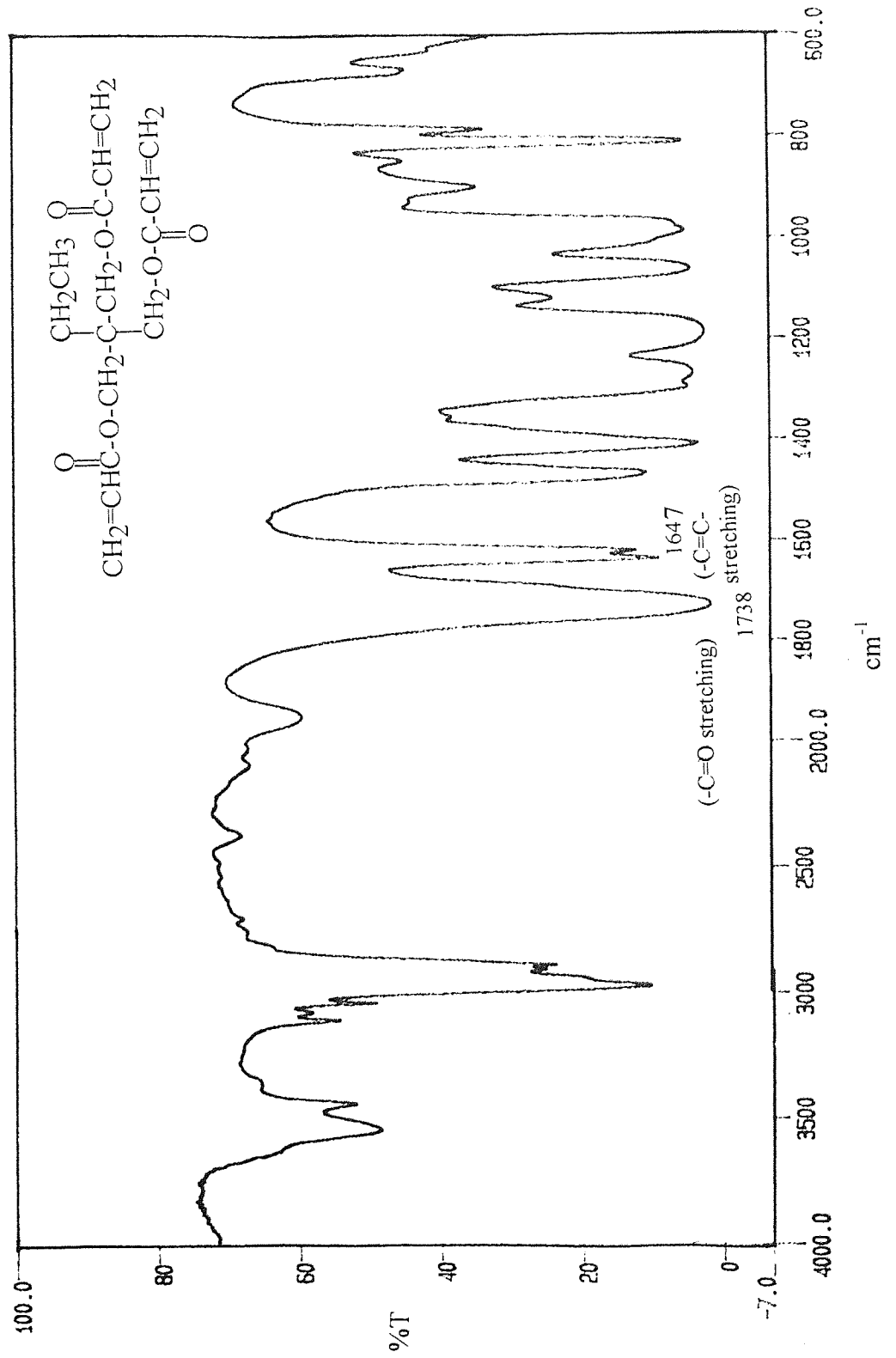
Fig 2.4: Infrared spectra of 2,5-dimethyl 2,5-ditertiary butylperoxy hexane (T101) (between KBr disk)
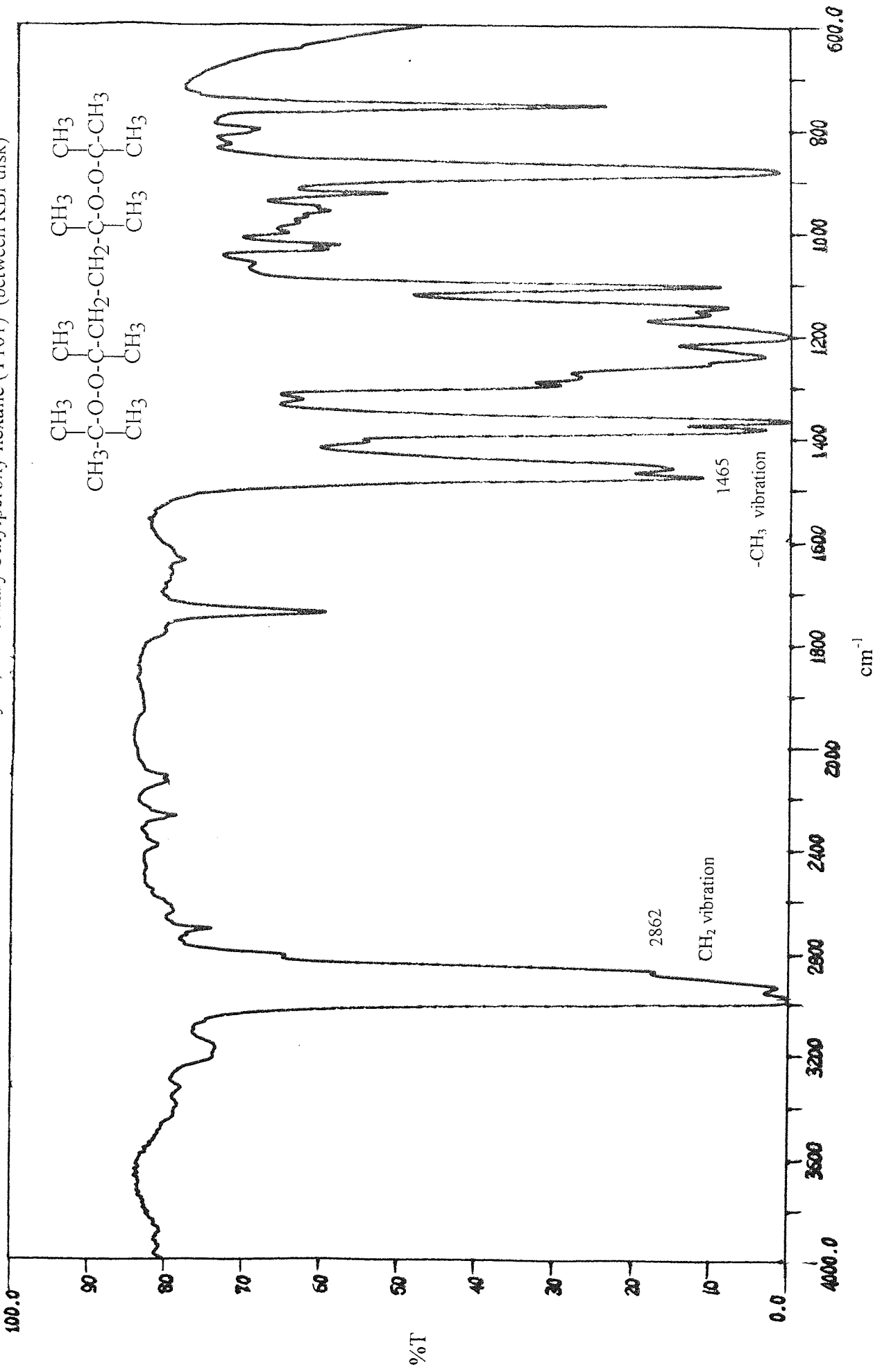
Fig. 2.5: Infrared spectra of hexamethylene diamine (HEMDA) (KBr disk)

$H_2N-(CH_2)_6-NH_2$
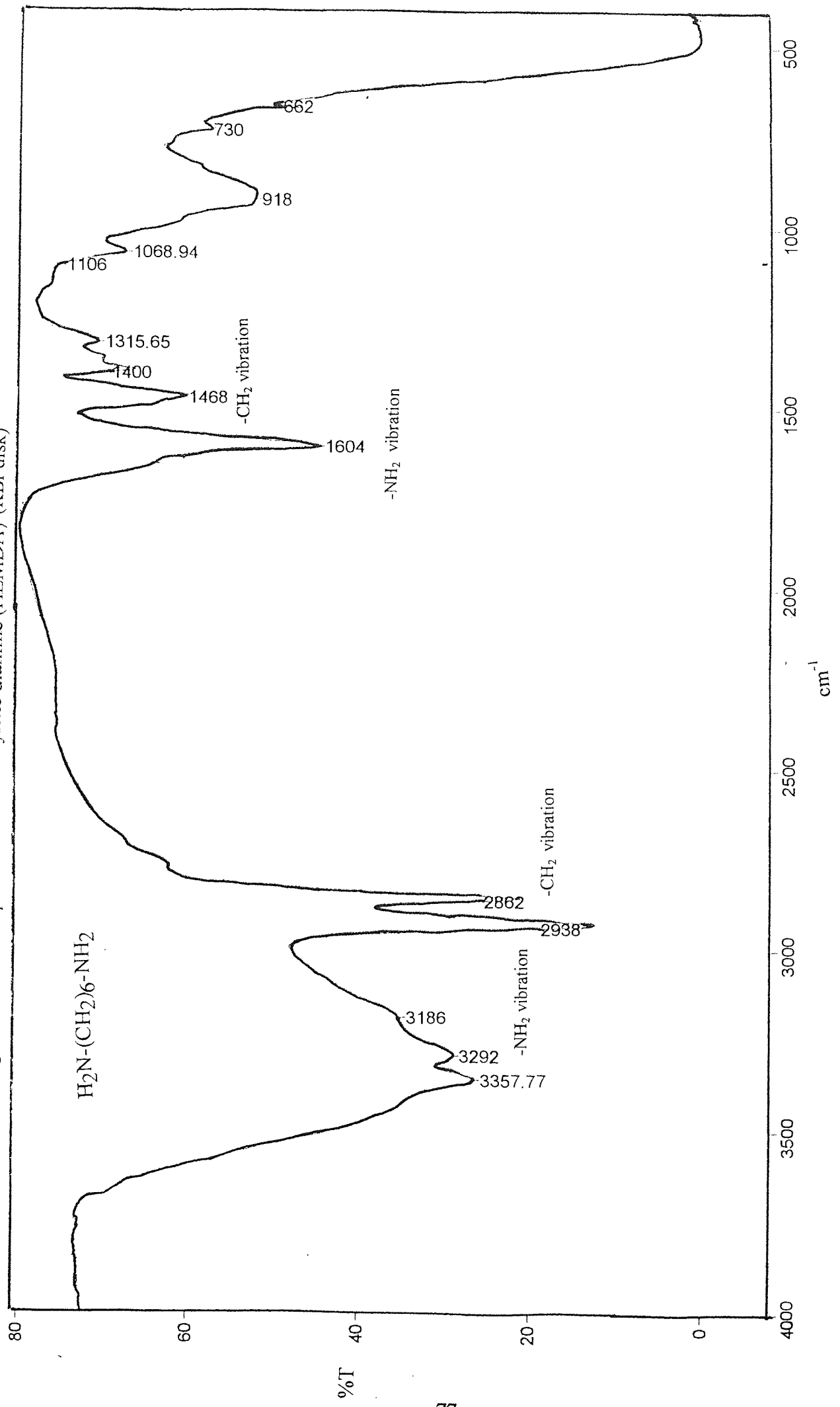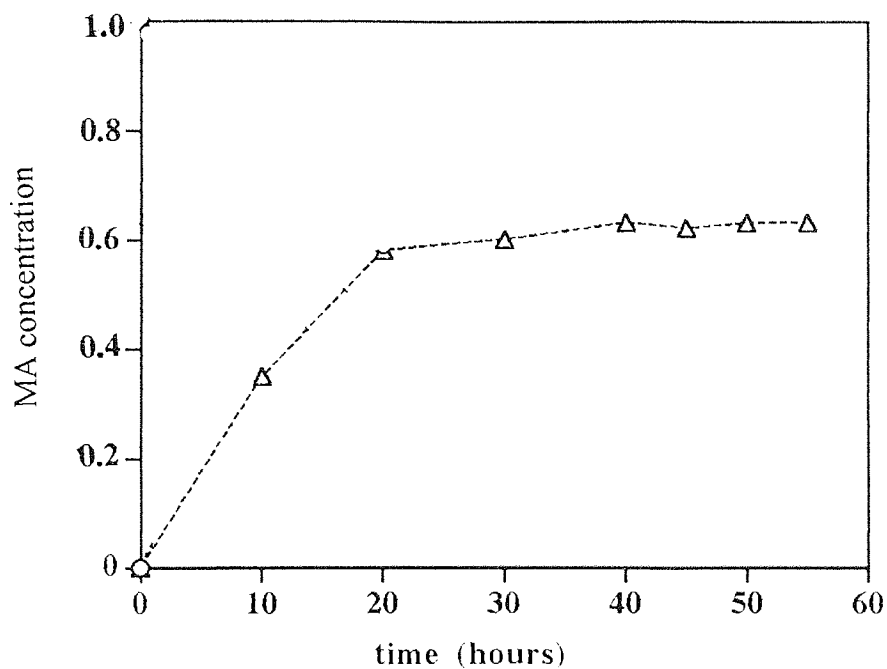
Figure 2.6: Concentration of maleic anhydride (MA) in a maleated PP film after Soxhlet extraction in DCM at various time intervals. The maleated PP was a product of PP processed with 6 phr MA in the presence of 0.005 molar ratio (m.r) of T101

Fig. 2.7: Infrared spectrum of maleated polypropylene film
(PP processed with 6phrMA in the presence of 0.005 m.r T101)
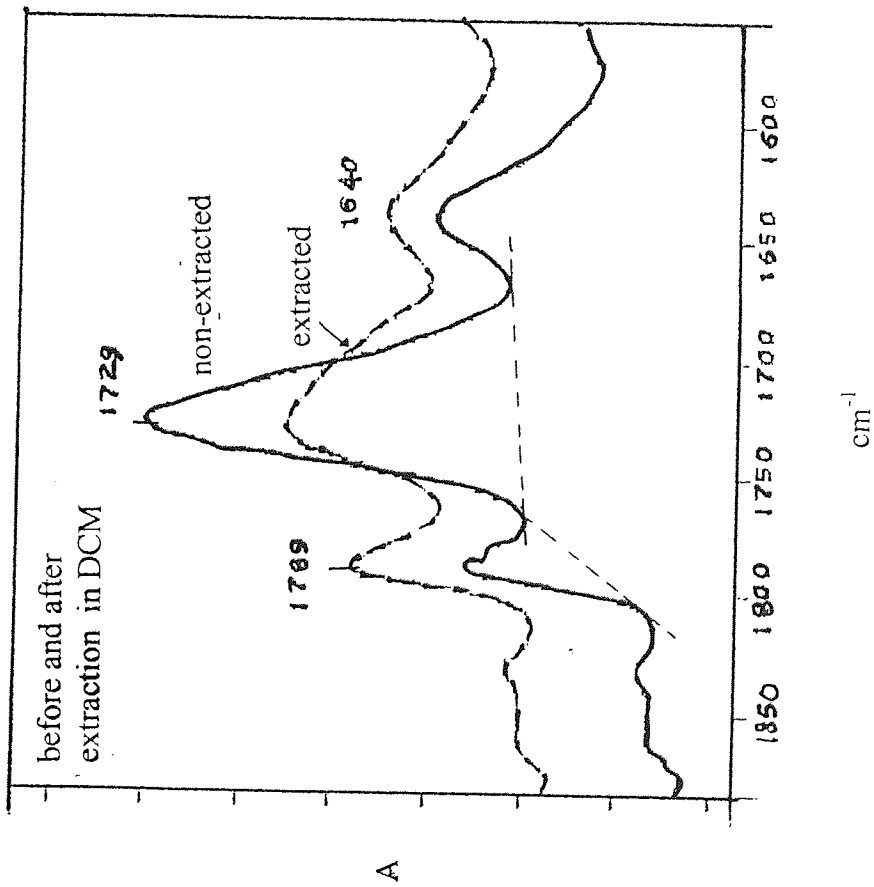
Fig: 2.9: The carbonyl region in the Infrared spectrum of succinic acid in glyme

Fig: 2.8: The carbonyl region in the Infrared spectrum of succinic anhydride in glyme
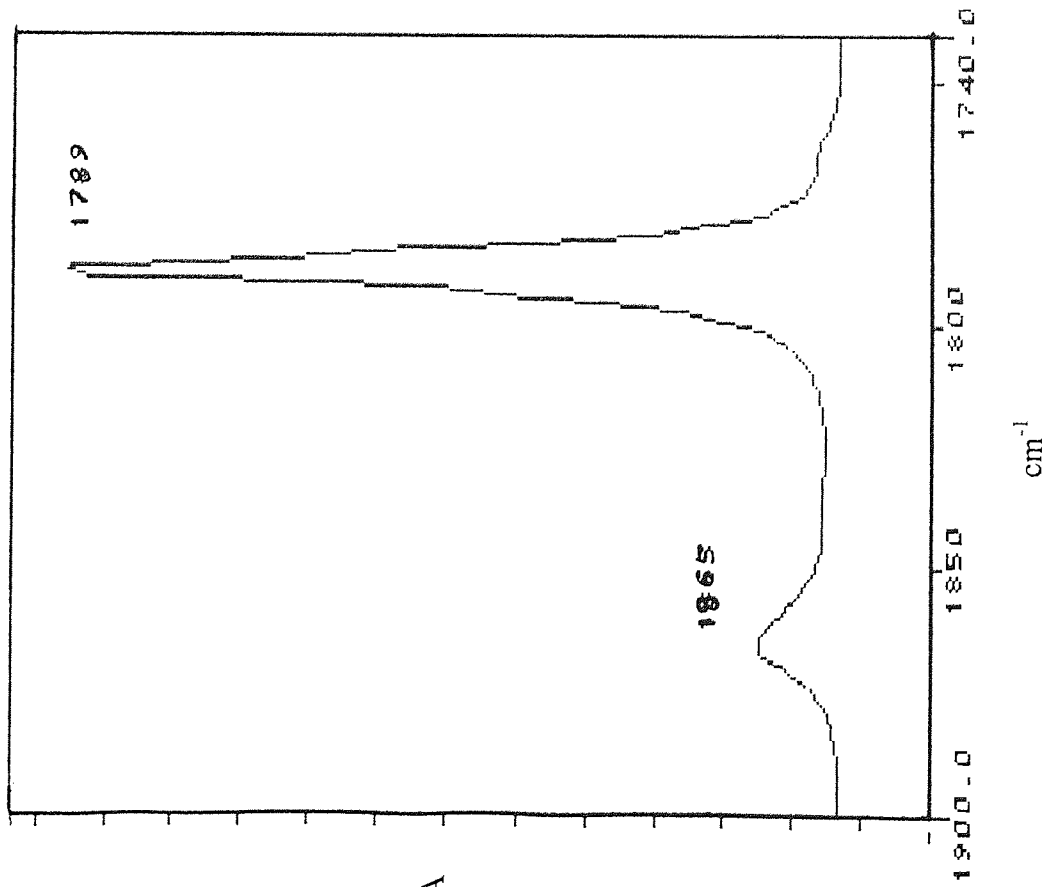
80
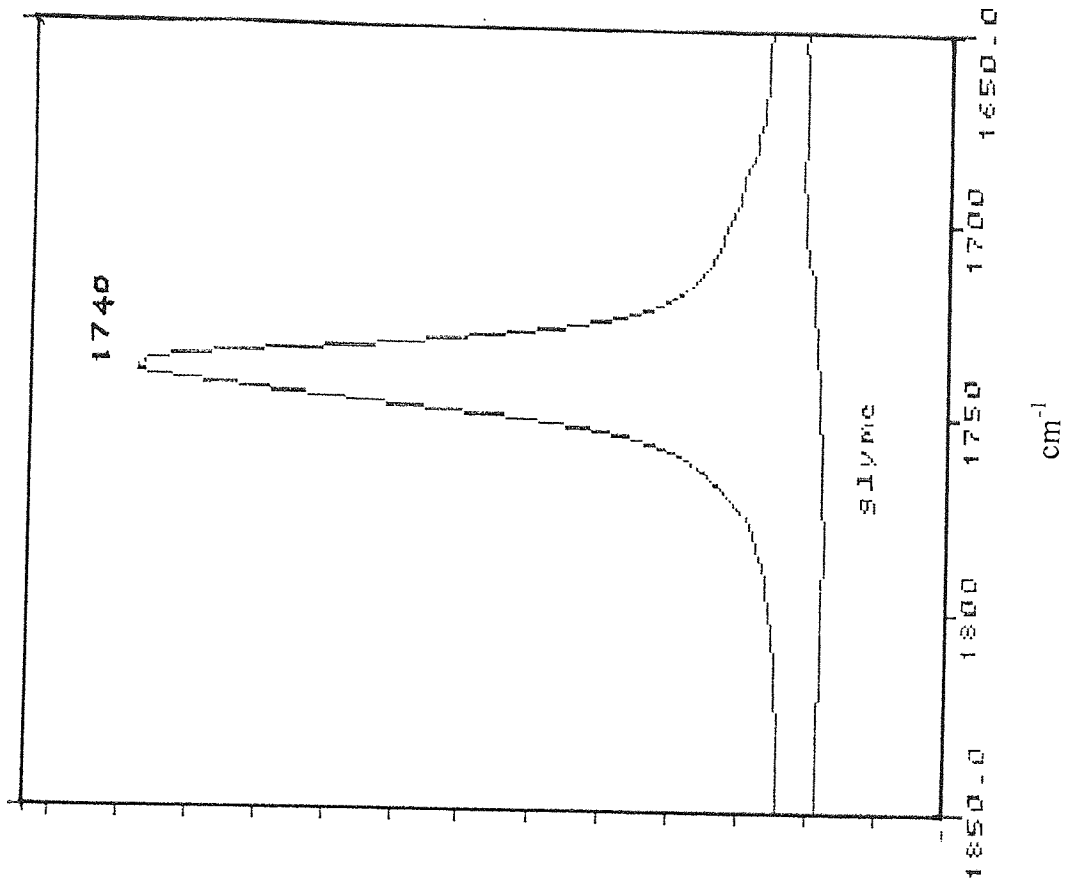
Fig. 2.10: Infrared spectra of pure liquid of glyme (in between KBr disk)

cm⁻¹

1690

1960

2060

%T

81
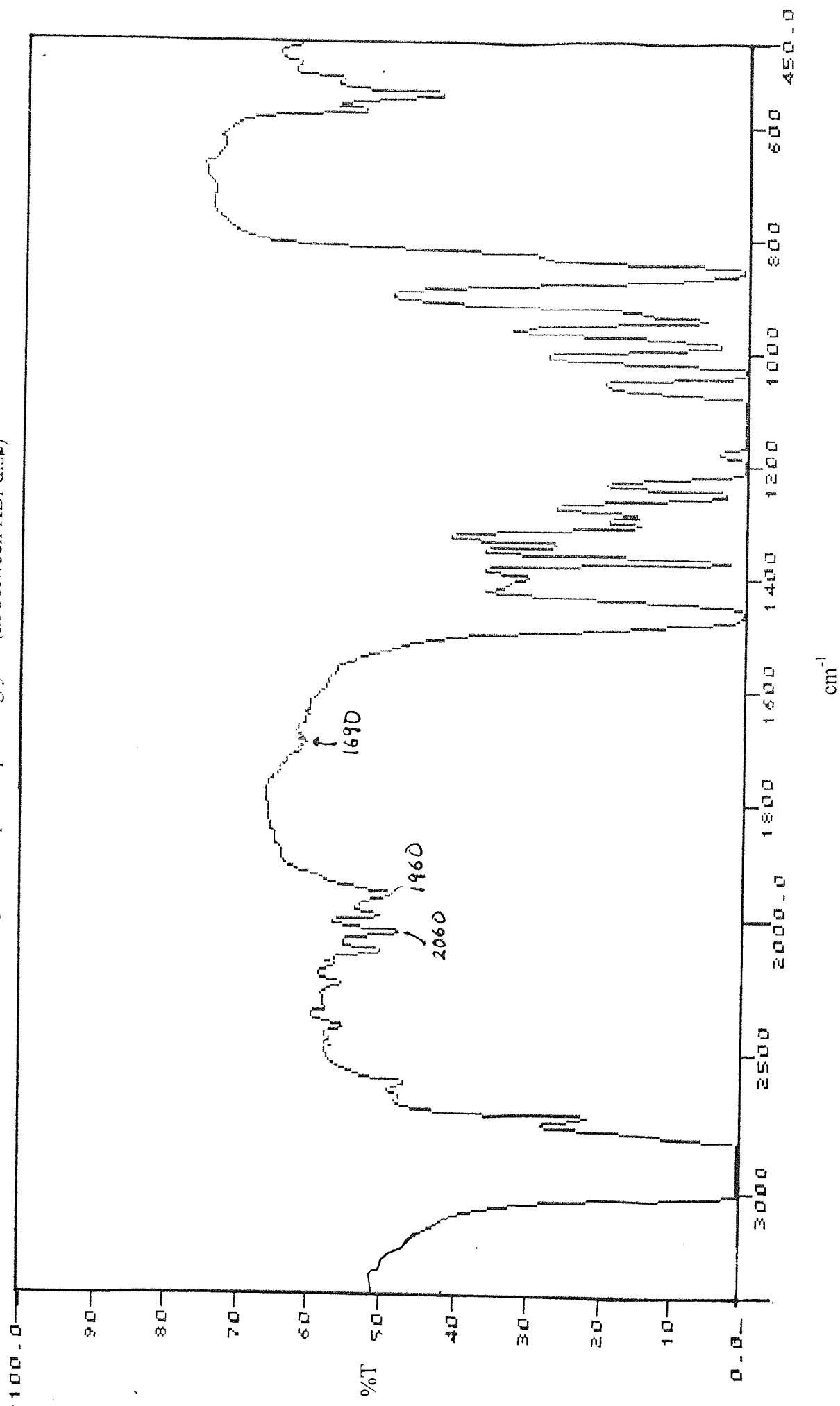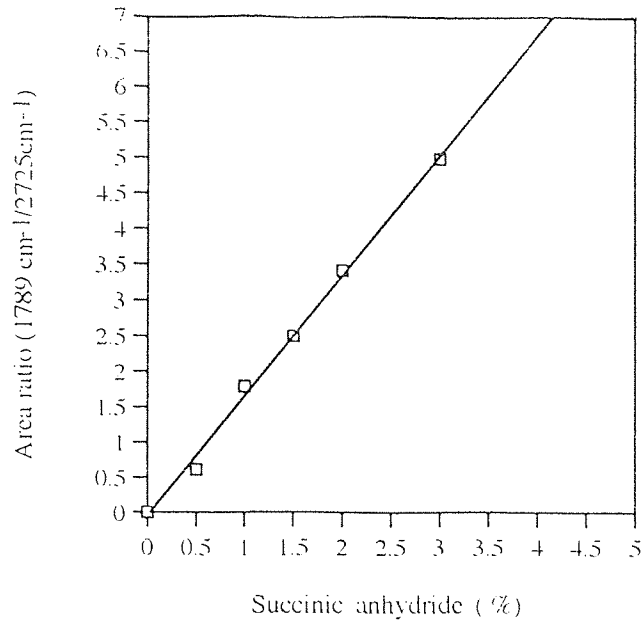
(A)
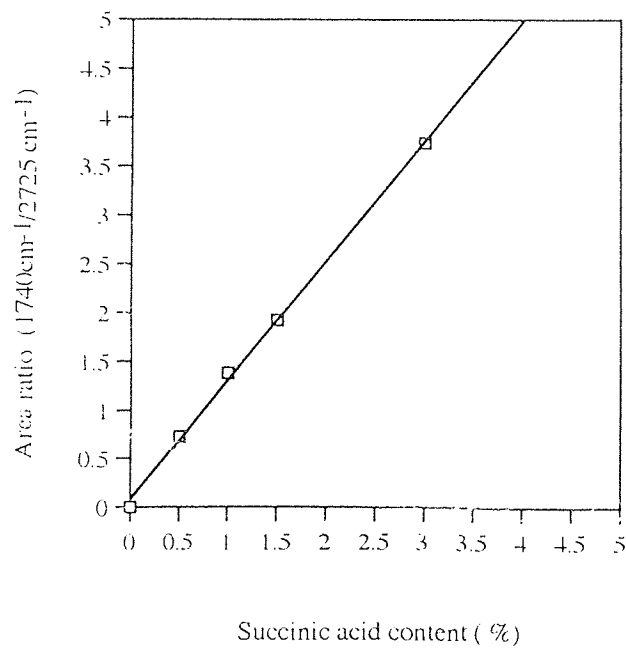
(B)

Fig. 2.11: Infrared calibration curve: relation between concentrations of succinic anhydride (A) and succinic acid (B) in glyme, and area ratio of anhydride peak at 1789 cm^{-1} and acid peak at 1740 cm^{-1}, respectively.
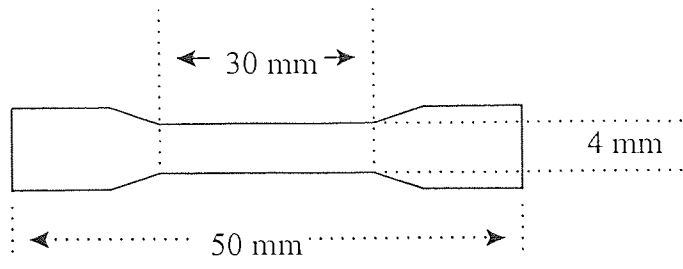
Fig. 2.12: Dumb-bell shaped tensile test specimen
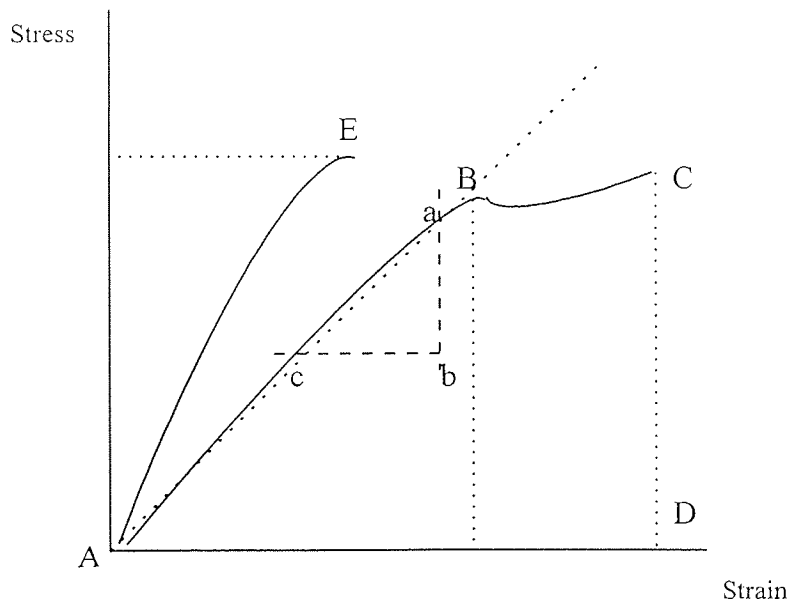
Figure 2.13: Idealised tensile stress-strain curve

CHAPTER THREE

FUNCTIONALISATION OF POLYPROPYLENE, EPDM AND POLYPROPYLENE - EPDM BLEND WITH MALEIC ANHYDRIDE BY REACTIVE PROCESSING

3.1 OBJECTIVE AND METHODOLOGY

A great deal of work has been done on grafting of maleic anhydride, **MA (I)**, onto polyolefins either in polymer melt, in the solid or in solution [49,50,52-55,114]. The overall aim is to increase the polarity and to functionalise the non-polar polyolefins. In most cases the grafting reactions of MA onto polyolefins has been carried out in the melt, with grafting yield generally less than 1 phr. [41]. To obtain these values, extremely high initiator concentration of up to 50 mol-% related to MA were used [115]. Unfortunately, this approach leads to degradation of the polymer backbone and consequently to reduction of the desired physical properties of the polymer . A novel approach to functionalisation of polymers has been developed at Aston University, with the main object of enhancing the grafting efficiency of a wide range of functional monomers [76, 107a, 107b, 116]. This is based on the reaction of vinyl monomers (an agent) in the polymer melt carried out in either extruder or internal mixer, in the presence of a small concentration of a free radical initiator and a co-monomer containing two or more reactive functions (a co-agent).

The work described in this chapter describes a study of the efficiency of grafting of MA onto PP, EPDM and PP/EPDM mixtures, in the presence of a trifunctional co-agent trimethylolpropane triacrylate **TRIS (II)**, during reactive processing in an internal mixer. The MA functionalised polymers (referred to as 'maleated polymers') will be used in

84

subsequent synthesis of PP/EPDM copolymers to be used for the compatibilisation of PP/EPDM blends. A preliminary work to study TRIS reactivity onto PP and EPDM was first conducted before the functionalisation of the polymers with MA.

All reactive processing methods used were performed in a closed system of an internal mixer under a standard condition i.e. 180^0 C, rotor speed 60 rpm and processing time 10 minute as detailed in Section 2.2. The functionalisation of polymers with MA was performed in the presence or absence of various concentration of FRI (**T101**), III, and TRIS. Different methods of addition of the reactive agents (as shown in Scheme 3.1, 3.2 and 3.3) were studied. Methods of analysis of samples were as described in relevant sections in Chap. 2.
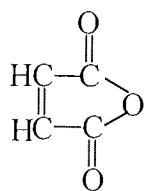
(**I**)
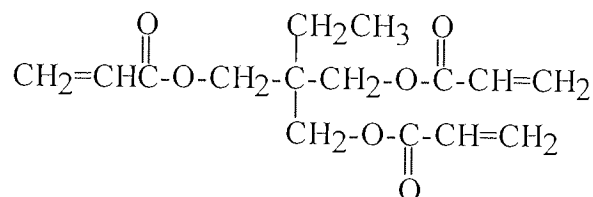
(**II**)
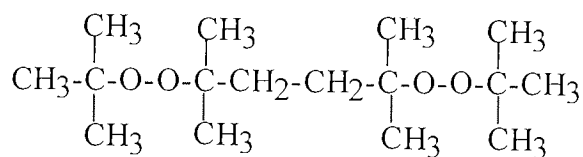
(**III**)

3.2 RESULTS

3.2.1 Methods of Addition of the Reactive Agents

Three methods were assessed with an objective to optimise the method of addition of reactive agents i.e. MA and TRIS, that will result in optimum grafting efficiency of MA. A standard mixture of 35 g of sample containing 90 phr PP, 7 phr MA, 3 phr TRIS and 0.002 m.r. T101, were used in the study. The major variable in those methods was the sequence of addition of agents MA, co-agent TRIS and FRI T101.

In **Method A** as described in Scheme 3.1, all ingredients were premixed before processing in the internal mixer under standard condition.

In **Method B,** as described in Scheme 3.2, PP and MA were tumbled mixed before processing in the internal mixer under standard condition. After 3 minutes, the loading ram was lifted-up and while the mixing continued, a mixture of TRIS and FRI was directly added into the polymer melt in the internal mixer, using a long needle syringe. The addition was completed within 20 seconds. The ram was immediately lowered down and the processing was continued to completion for 10 minutes.

In **Method C,** as described in Scheme 3.3, PP, TRIS and FRI were premixed before processing in the internal mixer under standard condition. After 3 minutes, loading ram was lifted-up (less than 20 s) and while the mixing continued, pure MA in the powder

form was directly added into the polymer melt using a self made non-stick paper spoon. The ram was immediately lowered down and the processing was continued to complete in 10 minutes.

In all methods described above, after completion of each of the processing operation, the hot maleated PP (**PMA**) melt was immediately shredded to small pieces to facilitate cooling before being kept in an air tight polyethylene small bag. Since MA, in the maleated PP, was present in non-grafted and grafted forms, the level of grafted MA onto PP was determined after all non-grafted MA was removed by Soxhlet extraction in hot DCM for 48 hours as detailed in Section. 2. 3.1

The MA content in non-extracted and extracted maleated PP sample were determined titrimetrically as described in Section 2.4.2. The results (see Table 3.1) show that MA content in extracted maleated PP i.e. grafted MA onto PP, prepared in accordance with **Method A** is higher than that of Method B and Method C. The grafting efficiency was about 49% compared to 39% and 43% for Method B and Method C, respectively. Based on the above results, Method A was adopted for the rest of functionalisation of PP and EPDM with MA.

Table 3.1 also shows that only 67%, 40% and 30% MA remained in the polymer after processing (before extraction) relative to the amount of MA initially introduced (the introduced MA was 7 phr - refer Table 3.1) in the case of Method A, Method B and Method C, respectively. It is known [47] that the vapour pressure of MA is low; about 3 mm of Hg. at melting point temperature 52.8 °C, and about 500 mm Hg. at 180 °C. With

this easy-to-sublime property, part of the MA was assumed to have been lost via sublimation during the reactive processing stage. Furthermore, acrid odour and eye irritating vapour was produced which was most probably due to the sublimation of MA, especially when the ram of the internal mixer was opened at 3 minutes during the reactive processing (for Methods B and C), as well as at the end of the processing (All the processing involving MA was conducted under an air extractor).

A typical torque change during the processing of MA via the three methods is shown in Fig. 3.1. All Methods show similar trend of torque curve although with Methods B and C opening the ram at 3 minutes during processing caused a sudden drop in torque values, but this was recovered upon closing the ram. The torque reached a stable plateau after 6 minutes and this indicated that 10 minutes processing was sufficient for grafting MA onto the polymer

3.2.2 Grafting efficiency of TRIS onto PP and EPDM

A series of PP and EPDM processed in the presence of various concentration of peroxide and TRIS were prepared in accordance with Method A Scheme 3.1 but with exclusion of MA. The work was conducted in order to study the grafting efficiency of TRIS onto PP and EPDM. The TRIS grafting level was evaluated from FTIR spectra of thin sample films, before and after exhaustive Soxhlet extraction in DCM, by measuring carbonyl area ratio: area of carbonyl peak (1690 - 1780 cm^{-1}) Fig. 3.2 with reference to an area peak of a constant IR absorption of the polymer ($>CH_2$) at 2725 cm^{-1}; this was conducted in order to take any changes in polymer film thickness into account.

3.2.2.1 The use of FTIR to Identify TRIS Grafting onto Polymer

The Infrared (FTIR) spectrum of TRIS in KBr disk (Fig. 2.3) shows two selected major peaks at 1738 cm^{-1} for unsaturated ester group, and 1647 cm^{-1} for acrylate double bond. A comparison of IR spectra of a PP film containing 2 phr TRIS processed in the absence (Fig. 3.2a) and presence (Fig. 3.2b) of FRI, with that of fresh TRIS (Fig.2.3) show that the carbonyl group peak absorption of fresh TRIS at 1738 cm^{-1} (Fig 2.3) was shifted to lower wave-numbers around 1730 cm^{-1} after grafting onto PP (Fig. 3.2a and Fig.3.2b), while the acrylate double bond peak absorption of fresh TRIS at 1647 cm^{-1} was shifted to 1640 cm^{-1} with very low peak intensity. Upon Soxhlet extraction of the sample in DCM the intensity of the 1730 cm^{-1} peak was reduced while 1647 cm^{-1} peak was completely eliminated (Fig. 3.2a and Fig. 3.2b). Similar results were observed for the FTIR spectra of EPDM functionalised with TRIS (Fig.3.3).

3.2.2.2 Effect of TRIS and FRI concentration on TRIS grafting yield

The grafting efficiency of TRIS onto PP is shown in Fig. 3.4. The grafting yield of TRIS increases with higher TRIS concentration. Addition of FRI drastically improved the TRIS grafting level which reached to above 80 % efficiency at 0.005 m.r. FRI. Similar results were observed for EPDM samples (Fig. 3.5). In the presence of 0.005 m.r FRI, the TRIS grafting efficiency was 100 % .

The presence of TRIS (alone without FRI) in the samples did not have any appreciable effect on the melt property of PP (Fig.3.6 and 3.7) . In this part of the work the MFI

values were measured using standard diameter die size (Section 2.7). Addition of small amount of FRI drastically increased the MFI values (Fig.3.7). On the other hand, at constant FRI concentration, addition of higher TRIS concentration reduces MFI values (Fig. 3.6). The lower MFI values, at higher TRIS concentration, could be related to both lower PP backbone degradation and crosslinking between PP molecules initiated by TRIS. The crosslinking was confirmed from the formation of small amount of gel (sample Soxhlet extracted in xylene, refer to Section 2.6) in these samples (see Table 3.2). On the other hand Table 3.3 shows high amount of gel is formed from EPDM processed with TRIS and free radical initiator. The high gel amount is a reflection of excessive crosslinking.

3.2.3 Functionalisation of PP and EPDM with Maleic Anhydride in the presence and absence of co-agent

The affinity of MA towards PP and EPDM was studied by reactively processing PP or EPDM with MA in the absence and presence of various concentration of organic peroxide T101 but without the co-agent TRIS, in accordance with Method A (Scheme 3.1). Three purification methods namely Soxhlet extraction, heating in vacuum oven and precipitation in xylene-acetone system (as detailed in Sections 2.4.1, 2.4.2 and 2.4.3, respectively) were used to remove any non-grafted MA and its derivative maleic acid, from the maleated polymers. The grafting efficiency was determined from FTIR spectroscopy (Section 2.5.1) and by titration (Section 2.5.2). The efficiency of the purification methods will be compared and discussed.

3.2.3.1 Proof of MA grafting

Infrared spectroscopy is a common method which has been used frequently [109, 117-119] to follow grafting reactions of MA onto polyolefins, due to the strong carbonyl absorption of the cyclic anhydrides which appears in a region rarely superimposed by other bands. Fig. 3.8 shows the carbonyl region in the IR spectrum of MA in a solvent (DCM), within the wavelength region of interest from 1700 cm^{-1} to 1900 cm^{-1}. Absorption peaks at 1781 cm^{-1} and 1850 cm^{-1} are characteristic of a cyclic anhydride with 5-ring structure. This doublet is usually ascribed to mechanical coupling of carbonyl vibration. The high frequency band (1781 cm^{-1}) is related to the symmetric (in-plane) stretching mode and the low frequency band (1850 cm^{-1}) is to asymmetric (out-of-plane) mode. Existence of these two peaks in a purified maleated polymer is therefore an evidence to the presence of grafted MA. MA in the grafted form exists as succinic anhydride (SAn). MA and SAn, like most other anhydrides, could be hydrolysed to the corresponding acids. Infrared spectra of SAN shown in Fig. 3.9 reveals two peaks at 1789 cm^{-1} and 1865 cm^{-1}, and the infrared spectrum of the hydrolysed form of MA, succinic acid (SA) Fig. 3.10 shows only a single peak at 1740 cm^{-1}.

Infrared spectrum of PP film processed with 6 phr MA alone (hereafter called PMA1) Fig. 3.11 shows a new small absorption peak at 1789 cm^{-1} which could be related to carbonyl group vibration of MA in the form of SA. However the absorption peak intensity is very low. A new low intensity peak is also observed at 1725 cm^{-1}. Exhaustive Soxhlet extraction of the PMA1 films in DCM has almost eliminated peaks 1789 cm^{-1} and 1725

91

cm^{-1}. The overall IR spectrum of the extracted PMA1 film now resembles that of the control PP film. (Fig. 3.11).

A typical IR spectrum of PP processed with MA in the presence of free radical initiator is shown in Fig. 3.12. The carbonyl vibration of MA appeared at 1787 cm^{-1} and a new peak observed at 1729 cm^{-1}. The intensity of both peaks in an extracted sample film are stronger than that of PMA1, which is an indication of higher grafted MA. The existence of new peak at 1729 cm^{-1} is related to acid function, from hydrolysis of MA. Similar peaks are observed in a commercial maleated PP ex-Fusabond MD278D supplied by DuPont (Fig. 3.13).

A typical IR spectra of the PP processed with MA in the presence of both organic peroxide and co-agent TRIS is shown in Fig. 3.14. A comparison between Fig. 3.14 with Fig. 3.12 indicates that intensity of carbonyl vibration of MA at 1789 cm^{-1} and 1850 cm^{-1} are drastically increased with the addition of the co-agent TRIS during reactive processing. After exhaustive Soxhlet extraction in hot DCM, the high intensity of the peaks shown in Fig. 3.14 is retained. This indicates higher grafting level of MA onto the polymer.

Fig. 3.15 is a typical IR spectra of EPDM processed with MA in the presence of free radical initiator and co-agent TRIS. Generally maleated EPDM exhibits similar IR peak related to the MA.

3.2.3.2 Analysis of MA grafting yield

In a functionalisation reaction of a polymer with a reactive monomer, it is important to be able to determine the characteristics of the graft copolymer resulting from the process. One of the common tests applied is 'graft efficiency' analysis. It is defined as the percentage of the grafting monomer which is ultimately bonded to the polymer backbone, the remainder being non-attached or free monomer [108,120]. Before analysis of the MA grafting level in the maleated polymers, it is imperative to remove all impurities that could directly interfere with the measurements of grafted MA. In a maleated polymer, the impurities are primarily based on the non-grafted (free) MA and hydrolysed MA present as maleic acid. Three methods have been widely utilised in the literature to remove the impurities mentioned [55,98,108, 121-124]. These are extraction in a selected solvent, hot drying in a vacuum oven and precipitation from xylene-acetone solvent system. All these methods (detailed in Sections 2.4.1, 2.4.2 and 2.4.3) were used in this work, and the efficiency to remove impurities was compared.

Analysis of grafting yield in maleated PP processed without the co-agent was determined by either FTIR method or titration. For maleated polymers processed in the presence of the co-agent TRIS, FTIR method could not be used confidently because the peak of the acid moiety would be superimposed with carbonyl peak of the co-agent TRIS. Therefore the grafting yield of MA in all TRIS containing samples was determined titramatrically.

For all maleated EPDM samples, MA content was determined by titration. Effort to determine MA content in maleated EPDM by FTIR method was unsuccessful due to difficulty in sample film preparation which consequently resulted in poor and inconsistent IR spectra. It was found that the maleated EPDM samples stick strongly to laminating films, and this caused peeling difficulty of the samples with acceptable thickness for FTIR measurement. Immersion of the sample films in water could easily separate the laminating films but on the other hand will cause hydrolysis of the MA content. IR spectra was therefore used only to check qualitatively the presence of anhydride peak in the maleated EPDM.

3.2.3.3   Grafting of MA onto PP without co-agent

Results shown in Section 3.2.3.1 indicate that in a maleated polymer, the anhydride exists in both the anhydride and acid forms. The existence of acid is suspected as a result of hydrolysed MA or SAn. Heating a maleated polymer film in a vacuum oven at 120^0C is intended to remove non-grafted MA and more importantly to revert any acid back to anhydride form [48]. Inspection of IR spectra of maleated PP films processed in the presence of peroxide only, revealed that the acid peak (at 1725 cm^{-1}) is clearly observed after 72 hours heating in vacuum oven. This suggest that the heating in vacuum is unable to completely reverted all the acid to the anhydride form. Similarly, FTIR spectra of maleated PP films purified by Soxhlet extraction and purified by precipitation from xylene-acetone, display both anhydride and acid peaks after heating in vacuum oven (at 120^0C) for 72 h. This observation suggests that anhydride moiety always exist in both the anhydride and the acid forms. To quantitate the amount of grafted MA, a calibration curve

for each moiety was constructed from IR spectra of known concentration of pure succinic anhydride and succinic acid dissolved in 1,2-dimethoxyethane (known as glyme) , as detailed in Section 2.5.1 The curves were then used to calculate the amount of grafted anhydride and acid moieties in the maleated polymer which represent the sum of the total amount of grafted MA in the polymer samples.

The level of MA in the maleated polymer was also determined by aqueous titration of the grafted polymer (see Section 2.5.2). Dissolving the maleated polymer in boiling xylene in the presence of small amount of water converts all the anhydride to acid which could be then titrated (hot) with ethanolic solution of NaOH to a phenophthalein end point.

It has been noted that three methods were used in this work to wash out non-grafted MA from maleated PP. The effect of each purification method on the MA grafting yield of MA in different PP maleated samples (analysed by either FTIR spectra or titration) was tabulated in Table 3.4. The performance of each purification methods could be observed from the grafting yield as presented in Fig.3.16 A, B and C for heating in vacuum, Soxhlet extraction, and precipitation from xylene/acetone solvent system, respectively. The grafting yields were analysed by FTIR spectra using the calibration curves. The Figures indicate that all three purification method used show relatively equivalent efficiency for the removal of non-grafted MA from the maleated PP (see Fig. 17 A and B). The Soxhlet extraction method (using DCM) was found very convenient, not laborious and simple, involving only a small amount of solvent (about 100 ml.). On the other hand, precipitation method from xylene/acetone solvent system is laborious and time consuming. Furthermore samples used for this method have to be dissolved in hot xylene (120 °C) and

require quite a large volume of acetone (about 200 ml for each sample) which was not recycleable. The vacuum purification method requires very long heating times of more than 72 hours and high temperature of 120^0C. Prolong heating might cause thermal degradation on the polymer backbone. For the rest of the samples, purification were carried out by Soxhlet extraction in DCM.

Figure 3.18 compares effectiveness of FTIR and titration methods in measuring the grafting yield of MA processed in PP in the absence of a co-agent. The figures indicate that both methods show statistically similar grafting yield. The results show that both methods are equivalently effective in determining the amount of MA in the maleated samples. A commercial maleated PP, Fusabond MD278D was used as a reference to check the accuracy of the above purification and analysis methods. Titration analysis on this reference sample, purified by Soxhlet extraction revealed that the MA grafting yield in the Fusabond was 0.96 phr. This result is quite close to the grafting yield specified by the manufacturer which is 0.85 phr. The FTIR method was found not suitable to determine MA grafting yield in the Fusabond sample because, as could be clearly seen in Fig. 3.13, a very strong peak at around 1730 cm^{-1} could be contributed not only by succinic acid but may by other unknown material.

Figure 3.16 also shows that the grafting yields of MA in all samples are low, less than 0.65 phr. Furthermore, the grafting yield is found to be non-monotonic function of MA initial concentration. It initially increases with increasing MA initial concentration and reaches a maximum value at about 6 phr MA introduced, however grafting level decreases with further increase in introduced MA concentration. The amount of grafting yield is also

effected by the level of free radical initiator concentration used with higher grafting at higher free radical concentrations. Addition of higher free radical initiator concentration during the reactive processing, however, results in severe degradation of the polymer (Fig.3.19). Reaction of PP with MA alone does not significantly alter MFI of the pure PP. However addition of FRI (traces amount of 0.002 - 0.005 m.r) drastically increases the MFI value which indicated severe polymer backbone degradation. It is noteworthy that an attempt to measure MFI values using standard die were unsuccessful due to fluidly nature of these maleated PP samples from which collecting MFI extrudates were impossible. As an alternative, small diameter die was used to measure MFI values of all maleated PP samples. At constant FRI concentration, addition of higher MA concentration reduces the MFI value which is a sign of less polymer backbone degradation.

3.2.3.4   MA grafting onto PP in the presence of a co-agent

Various concentration of MA were reactively processed with PP in the presence of various concentration of FRI and co-agent TRIS, in accordance with Method A of Scheme 3.1 and grafting yield was determined by titration, see Table 3.5.

Fig. 3.20 compares MA grafting level of maleated PP processed in the presence of co-agent TRIS, and that in its absence. Addition of the co-agent TRIS brings about a significant increase in the MA grafting yields. At constant MA to TRIS ratio, within the range of MA concentration studied, the grafting yield increases proportionally with MA introduced; and   unlike maleated PP processed with MA only, maleated PP samples processed in the presence of TRIS show no maximum grafting yield. The magnitude of the MA grafting

increase (in presence of TRIS) is very visible when the amount of MA introduced is higher than 4 phr. The addition of TRIS during reactive processing of maleated PP has also significantly improved the melt properties as shown in Fig. 3.21. At constant MA to TRIS ratio, and FRI concentration 0.002 m.r., MFI values improve with higher MA and TRIS concentration, at which the MFI value is almost similar to MFI value of pure PP. Low MFI value and low gel content of the maleated PP (Table 3.5) indicate little PP backbone degradation and polymer crosslinking, respectively.

Fig. 3.22 shows effect of various ratio of MA to TRIS on MA grafting yield. Grafting yields increased at higher MA to TRIS ratio, with MA to TRIS ratio 6:4 exhibiting highest grafting yield. It was also shown that the grafting yield increased with higher FRI concentrations with an optimum effect at 0.001 m.r FRI. Further increase in FRI concentration improved the grafting yield only moderately.

The MFI values of maleated PP processed in the presence of TRIS were found not dependent on MA to TRIS ratio (Fig.3.23) but were influenced seriously by the FRI concentration (Fig. 3.24). Without FRI, MFI values of maleated PP at various MA to TRIS ratio are closed to that of pure PP. The MFI values increased exponentially with addition of FRI; MFI values increase about 2.5 fold and 5 fold with addition of 0.001 m.r. and 0.002 m.r of FRI, respectively.

3.2.3.5 MA grafting onto EPDM

EPDM was reactively processed with various concentrations of MA in the presence of free radical initiator (0 to 0.005 m.r) and co-agent TRIS (0 - 4 phr), in accordance with Method

98

A (Scheme 3.1). The results of MA grafting yields determined by titration method are presented in Table 3.6. The results indicate that in the absence of a free radical initiator, some MA becomes grafted onto EPDM with reasonably low gel content. The presence of grafted MA onto EPDM could be observed from FTIR spectra of extracted maleated EPDM shown in Fig.3.25. Addition of a trace amount of free radical initiator enhanced the MA grafting yield, but followed by increases in gel content. The amount of MA grafting yield was further enhanced with addition of the co-agent TRIS (see Fig.3.26). Fig. 3.27 illustrates the effect of MA to TRIS ratio on the grafting level, at different FRI concentrations. It is clear that, the grafting yield does not depend, to any appreciable extent, on the MA to TRIS ratio, however it is significantly influenced by the FRI concentration. At constant MA to TRIS ratio, MA grafting yield increased with higher FRI concentration. Addition of higher FRI concentration (although at minute amount) to the EPDM system however produced higher gel content which was a result of substantial crosslinking during reactive processing of maleated EPDM.

The pattern of torque behaviour against processing time observed during reactive processing of TRIS with MA in the presence of different concentration of FRI (see Fig. 3.28) supports the formation of high gel content (higher torque level at the end of processing compared to pure EPDM). Unlike pure EPDM, incorporation of MA into EPDM with or without TRIS, during reactive processing drastically increased torque values. After reaching the maximum torque value, the torque decreased with time to a stable plateau. Both values of maximum torque and stable plateau become higher with high FRI concentrations. The high gel content in the maleated EPDM may effect the measurement accuracy of MA grafting level by titration. It was observed that the

99

maleated PP did not fully dissolve in boiling xylene i.e. part of the sample was only swollen, and this could prevent complete hydrolysis of the anhydride moiety to acidic form (refer Section 2.5.2), required for titration, consequently the MA concentration would not be fully assessed resulting in underestimated grafting values.

3.2.3.6 Grafting of MA onto PP/EPDM blend.

PP/EPDM blends at ratio 75PP and 25 EPDM were processed with various ratios of MA to TRIS in the presence of various concentrations of free radical initiator, see Scheme 3.4. MA grafting yield in the maleated PP/EPDM samples, purified from Soxhlet extraction (Section 2.4.1) were determined by titration (Section 2.5.2). The results are presented in Table 3.7. The presence of grafted MA in the PP/EPDM blend samples was checked from FTIR spectra. Compared with the FTIR spectrum of pure PP/EPDM (Fig. 3.29a), IR spectra of purified maleated PP/EPDM (Fig 3.29b) shows dominant acid peaks at 1720 cm^{-1} and anhydride absorption peaks at 1781 cm^{-1} and 1853 cm^{-1}.

Effect of the co-agent TRIS concentration on the MA grafting level is shown in Fig. 3.30. At constant MA ratio (6 phr) and FRI (0.002 m.r.), and within TRIS concentration studied, MA grafting yield increases exponentially with addition of higher TRIS concentration. The effect of MA to TRIS ratio on the grafting yield was studied. The result as Fig.3.31 indicates that 6 to 4 ratio give optimum MA grafting yield. Similar to PP and EPDM, the grafting yield was effected by the FRI concentration where higher FRI concentrations resulted in higher MA grafting level (Fig. 3.32).

100

Effect of PP/EPDM ratio on the MA grafting yield was briefly studied. PP/EPDM blends at ratio 60 to 40 was processed using the optimum MA to TRIS ratio in the presence of various FRI concentration and the results were presented in Table 3.8. It was found that at FRI concentration up to 0.002 m.r., MA grafting yields in the PP/EPDM 60/40 were similar to that of PP/EPDM75/25. At higher FRI concentration, MA grafting yields in the former was higher than in the later.

3.3   DISCUSSION

Experimental results show that maleic anhydride (MA) have been successfully grafted onto polypropylene (PP), EPDM and blends of PP/EPDM. When MA alone is grafted onto PP, the MA grafting yield is low, about 0.1 phr (Table 3.4) and this is very low for any meaningful application. The addition of MA does not affect the melt stability of the maleated PP samples when compared to pure non-stabilised PP. In the absence of FRI, the number of free macro-radical formed via mechano-scission is limited and are insufficient for the production of high grafting yields of functional monomers. This could be overcome by addition of a small amount of free radical initiator (FRI) (0.001 to 0.005 molar ratio) during the reaction of PP with MA. At an elevated temperature, the peroxide molecules are decomposed into primary radicals with sufficient energy to abstract tertiary hydrogen atoms from polymer backbone [125]. In the presence of FRI only, PP macro-radicals undergoes β-scission rather than crosslinking [126-127] as shown in Scheme 3.5. This leads to higher MFI values i.e. lower molecular weight (see PMA 24 in Table 3.4). In the case of EPDM, crosslinking reaction dominant [128, 129] In the presence of MA,

PP macro-radicals react with the double bond of the MA, forming grafted MA onto PP. As shown in Fig. 3.16 the higher the MA grafting yield

$$
\begin{array}{ccc}
\text{CH}_3 \quad \text{CH}_3 & \xrightarrow[\text{(a) RO}^*]{\text{shear, heat}} & \text{CH}_3 \quad \text{CH}_3 \\
-\text{CHCH}_2\text{-C-CH}_2\text{-} & & -\text{CHCH}_2\text{-C-CH}_2\text{-} \\
\quad\quad\quad\text{H} & & \quad\quad\quad* \\
\text{polypropylene} & & \text{PP macro-radical}
\end{array}
$$

(c) O_2 excess   (b) O_2 deficiency

CH₃ CH₃
-CHCH₂-C-CH₂-
       OOH

(d)

$-\text{C-}^* \quad + \quad \text{CH}_2=\text{CH-CH}$

$^*\text{CH} + -\text{CHCH}_2\text{-C-CH}_2\text{-} \quad\longrightarrow\quad -\text{CHCH}_2\text{-C}=\text{O} + \;^*\text{CH}$
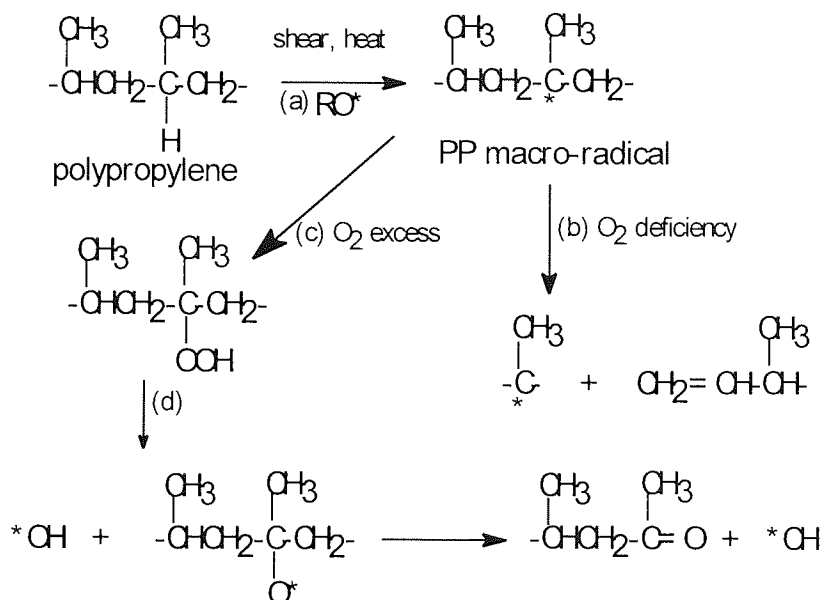
Scheme 3.5 : Mechanochemical chain scission in polypropylene during processing in the presence of free radical initiator during melt processing

required, the greater the FRI concentration is needed and consequently higher MFI valueswould result (Fig. 3.19). The melt property is of a prime importance in polymer processing and is an indirect indication of what type of reactions would occur. High MFI values indicate more intensive PP backbone degradation via chain scission.

However at a constant FRI concentration, the overall grafting efficiency is dependent on the MA solubility in the polymer melt [41]. It was clearly shown that the grafting efficiency of MA passes through an optimum with increasing amount of added MA (Fig.

3.16). The existence of a maximum for the MA grafting yield is associated with the limited solubility of MA in the molten PP [41]. In the presence of excess MA concentration, the PP/MA/FRI mixture changes from a single phase to diphasic system with MA/FRI droplets dispersed in the molten PP [41]. The two phase-system may causing the loss of the initiator to the MA phase, thereby lowering the effective concentration of the initiator. The partition of peroxides over the PP and MA phases results not only in a decrease in grafting efficiencies, but also in reduction of PP backbone degradation, as shown in Fig. 3.19. During the free-radical grafting of MA onto PP, once the PP macro-radicals are formed they will undergo either the desired grafting or the undesired PP degradation by β-scission. At elevated temperatures, the degradation process of PP tertiary macroradicals is a very fast process [125]. The low MA grafting yield implies that MA is not reactive enough towards the tertiary PP macroradicals. Low levels of MA grafting on various polymers including PP, PE, PS, EPDM and ABS has been demonstrated in the literature [102,105,106,117].

In order to promote the grafting efficiency of MA with a lower PP backbone degradation, a co-reactive agent was used utilising an approach developed at Aston University [107]. The key to this approach is the *in situ* co-grafting of a small amount of a multifunctional co-monomer having higher reactivity than the functional monomer (i.e. MA) is used as a reactive co-agent. The strategy is that instead of grafting MA directly onto PP chains, the reactive comonomer is used to serve as a mediator to bridge the gap between the PP macroradicals and the MA monomer. The success of this method lies in achieving a delicate balance between the composition of the chemical system (vinyl monomer, co-

agent, and free radical initiator) and the processing conditions (e.g. temperature, mixing speed).

When TRIS (III), the reactive multifunctional comonomer is used, the MA grafting yield was shown to increase significantly (Fig. 3.20). Furthermore, within the MA concentration studied the MA grafting yield in the PP/MA/TRIS system does not shows a maximum peak in the grafting yield; MA grafting yield increases virtually linearly with increasing concentration of added MA. This contrast the peak formation shown in the absence of TRIS, see Fig. 3.20, which in the latter case indicates low solubility of MA in the polymer. Similar behaviour was observed when MA (alone) was grafted on PP using extruders [41]. The absence of a grafting peak when TRIS is used (Fig. 3.30) suggests formation of TRIS-MA copolymer which is expected to be more soluble than MA in PP melt.

Similarly MA grafting yield in the EPDM was improved when the comonomer TRIS was added. At a given MA , TRIS and FRI concentration, the MA grafting yield in EPDM was shown to be higher than that in PP (Fig. 3.33). However this high yield of MA grafting in the former was accompanied by high gel content which was a result of excessive EPDM crosslinking (see Table 3.6).

The improvement in the MA grafting level in PP in the presence of TRIS could be due to rapid reaction between TRIS with PP macroradicals when compared to that of PP and MA. The triacrylate co-agent TRIS was very reactive towards PP with grafting yield reaching 90% efficiency at 0.005 m.r FRI (Fig. 3.4). Similarly high grafting yield was achieved in EPDM (Fig.3.5). High TRIS grafting yields observed in both PP and EPDM, could also be

104

contributed partly from polymerised TRIS. Few workers [130-131] have reported that in the presence of radical initiator, triacrylate co-agent TRIS is readily polymerise or copolymerise through classical free radical chain reaction mechanism . The resulting PP/TRIS radicals could copolymerise with the MA readily. Addition of TRIS during processing of PP in the presence of FRI also improved PP melt property i.e. the MFI value of the maleated PP was reduced (Fig. 3.21). It could be a result of high reactivity of TRIS towards PP macroradicals that reduced the unwanted β-scission of PP backbone. It also could be attributed to a small amount of gel formed in the maleated PP. In fact such multifunctional monomer have been used to improve PP crosslinking efficiency [25, 132]. The double bonds of the multifunctional monomer are sites for trapping macroradicals of PP. Especially when the PP radical is a tertiary one, the multifunctional monomer reduces the disproportionation reaction significantly and augments crosslinking efficiency. This behaviour could be observed from torque behaviour of PP reactively processed with MA (7 phr), coagent TRIS (3 phr) and free radical initiator T101 (0.002 m.r), as shown in Fig. 3.1. Figure 3.1 shows that a small increase in torque values was observed at about minute 2 during the processing. This increase in torque values at about 2 minutes after processing was more prominent in the torque behaviour of PP/EPDM (see Fig.3.34). The torque values increase is an indication of some initial transient crosslinking in the reaction system. With further processing, preferential chain scissions seems to occur resulting in lower torque values. This behaviour was observed with TRIS when used with a number of other functional monomers [130,131]. A suggested reaction mechanism of PP with MA in the presence of TRIS and small amount of FRI is shown in Scheme 3.7.

GRAFTING OF MA ONTO PP METHOD A

| Polymer
Polypropylene
90 phr | Coagent
TRIS
3 phr | Free radical
T101
0.005 m.r. | Agent
Maleic anhydride
7 phr |

Tumble mixed

torque values monitored

Processed in internal mixer, closed system. 180 C, and rotor speed 60 rpm.
Discharge after 10 min. and shredded to small pieces

t = 0 min. start processing

t = 10 min. stop processing

MA functionalised PP → Melt flow index

Analysis of MA grafting level

Scheme 3.1 : Method A - Flow chart for grafting maleic anhydride onto polypropylene

GRAFTING OF MA ONTO PP METHOD B

Polymer
Polypropylene, 90phr

Agent
Maleic anhydride,7phr

↓

Tumble mixed

↓

Processed in internal mixer, closed system, 180 C, and rotor speed 60 rpm

t = 0 min. start processing

t = 3 min., open ram (<20 s)

torque values monitored

after 3 min. loading ram lifted while mixing is continued. Addition of co-agent and peroxide then lowering of ram

← Co-agent (3%) and peroxide (0.005 m.r)

t = <4 min., close ram

continue processing to total time of 10 min. Sample removed and shredded to small pieces

t = 10 min. stop processing

↓

MA functionalised PP

↓

Analysis of MA grafting level

Scheme 3.2 : Method B - Flow chart for grafting maleic anhydride (MA) onto polypropylene (PP)

GRAFTING OF MA ONTO PP METHOD C

```
┌──────────────┐  ┌──────────────┐  ┌──────────────┐
│   Polymer    │  │   Co-agent   │  │ Free radical │
│ Polypropylene│  │    TRIS      │  │    T101      │
│    90phr     │  │    3phr      │  │  0.005 m.r   │
└──────┬───────┘  └──────┬───────┘  └──────┬───────┘
       └─────────────────┼─────────────────┘
                         │
                 ┌───────────────┐
                 │  Tumble mixed │
                 └───────┬───────┘
                         │
```

torque values monitored

```
        ┌──────────────────────────────────┐      t = 0 min. start process
        │  Processed in internal mixer,    │
        │  closed system. 180 C, and       │
        │     rotor speed 60 rpm           │      t = 3 min., open ram (<20 s)
        └──────────────┬───────────────────┘
                       │
        ┌──────────────────────────────────┐          ┌──────────────────┐
        │  after 3 min. loading ram lifted │          │ Maleic anhydride │
        │ while mixing is continued. Addition│◄────────│      7phr        │
        │      of maleic anhydride         │          └──────────────────┘
        │     then lowering of ram         │
        └──────────────┬───────────────────┘      t = <4 min., close ram
                       │
        ┌──────────────────────────────────┐
        │ continue processing to total time│
        │ 10 min. Remove sample and shredded│
        │         to small pieces          │
        └──────────────┬───────────────────┘      t = 10 min. stop process
                       │
              ┌──────────────────┐
              │ MA functionalised PP │
              └─────────┬────────┘
                        │
         ┌────────────────────────────┐
         │ Analysis of MA grafting level │
         └────────────────────────────┘
```

Scheme 3.3 : Method C - Flow chart for grafting maleic anhydride (MA)
onto polypropylene (PP)

GRAFTING OF MA ONTO PP/EPDM

| Polymer Polypropylene | Co-agent TRIS | Free radical T101 | Agent Maleic anhydride | Polymer EPDM |

Tumble mixed

Processed in internal mixer, closed system, 180 C, and rotor speed 60 rpm then shredded to small pieces

torque values monitored

t = 0 min. start process

t = 10 min. stop process

MA functionalised PP/EPDM → Melt flow index

Analysis of MA grafting level
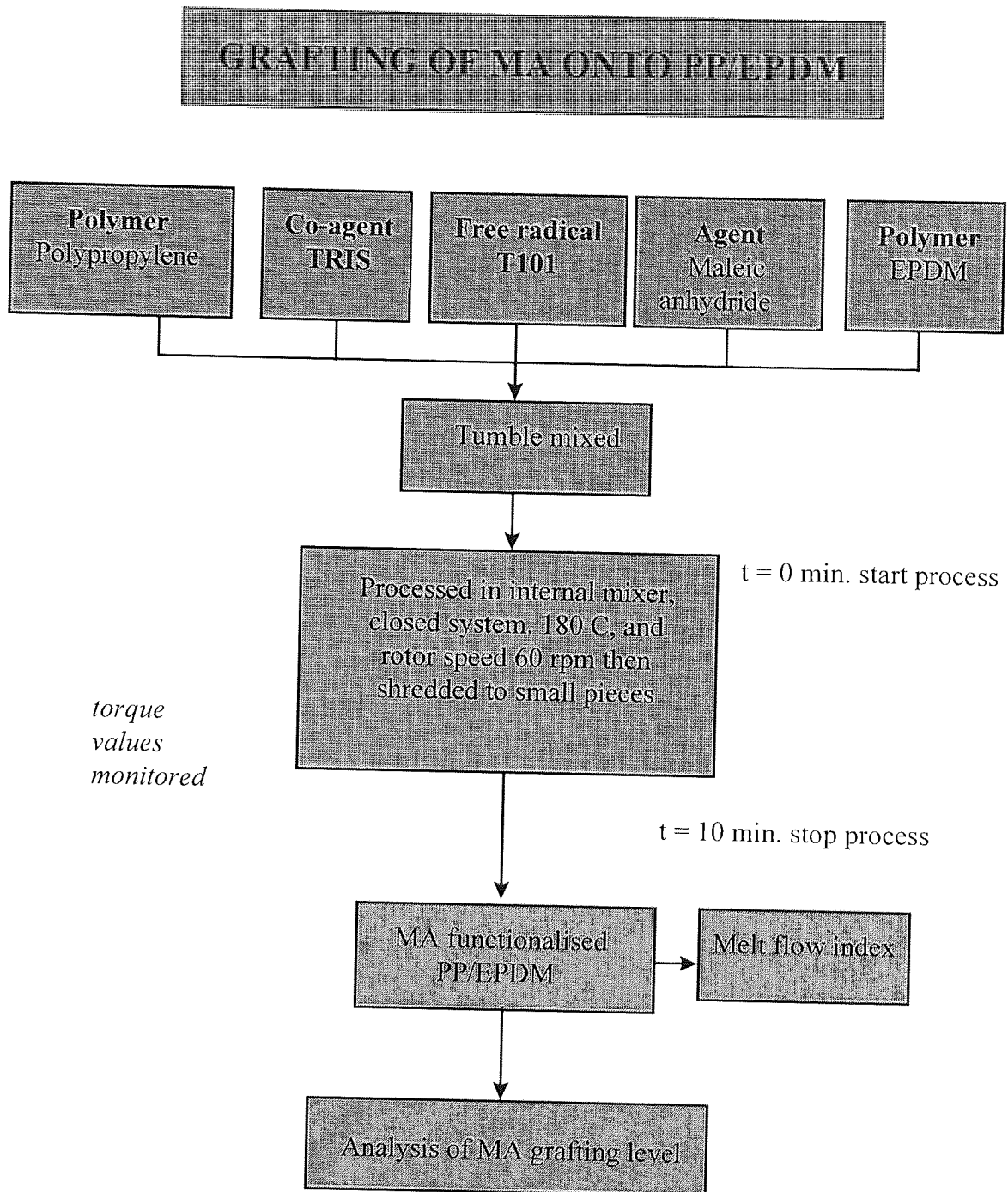
Scheme3.4: Functionalisation of MA onto PP/EPDM in the presence and absence of co-agent TRIS and free radical initiator T101.

ROOR
(free radical
initiator)
$\xrightarrow{\Delta}$ 2RO·

(polypropylene) $\xrightarrow{+ RO·}$ ROH + (PP macroradical)

$$C_2H_5-C\begin{cases}CH_2-O-CO-CH=CH_2\\CH_2-O-CO-CH=CH_2\\CH_2-O-CO-CH=CH_2\end{cases} + 3RO· \longrightarrow C_2H_5-C\begin{cases}CH_2-O-CO-\overset{·}{C}H-CH_2-OR\\CH_2-O-CO-\overset{·}{C}H-CH_2-OR\\CH_2-O-CO-\overset{·}{C}H-CH_2-O\end{cases}$$

(TRIS)

(MA) $\xrightarrow{+ RO·}$

$$C_2H_5-C\begin{cases}CH_2-O-CO-\overset{·}{C}H-CH_2-OR\\CH_2-O-CO-\overset{·}{C}H-CH_2-OR\\CH_2-O-CO-\overset{·}{C}H-CH_2-OR\end{cases} +$$

MA homopolymerisation
is unlikely at very low
free radical
initiator concentration

$$C_2H_5-C\begin{cases}CH_2-O-CO-CH-CH_2\\CH_2-O-CO-CH-CH_2\\CH_2-O-CO-CH-CH_2\end{cases}$$

MA grafting onto PP

$$C_2H_5-C\begin{cases}CH_2-O-CO-CH-CH_2\\CH_2-O-CO-CH-CH_2\\CH_2-O-CO-CH-CH_2\end{cases}$$

PP crosslinking

Scheme 3.7   Suggestion mechanism of reactive processing of grafted MA and TRIS
in PP, in the presence of free radical initiator, processed at 180°C
for 10 minutes in closed mixing condition.

Table 3.1 : Effect of method of addition of reactive agents on grafting efficiency (via titration) of MA onto PP

| Method | Initial Reactants concentration (A) | | | MA content in samples | | | | |
| | | | | non-extracted | | extracted | | |
	MA, phr, (I)	TRIS, phr	FRI (m.r)	(phr) (II)	% from (I)	(phr)	% from (I)[1]	% from (II)[2]
A	7	3	0.005	4.7	67	2.3	33	49
B	7	3	0.005	2.8	40	1.1	16	39
C	7	3	0.005	2.1	30	0.9	13	43

Note : 1. Percentage of grafted MA from initial MA added
2. Percentage of grafted MA from total remaining MA concentration (after processing) in non-extracted maleated sample.

Table 3.2: List of TRIS functionalised PP and results of analysis

| Code | Initial Chemical composition | | Gel content % | Grafting level % | MFI (g/10 min.) small die |
	TRIS phr	FRI, m.r			
PP (processed)	0	0	0	0	0.65
PMA24	0	0.002	0	0	1.7
PMA35	1	0	0	22	0.65
PMA36	2	0	0	46	0.68
PMA37	3	0	0	60	0.52
PMA38	1	0.002	1	49	1.46
PMA39	2	0.002	1	80	1.43
PMA40	3	0.002	2	83	1.57
PMA41	1	0.005	2	81	3.55
PMA42	2	0.005	3	88	3.09
PMA43	3	0.005	2	90	2.34

Table 3.3: List of TRIS functionalised EPDM and results of analysis

Code	Initial Chemical composition		Gel content %	Grafting level %
	TRIS phr	FRI, m.r		
MAT40	1	0.001	15	20.2
MAT41	2	0.001	15	49.4
MAT42	3	0.001	13	56.5
MAT43	4	0.001	17	72.9
MAT44	1	0.002	21	73.0
MAT45	2	0.002	20	76.0
MAT46	3	0.002	24	82.8
MAT47	4	0.002	25	95.7
MAT48	1	0.005	40	97.7
MAT49	2	0.005	50	92.1
MAT50	3	0.005	40	109
MAT51	4	0.005	35	108

Table 3.4: MA grafting level of functionalised PP with MA only (no coagent) purified using different methods, melt flow index and gel content

Code	Chemical composition MA added, phr	FRI m.r.	MA Grafting level FTIR method heat@120°C A phr	%+	Extraction B phr	%+	Precipitation C phr	%+	Titration Extraction D phr	%+	MFI g/10min (small die)	Gel content phr
PP	nil	nil	0	0	0	0	0	0	0	0	0.65	0
PMA24	nil	0.002	0	0	0	0	0	0	0	0	1.7	0
PMA1	6	nil	0.1	1	0.1	1	0.1	2	0.1	2	0.7	0
PMA64	2	0.002	0.2	10	0.2	10	0.2	8	0.2	10	3.5	2
PMA65	4	0.002	0.3	6	0.3	7	0.3	7	0.3	7	3.2	3
PMA2	6	0.002	0.4	6	0.4	6	0.3	5	0.3	5	2.1	5
PMA66	10	0.002	0.2	2	0.3	3	0.2	2	0.3	3	2.0	4
PMA62	2	0.005	0.3	13	0.3	16	0.2	10	0.4	18	7.8	2
PMA63	4	0.005	0.5	13	0.5	11	0.4	10	0.5	13	7.2	4
PMA3	6	0.005	0.7	12	0.7	11	0.5	8	0.6	10	4.0	6
PMA61	10	0.005	0.5	5	0.5	5	0.5	5	0.5	5	2.6	5

NOTES: Maleated PP samples were purified from non-grafted MA by 4 different methods. (A) was heated at 120°C (B) and (D) were Soxhlet extracted in DCM for 48 hours and (C) was acetone precipitated from hot xylene. MA grafting level in purified samples was determined by Infrared spectroscopy for (A), (B) and (C), and by titration for (D)

+ % is the % of originally introduced MA amount.

113

Table 3.5: List of maleated PP samples, chemical compositions, melt flow index and gel content

Code	Chemical composition			Results		
	MA added, phr	TRI S phr	FRI m.r.	MA[1] grafted phr	MFI[2] g/10 min	Gel content phr
PP(processed)	0	0	0	0	0.65	0
PP(not processed)	0	0	0	0	0.55	0
Fusabond[3]	-	-	-	1	1.00	1
PMA6	9	1	0	0.9	0.33	2
PMA7	8	2	0	1.1	0.34	3
PMA8	7	3	0	1.3	0.29	2
PMA51	6	4	0	1.4	0.20	3
PMA32	9	1	0.001	1.8	1.24	5
PMA33	8	2	0.001	2.0	0.79	5
PMA34	7	3	0.001	2.2	0.77	7
PMA9	**9**	**1**	**0.002**	**1.9**	**1.49**	**9**
PMA10	8	2	0.002	2.1	1.40	7
PMA11	7	3	0.002	2.3	1.34	5
PMA52	6	4	0.002	2.6	1.30	9
PMA12	9	1	0.005	2.2	2.34	6
PMA13	8	2	0.005	2.3	2.29	8
PMA14	7	3	0.005	2.6	2.45	5
PMA53	6	4	0.005	2.8	2.64	9
PMA47	2	0.5	0.002	0.8	1.36	3
PMA48	4	1	0.002	1.4	1.12	4
PMA49	6	1.5	0.002	1.9	0.90	3
PMA50	10	2.5	0.002	2.7	0.85	5

NOTE:1. Purification via Soxhlet extraction in DCM and grafting calculation via titration method
2. Melt flow index (MFI) was measured using small diameter die (refer Section 2.7)
3. Fusabond is a commercial maleated PPMD278D supplied by DuPont.

Table 3.6: List of maleated EPDM samples, chemical composition, MA grafting level and gel content. Purification by Soxhlet extraction in DCM and grafting measured by titrations.

| Code | Chemical composition | | | Grafted | Gel |
	MA (phr)	TRIS (phr)	FRI (m.r)	MA phr	content %
MA1	5	0	0	0.5	5
MA2	5	0	0.001	0.8	9
MA10	5	0	0.002	0.9	12
MAT11	**9**	**1**	**0.005**	**2.8**	**29**
MAT12	8	2	0.005	3.4	26
MAT13	7	3	0.005	2.9	38
MAT14	6	4	0.005	3.1	36
MAT16	9	1	0.002	2.6	29
MAT17	8	2	0.002	2.2	45
MAT18	7	3	0.002	2.7	48
MAT19	6	4	0.002	3.4	46
MAT20	9	1	0.001	1.6	35
MAT21	8	2	0.001	1.6	42
MAT22	7	3	0.001	2.7	40
MAT23	6	4	0.001	2.3	41

Table 3.7. Chemical composition and MA content of maleated PP/EPDM 75/25 blends
Purification by Soxhlet extraction in DCM and grafting measured by titration.

| Code | Chemical composition | | | MA content (phr) | | Grafted MA |
	MA (phr)	TRIS (phr)	FRI (m.r)	in unextracted sample	grafted MA	%, based on added [MA]
MB70	9	1	0.001	4.1	0.7	8
MB71	8	2	0.001	2.8	1.1	14
MB72	7	3	0.001	3.9	1.4	20
MB73	**6**	**4**	**0.001**	**3.3**	**1.5**	**25**
MB61	7	0	0.002	2.4	0.3	4
MB64	9	1	0.002	4.5	0.7	8
MB63	8	2	0.002	4.2	1.2	15
MB62	7	3	0.002	3.8	1.4	20
MB65a	6	0	0.002	1.3	0.2	3
MB65b	6	0.5	0.002	1.4	0.3	5
MB65c	6	1	0.002	1.4	0.4	7
MB65d	6	2	0.002	1.0	0.8	13
MB65	**6**	**4**	**0.002**	**3.1**	**1.7**	**28**
MB74	9	1	0.005	2.7	1.3	14
MB75	8	2	0.005	4.4	1.5	19
MB76	7	3	0.005	4.1	1.8	26
MB77	**6**	**4**	**0.005**	**3.3**	**2.0**	**33**
MB90	7	3	0.01	3.6	1.6	23
MB91	6	4	0.01	3.6	2.2	37

Table 3.8. Chemical composition and MA content of maleated PP/EPDM 60/40 blends
Purification by Soxhlet extraction in DCM and grafting measured by titrations.

| Code | Chemical composition | | | MA content | | Grafted MA |
	MA (phr)	TRIS (phr)	FRI (m.r)	in unextracted sample (phr)	grafted MA	%, based on added [MA]
MB92	6	4	0.001	3.9	1.2	20
MB93	6	4	0.002	3.2	1.6	27
MB94	6	4	0.005	4.0	2.5	42
MB95	6	4	0.01	3.8	2.7	45
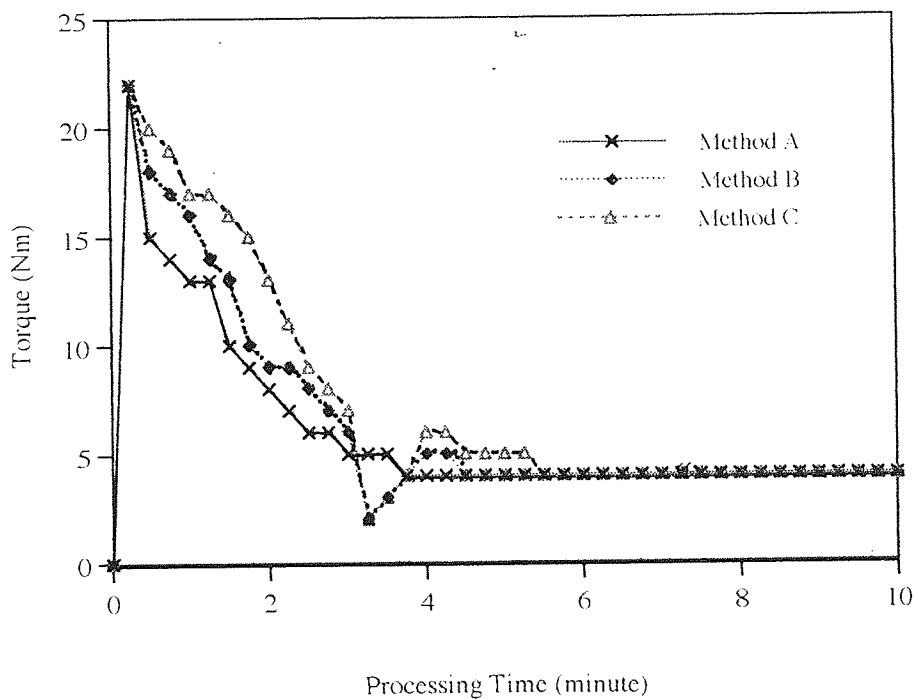
Figure 3.1: Torque behaviour of PP reactively processed with MA (7 phr),
TRIS (3 phr) and free radical initiator T101 (0.002 m.r) using
different method of addition of reactive agents

Figure 3.2a: Infrared spectrum of PP film processed in the presence of co-agent TRIS (2phr) only, before (BX) and after (X) 48 hr Soxhlet extraction in DCM.
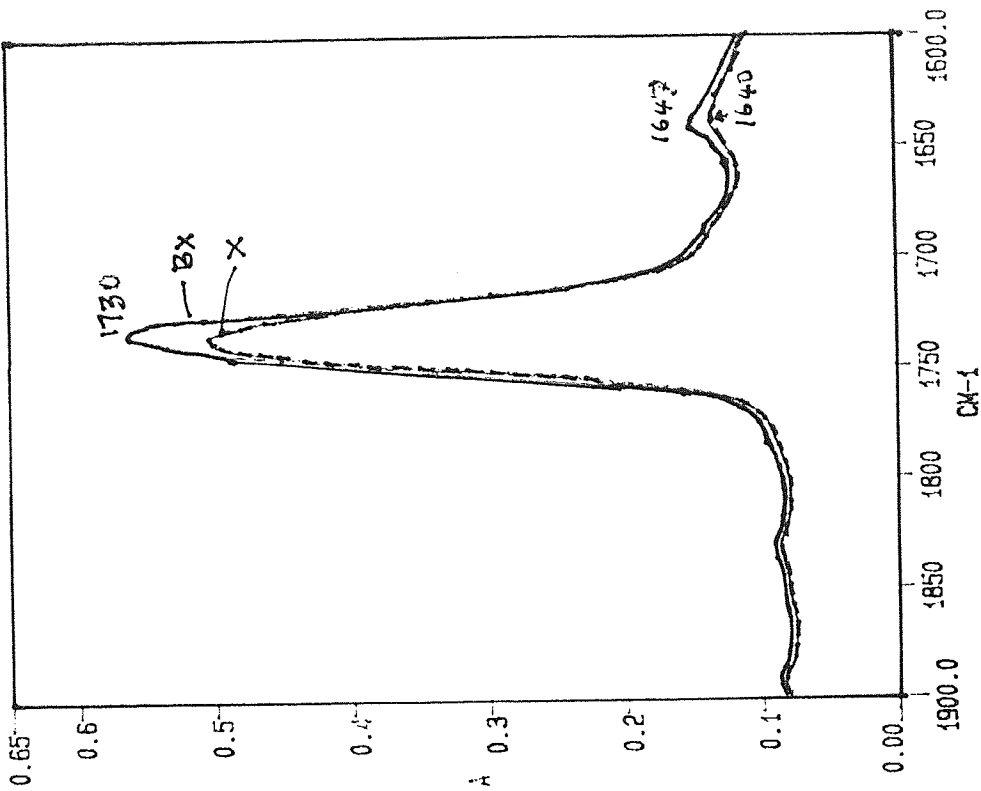
Figure 3.2b: Infrared spectrum of PP film processed in the presence of TRIS (2 phr) and FRI (0.002 m.r) before and after (X) 48 hr Soxhlet extraction in DCM.

118
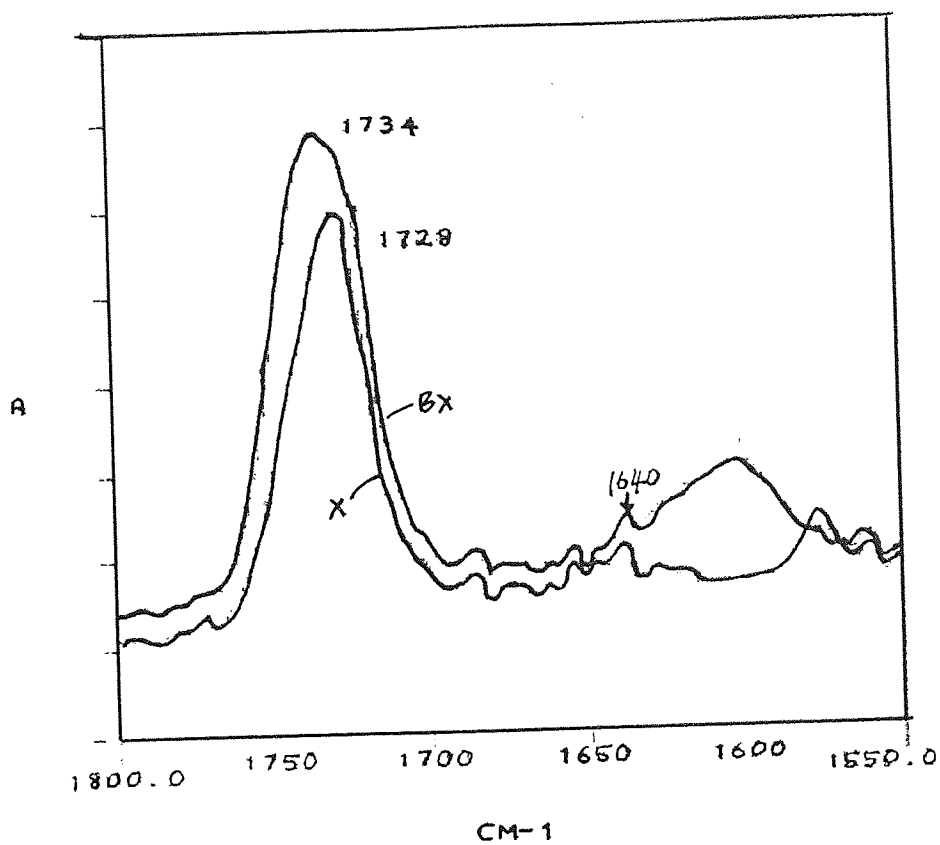
Figure 3.3: The carbonyl region in infrared spectrum of EPDM film processed in the presence of TRIS (2 phr) and free radical initiator T101 (0.002 m.r), before (BX) and after (X) 48 h Soxhlet extraction in DCM

119
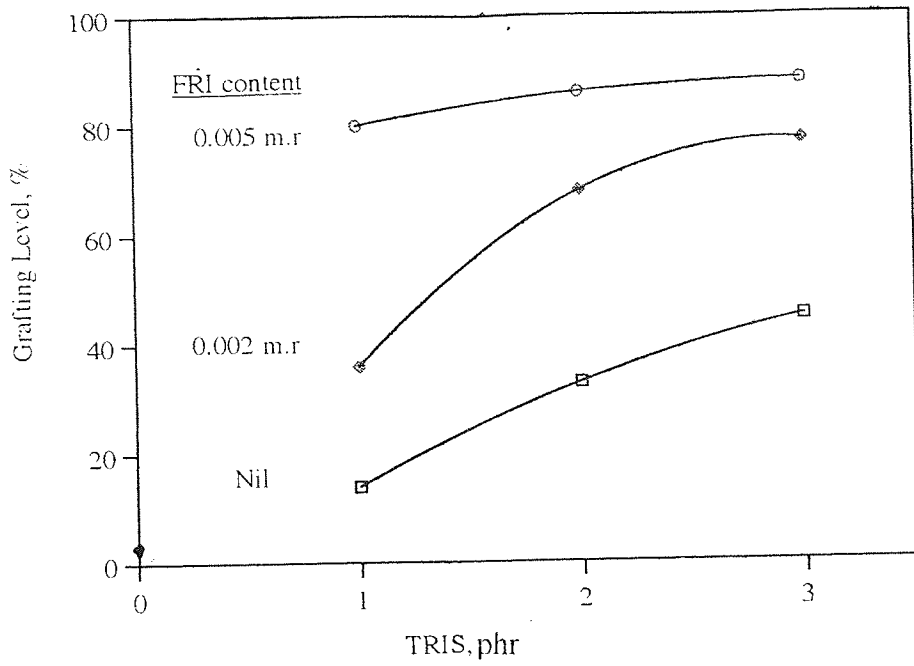
Figure 3.4:   Effect of TRIS and FRI concentration on TRIS grafting level
onto PP
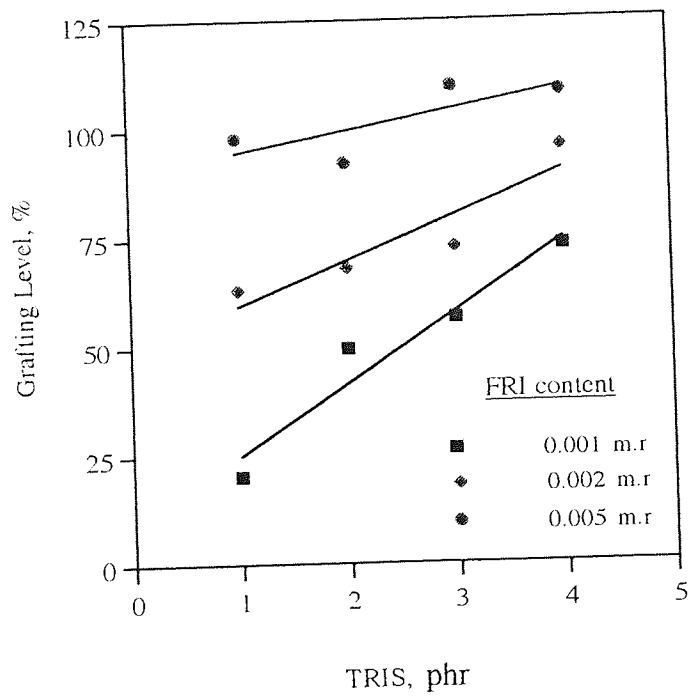
Figure 3.5:   Effect of TRIS and FRI concentration on TRIS grafting level
onto EPDM

120
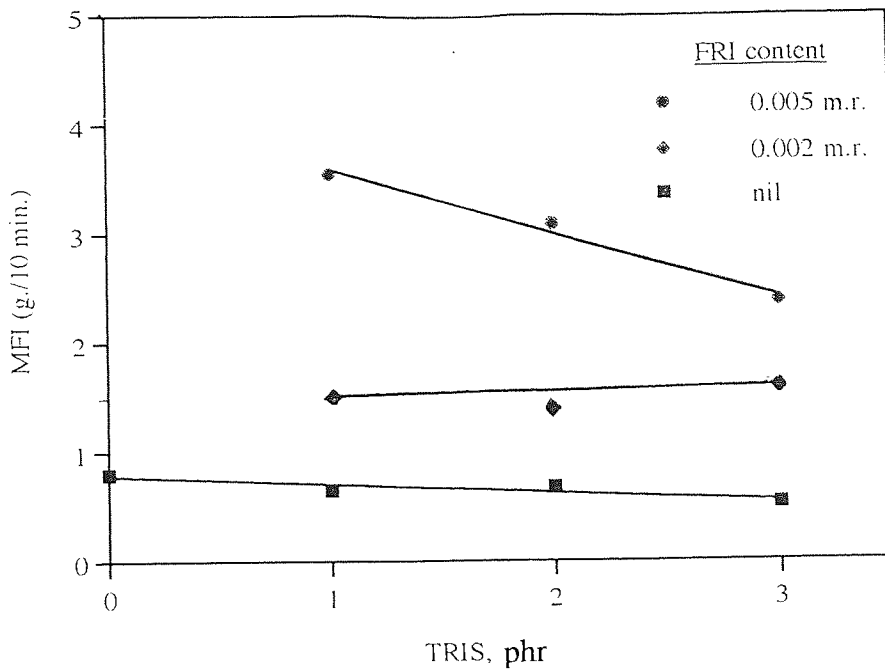
Figure 3.6: Effect of TRIS concentration on MFI values of PP processed in
the presence of various concentration of FRI.
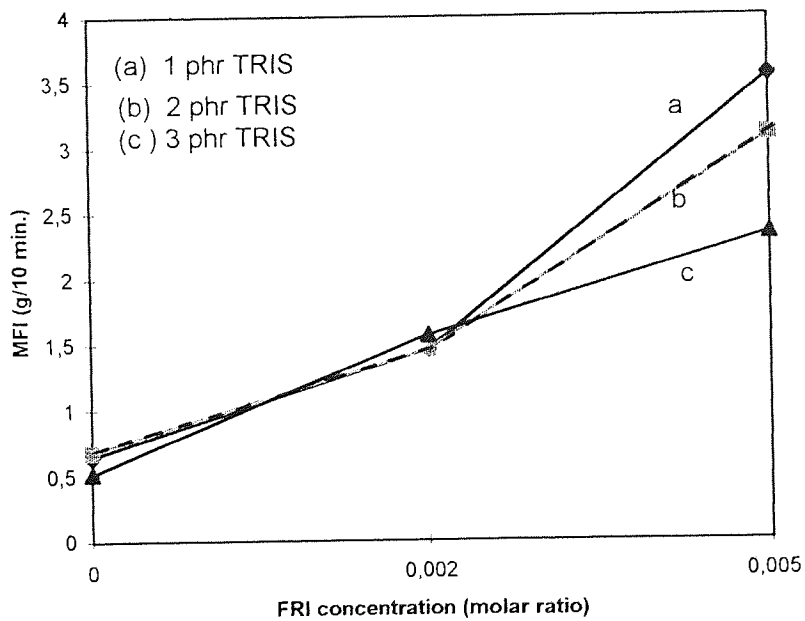
Figure 3.7: Effect of FRI concentration on MFI values of PP functionalised
with various concentration of TRIS.

121
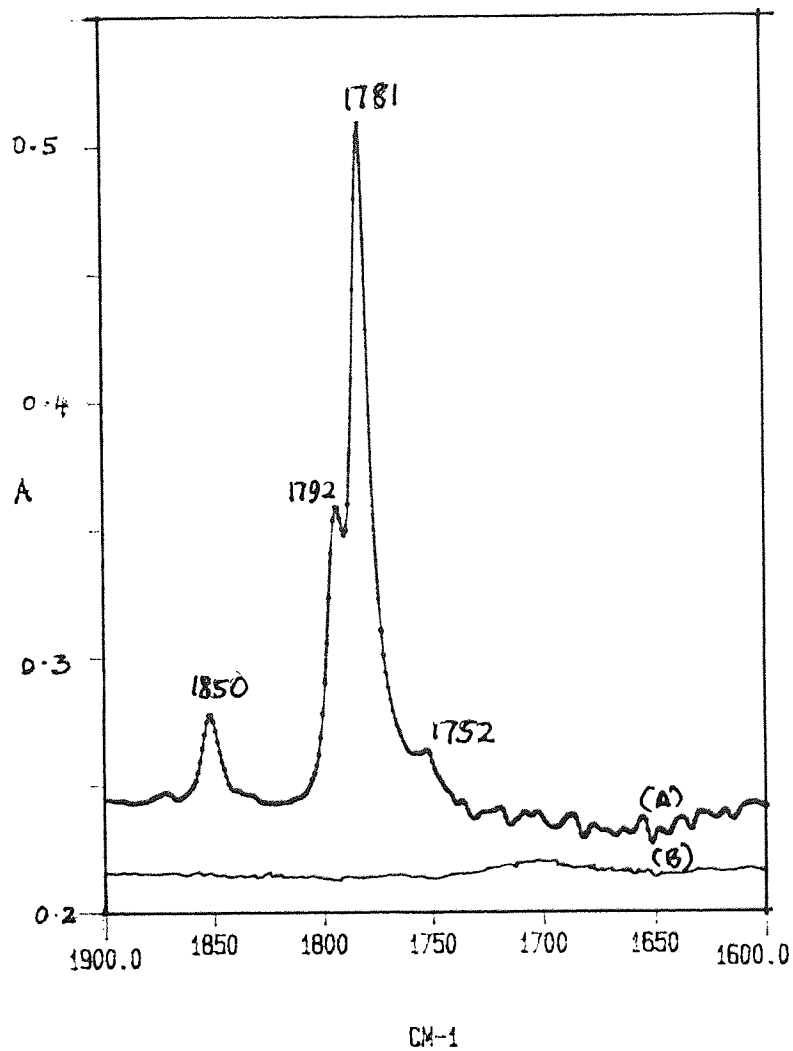
Figure 3.8 : The carbonyl region in infrared spectrum of maleic anhydride (MA) dissolved in DCM (A) and that of DCM (B)

Figure 3.10: The carbonyl region in infrared spectrum of succinic acid in glyme (reproduced from Fig. 2.9)

Figure 3.9: The carbonyl region in infrared spectrum of succinic anhydride in glyme (reproduced from Fig. 2.8)

123
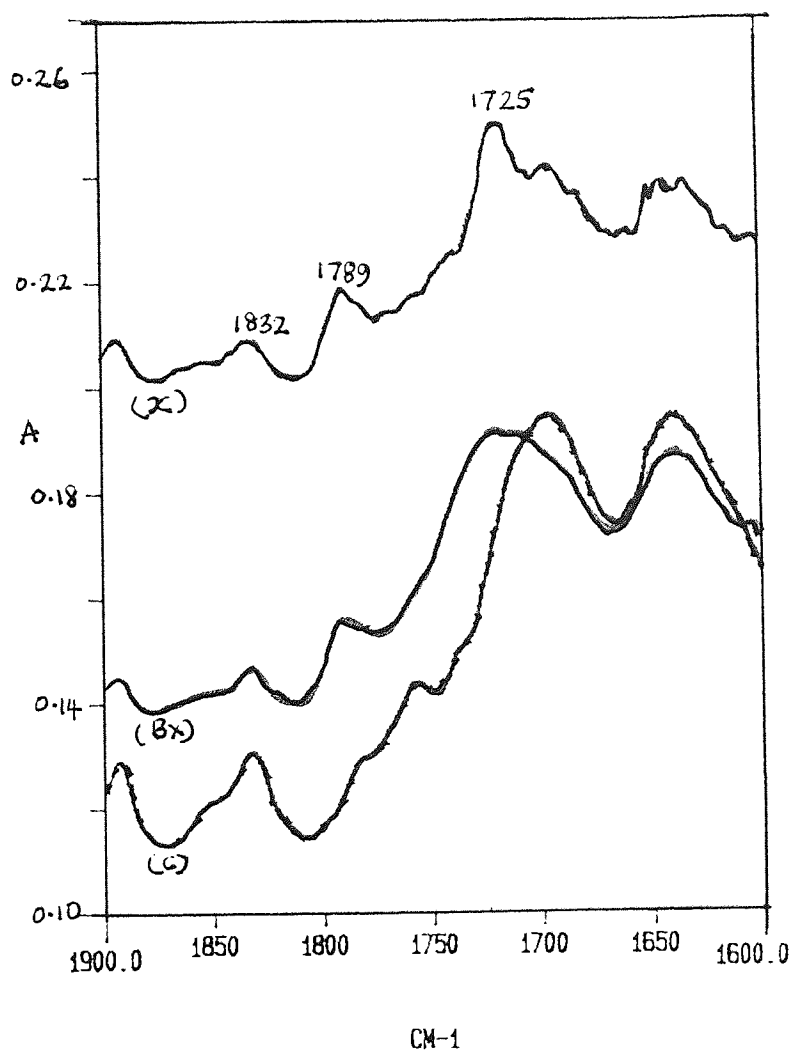
Figure 3.11: The carbonyl region in infrared spectra of PP film processed with MA (6 phr) only, before (BX) and after (X) 48 hr Soxhlet extraction in DCM. Infrared spectrum of pure PP (C) is inserted as a reference.

Figure 3.13: The carbonyl region in Infrared spectrum of a commercial maleated PP film (Fusabond MD278D) before and after (X) 48 hr Soxhlet extraction in DCM.

Figure 3.12: The carbonyl region in infrared spectrum of maleated PP film (initial MA concentration is 7%) processed in the presence of FRI (0.002 m.r), before (BX) and after (X) 48 hr Soxhlet extraction in DCM.

Figure 3.15: The carbonyl region in infrared spectrum of EPDM film processed with MA (8%) in the presence of FRI (0.002 m.r) and TRIS (2 %) before and after (X) 48 hr Soxhlet extraction in DCM.

Figure 3.14: The carbonyl region in infrared spectrum of PP film processed with MA (8%) in the presence of FRI (0.002 m.r.) and co-agent TRIS (2%) only, before (BX) and after (X) 48 hr Soxhlet extraction in DCM.
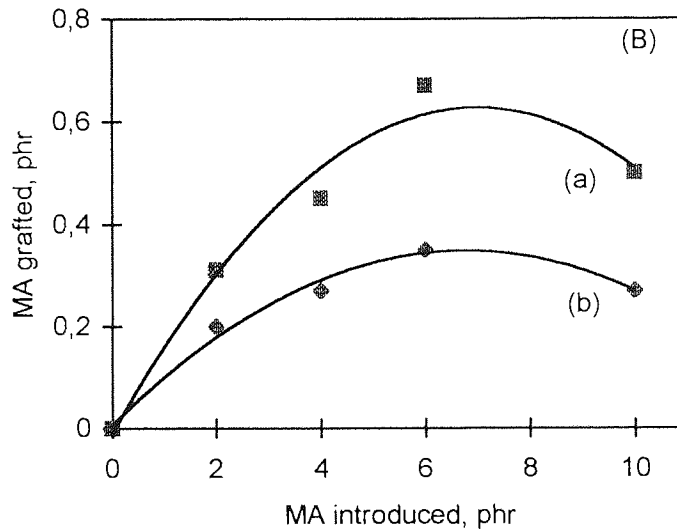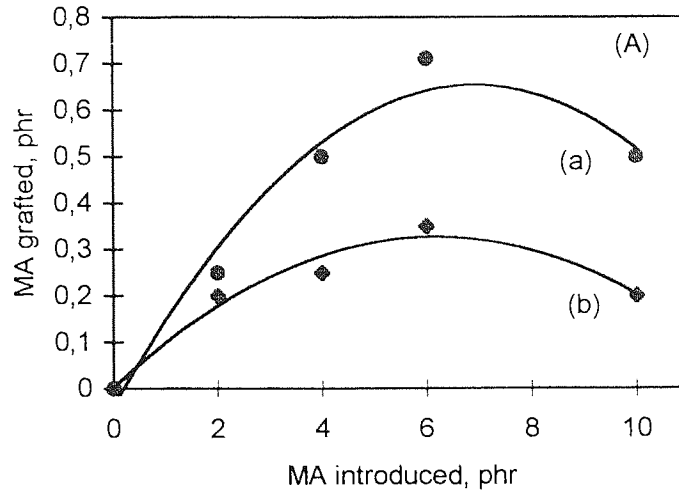
Figure 3.16: Maleic anhydride grafting yield in maleated PP prepared in the presence of FRI (a) 0.005 m.r and (b) 0.002 m.r. , without co-agent TRIS, as a function of the initial MA introduced. Samples were purified by (A) heating in vacuum oven at 120 ^{0}C for 72 hr., (B) 48 hr Soxhlet extraction in DCM, (C) precipitation from xylene/acetone solvent system, before analysing MA grafting yield using FTIR calibration curve. For (D) the samples were Soxhlet extracted before titrated to determine MA grafting yield.
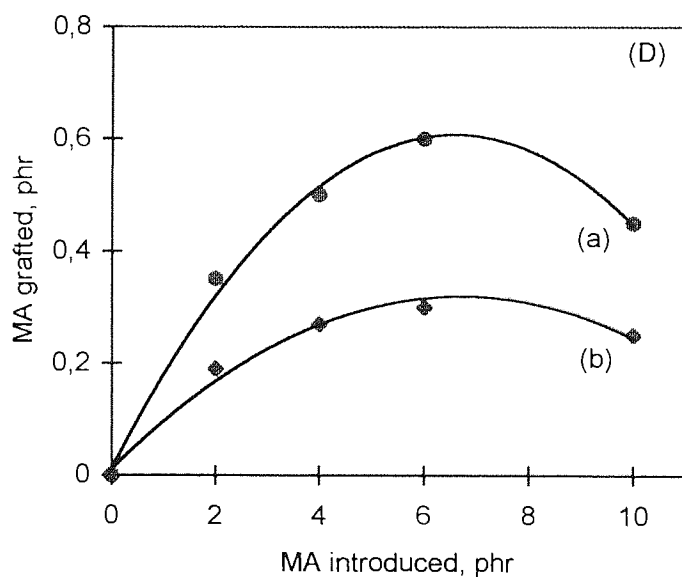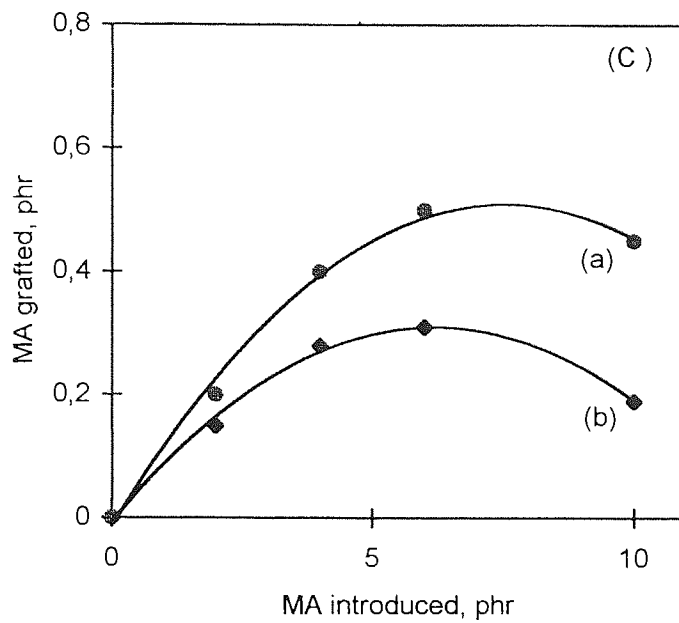
Figure 3.16:   continue
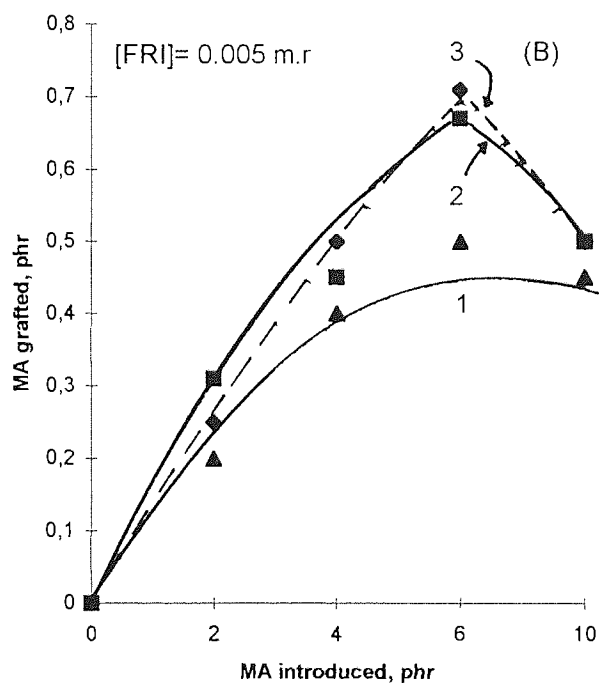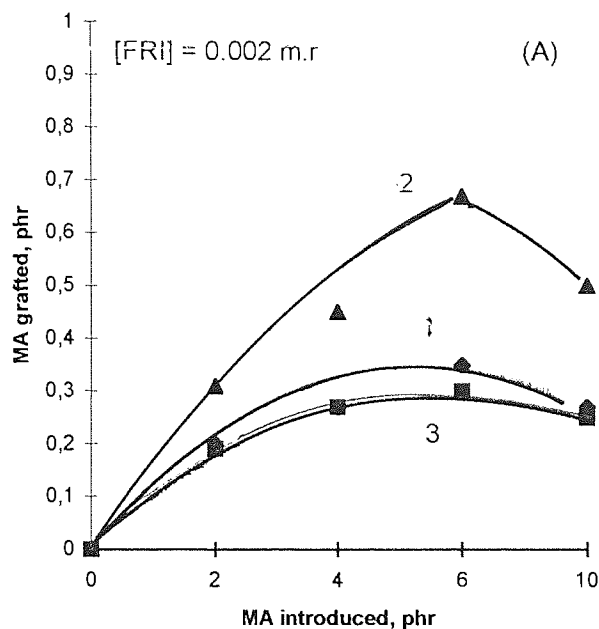
Figure 3.17: Maleic anhydride grafting yield onto PP as a function of the initial MA concentration introduced. Efficiency comparison between different methods used for purification of maleated PP prepared in the presence of FRI (1) 0.005 m.r (2) 0.002 m.r. , without co-agent TRIS. Samples were purified by (A) heating in vacuum oven at 120 °C for 72 hr., (B) 48 hr Soxhlet extraction in DCM, (C) precipitation from xylene/acetone solvent system, before analysing MA grafting yield using FTIR calibration curve.
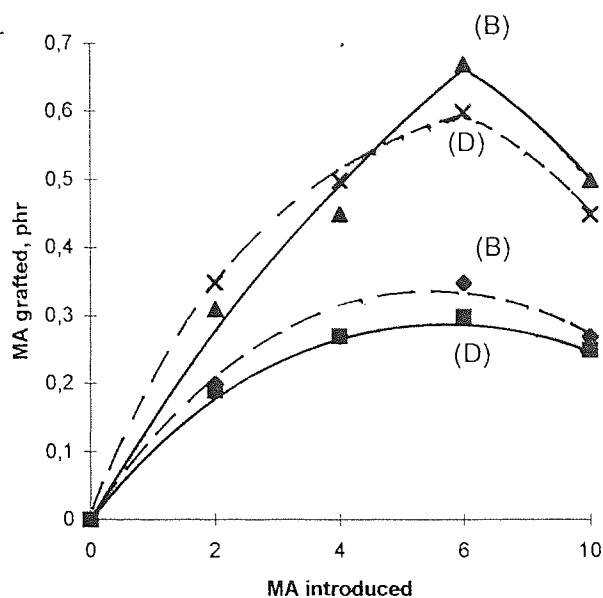
Figure 3.18: Maleic anhydride grafting yield onto PP as a function of the initial MA concentration introduced. Efficiency comparison between FTIR (B) calibration curve and titration (D) in determining the MA grafting yields.
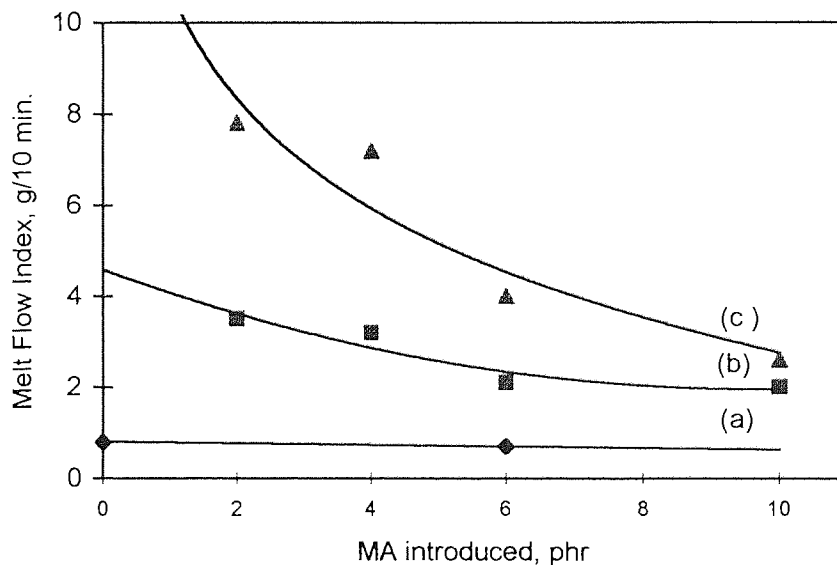
Figure 3.19: Melt Flow Index (MFI) of maleated PP processed in the presence of various concentration of MA and FRI but without co-agent TRIS, as a function of initial MA concentration introduced; (a) nil (b) 0.002 m.r. (c) 0.005 m.r.

130
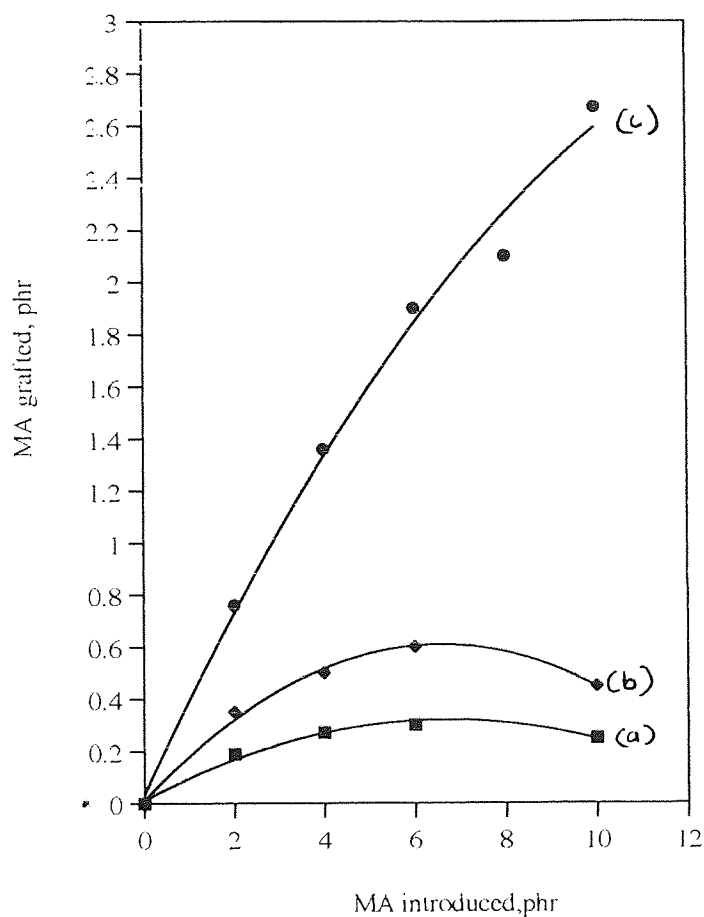
Figure 3.20: Maleic anhydride grafting yield onto PP as a function of the
initial MA concentration introduced . (a) and (b) were processed
in the presence of 0.002 m.r and 0.005 m.r FRI, respectively but
no co-agent added, while (c) processed in the presence of 0.002
m.r FRI and co-agent TRIS, where MA to TRIS ratio was kept
constant at 8 to 2. Purification of all samples via Soxhlet
extraction in DCM. MA   grafting yields were determined by
titration.

131
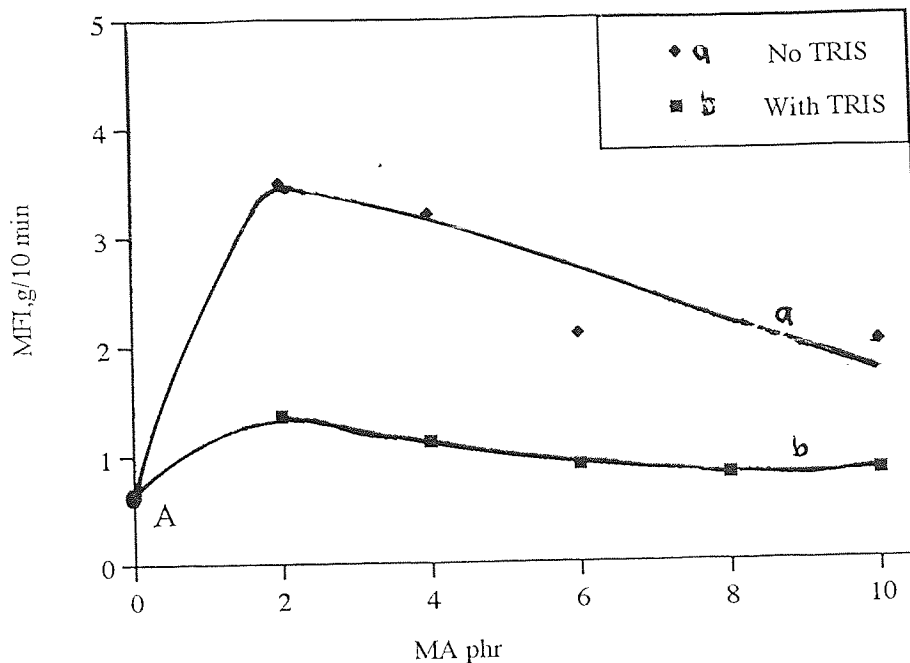
Figure 3.21: Melt Flow Index (MFI) of maleated PP as a function of the initial MA introduced. For maleated PP processed with TRIS, the MA to TRIS ratio is always 8 to 2. The FRI concentration was 0.002 m.r. (A) is MFI value of processed PP control containing no additives.
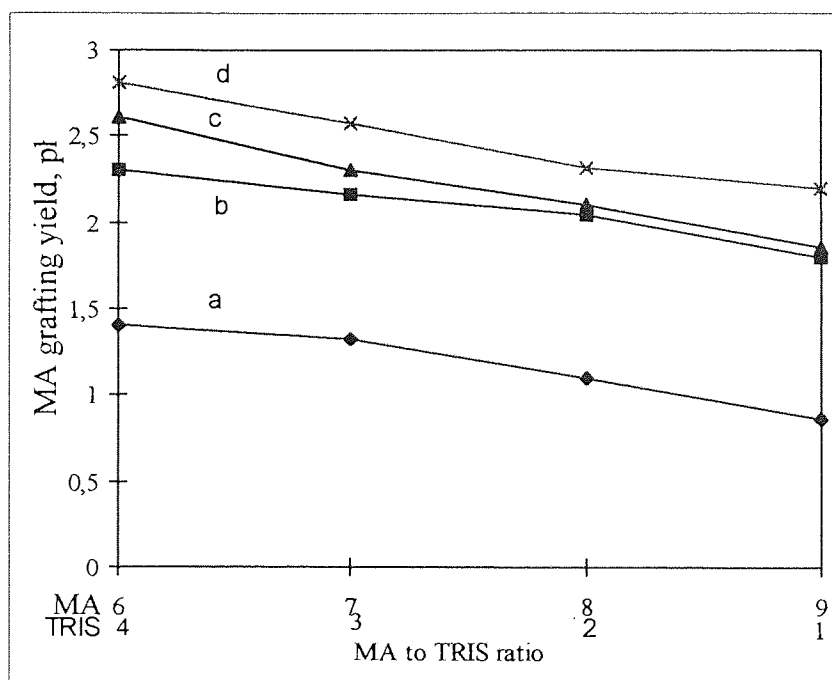
Figure 3.22 : Maleic anhydride grafting yield onto PP as a function of MA to TRIS ratio at various FRI concentration (a) 0 m.r, (b) 0.001 m.r (c)0.002 m.r (d) 0.005 m.r.
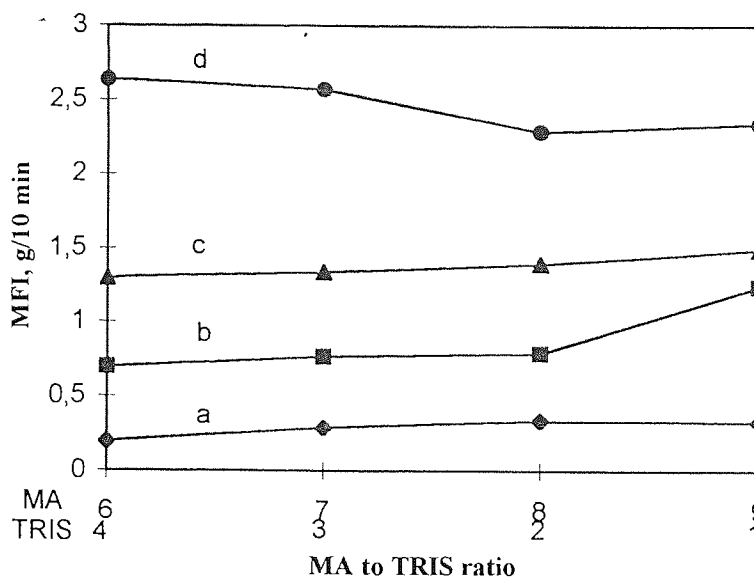
Figure 3.23: Melt Flow Index (MFI) of maleated PP as a function of MA to TRIS ratio at various FRI concentration (a) 0 m.r, (b) 0.001 m.r (c)0.002 m.r (d) 0.005 m.r.
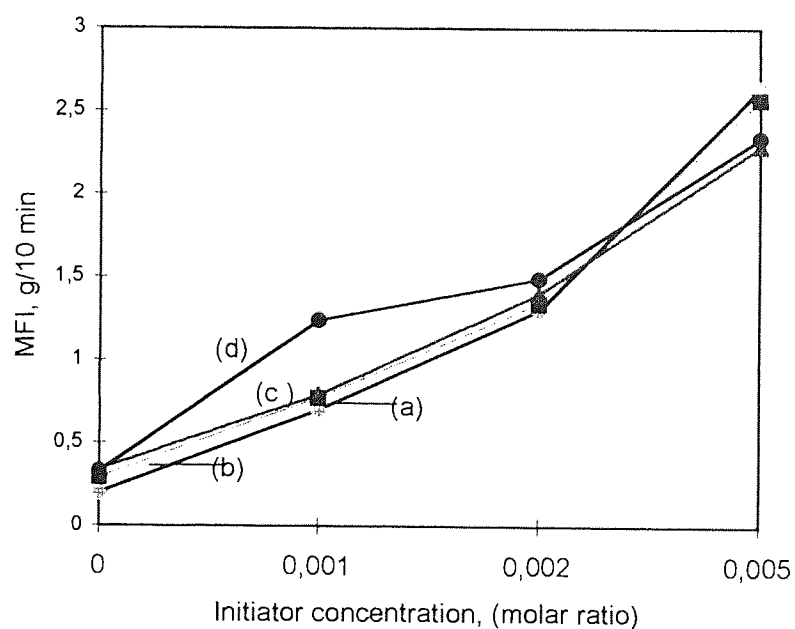
Figure 3.24: Effect of FRI concentration on MFI values of maleated PP processed with various ratio of MA to TRIS. MA to TRIS ratio is (a) 6:4 (b) 7:3   (c) 8:2 and (d) 9:1

133
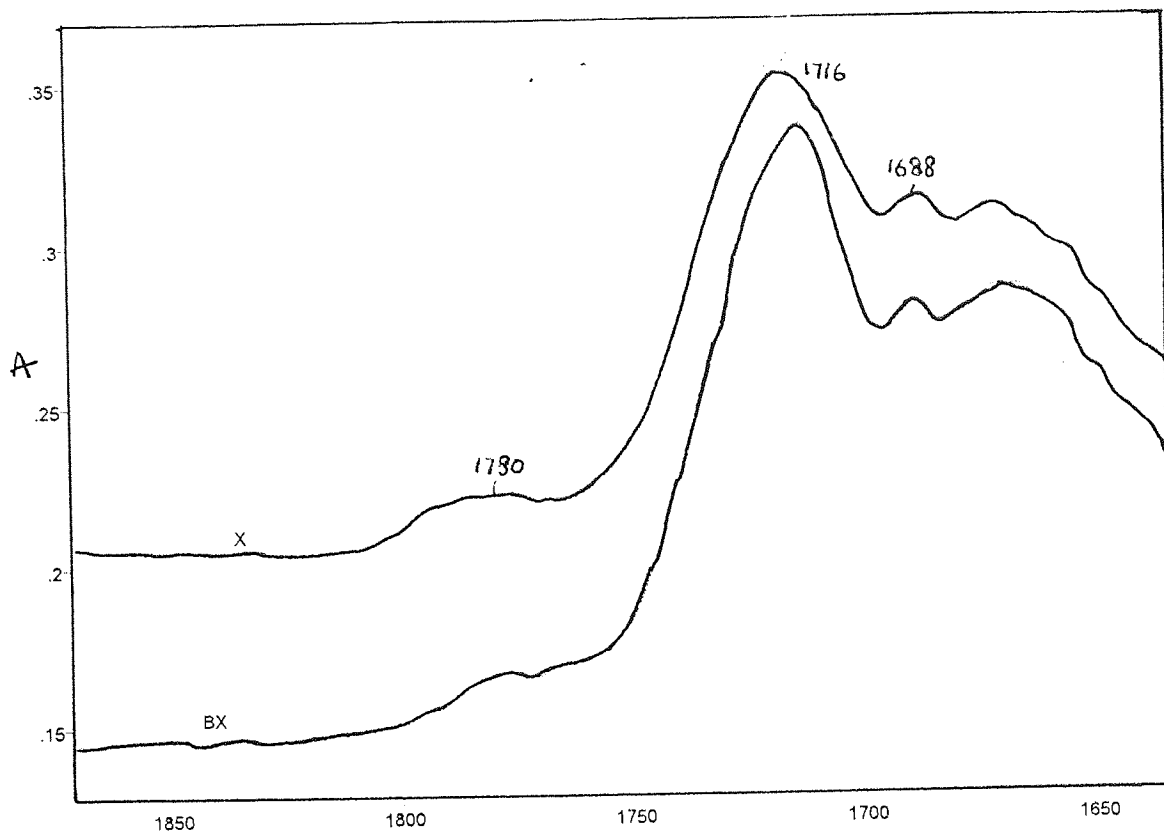
Figure 3.25: The carbonyl region in infrared spectrum of EPDM processed in the presence of MA and without free radical initiator and co-agent.
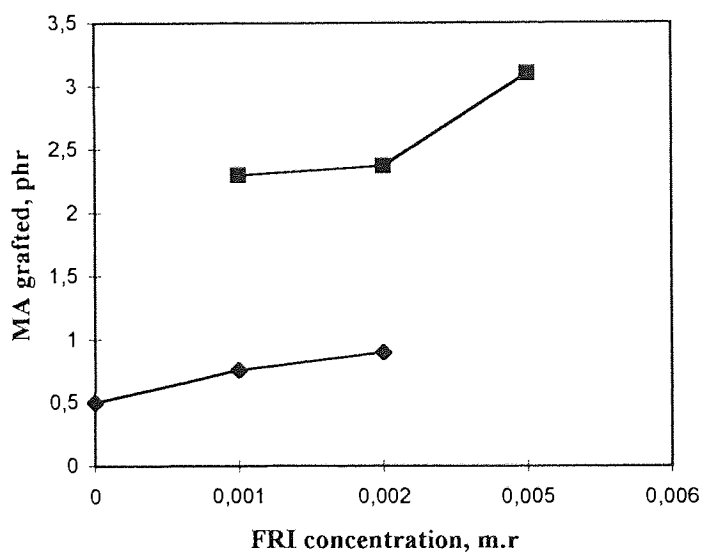
Figure 3.26 : Effect of coagent TRIS and FRI concentration on the MA grafting yield in EPDM. (a) no TRIS (b) with TRIS. MA to TRIS ratio is 6 to 4
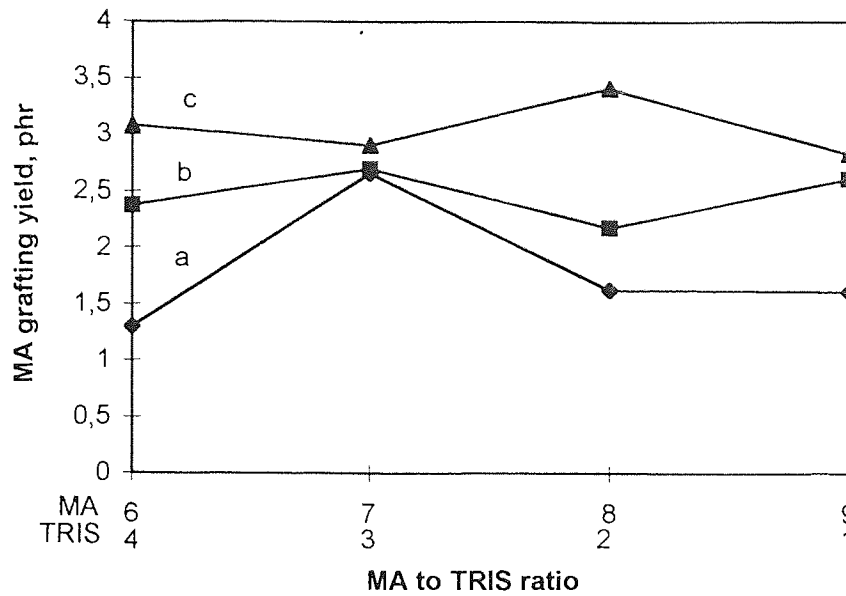
Figure 3.27: Maleic anhydride grafting yield in EPDM as a function of MA to TRIS ratio at various FRI concentration (a) 0.001 m.r. (b) 0.002 m.r and (c) 0.005 m.r.
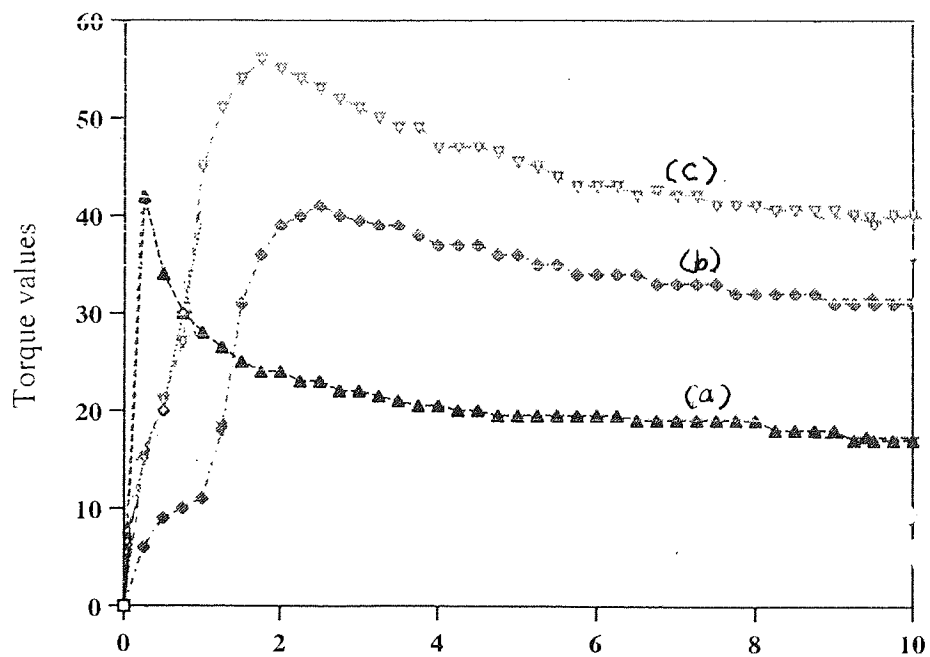
Figure 3.28: Torque behaviour of EPDM reactively processed with (b) MA (5 phr) in the presence of 0.002 m.r FRI (no TRIS), and (c) MA (6 phr) in the presence of 0.002 m.r. FRI and 4 phr TRIS, compared with that of pure EPDM (a).
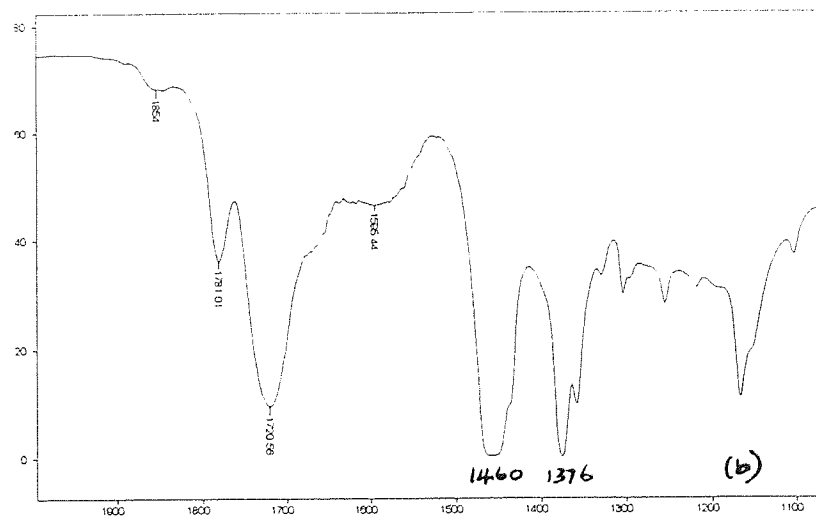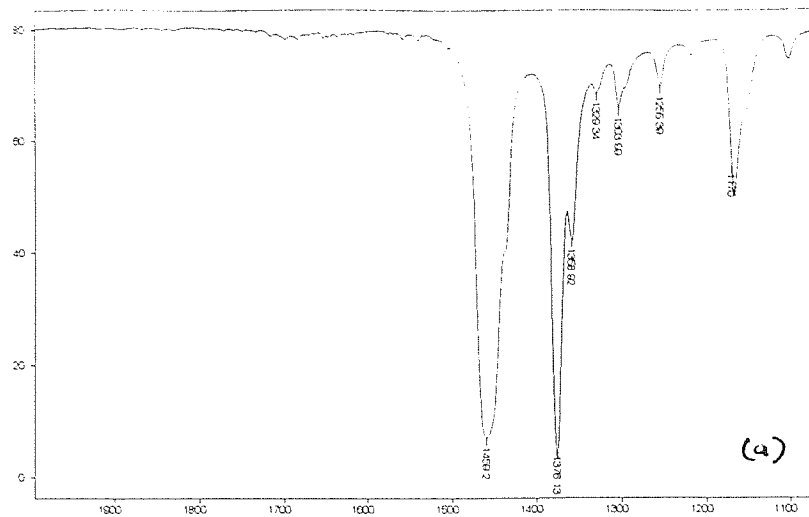
Figure 3.29: Infrared spectra of PP/EPDM at 75/25 ratio. (a) pure PP/EPDM , and (b) processed with 6 phr MA, 4 phr TRIS and 0.002 m.r FRI (after 48 hr Soxhlet extraction in DCM).

136
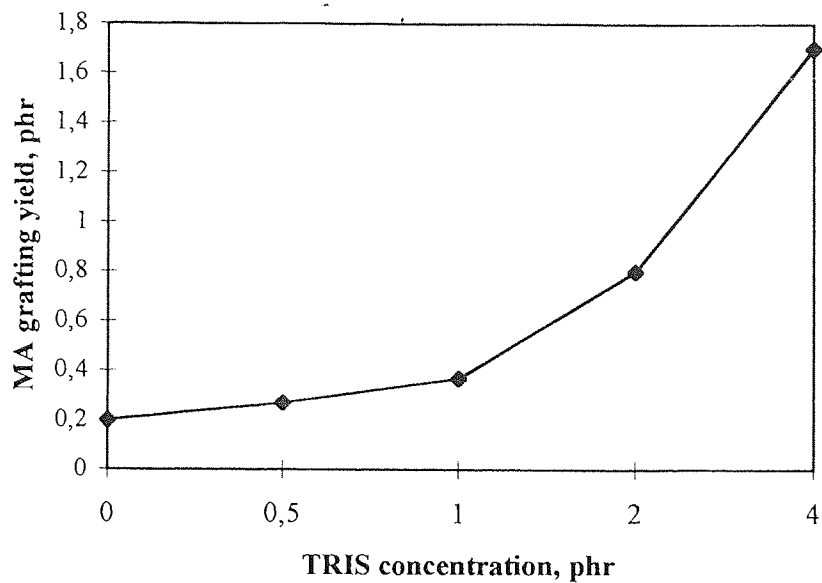
Figure 3.30 : Effect of co-agent concentration TRIS onto MA grafting yield in PP/EPDM blends. The maleated PP/EPDM samples were processed with 6 phr MA in the presence of 0.002 m.r FRI.
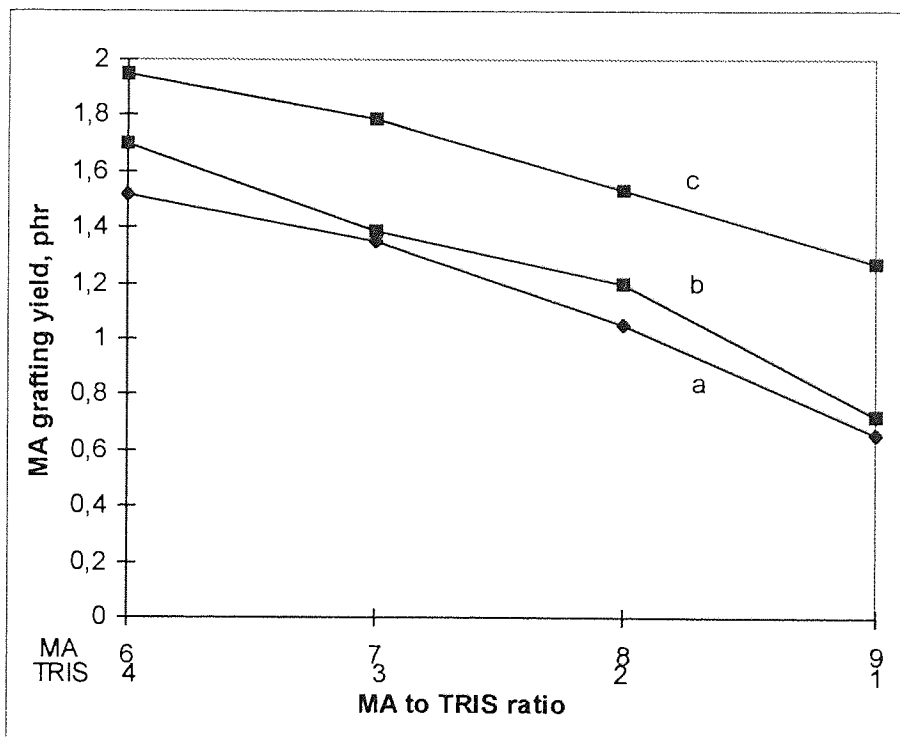
Figure 3.31 : MA grafting yield on PP/EPDM blend as a function of MA to TRIS ratio in the presence of various concentration of FRI (a) 0.001 m.r (b) 0.002 m.r and (c) 0.005 m.r.

137
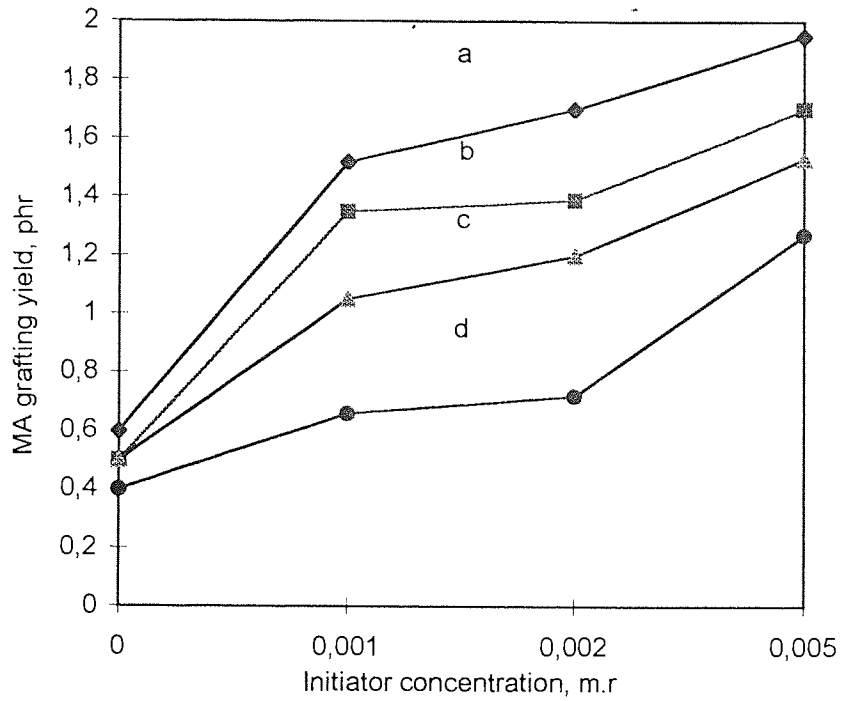
Figure 3.32 Effect of free radical initiator concentration on MA grafting yield in PP/EPDM blend. MA to TRIS ratio is (a) 6:4 (b) 7:3 (c) 8:2 and (d) 9:1.
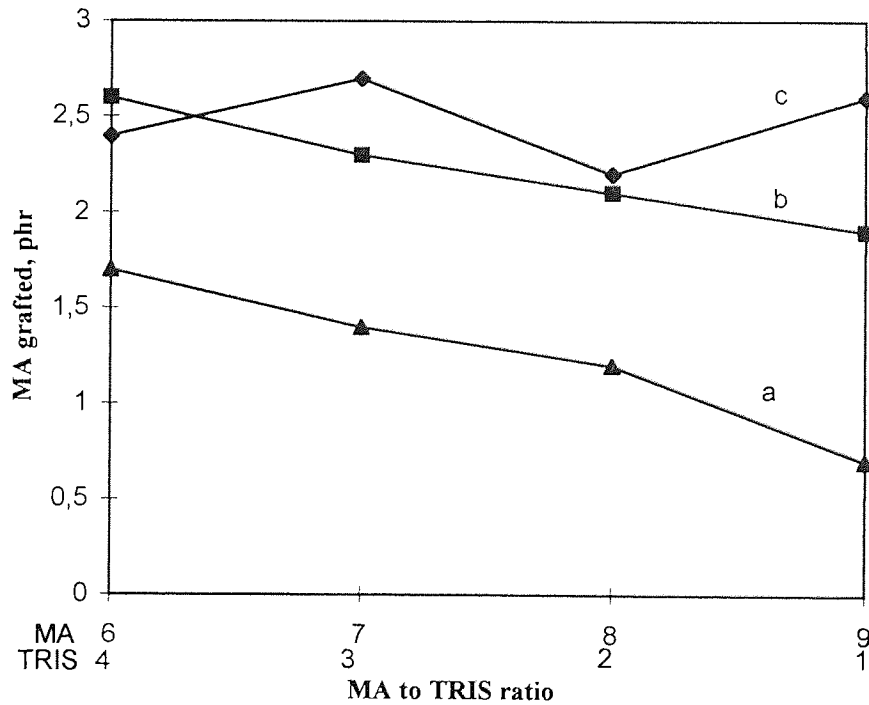
Figure 3.33: Comparison of MA grafting yield in (a) PP/EPDM (b) PP(c) EPDM, processed in the presence of 0.002 m.r FRI and various MA to TRIS ratios.
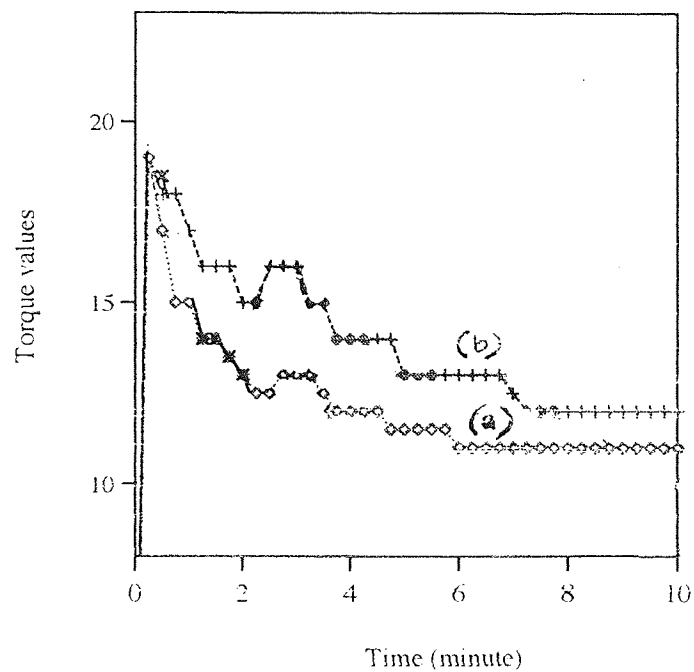
Figure 3.34. Torque behaviour of PP/EPDM blend (75/25) processed with various ratio of MA to TRIS, in the prersence of 0.001 m.r FRI. (a) 8 phr MA and 2 phr TRIS, (b) 6 phr MA and 4 phr TRIS.

CHAPTER 4

IN-SITU SYNTHESIS, USING REACTIVE PROCESSING METHODS, OF FUNCTIONALISED PP/EPDM COPOLYMERS FOR USE AS SOLID PHASE DISPERSANTS

4.1 OBJECTIVES

It was demonstrated, in Chapter 3, that maleic anhydride (MA) was successfully grafted onto PP and EPDM melt via reactive processing. The level of grafted MA was significantly enhanced when the chemical modification of the polymers was carried out in the presence of the co-agent TRIS and the organic peroxide Trigonox 101 (T101). Similar results were also obtained during the functionalisation of PP-EPDM mixtures with MA. The functionalised polymers (either as a homopolymer or a mixture of two polymers) contain a pendant electrophilic anhydride (and/or carboxylic) moiety which acts as a reactive site capable of forming covalent bonds with a co-reactive nucleophilic functionality. It is known that diblock copolymers (A-B type) containing two different homopolymers (A and B) linked by a covalent bond is one of the most effective compatibiliser [15,20,133] in two phase blends of homopolymers A and B. Blending two incompatible homopolymers with the corresponding diblock copolymer provides means for achieving a fine dispersant and enhanced interfacial adhesion, and consequently improvement in mechanical properties. The success in grafting MA onto PP and EPDM homopolymers as well as in PP/EPDM mixtures provides opportunities to synthesise functionalised PP/EPDM copolymers suitable for the compatibilisation of PP/EPDM polymer blends.

140

The object of this part of the work was to synthesise MA-functionalised copolymers of PP/EPDM from maleated PP (PP_{gMA}) and maleated EPDM (EP_{gMA}), or maleated PP/EPDM. Hexamethylene diamine (HEMDA) was used as an interlinking agent. The functinalised f(PP/EPDM) copolymers (also referred solid phase dispersant, SPD) will be used subsequently as compatibilisers in PP/EPDM blends and this will be discussed in Chapter 5.

4.2 RESULTS

4.2.1 Methodology for Synthesis of PP/EPDM Copolymers

Two potential routes for copolymer synthesis were examined. The first was based on the copolymerisation of two separately functionalised maleated polymers (maleated PP and maleated EPDM), and the second route was via the copolymerisation of maleated PP/EPDM blends. Initial work was conducted to analyse the effectiveness of each type of copolymer as SPD for PP/EPDM blends. The copolymer that leads to optimum compatibilisation in the binary PP/EPDM blends would be subjected to further tests.

4.2.1.1 METHOD A: Two-Step Synthesis of PP/EPDM Copolymers from Maleated PP and Maleated EPDM using Hexamethylene diamine (HEMDA) as an Interlinking Agent.

A series of PP/EPDM copolymers which are referred to here as solid phase dispersants (SPD) were synthesised by imidisation of mixtures of maleated PP and maleated EPDM using different concentrations of the interlinking agent HEMDA in an internal mixture

141

under standard condition (180⁰C, 60 rpm, 10 min.). The general methodology of the imidisation reaction is described in Scheme 4.1. Maleated PP and maleated EPDM used in the synthesis of the SPD were PMA 9 (containing 1.9 phr grafted MA, see Table 3.5) and MAT 11 (containing 2.83 phr grafted MA, see Table 3.6) respectively. The ratio of PMA9 to MAT11 was 80/20.

Various concentrations of SPDs were premixed and blended with PP and EPDM (PP to EPDM ratio is 80:20) in the internal mixer under the standard condition. The effectiveness of the copolymers as SPD for PP/EPDM blends were monitored from tensile properties of 1 mm thick hot pressed sheets tested in accordance with Section 2.10. The general methodology of the blending process is described in Scheme 4.1. The list of compatibilised PP/EPDM (CPB), chemical composition of solid phase dispersants (SPD), and tensile properties of CPB are presented in Table 4.1.

Table 4.1 indicates that compatibilised PP/EPDM blends show overall lower tensile properties than the control PP/EPDM blend of ratio 80:20 (the binary blend containing no SPD - coded 8020). Elongation at break (E_b) and toughness factor (TF) of the compatibilised blends are the most adversely effected. Visual inspection on the tensile test samples revealed scattered tiny brownish solid spots which were almost certainly responsible for the premature failure observed during tensile testing. The unfavourable tensile properties of the compatibilsed PP/EPDM synthesised in accordance with Method A led to the investigation of an alternative method for synthesising the PP/EPDM copolymers (Method B).

142

4.2.1.2 METHOD B: One-Step Synthesis of PP/EPDM Copolymers from Maleated PP/EPDM using Hexamethylene diamine (HEMDA) as an Interlinking Agent.

Work described in Chapter 3 indicated that maleated PP/EPDM having an initial chemical **composition 6 phr MA, 4 phr TRIS and various FRI concentration** gave optimum MA grafting levels; the chemical composition is reproduced in Table 4.2 for reference. The work described here aims at synthesising PP/EPDM copolymers by imidisation of selected PP/EPDM mixtures (using 75/25 and 60/40 ratios), containing the optimum chemical compositions, using HEMDA. It was assumed that MA grafting level onto PP/EPDM is reproduced during the 'functionalisation' reaction stage, see Scheme 4.2.

HEMDA was added into the reaction system at one of two stages. In the first route, HEMDA was premixed with all the reactants before processing in the internal mixer. This approach was intended to minimise the loss of MA via sublimation as discussed in Section 3.2.1. Unfortunately this approach had to be abandoned due to vigorous reaction between MA and HEMDA during the premixing forming a yellowish substance.

In the second route, a mixture of PP/EPDM was first functionalised with MA in the presence of TRIS and FRI as shown in 'Functionalisation' part of Scheme 4.2. The functionalisation process was allowed to be completed within 10 minutes before the ram was opened (less than 20 s) to add HEMDA. The process was continued for another 10 minutes as shown in the 'Imidisation' part of Scheme 4.2. The changes in torque values

143

were noted every 15 seconds. The copolymers were then compression moulded into 1 mm thick sheets for tensile test measurements.

4.2.2 Effectiveness of PP/EPDM Copolymers Synthesised by Method B as Solid Phase Dispersants for PP/EPDM Blends

A series of PP/EPDM copolymers (as solid phase dispersant - SPD) synthesised via Method B were used as compatibilisers for a mixture of PP and EPDM (75:25 ratio). The SPD chemical composition and tensile properties of the compatibilised blends are tabulated in Table 4.3. The tensile properties were plotted and shown in Fig. 4.1A and B.

Fig. 4.1 shows clearly that SPDs synthesised by Method B give better compatibilisation in PP/EPDM blends than those synthesised via Method A (Table4.1). The former SPDs improved tensile and Young' modulus properties of the control binary blend PP/EPDM (code 7525). However the addition of the SPD reduced the elongation at break and toughness factor.

4.2.3 Infrared Spectroscopy Investigation of Imidisation Reaction in PP/EPDM Copolymers

The imidisation reaction between the anhydride and carbonyl functional groups attached onto PP/EPDM with amino group of the interlinking agent HEMDA was conveniently monitored using the carbonyl region in the FTIR spectra of PP/EPDM copolymers. FTIR spectra of HEMDA (in KBr disk) is shown in Fig. 2.5. FTIR spectra for a control PP/EPDM solid phase dispersant (PP/EPDM processed with MA in the presence of TRIS

and FRI but without interlinking agent HEMDA), and a PP/EPDM solid phase dispersant (PP/EPDM processed with MA in the presence of TRIS, FRI and interlinking agent HEMDA) are shown in Fig. 4.2 and Fig.4.3, respectively. Principle absorption peaks along with probable functional assignment are detailed in the respective figures.

FTIR spectrum of HEMDA , Fig.2.5, shows peak of interest at 1604 cm^{-1} due to vibration of amino group (-NH_2). FTIR spectrum of the control copolymer (copolymer processed without the interlinking agent HEMDA), Fig.4.2, shows three peaks of interest at 1854 cm^{-1}, 1781 cm^{-1} and 1720 cm^{-1}. The first two peaks are related to vibration of carbonyl (C=O) functional group in a cyclic anhydride attached to PP/EPDM backbone. The broad absorption peak at 1720 cm^{-1} could be assigned to an overlaping peak of carbonyl groups from TRIS and from hydrolysed anhydride moiety.

The introduction of HEMDA into a maleated PP/EPDM leads to disappearance of absorption bands related to MA at 1854 cm^{-1} and 1781 cm^{-1} (Fig.4.3). This indicates that MA moiety in the sample has completely reacted with the amino group in HEMDA. The formation of imide, as maleimide through cyclisation of the acid/amide, see **reaction scheme 4.1**, can be identified by new additional absorption band at 1773 cm^{-1} and a strong absorption at 1700 cm^{-1} (Fig.4.3) which are attributed to a carbonyl group (>C=O) absorption in a cyclic 5-ring imide [134]. Another new peak at 1403 cm^{-1} is related to vibration of cyclic-imide nitrogen to carbon covalent bond (>N-CH_2-). The carbonyl stretching vibration of the amide, which usually occurs at around 1620 cm^{-1} , is not

145

observed. This indicates that the reaction between all the grafted MA with the primary diamine was converted directly to the imide form, see **reaction scheme 4.1.**

4.2.4 Effect of TRIS Concentration on Tensile Properties of the Copolymers

A series of PP/EPDM (75/25) copolymers were processed with 6% MA , 0.002 m.r FRI and various concentration of TRIS (0 phr - 4 phr) in the presence of 5 phr HEMDA using Method B. The results (shown in Table 4.4 and in Fig. 4.4) show that the tensile properties increase with TRIS concentration. The improvements could be related to the higher grafting levels of MA in the copolymers at high TRIS concentration, see Fig. 4.4.

4.2.5 Effect of MA to TRIS Ratio on Tensile Properties of Copolymers.

Effect of MA to TRIS ratio on tensile properties of copolymers was studied in PP/EPDM blends at 75/25 ratio. Table 4.4 and Fig.4.5 show that at constant radical initiator and interlinking agent concentration, **(SPD80)** with MA to TRIS ratio of 6:4 exhibits overall optimum tensile properties that may be related to the higher MA grafting level.

4.2.6 Effect of MA Grafting Level on Tensile Properties of PP/EPDM Copolymer

Work described in Section 3.3.2.5 shows that at a ratio of **6 % MA to 4 % TRIS,** optimum tensile properties of PP/EPDM 75/25 copolymers are obtained. To study the effect of free radical initiator concentration and hence MA grafting level on tensile properties of blends, a series of PP/EPDM copolymers at ratios of 75/25 and 60/40 were

146

synthesised in accordance with Method B of Scheme 4.2 in the presence of 6 % MA, 4 % TRIS , various concentration of free radical initiator and 5 phr of HEMDA. The tensile properties of the copolymers are presented in Table 4.5 and Fig. 4.6 A to D. The relation between MA grafting level and radical initiator concentration (FRI) used during the reactive processing is illustrated in Fig. 4.7.

The data revealed that in the case of copolymers based on 75/25 PP/EPDM, sample **SPD80** (processed in the presence of 0.002 m.r T101 and containing 1.70 phr grafted MA) gave overall optimum tensile properties, (see Table 4.5). The tensile properties of these 75/25 PP/EPDM copolymers increased significantly, with increasing radical initiator concentration from 0.001 m.r to 0.002 m.r. (higher MA grafting level at higher radical initiator concentration), a further increase in radical initiator concentration and MA grafting level, led to a general reduction in tensile properties (see Table 4.5). Similar trend is observed for copolymers based on 60/40 PP/EPDM. Sample **SPD140** processed in the presence of 0.005 m.r of T101 and containing 2.46 phr grafted MA shows overall optimum tensile properties (see Table 4.5).

4.2.7 Effect of HEMDA Concentration

The performance of a copolymer of PP/EPDM is expected to be influenced by the extent of the interlinking (i.e. imidisation) reaction between the maleated PP and EPDM in maleated PP/EPDM and the diamine interlinking agent. A series of PP/EPDM 75/25 copolymers processed in the presence of various concentrations of the interlinking agent

HEMDA were synthesised (see Table 4.6). The effect of MA grafting level was also studied.

Fig. 4.8 shows that PP/EPDM copolymers processed with 5 phr HEMDA reveal optimum tensile properties except for copolymers synthesised in the presence of 0.001m.r and 0.005 m.r FRI which show optimum modulus at 3 % HEMDA and 10 % HEMDA, respectively. Fig. 4.8 also shows the tensile properties are effected by FRI concentration used during functionalisation of PP/EPDM with MA and hence the MA grafting level. The copolymer samples processed in the presence of 0.002 m.r. T101 with 5 % HEMDA exhibited better overall performance, especially with respect to toughness factor which reflects higher toughness of the sample (see Table 4.6, sample SPD80).

4.3 DISCUSSION

Synthesis of block graft copolymer containing polyolefins constituents is very challenging [97,135,136]. The difficulty in making compatibilisers for PP and EPDM blends lies in the different natures of the two polymers and the ways by which they are polymerised [97, 98, 137]. PP is a semi-crystalline thermoplastic polymer, generally made with a heterogenous catalyst that leads to stereoregular incorporation of propylene monomer. The EP copolymers are made with homogenous catalysts which do not exhibit polymerisation kinetics that facilitate block polymer synthesis.

The results presented in this chapter show that MA-grafted PP/EPDM copolymers (60/40 and 75/25 ratios) have been successfully synthesised via **one-step reactive processing** in the melt. These copolymers were synthesised in a two routes process (Method B). The first synthetic route was based on the functionalisation of PP/EPDM mixture with MA, in an internal mixer at 190 $^{\circ}$C using a peroxide free radical initiator in the presence of a multi-functional monomer TRIS. Possible chemical reactions involved in the grafting of MA onto the mixture of PP and EPDM were discussed in Section 3.4 and reaction scheme 3.6. In accordance with literature finding most of the PP and EPDM have only a single MA graft per-polymer molecule [63-65,72,115] and/or short poly(maleic anhydride) chain, and located at the end chain of the homopolymers [63,73,138]

In the second synthetic route, the grafted MA (i.e. maleated PP/EPDM) was reacted with a symmetrical primary diamine HEMDA. Amines are good bases and nucleophiles which can be made to react with carboxylic acid or anhydride moieties that are grafted onto polymers [129, 139]. The selection of a primary amine in this work was based on the fact that it has the highest reactivity towards anhydride or carboxylic acid group when compared to than secondary and tertiary amines [139]. It has been reported [139, 140] that an anhydride group attached to a polymer has a higher reactivity towards secondary or primary amino groups compared to carboxylic acid group in nucleophilic acyl substitution reactions. FTIR analysis of functionalised PP/EPDM copolymers (Section 4.3.2) proved that the primary amine group in the diamine molecule HEMDA preferentially reacts with the succinic anhydride grafted on PP and EPDM. Since the

unsaturation in the maleic anhydride is lost upon grafting, the resulting grafted succinic anhydride moiety, has the chemical reactivity of a saturated acid.

Reaction Scheme 4.1 illustrates a suggested mechanism for the formation of the functionalised graft PP-EPDM copolymer. The reaction of anhydride with an amine results readily in a covalent bond formation. The initially formed amic acid undergoes ring closure leading to a thermally stable imide functioned formed at the elevated temperature used in the internal mixer. The reactivity of amines depends on their basicity and nucleophilicity. An amine can react with carboxylic acid as a base by withdrawing the proton of the hydroxyl group to form an amine salt or as a nucleophile by attacking the electron-deficient carbon of the acyl group to form an amide. The basicity of amines has the following trend according to K_a value [141]: secondary $\geq$ primary > tertiary. On the other hand, the formation of amides through nucleophilic acyl subtitution depends on the nucleophilicity of the amines. The nucleophilicity of the amines decreases in the order: primary > secondary > tertiary due to the size effect [139, 141]. Thus, the primary diamine having the highest nucleophilicity and a moderate basicity could produce mainly an irreversible amide crosslink. Upon further heating, condensation reaction between the amide and the acid groups takes place to form an imide linkage.

The reaction of diamines with anhydride in polymers should result in crosslinks which, in turn should result in an increase in molecular weight and viscosity. This is expected to be manifested by a significant increase in torque during the melt processing. The extent of

grafted MA-TRIS on PP + H2N(CH2)6NH2 + grafted MA-TRIS on EPDM

(An amide)

(An imide)

a copolymer of PP-g-EPDM
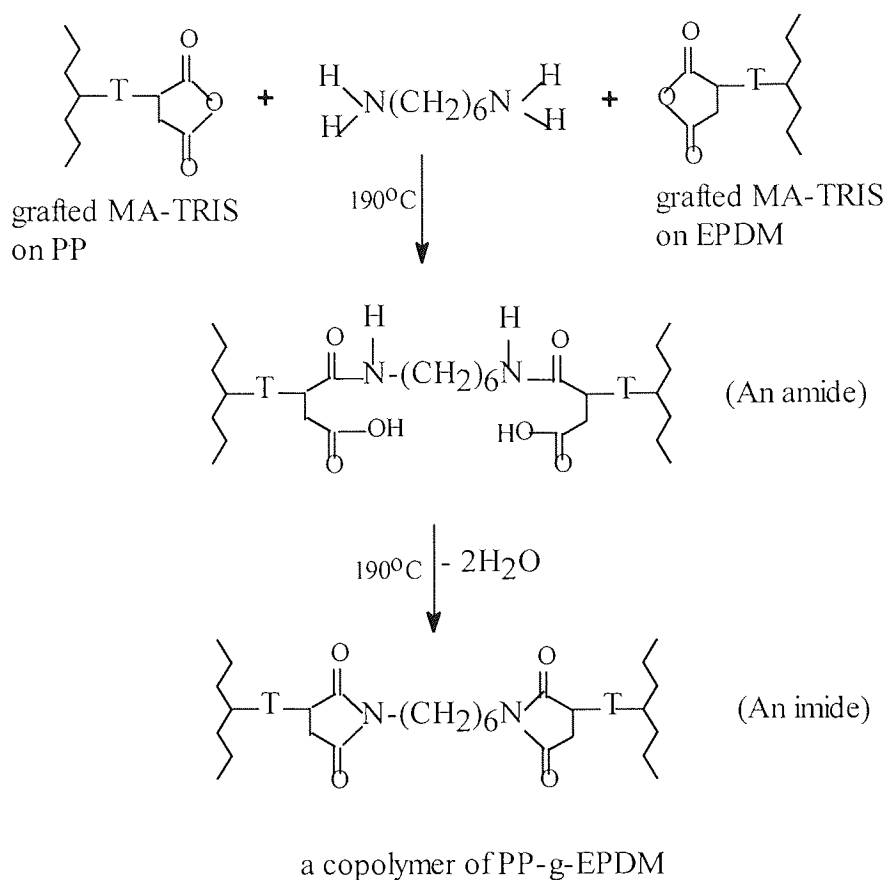
Reaction scheme 4.1: Proposed reaction mechanism in the melt between grafted maleic anhydride with amino group in HEMDA. Letter 'T' represent coagent TRIS. See Reaction scheme 3.6 for proposed mechanism of MA grafting onto PP.

torque increase varies according to the extent of crosslinking. A general pattern of torque-time relationships for the reaction of maleated PP/EPDM with primary diamine HEMDA is shown in Fig. 4.9. In the fist 10 minutes of processing functionalisation of PP/EPDM with MA was carried out in the presence of peroxide and a co-agent (TRIS). The pattern of the torque values of this 'functionalisation reaction' shown in Fig. 4.9 resembles that of the torque behaviour of PP/EPDM copolymer (see Fig.3.34) and has been discussed in detail in Chapter 3. After 10 minutes processing, HEMDA was

151

introduced to the polymer mixture by lifting the ram, hence reduced the torque to a minimum (within less then 20 s the ram was lowered to close the mixing chamber). A vigorous reaction was observed after addition of HEMDA which reflected by a rapid torque values increased to a distinct peak to a value well above the reference, PP/EPDM copolymer sample processed without the addition of HEMDA (see Fig. 4.9). The torque peak decayed on further mixing, but remained at a high final level. Torque gains significantly higher than control levels could be accounted for by effective crosslinking between the maleated PP and EPDM and HEMDA(see reaction Scheme 4.1). The formation of a torque peak could be rationalised by changes at a molecular level. At the point of maximum torque (Tq_m), crosslinking would be intensive, yielding high viscosity, but further shear in the internal mixer combined with entanglement stresses, results in mechanochemical scission of crosslink network and polymer backbones, thus reducing melt viscosity until an equilibrium position is maintained, resulting in a steady torque. [116, 130].

The effectiveness of HEMDA in crosslinking maleated PP/EPDM could be observed from changes in the physical properties of the functionalised PP/EPDM copolymers. Addition of HEMDA to maleated PP/EPDM copolymers during reactive processing, results in significant improvement in tensile properties over the control (SPD65, Table 4.7). Within the chemical compositions studied, the optimum tensile properties for both SPD6040 and SPD7525 were achieved at HEMDA concentration of about 5 to 10 %, with the SPD7525 showing overall better performance.

152

However the tensile properties of the SPD was not only effected by the concentration of HEMDA but also by the level of MA grafting and more importantly by the free radical initiator concentration. The concentration of MA grafted onto PP and EPDM determined the extent of effective imide crosslinking that consequently determined the final physical properties of the copolymers. All level of MA grafted concentration used within this studies greatly improved the strength and stiffness of the copolymers but on the other hand showed low values of elongation at break (E_b) and toughness factors (TF). Elongation at break and toughness factors give an indication of the material toughness. Figures 4.10 (a and b) shows typical SEM micrographs of the tensile fracture surface of binary PP/EPDM 75/25 blend and SPD, respectively. Compared to the PP/EPDM binary blend which clearly demonstrate a two-phase morphology, the SPD shows very fine disperse phase which reflects a good adhesion between PP and EPDM phases. The good adhesion could be a result from imide linkage between PP and EPDM. The SEM micrograph also indicated that the SPD experienced brittle failure which related to low elongation at break hence low tensile toughness. The SPDs processed with free radical initiator concentration higher than 0.002 m.r. for SPD6040 (Table4.5) and 0.005 m.r. for SPD6040 (Table 4.6), although exhibit comparatively good strength and stiffness but suffer low elongation capabilities and consequently unable to sustain higher energy before break. During the reactive processing of PP/EPDM mixture, radical initiator might have caused two opposite effects. Although higher radical initiator could improved crosslinking density in EPDM but on the other hand could severely degrade PP backbone. As has been discussed in Chapter 3, the presence of MA during the reactive processing lead to further degradation of the PP backbone. The presence of both peroxide and MA

during the processing, but without HEMDA, had reduced tensile properties of PP/EPDM (SPD65 in Table 4.7) to a level lower than binary mixture of PP/EPDM (7525 in Table 4.7). The minimally crosslinked EPDM proven with low gel content as measured in Chapter 3, unable to sustain strength of the PP/EPDM and more importantly the copolymer was broken at low stress.

Copolymer containing higher MA grafting level show relatively better tensile properties however the correlation is not linear. The data indicates that improvement of MA grafting level from 0.8 phr to 1.70 phr (about 100% increase) only moderately improved tensile strength and toughness factor from 21.4 MPa and 30 MPa to 24 MP and 32 MPa, respectively.

SYNTHESIS OF SOLID PHASE DISPERSANTS METHOD A

	STEP-1

FUNCTIONALISATION OF PP AND EPDM
with MA, see Method A Scheme 3.1

Imidisation reaction

PMA9 80%	MAT11, 20%	HEMDA,2-5%

tumble mixed

STEP-2

Processed in internal mixer, closed mixing, 180 C
for 10 min.,Copolymerwas then sheeted to thin film
and cooled to room temperature

Copolymer
(or solid phase dispersant

Blending

PP, 80%	Copolymer, 2-5 %	EPDM, 20%

Processed in internal mixer, closed
mixing, 180 C for 10 min.,60 rpm

STEP-3

compatibilised blend

tensile test

Scheme 4.1: General experimental procedure for the imidisation of maleated PP (PMA) and maleated EPDM (MAT) with HEMDA as an interlinking agent, and compatibilisation of PP/EPDM. PMA is PMA9 containing 1.9 phr grafted MA, and MAT is MAT11 containing 2.8 phr grafted MA, see Tables 3.5 and 3.6 respectively.

SYNTHESIS OF SOLID PHASE DISPERSANT METHOD B

| PP 60-75 phr | EPDM 25-40 phr | MA 0-9 phr | TRIS 0-4 phr | T101 0-0.1 m.r |

Functionalisation

ONE STEP

tumble mixed

process in internal mixer closed ssytem, 180 C
t = 0
t = 10 min.

MA grafting level analysis

Continue processing, lift-up ram, add HEMDA (less than 20 sec.) and ram down to close chamber

HEMDA 1-15%

Imidisation

t = 20 min

non extracted SPD

hot pressed to 1 mm thick sheet, 4 min. at 180 C

Tensile test

SEM

Scheme 4.2: General one-step procedure for synthesis of solid phase dispersant (SPD) of PP/E
The synthesis reaction include functionalisation of maleic anhydride (MA) onto PP/EPDM in the presence or absence of co-agent TRIS and free radical initiator T101, then followed by imidisation of maleated PP/EPDM with an interlinking agent HEMDA.

Table 4.1 : Effect of PP/EPDM copolymers on tensile properties of PP/EPDM blends (ratio 80/20). The copolymers were synthesised via imidisation of maleated PP (PMA9) and maleated EPDM (MAT 11) with HEMDA, using Method A (see Scheme 4.1). Full data is in Appendix 4.1.

PP:EPDM blend, 80:20 code	PP/EPDM copolymer composition X PMA9 + Y MAT11 + Z HEMDA			Copolymer in blend,%	Tensile properties of blends			
	X %	Y %	Z %		TS, MPa	YM, MPa	Eb, %	TF MPa
CPB12	76.0	19.0	5	5	18.6	434	35	13.5
CPB13	76.0	19.0	5	2	18.6	487	48	14.9
CPB19	76.0	19.0	3	5	17.0	450	60	17.1
CPB20	76.0	19.0	3	2	18.0	500	54	19.0
CPB21	57.0	38.0	5	5	17.7	395	25	12.0
CPB22	57.0	38.0	5	2	19.4	420	30	16.0
CPB23	57.0	38.0	3	5	18.2	485	45	15.1
CPB24	57.0	38.0	3	2	18.3	490	52	18.6
8020	nil	nil	nil	nil	21.5	550	474	70.4

Table 4.2 : Optimum chemical composition of maleated PP/EPDM. (reproduced from Tables 3.7 and 3.8). Full data is in Appendix 4.2.

Maleated PP/EPDM		Chemical composition (PP+EPDM+MA+TRIS+FRI)			MA grafting level %	MA grafted of original %
code	PP/EPDM ratio	MA,%	TRIS,%	FRI, m.r		
MB73	75/25	6	4	0.001	1.5	25
MB65	**75/25**	**6**	**4**	**0.002**	**1.7**	**28**
MB77	75/25	6	4	0.005	2.0	33
MB92	60/40	6	4	0.001	1.2	19
MB93	60/40	6	4	0.002	1.6	27
MB94	**60/40**	**6**	**4**	**0.005**	**2.5**	**41**
MB95	60/40	6	4	0.01	2.7	45

Table 4.3: Effect of PP/EPDM copolymers (solid phase dispersant, SPD) on tensile properties of compatibilised PP/EPDM blends, CPB (ratio 75:25). The copolymers were synthesised via imidisation of maleated PP/EPDM with HEMDA, in accordance with Method B (see Scheme 4.2). Refer to Figure 4.1 in connection with this Table. Full data is in Appendix 4.3

Compatibilised PP:EPDM blend, 75:25 code	Copolymer (SPD) composition (PP/EPDM (60/40) + 6%MA 4%TRIS + X m.r T101 + Y%HEMDA)		SPD in blend	Tensile properties of compatibilised blend			
	X m.r	Y %	%	TS, MPa	YM, MPa	Eb, %	TF MPa
CPB131	0.001	5	3	19.5	696	261	46.4
CPB125	0.002	5	3	19.5	547	225	41.5
CPB133	0.005	5	3	19.8	602	294	52.4
7525	nil	nil	nil	17.5	387	440	69.4

Table 4.4: Chemical composition and tensile properties of copolymers (SPD) prepared from PP/EPDM (75/25) processed with various ratio of MA to TRIS, in the presence of 0.002 m.r FRI and 5 phr interlinking agent HEMDA. Refer to Figures 4.4 and 4.5 in connection with this Table. Full data is in Appendix 4.4.

Co-polymer code SPD	Chemical composition of copolymer					Tensile properties of copolymer			
	MA phr	TRIS phr	FRI m.r	MA grafted, phr	HEMDA phr	TS MPa	YM MPa	Eb %	TF MPa
119	9	1	0.002	0.7	5	19.1	443	127	23.0
120	8	2	0.002	1.2	5	19.5	541	110	22.4
121	7	3	0.002	1.4	5	21.0	522	103	21.4
80	**6**	**4**	**0.002**	**1.7**	**5**	**24.0**	**562**	**137**	**32.0**
124	6	0.5	0.002	0.3	5	20.2	489	116	23.0
123	6	1	0.002	0.4	5	21.2	499	121	27.8
122	6	2	0.002	0.8	5	21.4	518	123	30.0
204	6	0	0.002	0.1	5	17.9	400	110	20.0

Table 4.5: Effect of grafted MA and HEMDA concentration on tensile properties PP/EPDM copolymer synthesised by Method B. Refer Figures 4.6 and 4.7 in connection with this Table. Full data is in Appendix 4.5.

Copolymer		Chemical composition of copolymer					Tensile properties			
code SPD	PP/EPDM ratio	MA phr	TRIS phr	FRI m.r	MA grafted, phr	HEMDA phr	TS MPa	YM MPa	Eb %	TF MPa
78	75/25	6	4	0.001	1.5	5	21.5	489	114	24
80	**75/25**	**6**	**4**	**0.002**	**1.7**	**5**	**24.0**	**562**	**137**	**32.0**
82	75/25	6	4	0.005	2.0	5	24.1	431	82	18
106	60/40	6	4	0.001	1.2	3	12.6	230	183	20
107	60/40	6	4	0.002	1.6	3	15.4	246	219	29.3
108	60/40	6	4	0.005	2.5	3	17.9	292	221	35
109	60/40	6	4	0.01	2.7	3	18.0	286	110	14
102	60/40	6	4	0.001	1.2	5	14.8	270	178	22
103	60/40	6	4	0.002	1.6	5	17.8	295	216	34
104	**60/40**	**6**	**4**	**0.005**	**2.5**	**5**	**19.5**	**340**	**234**	**36.3**
105	60/40	6	4	0.01	2.7	5	20.5	303	116	21
6040	60/40	nil	nil	nil	nil	nil	11.9	299	328	33

Table 4.6: Chemical composition and tensile properties of copolymers prepared from PP/EPDM (75/25) processed with 6 phr MA and 4 phr TRIS in the presence of various concentration of FRI and interlinking agent HEMDA. Refer to Figure 4.8 in connection with this Table. Full data is in Appendix 4.6.

code SPD	Chemical composition of copolymer					Tensile properties			
	MA phr	TRIS phr	FRI m.r	MA grafted, phr	HEMDA phr	TS MPa	YM MPa	Eb %	TF MPa
98	6	4	0.001	1.5	3	17.8	497	74	12
78	6	4	0.001	1.5	5	21.5	489	114	24
79	6	4	0.001	1.5	10	20.2	536	108	20
84	6	4	0.001	1.5	15	17.9	377	138	23
99	6	4	0.002	1.7	3	20.0	472	79	13
80	**6**	**4**	**0.002**	**1.7**	**5**	**24.0**	**562**	**137**	**32**
81	6	4	0.002	1.7	10	22.3	470	133	27
85	6	4	0.002	1.7	15	19.5	379	132	21
100	6	4	0.005	2.0	3	21.9	503	66	13
82	6	4	0.005	2.0	5	24.1	431	82	18
83	6	4	0.005	2.0	10	24.1	439	78	17
86	6	4	0.005	2.0	15	18.2	316	71	11
88	nil	4	0.002	nil	nil	17.6	474	177	28
204	6	nil	0.002	0.2	5	21.9	512	147	25.7

Table 4.7: Chemical composition and tensile properties of various type of PP/EPDM copolymer. Full data is in Appendix 4.7.

code SPD	Chemical composition					Tensile properties			
	MA phr	TRIS phr	FRI m.r	MA grafted, phr	HEMDA phr	TS MPa	YM MPa	Eb %	TF MPa
80	6	4	0.002	1.7	5	24.0	562	137	32.0
88	nil	4	0.002	nil	nil	17.6	474	177	28.0
65	6	4	0.002	1.7	nil	16.4	459	49	7.7
204	6	nil	0.002	0.2	5	17.9	400	110	20.0
7525	nil	nil	nil	nil	nil	17.5	387	440	69.0
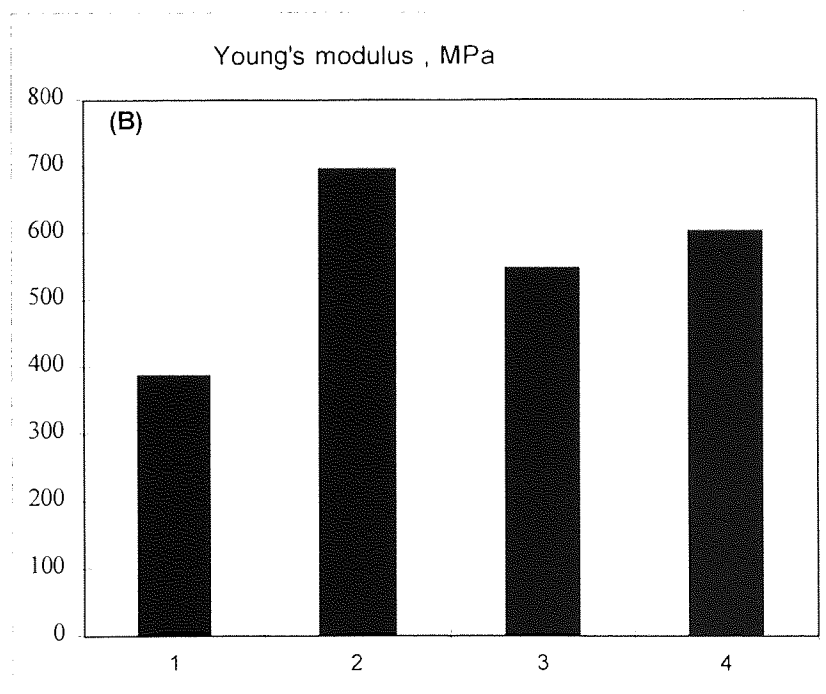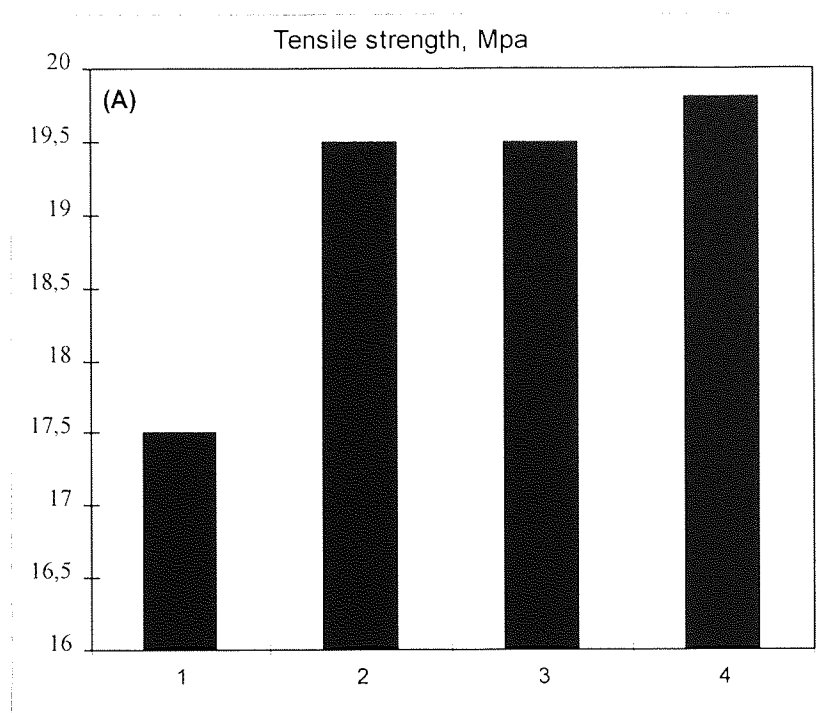
Fig 4.1: Effect of PP/EPDM copolymer on tensile properties of PP/EPDM blends 75/25 . (1) 7525 (2) CPB131 (3) CPB125 (4) CPB133. Refer to Table 4.3 for details.
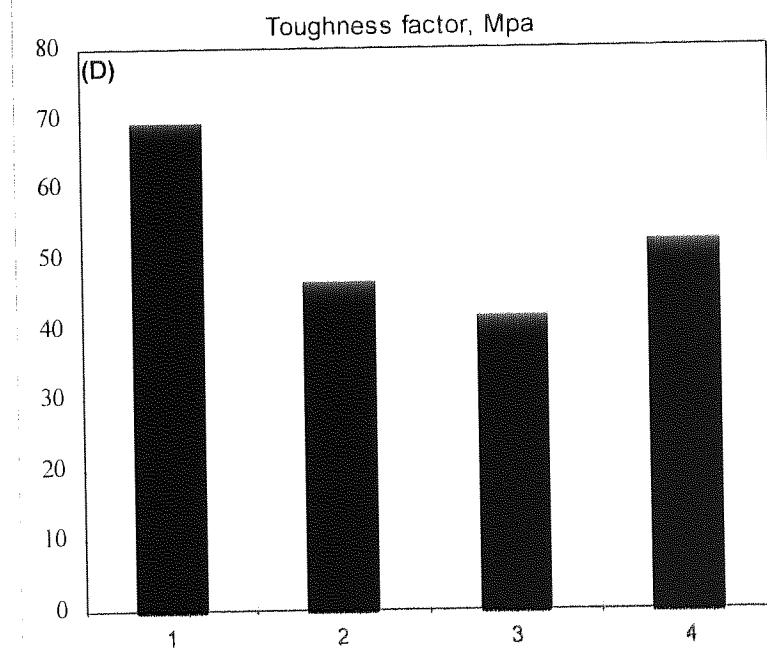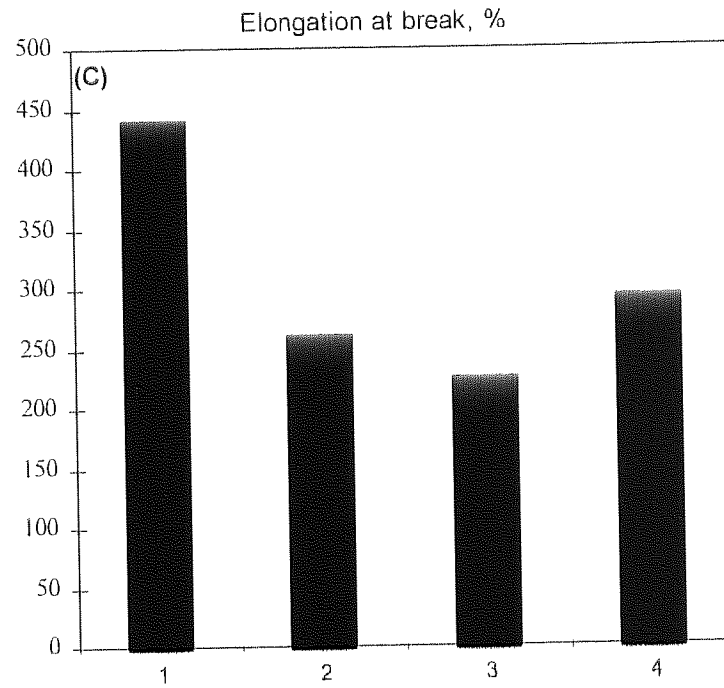
continue from Figure 4.1
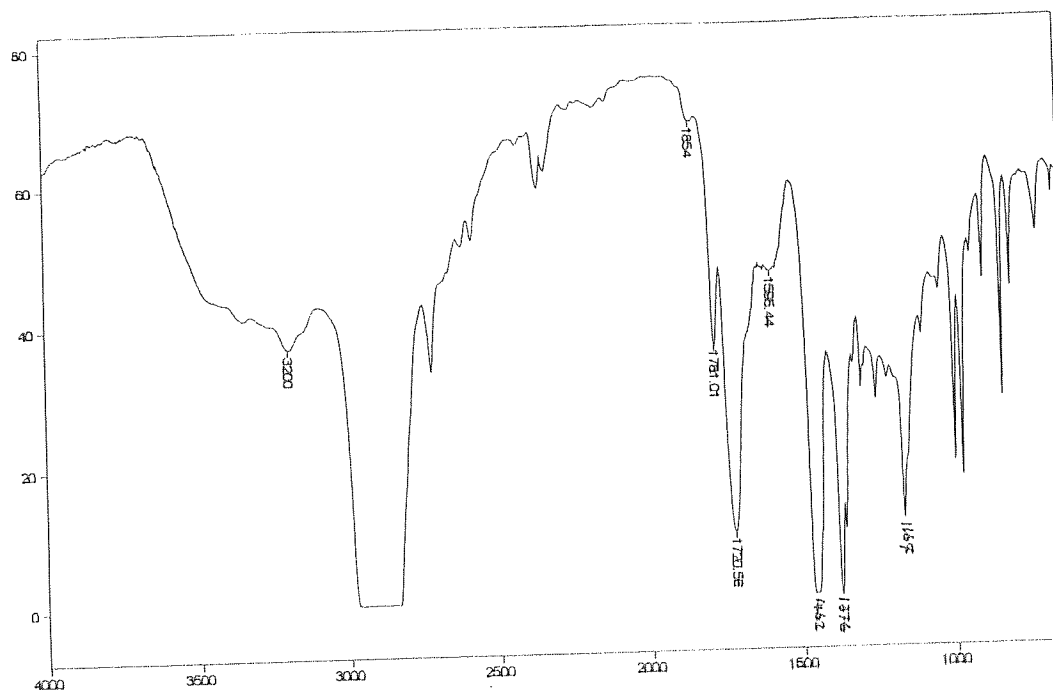
Figure 4.2 : FTIR spectrum of maleated PP/EPDM 75/25 (MB65). The chemical
composition was 6phr MA + 4 phr TRIS + 0.002 m.r. FRI (prepared by
Method B)

Major absorption bands and probable functional assignments

Peak (cm⁻¹)	Intensity	assignment
1854	weak	carbonyl asymmetric bonded in anhydride 5 cyclic ring
1781	strong	carbonyl symmetric stretching in anhydride 5 cyclic ring
1720	strong, broad	carbonyl vibration from hydrolysed anhydride
1462	very strong	methylene symmetrical C-H bending
1376	very strong	methyl C-H bending

163
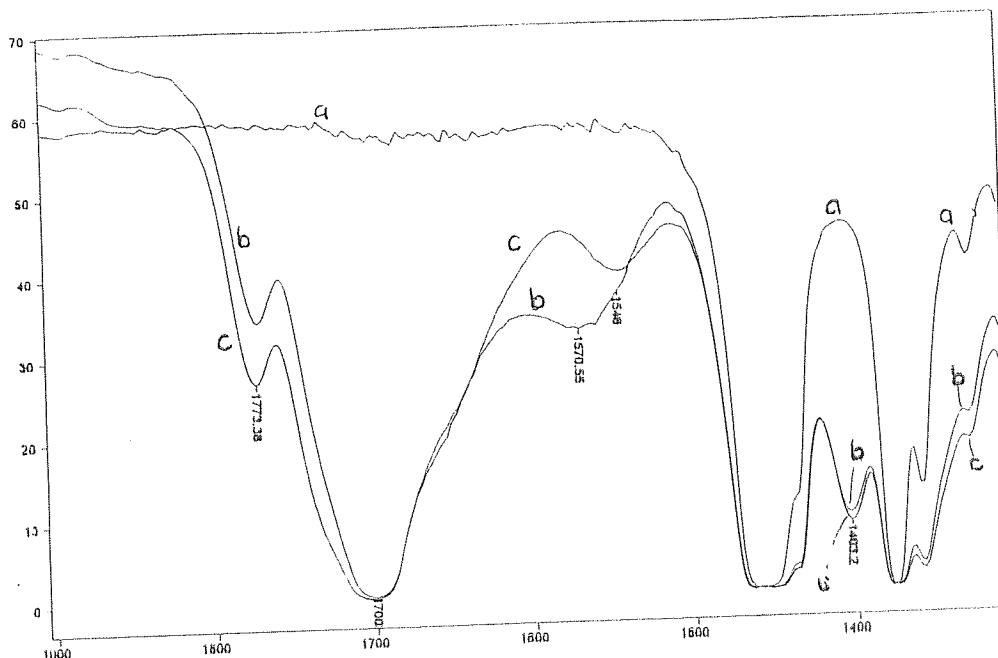
Figure 4.3: FTIR spectrum of PP/EPDM copolymer. Chemical composition of the copolymer (SPD80) was 6phr MA + 4 phr TRIS + 0.002 m.r. FRI + 5 phr HEMDA prepared by Method B. (a) PP/EPDM (b) maleated PP/EPDM before extraction, and (c) after extraction.

Major absorption bands and probable functional assignments in the infra-red spectrum of PP/EPDM copolymer (thin pressed film)

Peak (cm^{-1})	Intensity	assignment
1773	medium	carbonyl ($>C=O$) in a cyclic 5-ring imide
1701	broad, strong	carbonyl group in a cyclic 5-ring imide
1460	broad, strong	methylene symmetrical C-H bending
1403	medium	stretching vibration cyclic-imide nitrogen to carbon ($>N-CH_2-$)
1376	very strong	methyl C-H bending
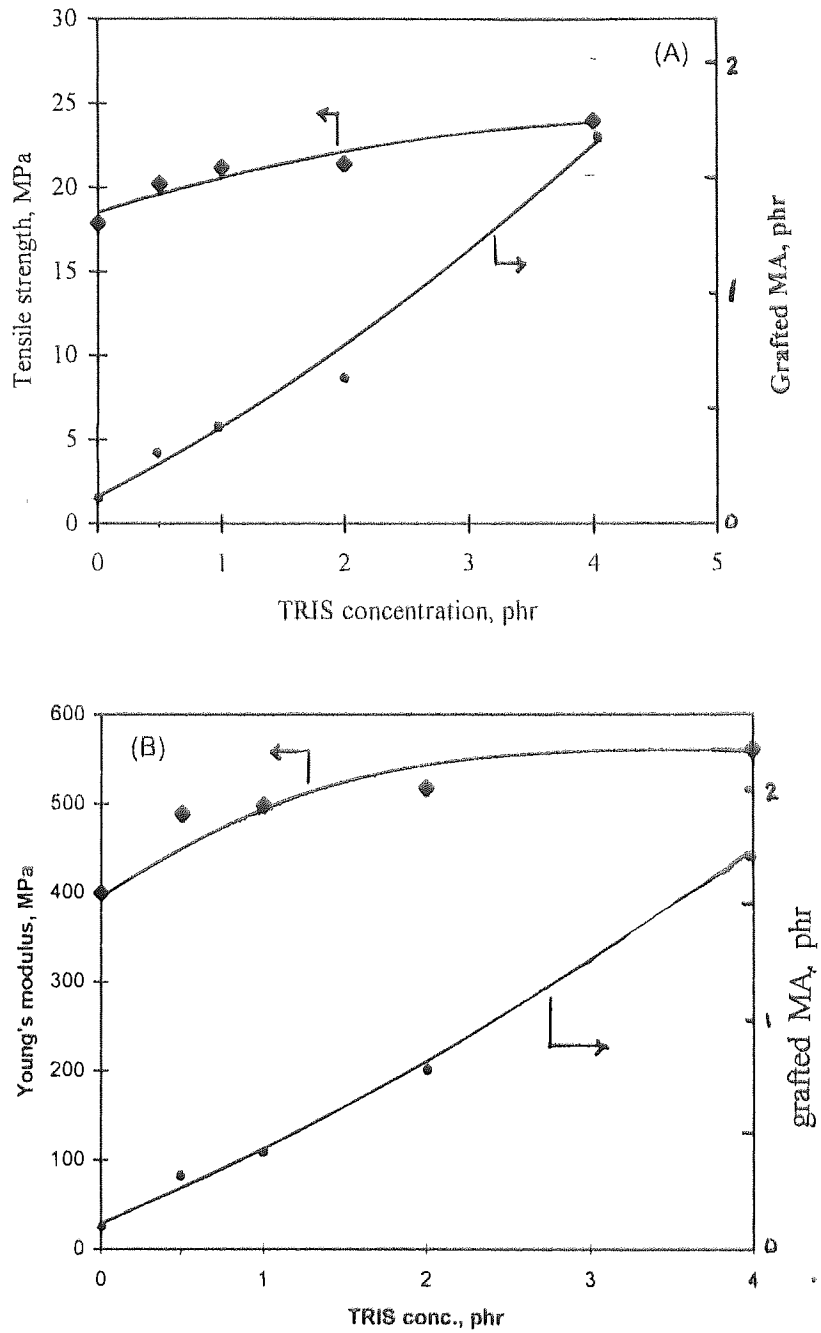
Figure 4.4 : Effect of co-agent TRIS and grafted MA concentration on tensile properties of PP/EPDM 75/25 copolymers. Refer to Table 4.4 for chemical composition.

(C)

(D)
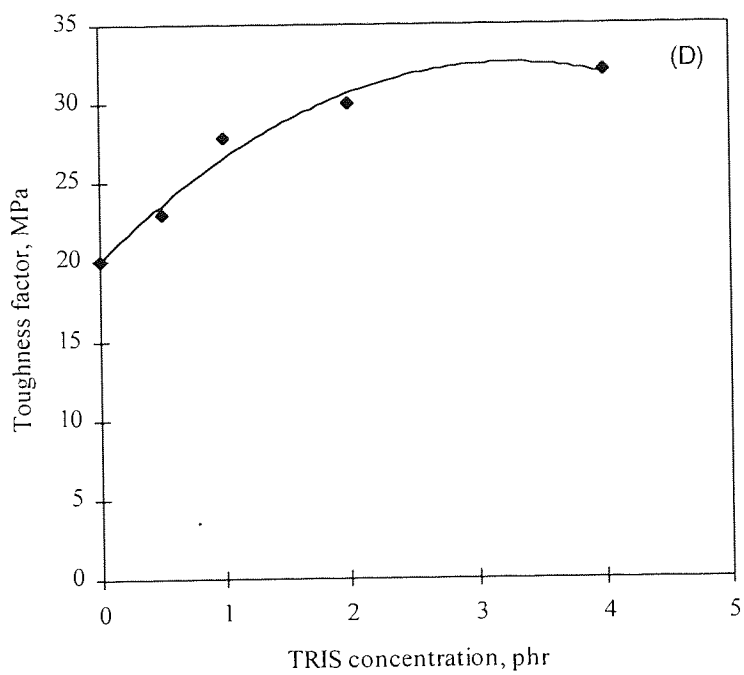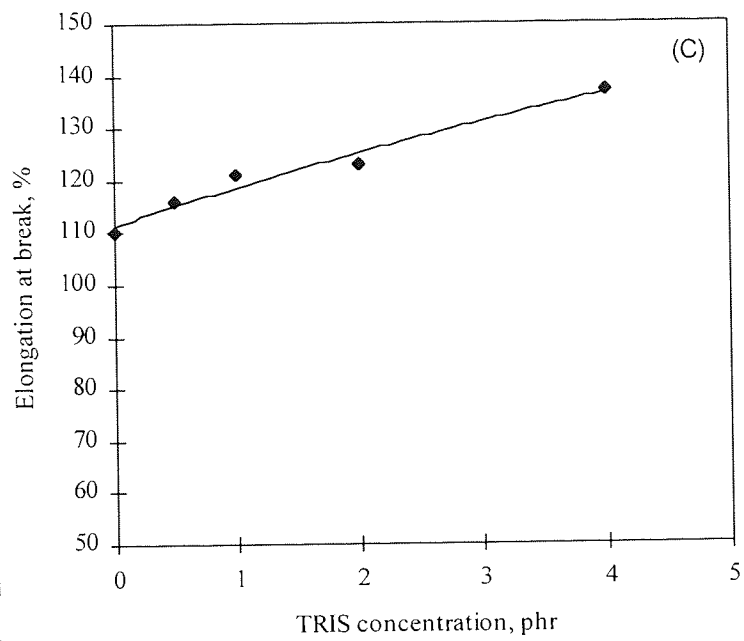
continue from Figure 4.4

166
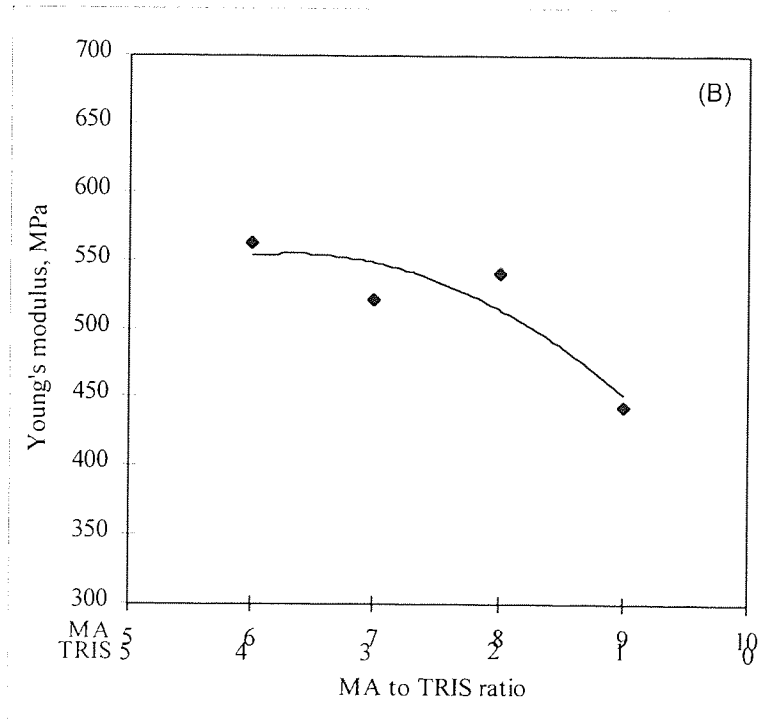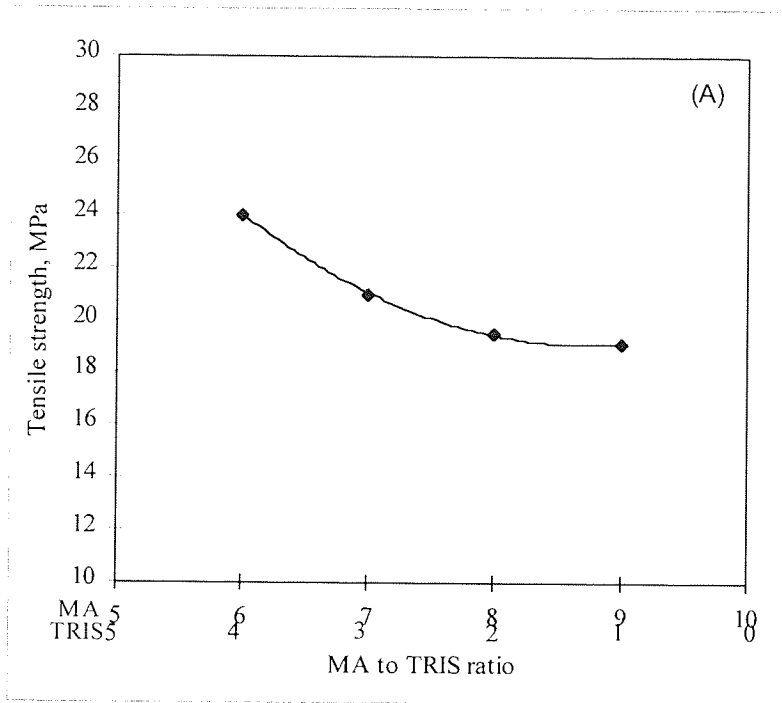
Figure 4.5: Effect of MA to TRIS ratio on tensile properties of PP/EPDM 75/25. Refer to Table 4.4 for related data.
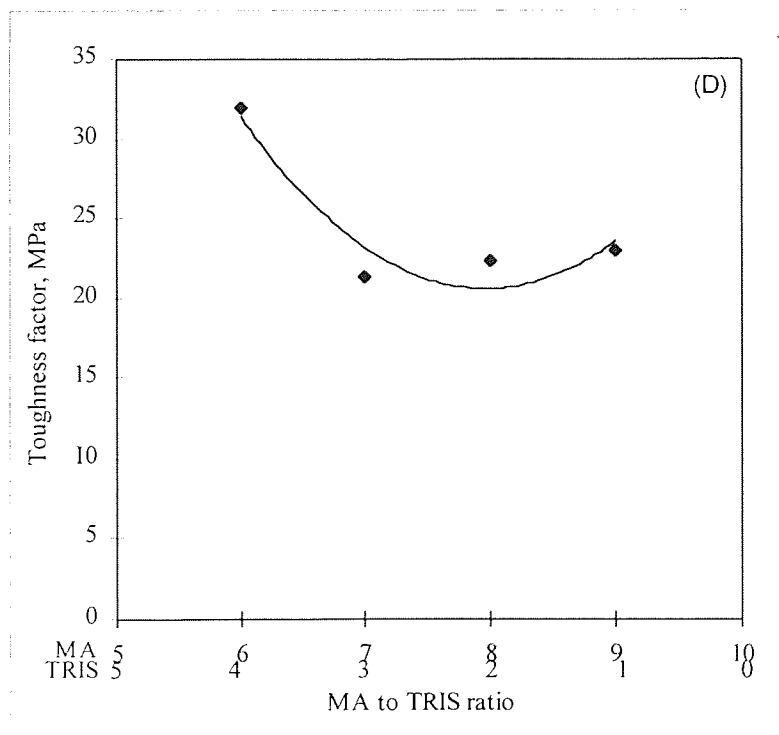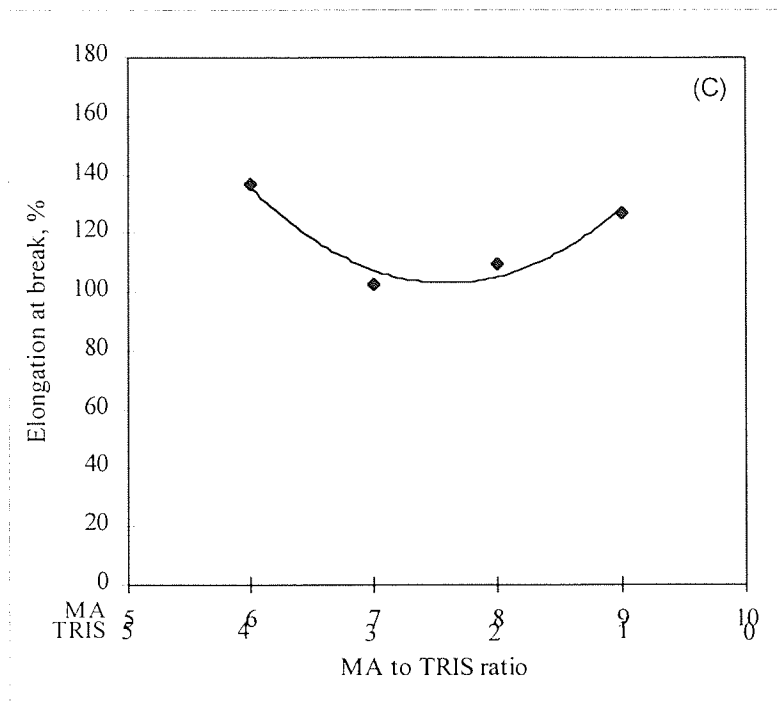
continue from Figure 4.5
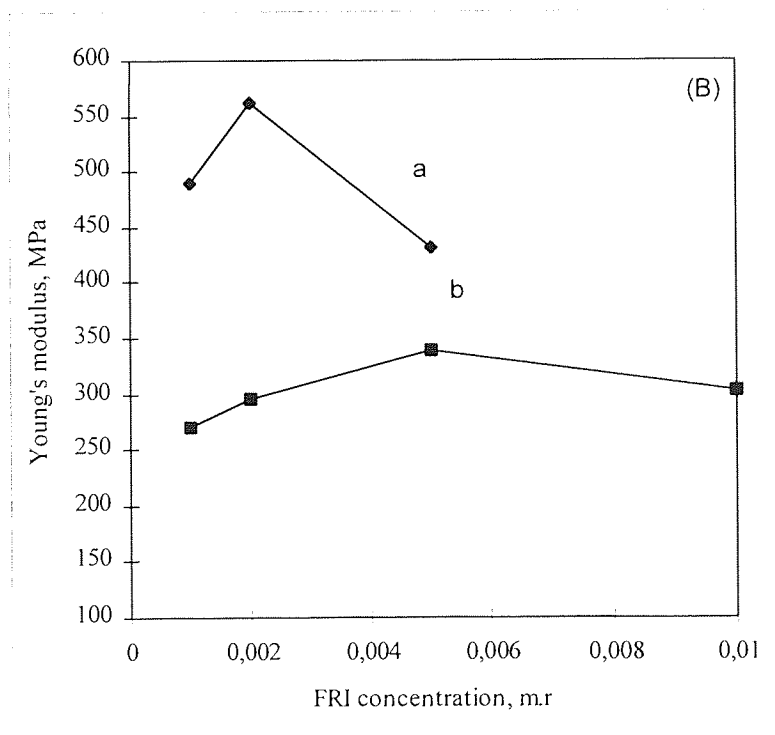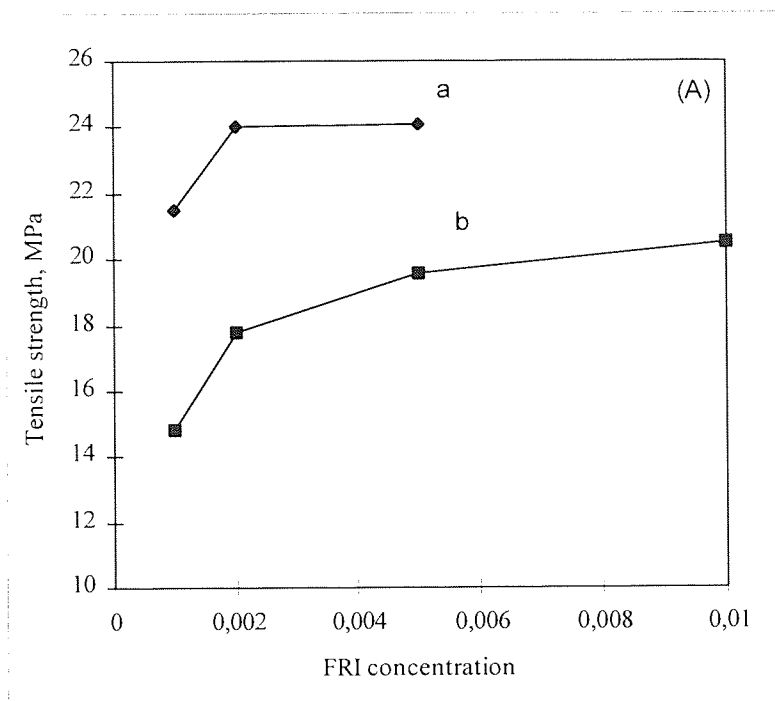
Figure 4.6: Effect of free radical initiator and interlink agent HEMDA concentrations on tensile properties of PP/EPDM 60/40 copolymers. Copolymers (a) containing 3 phr HEMDA, and (b) 5 phr HEMDA. Refer to Table 4.5 for details.
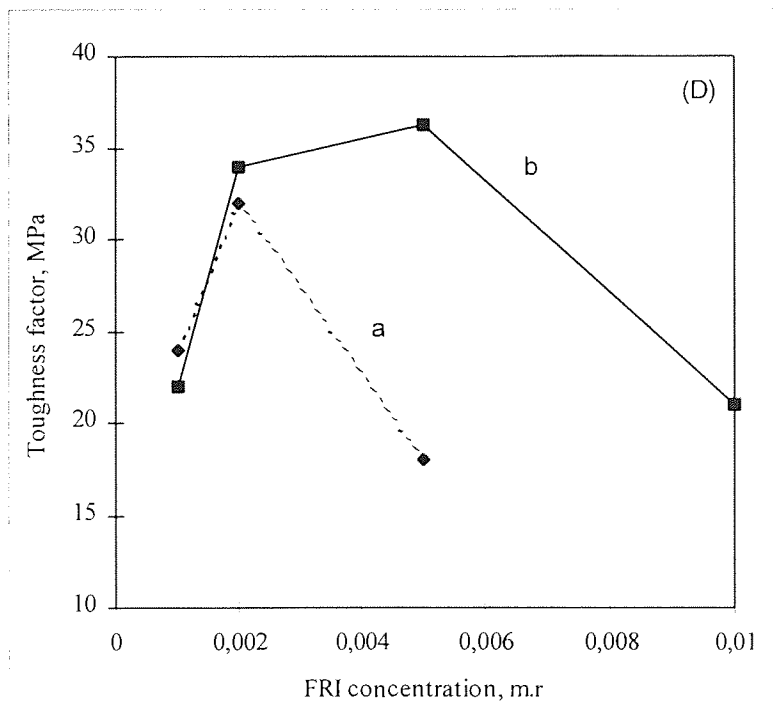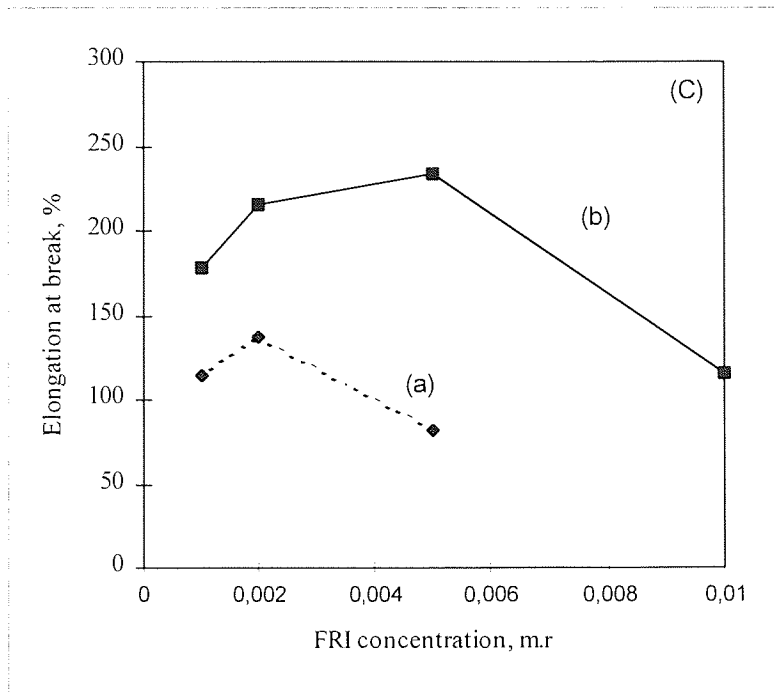
continue from Figure 4.6
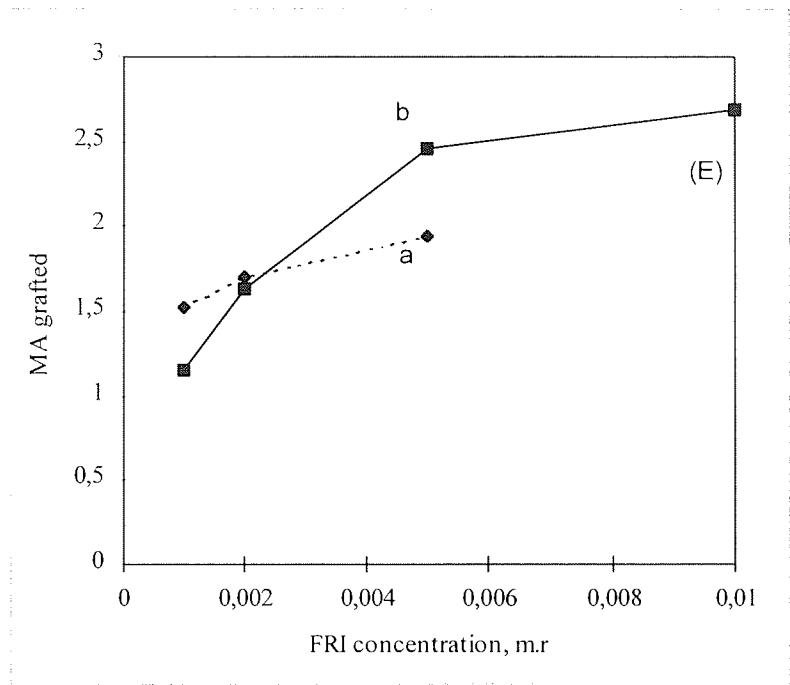
Figure 4.7: Effect of radical initiator concentration on MA grafting level onto PP/EPDM 75/25 (a), and PP/EPDM 60/40 (b). Initial MA and TRIS concentration is 6 phr and 4 phr, respectively. Refer to Table 4.5 for related data.
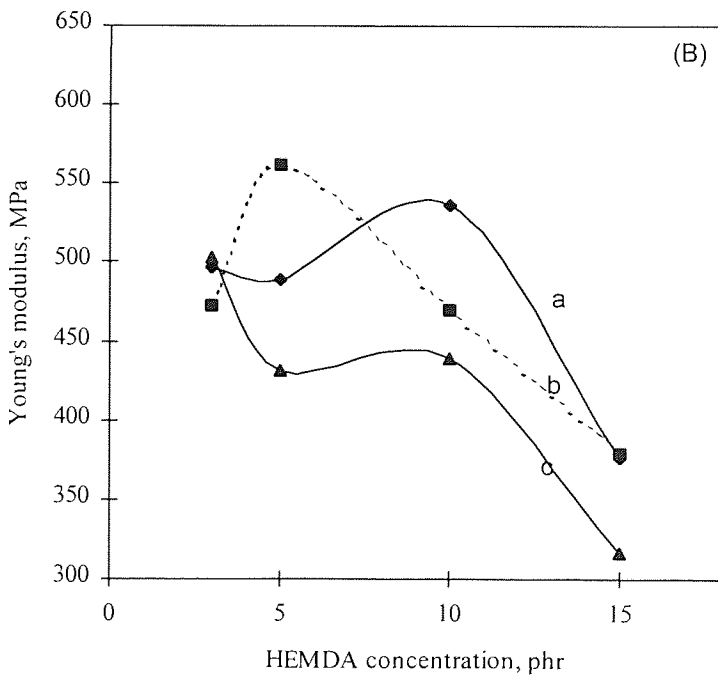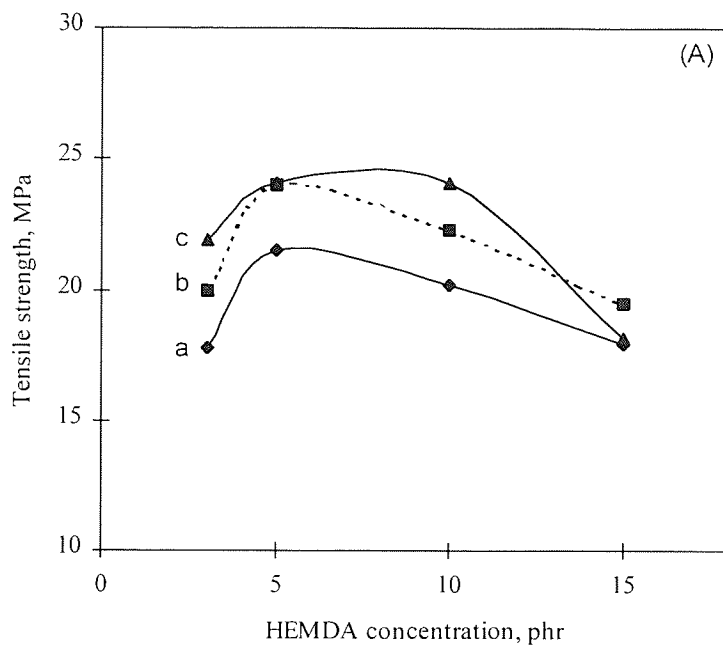
Figure 4.8: Effect of HEMDA concentration and level of MA grafted on tensile properties of the PP/EPDM 75/25 copolymers. MA grafting level (a) 1.5 phr (b) 1.7 phr (c) 2.0 phr. Refer to Table 4.6 for related data.
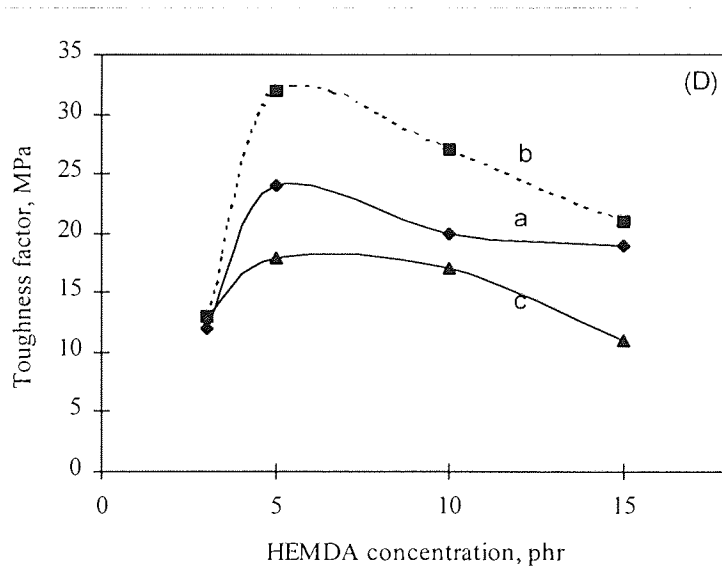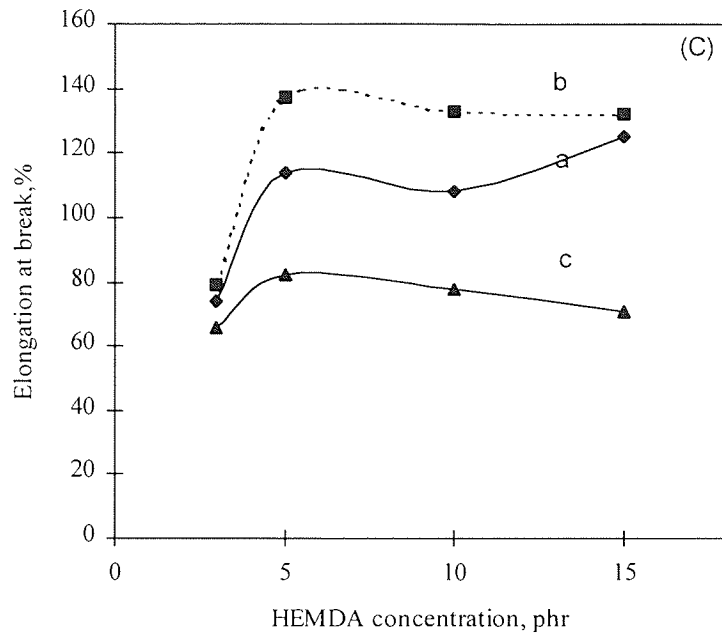
continue from Figure 4.8
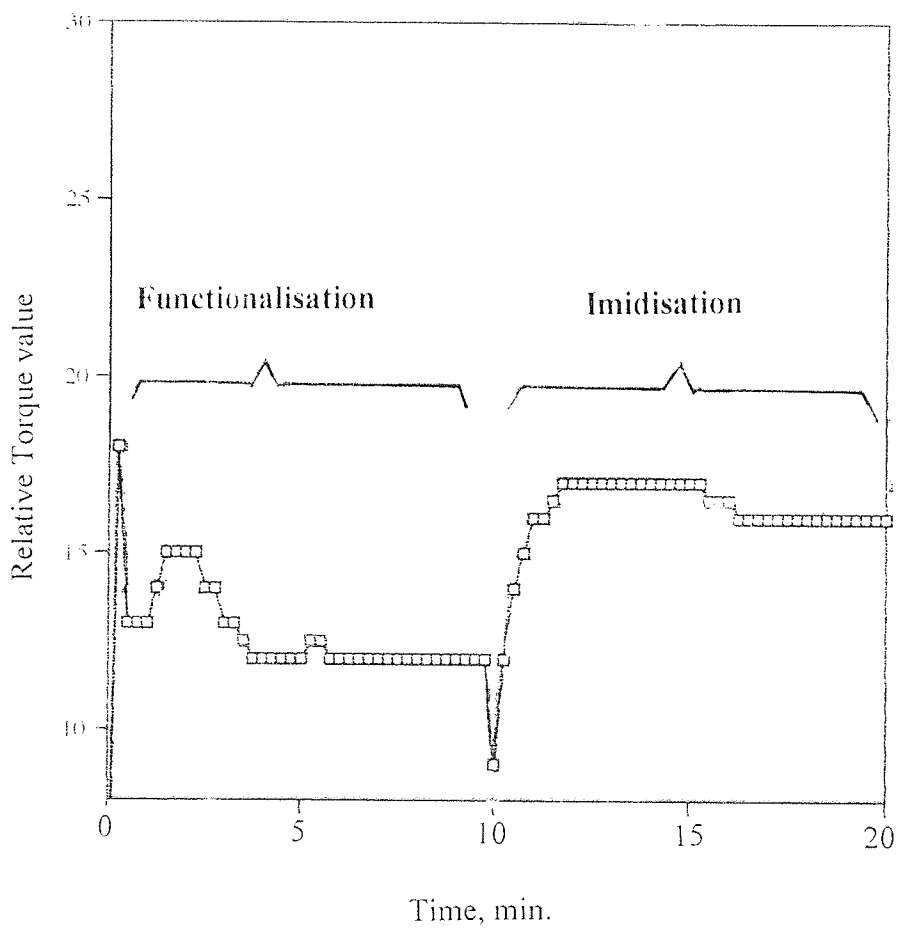
Figure 4.9: A typical torque - time curve for 'functionalisation' of PP/EPDM with MA, and 'imidisation' of maleated PP/EPDM by HEMDA.
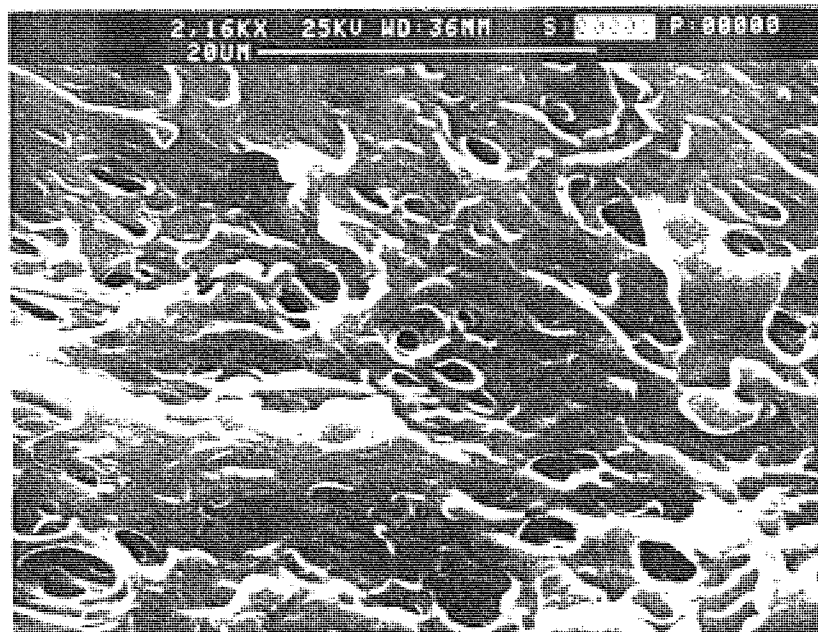
(a)
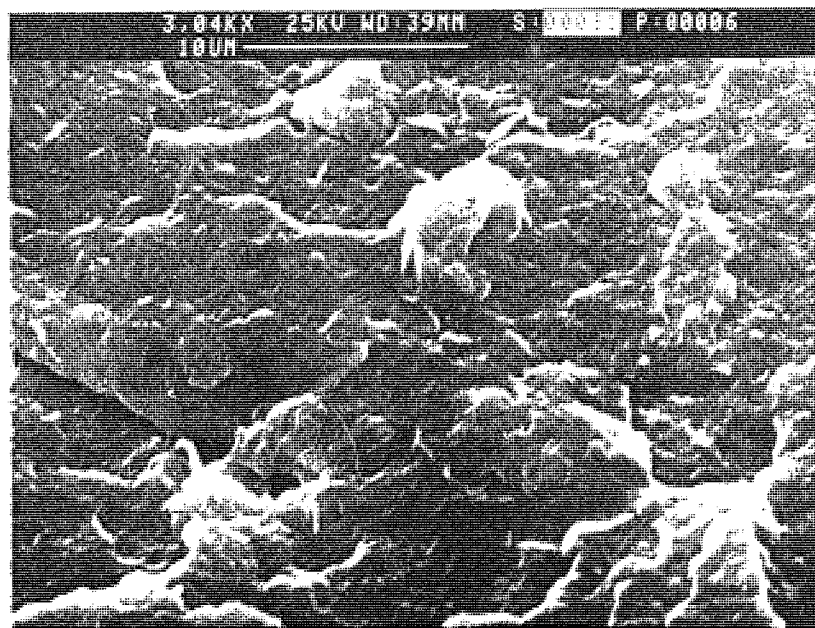
(b)

Figure 4.10: A typical SEM micrograph of binary blend PP/EPDM (a) and PP/EPDM copolymer. SPD 81 (b). The chemical composition of copolymer SPD 81 is PP/EPDM 75/25 – 6 phr MA – 4 phr TRIS – 0.002 m.r. T101 – 10 phr HEMDA. Note brittle mode of failure in SPD 81 (b).

CHAPTER 5

COMPATIBILISATION OF PP/EPDM BLENDS
USING PP/EPDM COPOLYMER

5.1 OBJECTIVE AND METHODOLOGY

Binary blends of PP and EPDM are immiscible under most conditions in both melt and solid state [80,89,94,]. Due to the difference in their viscosities, melt blends of most commercial grades of PP and EPDM have particle larger than optimum size [81,85], so there is a strong interest in finding ways to improve the dispersion. One such method is the addition of block or graft copolymers as compatibilisers. In the previous chapter, reactive processing of maleated PP/EPDM in an internal mixer in the presence of interlinking agent HEMDA was shown to form PP/EPDM copolymers via imidisation (imide linkage). It was expected that during the synthesis of the copolymers, maleated PP and maleated EPDM were linked via the amino groups of HEMDA to form copolymers of PP-HEMDA-EPDM (PP-g-EPDM). Because the segments of such copolymers are similar to the structure of the components of the blends i.e. homopolymer PP and homopolymer EPDM, the copolymers are expected to serve as effective compatibilisers for binary blends of PP/EPDM.

The object of the work described in this chapter is to investigate the effect of selected synthesised PP-g-EPDM copolymers (referred to here as solid phase dispersants - SPD) as compatibilisers for PP/EPDM blends. Various factors effecting tensile properties and morphologies of the ternary PP/EPDM/SPD blends (compatibilised blends, CPB) such as

176

SPD concentration, and SPD contents such as HEMDA concentration were investigated. The results from ternary and binary blends are also compared.

The general methodology for compatibilisation of PP/EPDM is described in Scheme 5.1. Mixtures of PP and EPDM at ratio 75/25, were blended in an internal mixer under standard condition (180^0C , closed mixing, 60 rpm within 10 minutes) in the presence of various concentration of SPDs used as compatibilisers. Two type of SPD used in this study were synthesised SPD based on 60/40 PP/EPDM and based on 75/25 PP/EPDM. The SPD used were either non-extracted SPD (SPD as described in Scheme 4.2 in Chapter 4) or extracted SPD (SPDx). The blends were compression moulded to 1 mm thick sheet for tensile test as procedure described in Section 2.15. Tensile fractured samples were used for examination of blend morphology under scanning electron microscopy (SEM).

5.2   RESULTS

5.2.1   Tensile Properties of Binary Blends

A series of binary blends containing various ratios of PP and EPDM as listed in Table 5.1 were prepared and the tensile properties were measured. Figure 5.1 shows that PP homopolymer exhibit good tensile strength (TS) and Young's modulus but very low elongation to break (E_b) and toughness factor (TF) when compared to PP-EPDM blends. As expected, the addition of EPDM drastically reduces the strength and stiffness of PP

but significantly improves the extension capabilities and toughness factor. At constant ratio of PP to EPDM, e.g. 75/25, the strength and modulus of PP homopolymer were reduced by about 100%, whereas the elongation at break and toughness factor were drastically enhanced from 15% to 440%, and 4.2 MPa to 69 MPa, respectively. As the ratio of PP to EPDM was increased , properties such a tensile strength, modulus also increased. The percentage of changes in tensile properties of the binary blends upon addition of the rubber component is dependant on the concentration of EPDM in the blends. Blends containing higher portions of the rubber component showed lower strength and stiffness but better elongation and toughness.

5.2.2 Tensile Properties of Ternary Blends of PP/EPDM

Binary 75/25 PP/EPDM blends were selected for compatibilisation work. The SPD used was either non-extracted SPDs (SPD) (see Scheme 4.2) or extracted SPD (SPDx) (see Scheme 5.2) of maleated PP/EPDM copolymers with 75/25 (SPD7525) and 60/40 (SPD6040) ratio components. List of compatibilised blends (CPB) i.e. ternary blends, and their tensile properties are tabulated in Table 5.2 to Table 5.5. The related data are plotted in Fig. 5.2 to Fig. 5.6. A typical stress- strain diagram for binary and compatibilised blends is shown in Fig. 5.7.

5.2.2.1 Effect of SPD concentration

Fig. 5.2 (see Table 5.2) shows that, within the SPD concentration studied, the addition of SPD6040 into the binary PP/EPDM blends have significantly increased both values of

178

tensile strength and modulus of the compatibilised blends but lowered the elongation and toughness factor of these blends. All compatibilised blends across the HEMDA and SPD concentration studied, suffered from lower elongation and toughness factor when compared to the control blend. An exception was for a blend compatibilised with 1 phr SPD6040 containing 3 phr HEMDA (CPB141 in Table 5.2).

Fig 5.2 also indicates that addition of higher SPD6040 concentration results in lowering effect on tensile properties of the compatibilised blends. This trend could be clearly seen in Fig. 5.3 (see Table 5.3). Addition of 1% SPD6040 significantly improved the tensile properties. Further increases in SPD concentration in these blends reduced the tensile properties, with extension to break and toughness factor were effected adversely.

The effect of SPD7525 on tensile properties of compatibilised blends is shown in Fig. 5.4 and Table 5.4. Similar to SPD6040, addition of SPD7525 into the binary PP/EPDM blends have drastically improved both tensile strength and modulus of all compatibilised blends. Contrary to the blends compatibilised by SPD6040, elongation at break and toughness factor for SPD7525 compatibilised blends showed very promising results. All blends compatibilised with up to 3 phr SPD7525 could be elongated up to 20% higher and about 160% improvement on toughness factor over the control blend.

5.2.2.2 Effect of HEMDA concentration in SPD

Fig. 5.2 and Fig. 5.4 show that, at constant SPD concentration, the effectiveness of SPD

in compatibilising PP/EPDM blends was effected by the amount of interlinking agent HEMDA introduced during the imidisation reaction in the SPD synthesis. However there was no direct correlation between HEMDA concentration and tensile properties. SPD6040 containing 3 phr HEMDA shows highest overall tensile properties however there was no clear trend in the case of SPD7525.

5.2.2.3   Effect of extracted SPD (SPDx) and HEMDA concentration in SPDx on tensile properties of blends

Work described in Chapter 3 disclosed that in the presence of the co-agent TRIS, the optimum grafting level of MA onto PP/EPDM was about 58 % of the total MA left after processing in the maleated PP/EPDM (sample SB77 Table 3.7). For the non-extracted SPD, some of the HEMDA introduced during the imidisation step (see Scheme 4.2) could react with the grafted MA and some could react with the non-grafted MA contained in the maleated PP/EPDM. To examine the effective concentration of HEMDA needed to optimise the tensile properties of compatibilised blends; it must be ensured that the amount of interlinking agent HEMDA introduced would react with grafted MA only and not with the non-grafted MA. In this work the maleated PP/EPDM copolymers were exhaustively extracted in hot DCM to remove any non-grafted MA before further reaction with HEMDA to synthesise SPDx, see Scheme 5.2. It was assumed that during the imidisation reaction one amino group attached at one end of HEMDA will react with MA grafted onto PP while the other amino group at another end of HEMDA will react with MA grafted onto EPDM.

A series of blends compatibilised by various concentrations of extracted SPD6040 (SPD6040x) were prepared and the tensile properties are shown in Table 5.5 and in Fig. 5.5. Various concentrations of HEMDA were introduced during the imidisation reaction step of SPD6040x. The counterpart blends compatibilised by non-extracted SPD6040 were listed in Table 5.2 and plotted in Fig. 5.2.

Removal of the non-grafted MA from maleated PP/EPDM before imidisation reaction step was found to affect the tensile properties of blends compatibilised with extracted SPD6040x. Generally all the tensile properties show similar trend as blends compatibilised with non-extracted SPD but with lower value (see Fig. 5.6).

5.2.3 Morphology of Blends

SEM micrographs of the tensile fractured surfaces of the binary blend of PP/EPDM 75/25 is shown in Fig. 5.8 which clearly demonstrates a two-phase morphology. The voids formed by the minor EPDM phase exists as a semi-continuous planar domain, is surrounded by the continuous PP matrix. The smeared out shape of rubber particles could be a result of mechanical blending operations. Many voids suggest that the dispersed rubber particles were pulled out during tensile-stress experiment because of the poor adhesion between the two phases. The fractured surface is very clean, the EPDM droplets were separated from the matrix, and their smooth surface appears practically not to be effected by the tensile stress. The size of the rubber particle is quite small with size varying from 0.5 μm to 5 μm.

181

Fig 5.9 shows the surfaces of a PP/EPDM 75/25 blend compatibilised with PP/EPDM75/25 copolymers, sample CPB179 (see Table 5.4). Addition of 1 phr compatibiliser has significantly modified the surface morphology which reflects the strong adhesion between PP matrix and EPDM particles in this case. The surface morphology is not very much affected with addition of higher compatibiliser concentration (Fig.5.10). Similarly the concentration of HEMDA in the SPD has no clear effect on the surface morphology of the compatibilised blends (Fig.5.11).

The SEM micrographs also indicate the mode of failure of the blends. It is clear that the binary blend (Fig.5.8) experienced a brittle mode of failure while the compatibilised blends experienced both brittle and ductile mode of failures (Fig.5.9 and Fig.5.10). Furthermore the compatibilised blends showed discrete rubber particle size of about 1 μm size which are homogeneously distributed across the surface.

5.3 DISCUSSION

The main reason for blending rubbers such as EPDM with PP is for improving the toughness of the thermoplastic polymer either at ambient temperature or sub-ambient temperatures, by providing a new energy-absorbing mechanism with minimum effect on other properties of the polymer components [83,94]. Fig.5.1 shows clearly that addition of EPDM has significantly improved tensile, elongation and toughness factor of PP while lowering tensile strength and modulus.

182

The incorporation of an elastomer as a minor phase in a thermoplastic-elastomer blend would induce one of the two mechanism's of failure; crazing or shear yielding in the semicrystalline thermoplastic polymer [142]. Rubbery particles differ from other inclusions in being able to delay the formation of a crack of catastrophic size. Shear deformation consists of a distortion of shape under stress without significant change in volume. The basis of the multiple crazing theory advanced by Bucknell and Smith [142] explains that rubber particles would both initiate and control the craze growth. Under tensile stress, crazes are initiated at points of maximum principle strain, which are usually near the equators of rubber particles, and propagate outwards, again following planes of maximum principal strain. Craze growth is terminated when the stress concentration at the tip falls below the critical level for propagation, or when a large rubber particle or other obstacle is encountered. The result is a large number of small crazes, in contrast with the small number of large crazes formed in the same polymer in the absence of rubber particles. Consequently the rubber modified thermoplastic can reach a much higher strain energy density before fracture.

In the binary PP/EPDM blends examined here, it seems that the failure termination mechanisms as stated above are less effective. Instead of stabilising the craze, a weakly bonded rubber particle is pulled out away from the matrix (see Fig.5.8) leaving a hole from which the craze can propagate further, and from which breakdown of the craze to form a crack becomes highly probable.

The adverse effect of weakly bonded rubber particles in the to PP matrix has been dealt with, in this work, through the use of compatibilisers which are based on synthesised block copolymers of PP-g-EPDM. Data presented in this chapter have clearly shown that synthesised PP-g-EPDM copolymers are effective compatibilisers (or solid phase dispersant, SPD), especially in the case of binary blends of PP/EPDM 75/25. A pronounced improvement in the properties of binary blends of PP/EPDM have resulted from compatibilisation (Fig.5.12). The evidence suggests that both crazing (see Fig.5.9a and Fig.5.10a) and shear yielding (Fig.5.9b and Fig.5.10b) failure mechanisms occur simultaneously in compatibilised PP/EPDM blends. SEM micrograph of compatibilised blends (Fig.5.9a) show a ductile mode of failure reflecting a pronounced adhesion between rubber particles and PP matrix with evidence of fabrils. Shear yielding takes place by slip on specific slip planes, as a result of dislocation glide as shown in Fig. 5.9b . The dislocation glide, and fabrils formation undoubtedly result from drawing of the EPDM discrete particles during fracture, an evidence to very strong adhesion between phases, consequently improve the physical properties of the blends. These micrographs definitely prove that the graft does play an interfacial role although this is not simple as the ideal visualised in Fig. 1.3 (in Chapter 1). Additional evidence of interfacial activity is the reduction in domain size accross the fractured surface attending efficient distribution of compatibiliser (compare Fig.5.8 , Fig.5.9b, Fig. 5.10b and 5.11).

The synthesised PP/EPDM copolymers have identical components with the blend components (PP and EPDM). For thermodynamic reasons, the two parts of PP/EPDM copolymers would penetrate preferentially into their respective polymer phases. By this

184

mechanism, the graft copolymer is expected to be capable of acting as interfacial agent in the polymer blends [143,144]. This could be related to the copolymer that serves to reduce the interfacial tension and helps strengthen the adhesion at the phase boundary, thus stabilises the morphology of the mixture. As a result, PP/EPDM 75/25 blends compatibilised with synthesised PP/EPDM copolymers show excellent strength and stiffness properties than binary 75/25 blend. It is shown in Fig. 5.12 that PP/EPDM blends compatibilised with up to 3 % PP/EPDM 75/25 copolymers exhibit overall better tensile properties over the binary blend. Of these, a series of blends compatibilised with 1 phr PP/EPDM75/25 copolymers which are interlinked with, within the concentration studied, up to 15 phr HEMDA, show optimum performance (Figures 5.12 and 5.13).

COMPATIBILISATION OF PP/EPDM BLENDS

```
┌─────────────────────┐   ┌──────────┐   ┌──────────┐
│  SPD or  SPDx       │   │   PP     │   │  EPDM    │
│   0 - 15 phr        │   │  75 phr  │   │  25 phr  │
│ SPD, see Sch. 4.2   │   └──────────┘   └──────────┘
│ SPDx, see Sch.5.2   │
└─────────────────────┘

              ┌──────────────┐
              │   tumble     │
              │   mixed      │
              └──────────────┘

      ┌──────────────────────────────┐
      │ Blending in the internal mixer,│
      │      180 C for 10 min.,        │
      └──────────────────────────────┘

         ┌──────────────────────┐
         │ Compatibilised blends │
         └──────────────────────┘

      ┌──────────────────────────────┐
      │ Pressed to 1 mm thick sheet   │
      │ at 180 C for 4 min. then cut  │
      │   to tensile test specimen    │
      └──────────────────────────────┘

      ┌──────────┐          ┌──────────────┐
      │   SEM    │          │ tensile test │
      └──────────┘          └──────────────┘
```
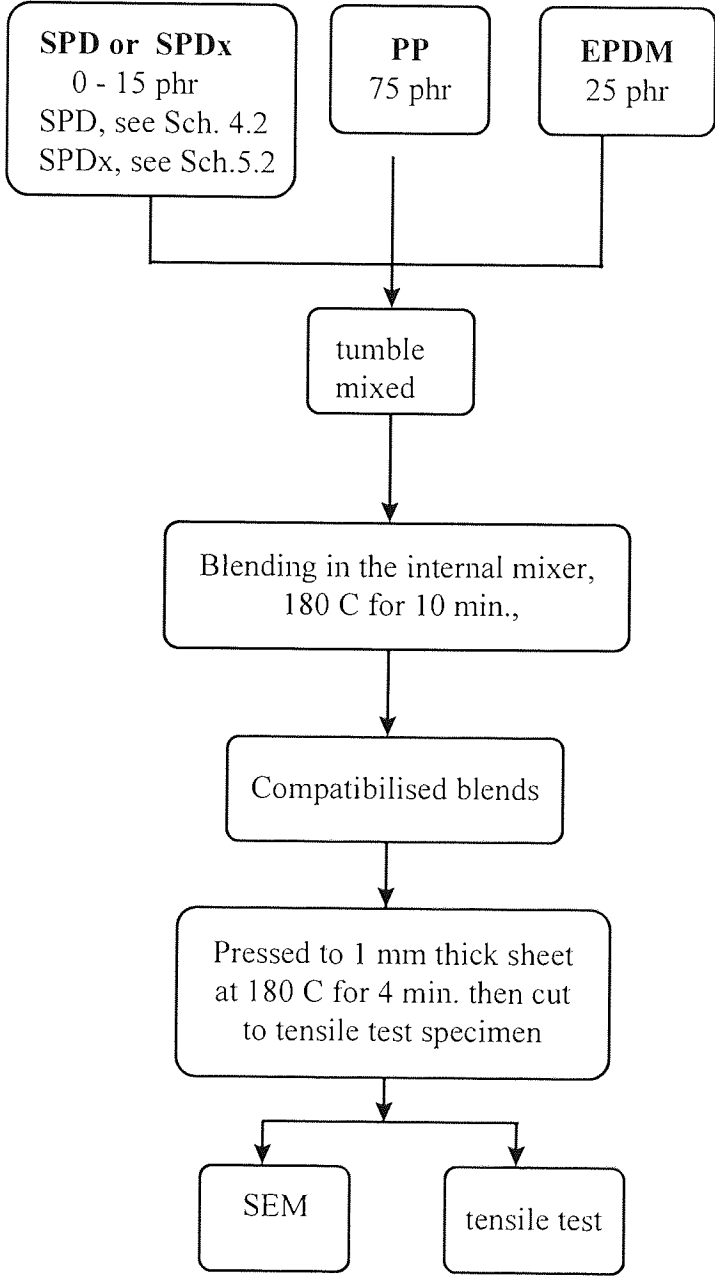
Scheme 5.1: Flow chart for compatibilisation of PP/EPDM blends using non-extracted solid phase dispersant (SPD) or extracted solid phase dispersant (SPDx). SPD was prepared according to Method B (see Scheme 4.2), and SPDx was prepared according to Scheme 5.2.

SYNTHESIS OF EXTRACTED SOLID PHASE DISPERSANT (SPDx) BASED ON EXTRACTED MALEATED BLENDS

```
┌──────────┐ ┌──────────┐ ┌────────┐ ┌─────────┐ ┌────────┐
│   PP     │ │  EPDM    │ │  MA    │ │  TRIS   │ │ T101   │
│75 or 60  │ │25 or 40  │ │0 - 6   │ │0 or 4   │ │        │
│  phr     │ │  phr     │ │ phr    │ │  phr    │ │        │
└──────────┘ └──────────┘ └────────┘ └─────────┘ └────────┘
```

Functionalisation of blends

```
          ┌───────────────────┐
          │   Tumble mixed    │
          └───────────────────┘

     ┌──────────────────────────────┐
     │ Processing in internal mixer │
     │ closed system, 180 C, 10 min.│
     └──────────────────────────────┘

        ┌────────────────────────┐
        │   Maleated PP/EPDM     │
        └────────────────────────┘
```

```
   ┌──────────────────────────────────────┐
   │ 48 hr. Sohlet extraction in DCM then  │
   │   dried overnight in vacuum at 60 C   │
   └──────────────────────────────────────┘
```

```
        ┌──────────────────────────┐
        │ extracted maleated PP/EPDM│
        └──────────────────────────┘
```

Imidisation

```
┌────────────────────────────────────────────────┐
│ Processing in internal mixer, closed system,    │        ┌────────┐
│ 180 C, lift-up ram (<20s) at 3 minutes to add   │◄───────│ HEMDA  │
│ HEMDA, closed system and continue processing    │        └────────┘
│ for 10 minutes                                  │
└────────────────────────────────────────────────┘
```

```
┌─────────────────────┐          ┌─────────────────────┐
│     extracted       │          │   Compatibilisation │
│ Solid Phase Dispersant│───────►│      PP/EPDM        │
│      (SPDx)         │          │  blend (Scheme 5.1) │
└─────────────────────┘          └─────────────────────┘
```

Scheme 5.2 : Flow chart for preparation of extracted solid phase dispersant (SPDx) from extracted maleated PP/EPDM

187

Table 5.1 : Tensile properties of PP and, PP/EPDM binary blends at various ratios. Detail data is in Appendix 5.1

PP/EPDM ratio	Tensile properties			
	TS, MPa	Ym, MPa	Eb, %	TF, MPa
60/40	11.9	299	328	33.0
75/25	17.5	387	440	69.4
80/20	21.5	474	550	70.4
PP	36.1	896	15	4.2

Table 5.2: Compatibilisation of PP/EPDM blends (75/25) using solid phase dispersant (SPD) containing non-extracted maleated PP/EPDM (60/40). The SPD is based on MB94[1] + **X** phr HEMDA. Detail data is in Appendix 5.2.

PP/EPDM 75/25 blends CPB	HEMDA in SPD[2] X phr	SPD[3] in blend phr	Tensile properties of compatibilised blends			
			TS, MPa	YM, MPa	Eb, %	TF, MPa
165	1	1	20.3	613	273	48.1
166	1	3	20.4	590	255	49.7
167	1	5	18.7	545	203	36.0
162	2	1	18.3	600	294	45.3
163	2	3	19.0	572	296	54.6
164	2	5	17.8	482	291	47.7
141	**3**	**1**	**21.5**	**661**	**475**	**98.8**
128	3	3	21.0	600	341	62.7
129	3	5	20.0	561	263	47.4
169	5	1	18.0	560	285	51.0
170	5	3	18.3	548	269	55.0
171	5	5	17.3	473	235	46.3
7525[4]	nil	nil	17.5	387	440	69.4
PP[5]	nil	nil	36.1	896	15	4.2

note :

1. MB94 (PP/EPDM 60/40 + 6phr MA + 4phr TRIS + 0.005m.rT101) see Table 4.2, contains 41% grafted MA (based on initial added MA concentration).
2. See Scheme 4.2 for synthesis of non-extracted SPD - Method B.
3. See Scheme 5.1 for compatibilisation
4. Blend 7525 is a binary blend of 75 phr PP and 25 phr EPDM used as a control.
5. PP is processed polypropylene homopolymer.

Table 5.3: Effect of nonextracted solid phase dispersant concentration on tensile properties of PP/EPDM blends (75/25). The SPD is based on MB94[1] + **3** phr HEMDA Detail data is in Appendix 5.3.

PP/EPDM 75/25 blends CPB	SPD in blend[2] phr	Tensile properties of compatibilised blends			
		TS, MPa	Ym, MPa	Eb, %	TF, MPa
141	1	21.5	661	475	98.8
128	3	21.0	600	341	62.7
129	5	20.0	561	263	47.4
143	7	18.8	599	247	43.3
130	10	17.2	481	248	37.6
7525	nil	17.5	387	440	69.4

Note: 1. MB94 (PP/EPDM 60/40 + 6phr MA + 4phr TRIS + 0.005m.rT101) , see Table 4.2, contains 41% grafted MA (based on initial added MA concentration).
2. See Scheme 5.1 for compatibilisation

Table 5.4: Effect of HEMDA concentration in **nonextracted solid phase dispersant** (SPD), and SPD concentration on tensile properties of compatibilised PP/EPDM blend (75/25). The SPD is based on MB65[1] + **X** phr HEMDA. Detail data is in Appendix 5.4.

PP/EPDM blends CPB	HEMDA conc.in SPD[2] X phr	SPD in blend[3] phr	Tensile properties of compatibilised blends			
			TS, MPa	Ym, MPa	Eb, %	TF, MPa
178	3	1	19.4	495	566	109
184	3	3	19.8	550	505	94.1
187	3	5	18.3	546	346	58.8
190	3	10	17.1	537	370	60.9
173	5	1	18.9	554	477	91.3
125	5	3	21.9	632	473	73.2
126	5	5	20.2	587	267	52.0
179	10	1	21.0	537	566	111.4
185	10	3	19.0	575	587	99.6
188	10	5	17.5	501	493	73.5
191	10	10	18.4	514	319	59.9
180	15	1	19.2	548	537	97.2
186	15	3	19.6	603	472	88.0
189	15	5	18.9	581	350	69.4

Note: 1. MB65 (PP/EPDM 75/25 + 6phr MA + 4phr TRIS + 0.002m.r T101) see Table 4.2 contains 28% grafted MA (based on initial added MA concentration).
2. See Scheme 4.2 for synthesis of non-extracted SPD - Method B.
3. See Scheme 5.1 for compatibilisation

Table 5.5: Effect of HEMDA concentration in **extracted solid phase dispersant** (SPDx), and SPDx concentration on tensile properties of compatibilised PP/EPDM blend (75/25). The SPD[1] is based on MB94 + **X** phr HEMDA. Detail data is in Appendix 5.5.

PP/EPDM blends CPB	HEMDA conc. in SPD$_x$ X phr	SPDx in blend phr	Tensile properties of compatibilised blends			
			TS, MPa	Ym, MPa	Eb, %	TF, MPa
1471	1	1	20.7	593	187	34.5
1473	1	3	19.5	587	162	27.7
1475	1	5	19.1	565	114	18.5
1481	3	1	19.6	555	267	38.9
1483	3	3	19.2	625	222	36.4
1485	3	5	18.5	610	212	31.6
1491	5	1	19.0	614	249	37.8
1493	5	3	18.0	602	168	25.6
1495	5	5	18.1	620	132	20.7

note:

1. MB94 (PP/EPDM 60/40 + 6 phr MA + 4phr TRIS + 0.005 m.r T101) contains 41% grafted MA (based on initial added MA concentration).
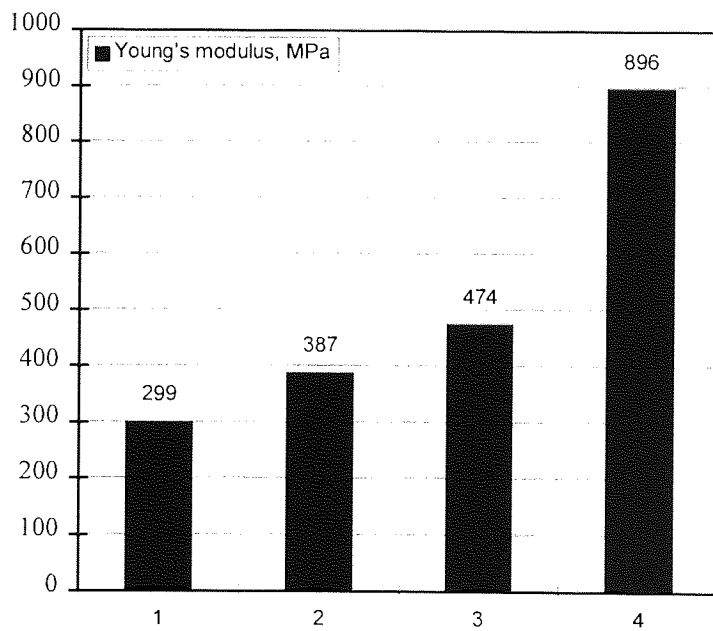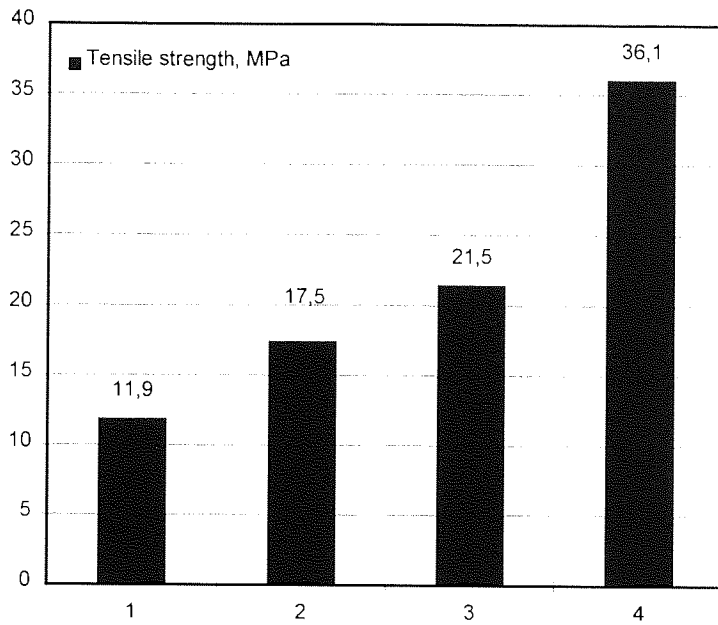
Figure 5.1: Tensile properties of PP and various ratios of PP to EPDM binary blends (1) 60/40 (2) 75/25 (3) 80/20 and (4) PP only
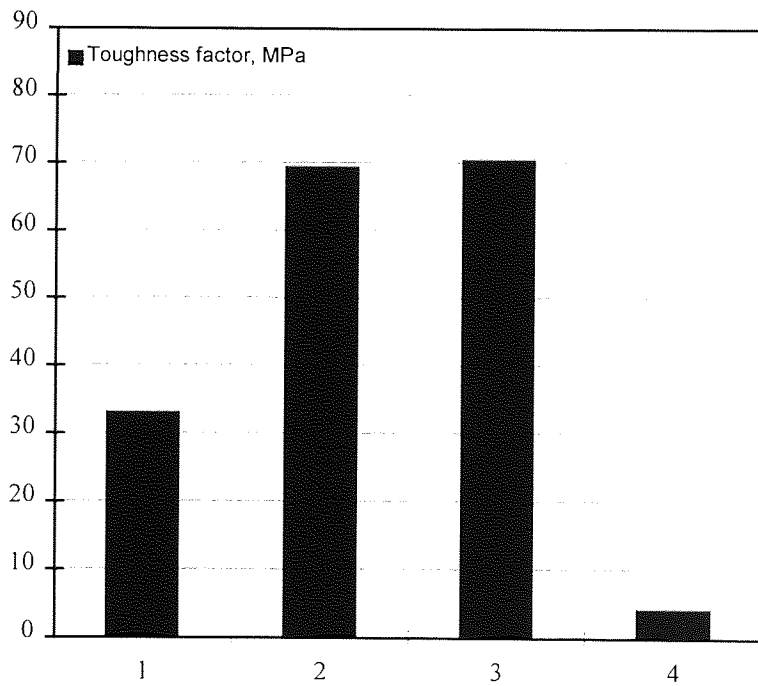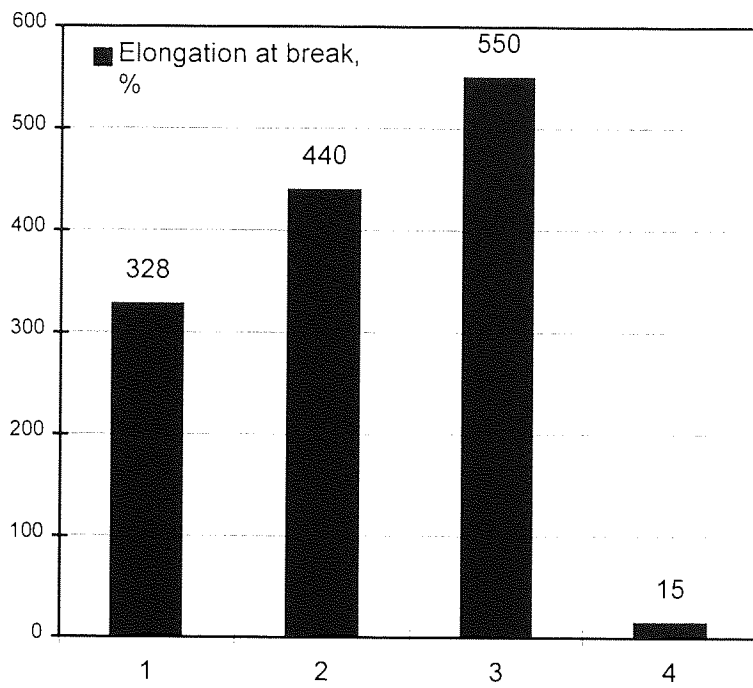
continue from Figure 5.1
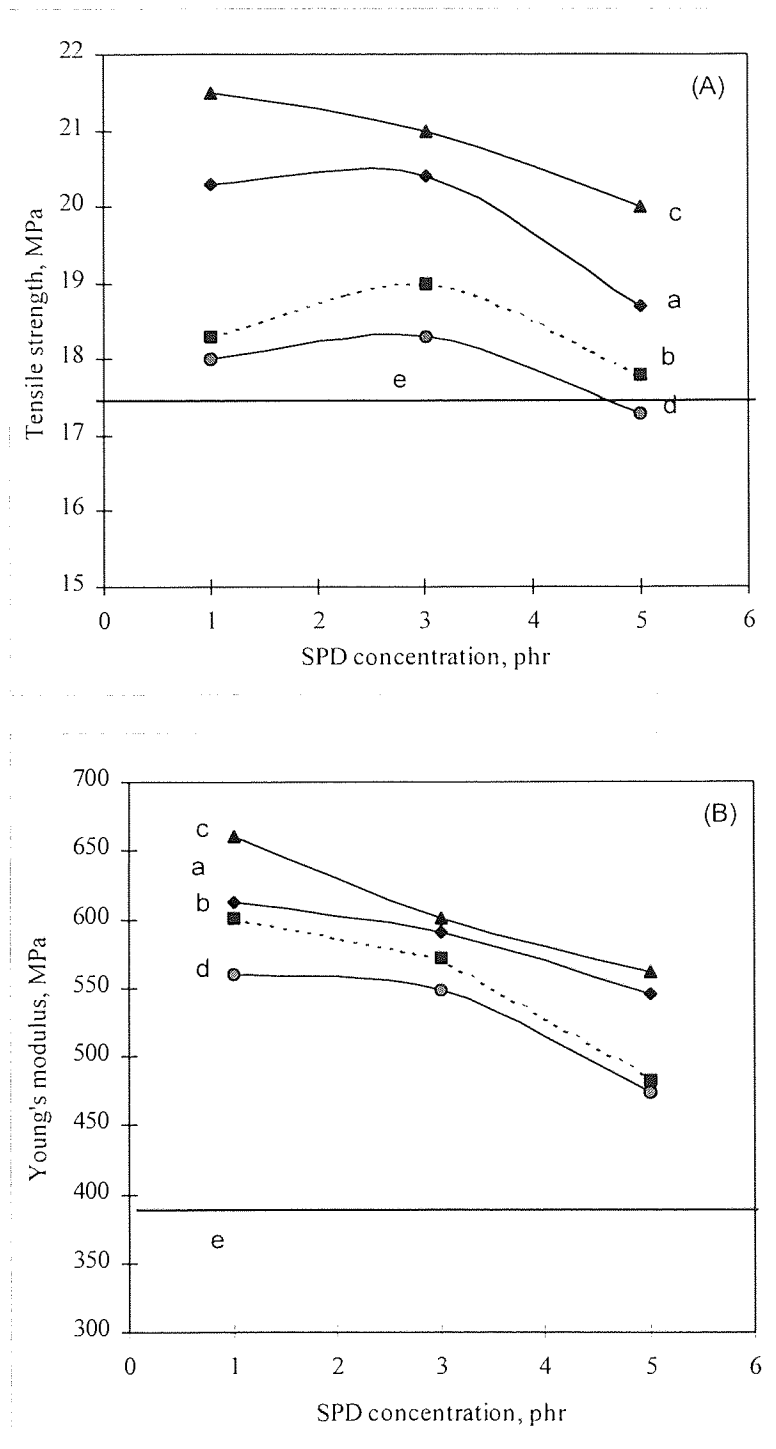
Figure 5.2: Effect of solid phase dispersant (SPD) containing non-extracted maleated PP/EPDM on tensile properties of PP/EPDM 75/25. The SPD is based on MB94 (PP/EPDM 60/40 + 6 phr MA + 4 phr TRIS + 0.005 m.r T101) + HEMDA. HEMDA concentration is (a) 1 phr (b) 2 phr (c) 3 phr and (d) 5 phr.. (e) is related binary blend value. Refer to Table 5.2 for related data.

193
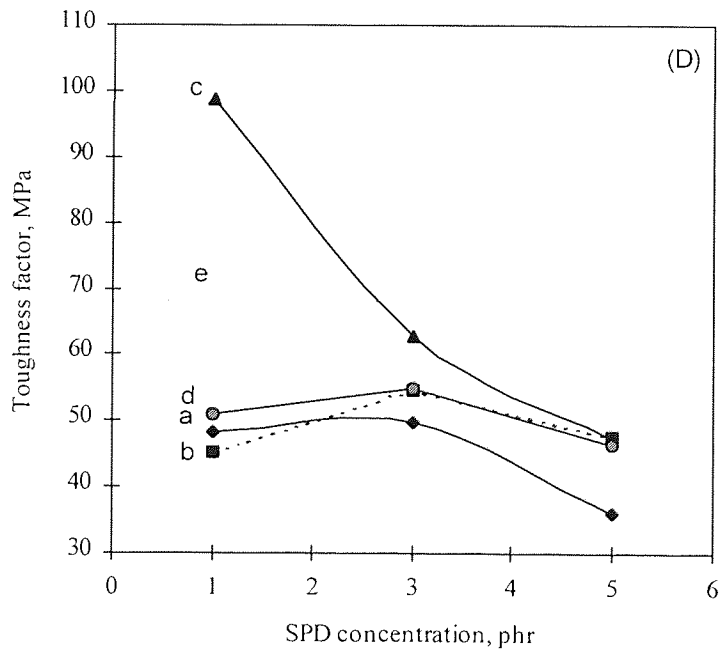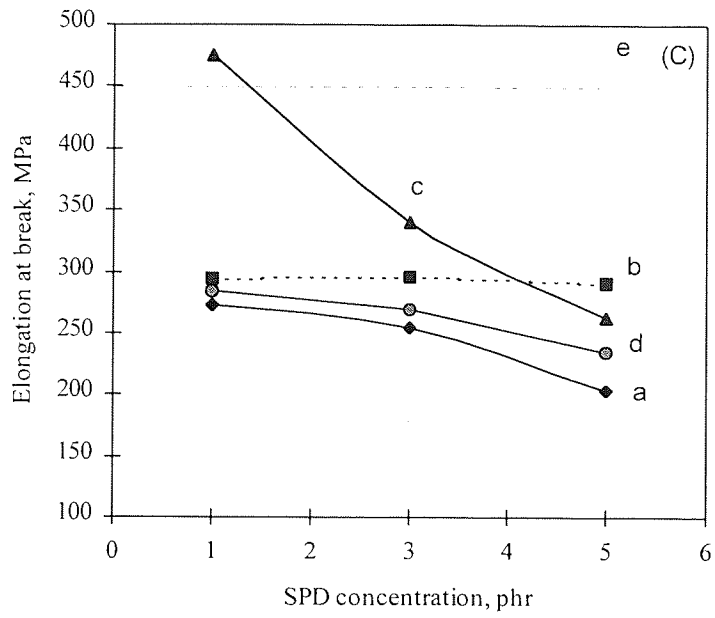
continue from Figure 5.2

194
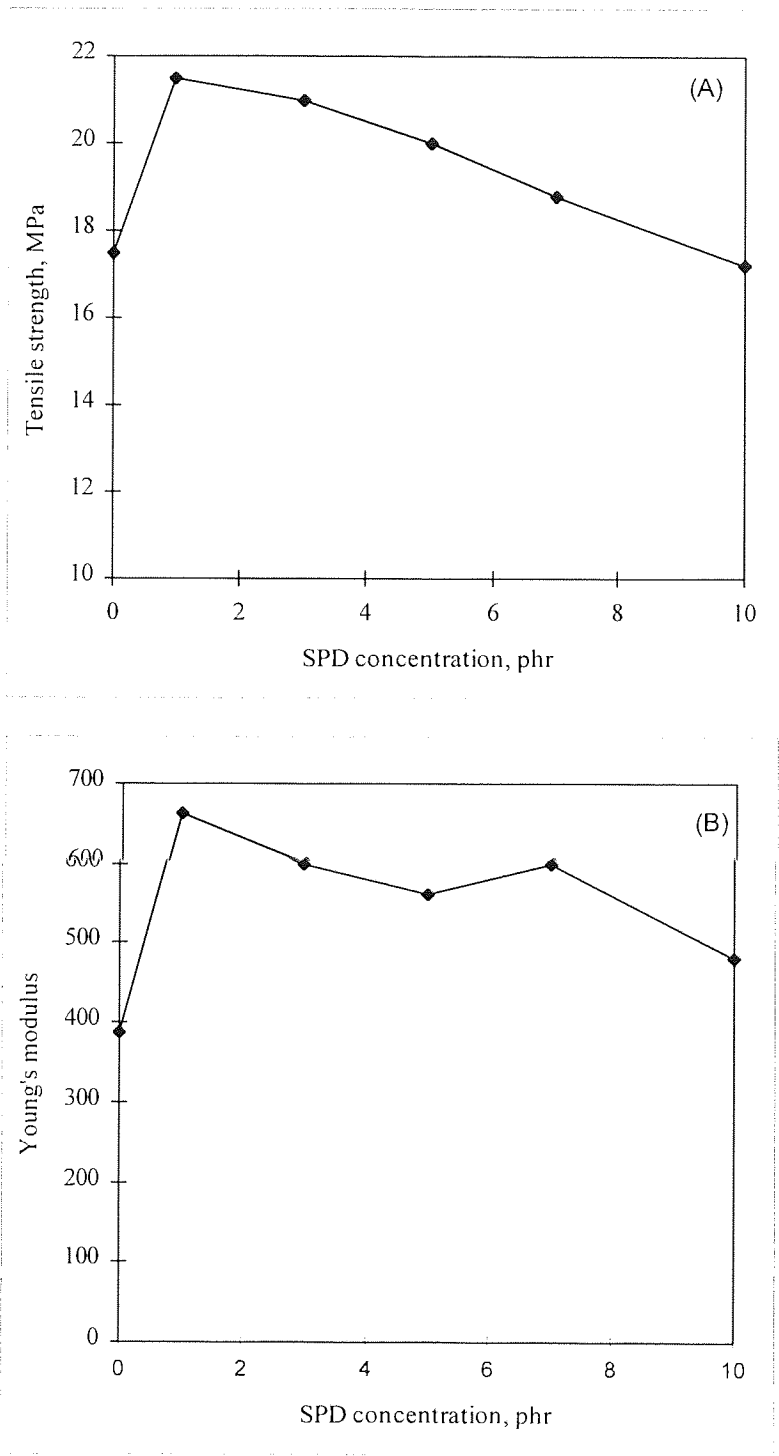
Figure 5.3: Effect of non-extracted SPD concentration on tensile properties of PP/EPDM blends 75/25. The SPD is based on MB94 + 3 phr HEMDA. Chemical composition for MB94 is PP/EPDM (60/40) + 6 phr MA + 4 phr TRIS + 0.005 m.r T101. Refer to Table 5.3 for related data.

(C)

(D)
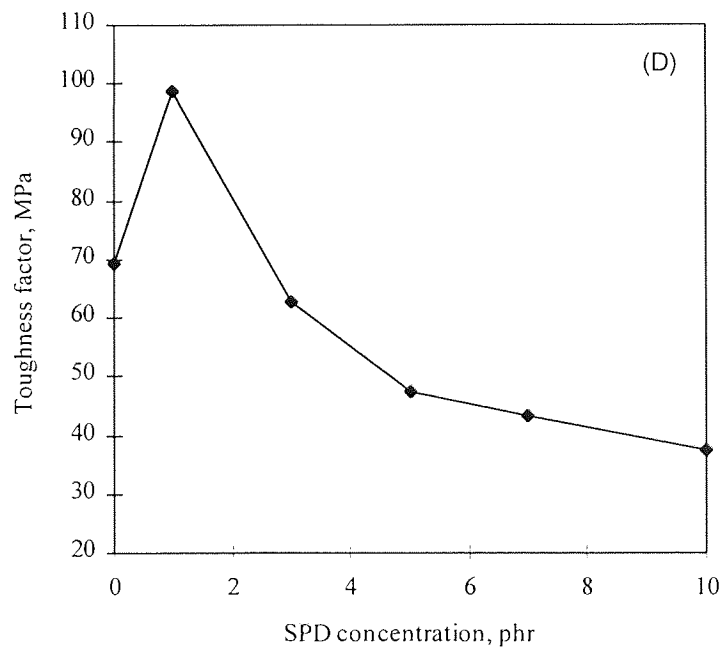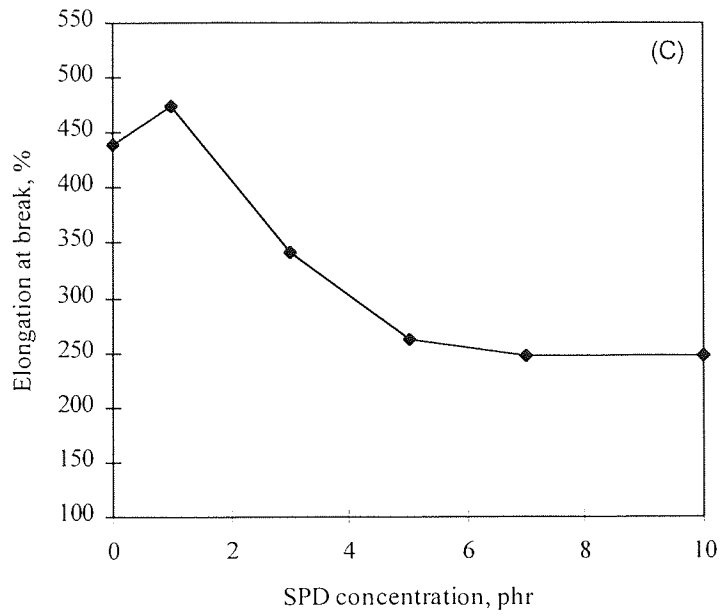
continue from Figure 5.3
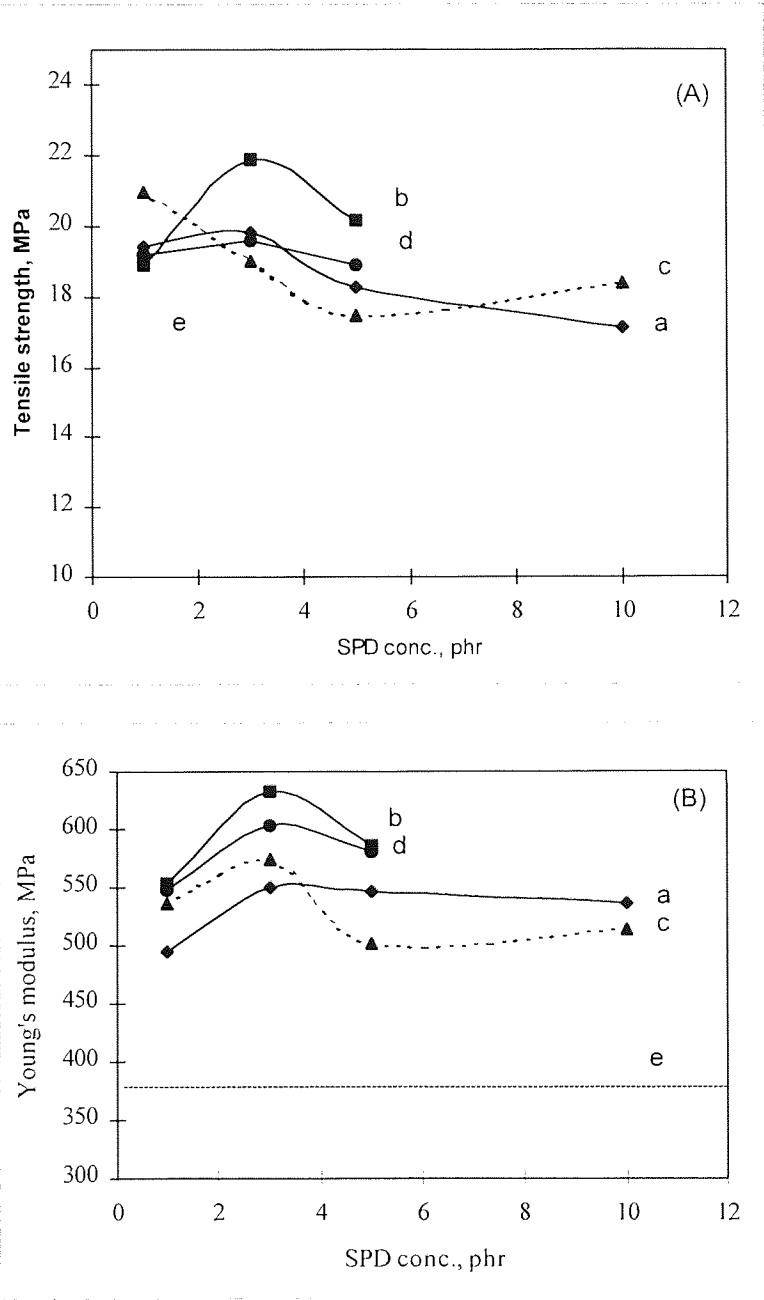
Figure 5.4: Effect of SPD and HEMDA concentrations in SPD on tensile properties of PP/EPDM 75/25. The SPD is MB65 + various concentration of HEMDA. HEMDA concentration is (a) 3 phr (b) 5 phr (c) 10 phr (d) 15 phr. (e) is related binary blend value. Composition for MB65 is PP/EPDM 75/25 + 6phr MA + 4phr TRIS + 0.002 m.r. Refer to Table 5.4 for related data.

197

(C)

(D)
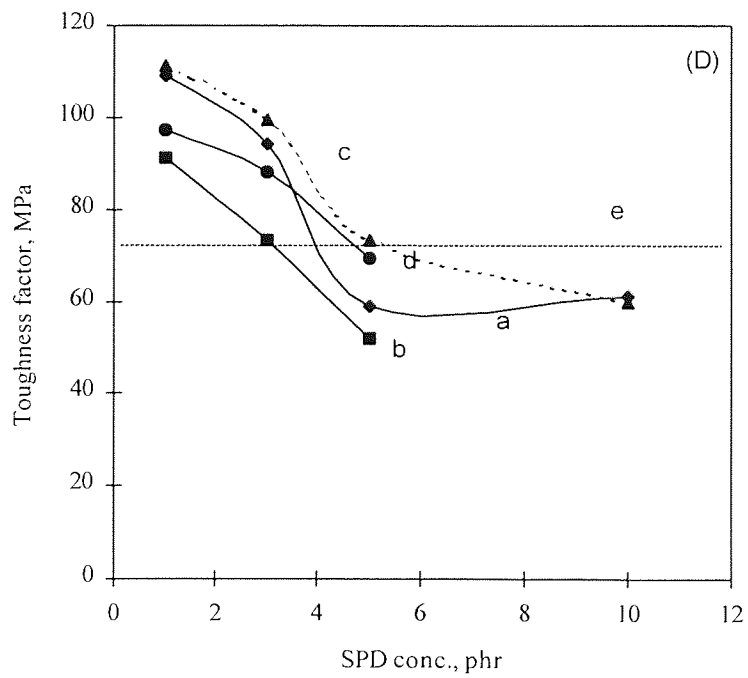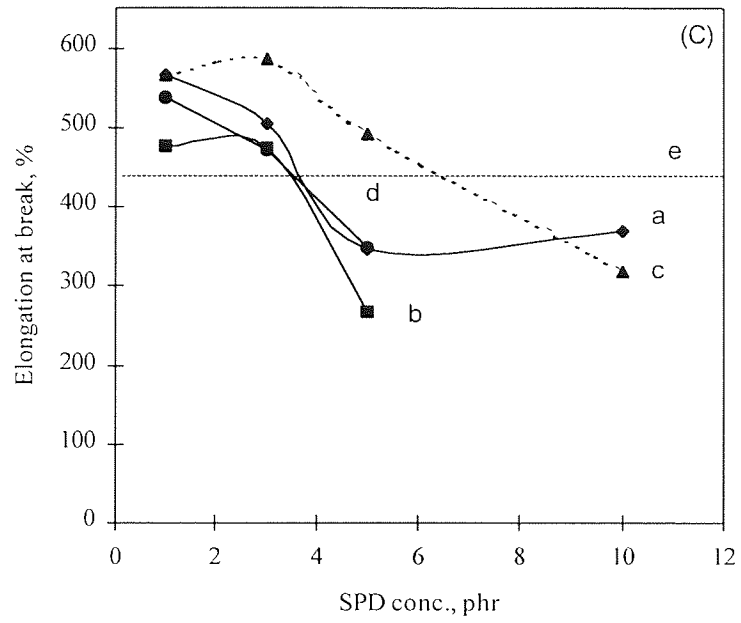
continue from Figure 5.4
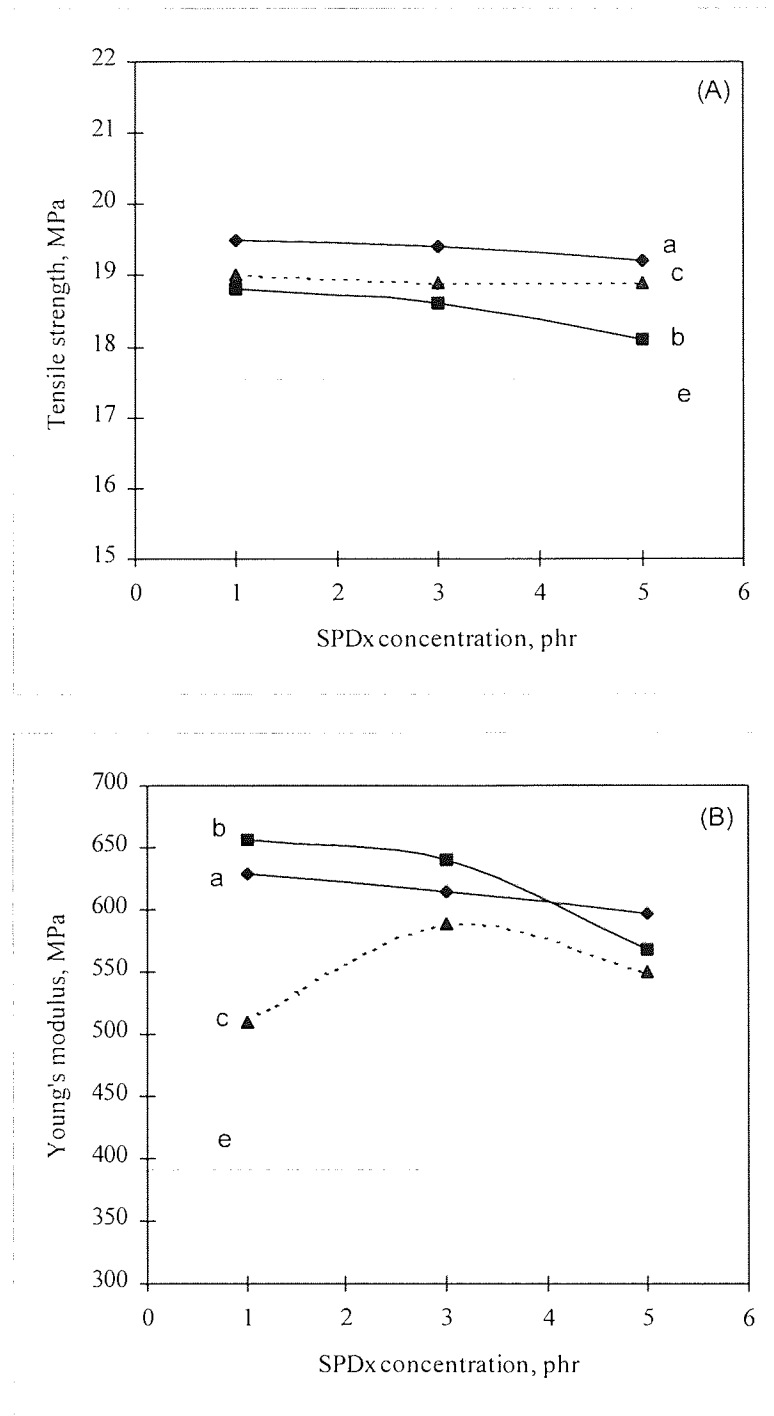
Figure 5.5: Effect of SPDx containing extracted maleated PP/EPDM (60/40) on tensile properties of PP/EPDM 75/25. The SPDx is extracted MB94 + various concentration of HEMDA. The MB94 is PP/EPDM 60/40 + 6phr MA + 4phr TRIS + 0.005 m.r. HEMDA concentration is (a) 1 phr (b) 3 phr and (c) 5 phr. (e) is related binary blend value. Refer to Table 5.5 for related data.

199

(C)

(D)
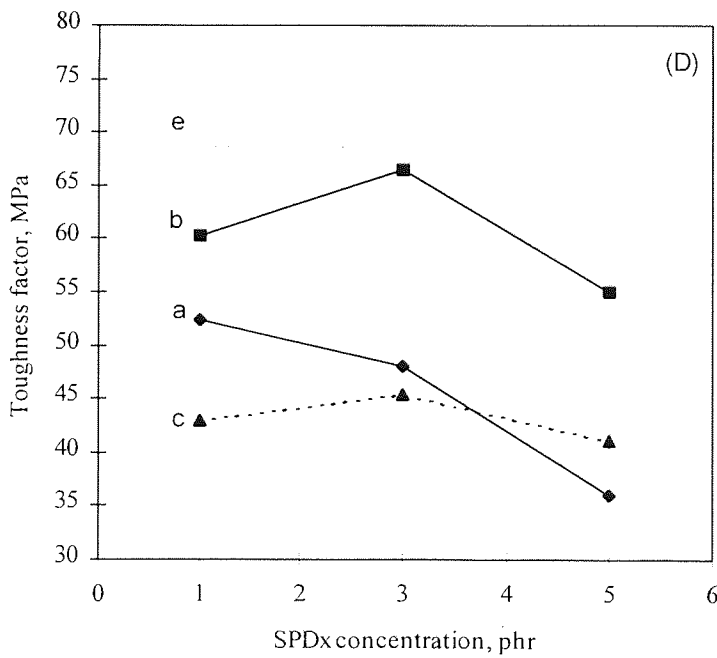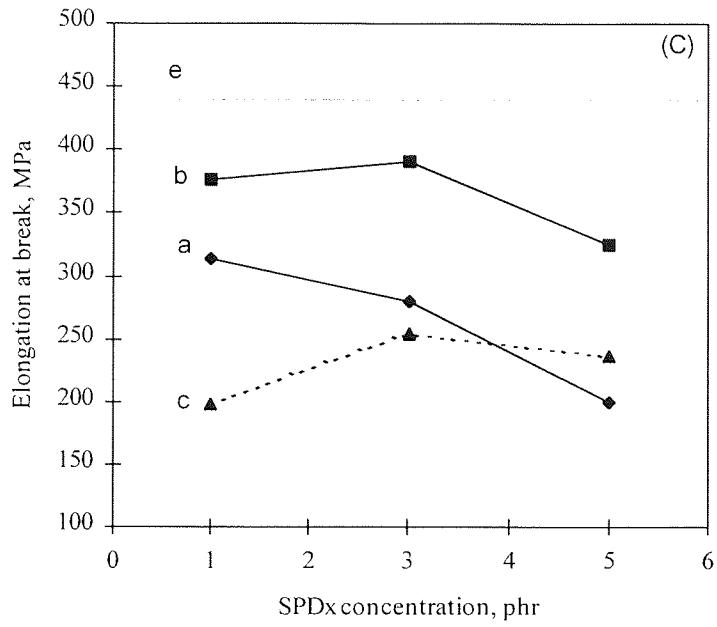
continue from Figure 5.5
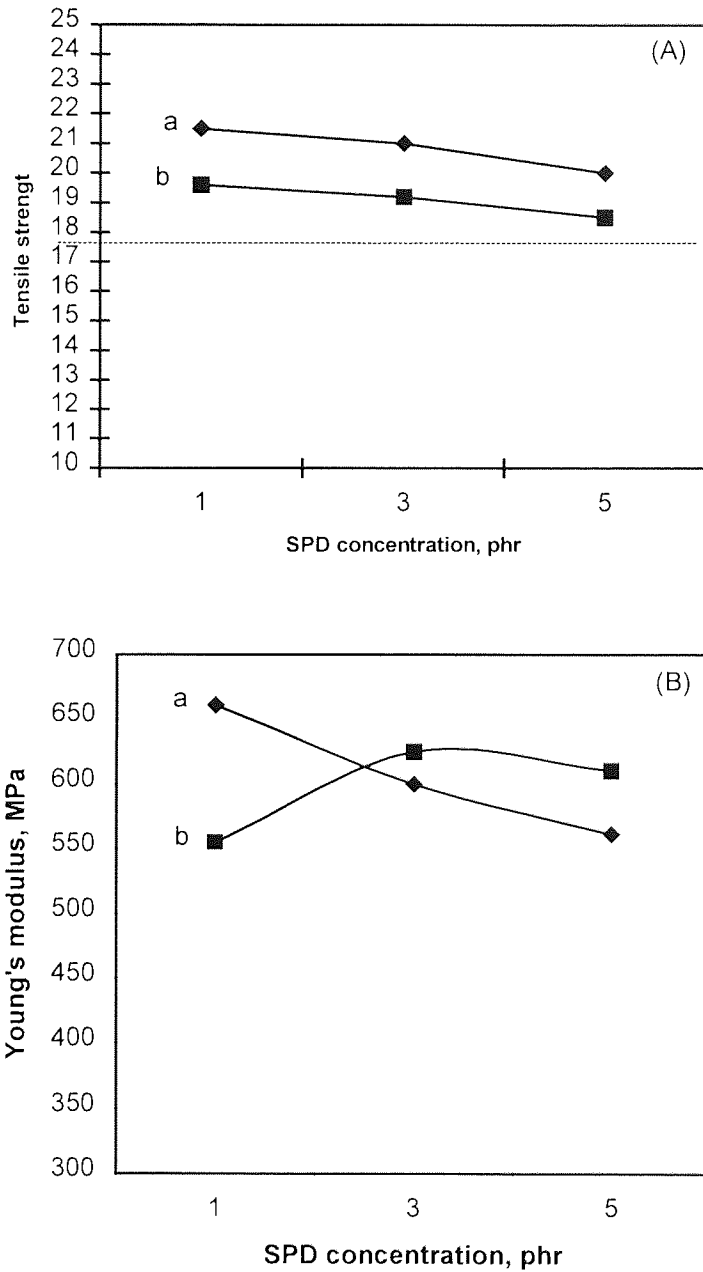
Figure 5.6 : Effect of non-extracted solid phase dispersant (SPD) (a) and extracted SPD (SPDx) (b) at various concentrations on tensile properties of PP/EPDM75/25. The SPD is based on MB94 (PP/EPDM 60/40 + 6phr MA + 4phr TRIS + 0.005 m.r T101 + 3 phr HEMDA. Refer to Table 5.2 for non-extracted SPD and Table 5.5 for extracted SPD.

201
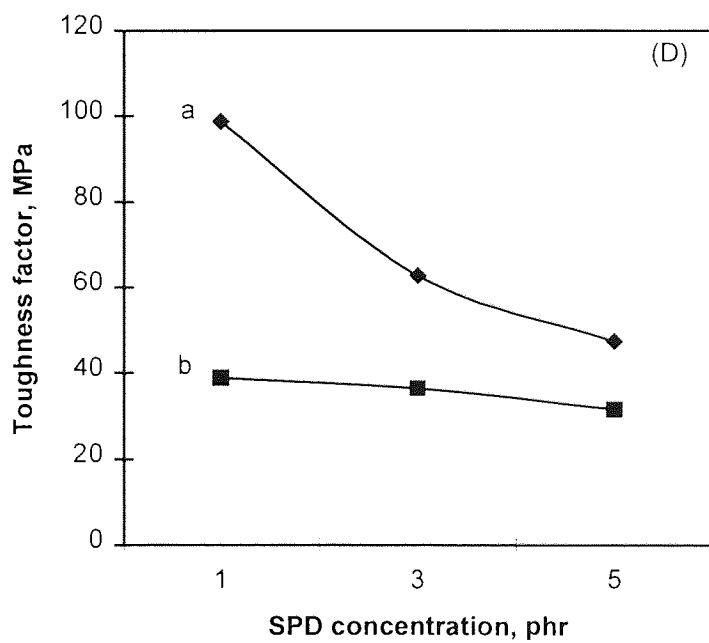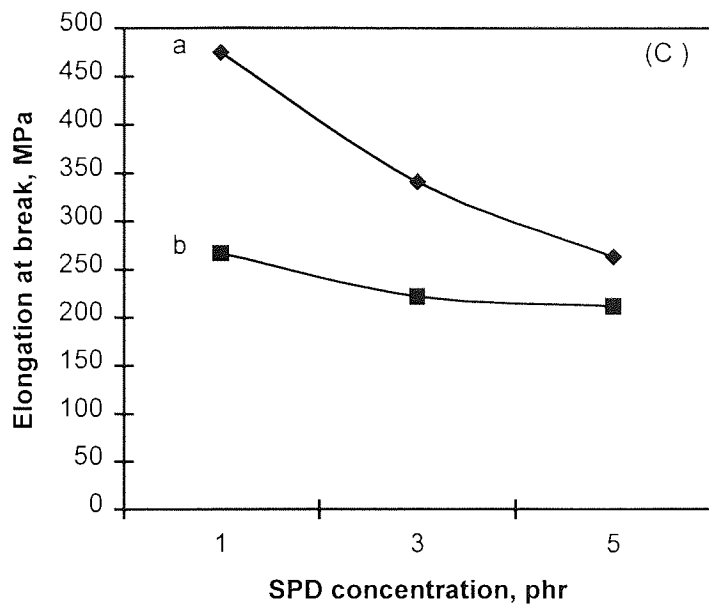
continue from Figure 5.6
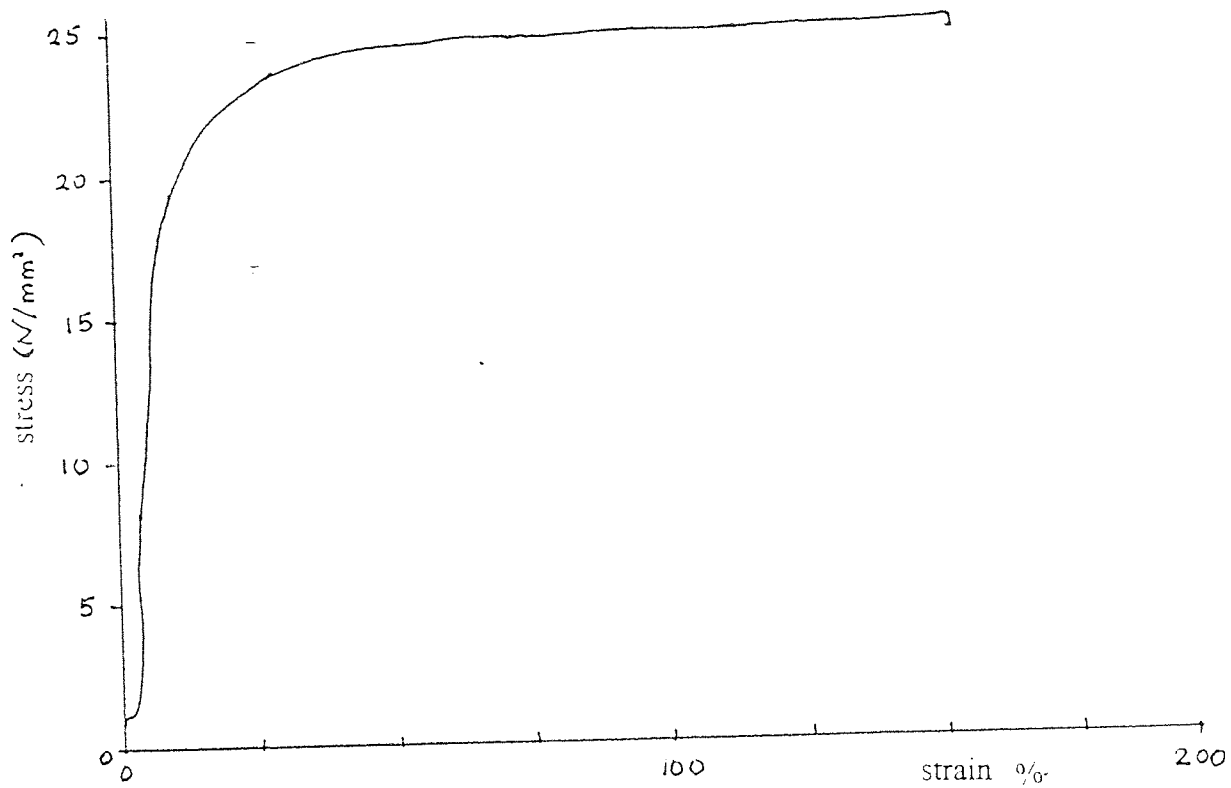
Figure 5.7: A typical stress-strain diagram for compatibilised PP/EPDM blends
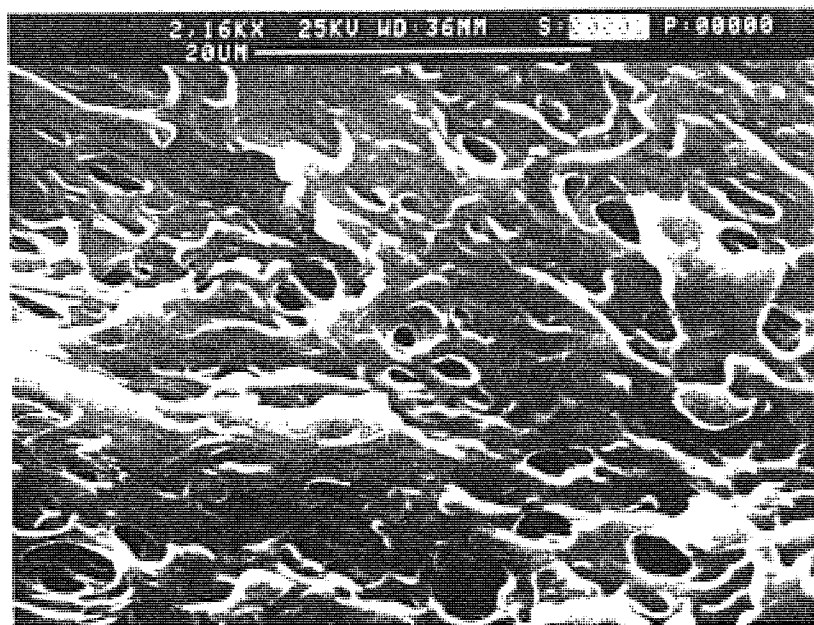
Figure 5.8: SEM micrograph of binary blend PP/EPDM 75/25. Note the two phases system and the brittle mode of failure
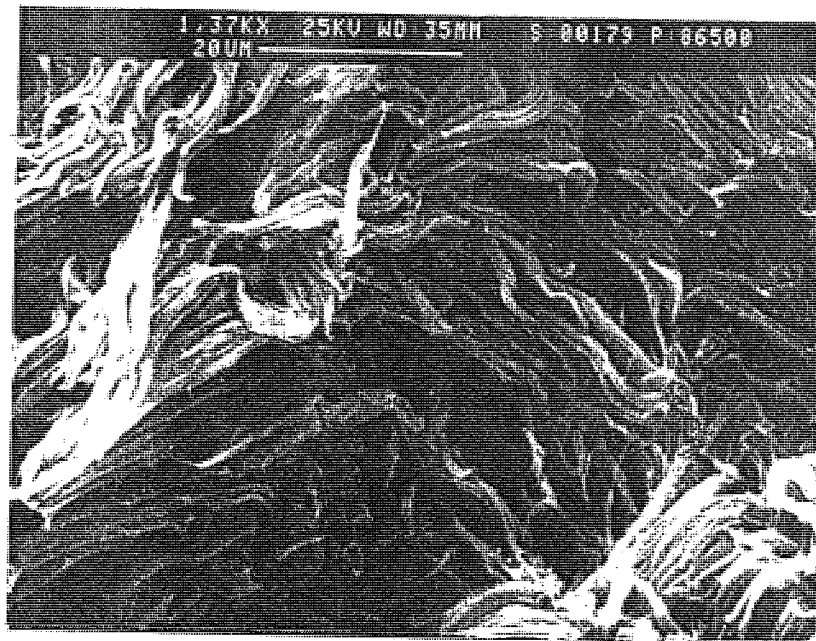
(a)
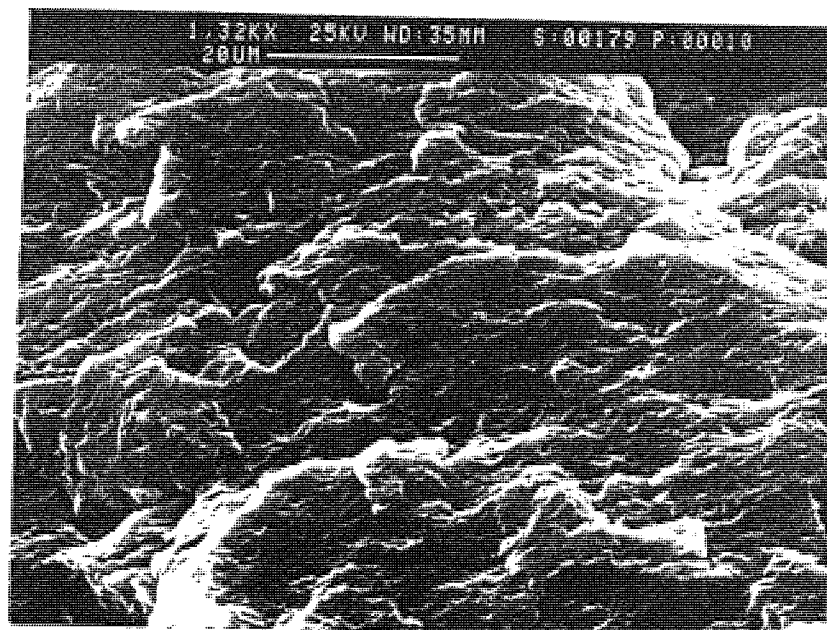
(b)

Figure 5.9: SEM micrographs of PP/EPDM 75/25 blend (CPB179, see Table 5.4) compatibilised with 1 % SPD. SPD composition is PP/EPDM 75/25 + 6%MA + 4%TRIS + 0.002m.r T101 + 10 % HEMDA. Note the ductile failures in (a) and brittle failure in (b), observed from the same sample (CPB179).
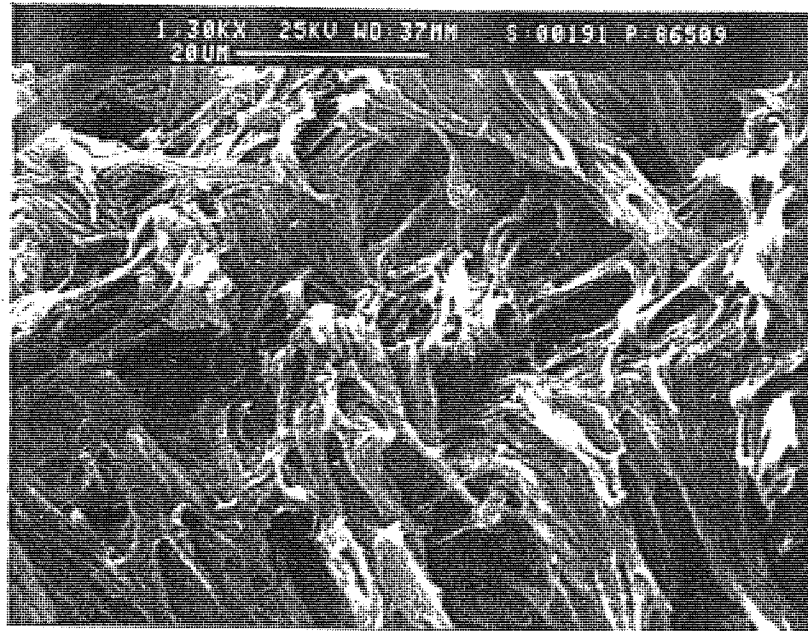
(a)
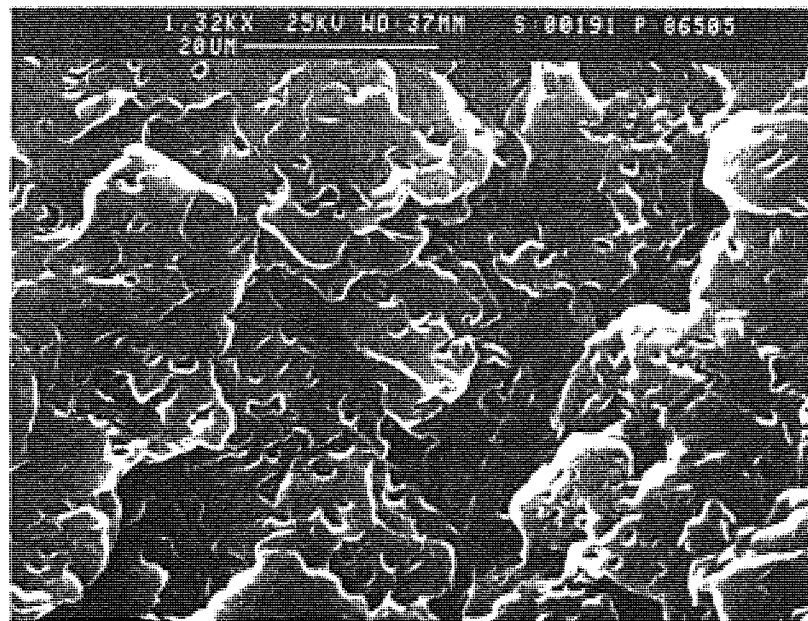
(b)

Figure 5.10: SEM micrographs of PP/EPDM 75/25 blend (CPB191, see Table 5.4) compatibilised with 10 % SPD. The SPD is based on MB65 (PP/EPDM 75/25 + 6%MA + 4%TRIS + 0.002m.r T101) + 10 % HEMDA. Note the ductile failures in (a) and brittle failure for (b), observed from the same sample (CPB191).
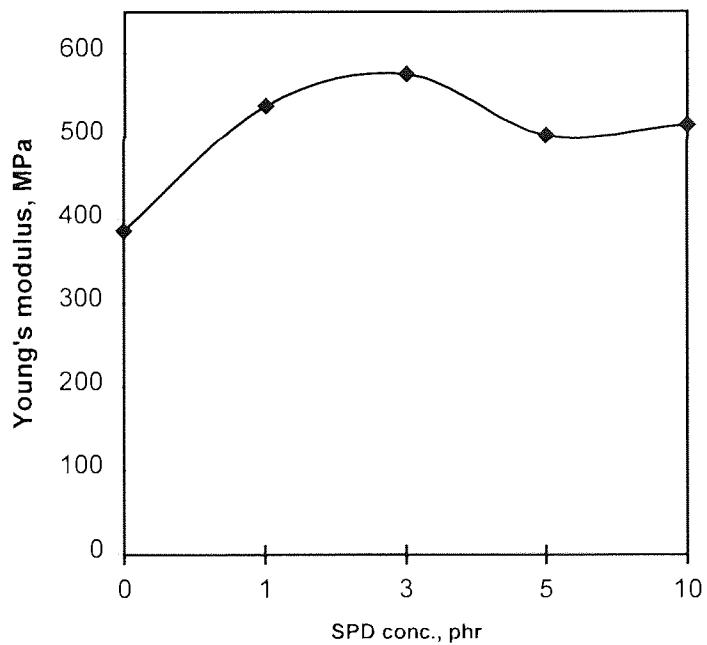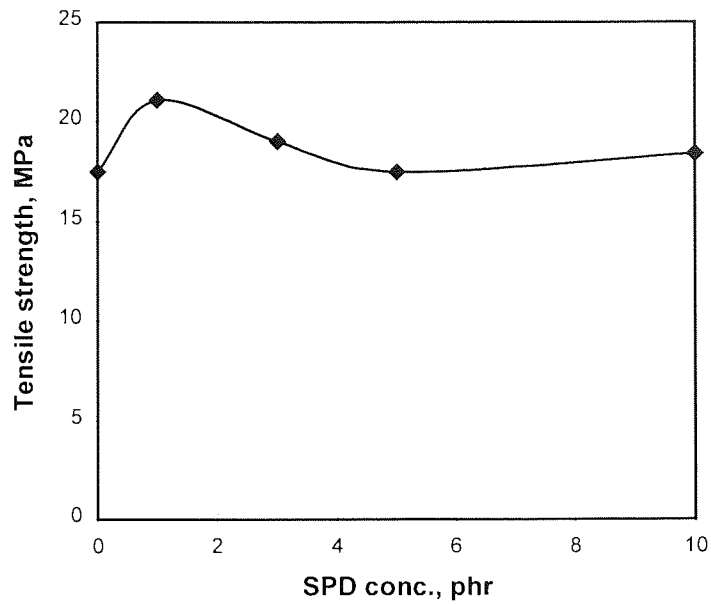
Figure 5.12: Effect of SPD concentration on tensile properties of PP/EPDM blends. The SPD is based on MB65 (PP/EPDM 75/25 + 6phr MA + 4phr TRIS + 0.002 m.r T101) processed with constant HEMDA concentration (10 phr). SPD concentration (0 phr) is binary PP/EPDM blend 75/25, (1 phr) is CPB 179, (3 phr) is CPB 185, (5 phr) is 188, and (10 phr) is CPB 191. Refer to Table 5.4 for related data.
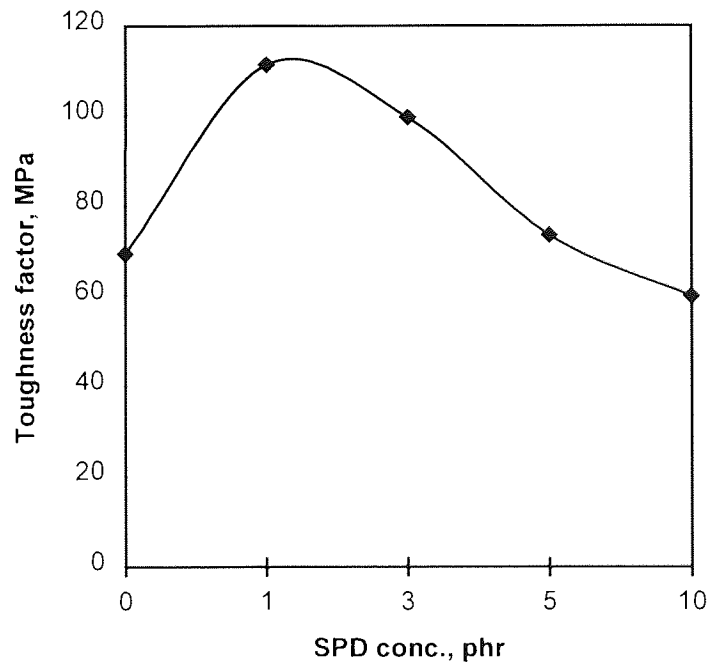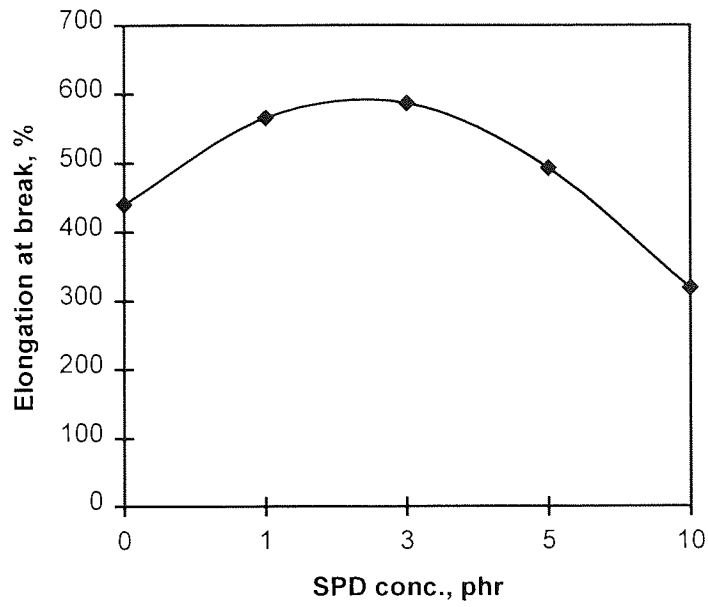
continue from Figure 5.12
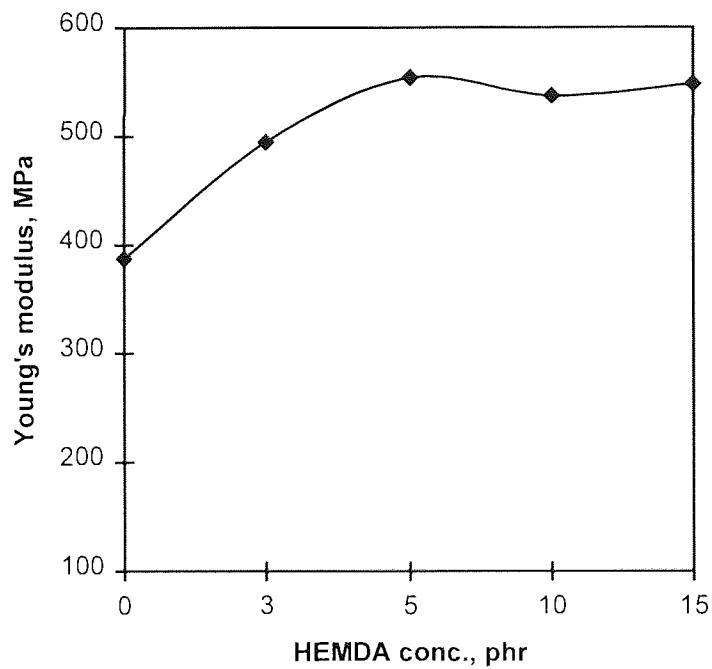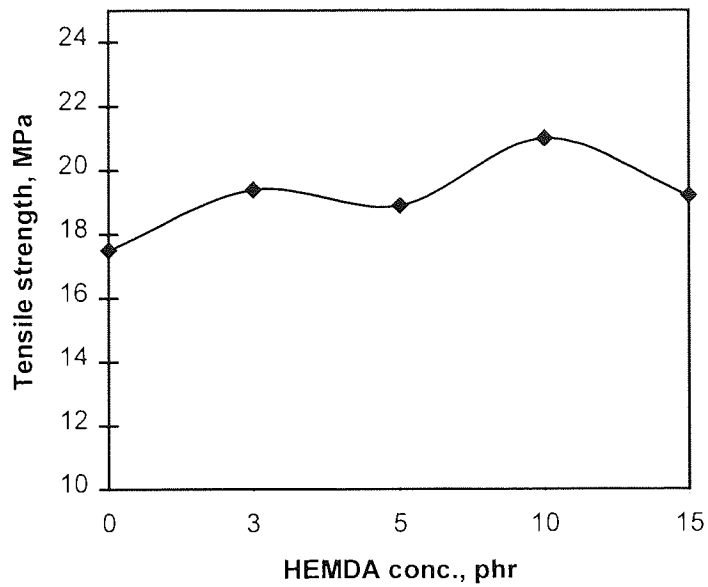
Figure 5.13: Effect of HEMDA concentration in SPD on tensile properties of PP/EPDM blends. The SPD (1 phr) is based on MB65 (PP/EPDM 75/25 + 6phr MA + 4phr TRIS + 0.002 m.r T101) + various concentration of HEMDA. HEMDA concentration (0 phr) is binary PP/EPDM blend 75/25, (3 phr) is CPB 178, (5 phr) is CPB 173, (10 phr) is 179, and (15 phr) is CPB 180. Refer to Table 5.4 for related data
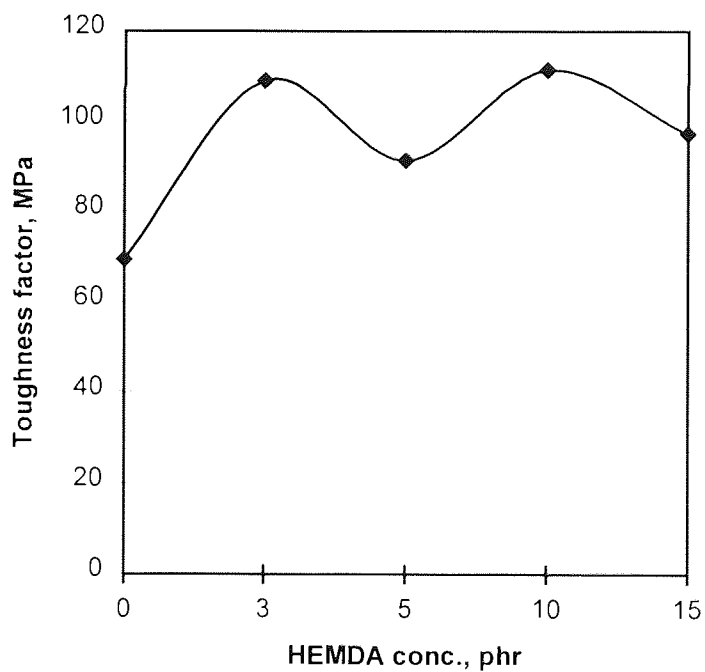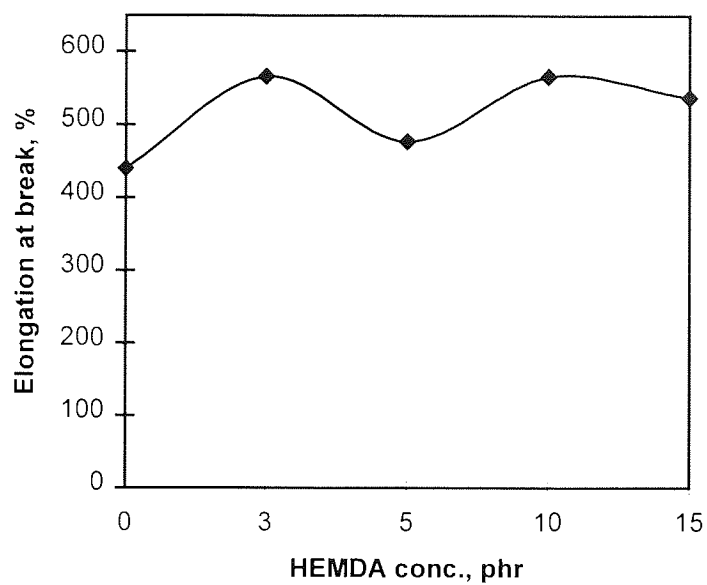
continue from Figure 5.13

CHAPTER SIX

CONCLUSIONS AND RECOMMENDATIONS
FOR FURTHER WORKS

6.1   CONCLUSIONS

These following conclusions can be drawn from the results discussed in Chapters 3 to 5:

6.1.1   Free radical-initiated reactive processing of maleic anhydride (MA) in polypropylene (PP) melt, resulted in a maximum grafting yield of 16 % (based on initial amount of MA added, Table 3.4 sample PMA62, page 113). At a constant free radical initiator (FRI) concentration, the grafting yield of MA is not linear function of the added MA concentrations; the grafting yield goes through a maximum at about 5 phr initial MA concentration (Fig. 3.16, page 127) before decreasing with a further increase in the added MA concentrations. This indicates that MA has a low solubility in the polymer. At a given MA concentration, on the other hand, the grafting yield increases with increasing the FRI concentration.

6.1.2   Shear-initated grafting of MA in PP (i.e. in absence of added FRI) resulted in low levels of grafting and low extent of polymer degradation (insignificant changes in melt flow index MFI values, see PMA1 in Table 3.4 page 113). Addition of a small amount of FRI (e.g. 0.002 m.r.) into the PP/MA system during reactive processing, however caused severe PP backbone degradation of the polymer

211

backbone through chain scission which was reflected in a drastic increase in MFI values (see Fig 3.19 curves (b) and (c) page 130 and Table 3.4 page 113). Increasing the MA concentration at a constant FRI concentration gave rise to a reduction in MFI, whereas the MFI increased when higher FRI concentrations were used. The low MA grafting yield and severe PP backbone degradation were related to the low solubility of MA in PP melt and low free radical reactivity of MA towards PP macroradicals.

6.1.3   The extent of grafting of the multi-functional monomer TRIS on PP and EPDM was shown to be very high (reaching to more than 90% as shown in Fig 3.4 and Fig 3.5 page 120) when compared to that of MA grafting on the same polymers. The latter gave less than 16 % grafting yield (Table 3.4, page 113). The high grafting yield of TRIS indicates the very high reactivity of TRIS towards PP macroradicals (much higher than that of MA radicals).

6.1.4   The experimental data in Chapter 3 have shown clearly that the use of a highly reactive multifunctional co-monomer, e.g. TRIS (coagent technology) is a very attractive route for grafting MA onto polyolefins. Addition of a small amount of TRIS (0.5 to 4 phr) during the radical initiated reactive processing of polymers has significantly increased the MA grafting yield in PP, EPDM and PP/EPDM blends. In the case of MA-functionalised PP, addition of TRIS seems to eliminate the 'solubility' limit (refer section 3.3 page 101) of MA in the polymer melt. The MA grafting yield increased virtually linearly with increasing MA concentration,

see Fig.3.20 page 131 up to a maximum yield of 2.7 phr. Furthermore, addition

of TRIS reduces the MFI value of maleated-PP which reflects lower extent of PP

backbone degradation by chain scission, see Fig. 3.21 curve b page 132.

6.1.5 Reactive processing of MA in EPDM in the presence of a trace amount of FRI (up

to 0.005 molar ratio) resulted in slightly higher MA grafting yield than that

achieved in PP, but the product contained high gel content due to high extent of

crosslinking (see Table 3.3, page 112). This intensive degree of crosslinking in

maleated-EPDM caused subsequently a great problem when conducting

compatibilisation of PP/EPDM blends with copolymers synthesised from

maleated-PP and maleated-EPDM (see Section 4.2.1.1, page 141). However this

problem of EPDM crosslinking led to the development of a new approach for the

grafting of MA onto PP and EPDM (maleated PP/EPDM). This was achieved by

processing MA in a mixture of PP (higher w/w ratio) and EPDM (low w/w ratio)

in the presence of FRI, see method summary in Scheme 3.4, page109. Maleated

PP/EPDM samples having initial chemical composition of 6 phr MA, 4 phr TRIS

and various FRI concentrations showed optimum MA grafting levels. (see Table

3.7 and Table 3.8 page 116). However at the same chemical composition, the

overall MA grafting level in the maleated-PP/EPDM was lower than that achieved

in each of the single polymers, i.e. maleated PP and maleated EPDM (see Fig.

3.33 page 138).

6.1.6 Various purification methods for maleated-polymers reported in the literature

such as precipitation from xylene/acetone solvent system, heating in vacuum oven

213

and Soxhlet extraction in DCM, as well as different methods of assessment of the grafting yield of MA e.g. FTIR and titration, were all used in this work for comparative purposes. The different procedures were found to give similar efficiencies in the polymers used. Soxhlet extraction however, was found to be very practical and convenient because the procedure required minimum number of man-hours and involved only a small amount of solvent (about 100 ml for each sample) which is reusable. On the other hand, the precipitation method involved dissolving the maleated-polymer samples in boiling xylene before washing with relatively large volumes of acetone which is non-recyclable. In the heating in vacuum oven procedure, prolong heating of the polymer samples at 120°C for 72 h may cause polymer degradation, especially the unstabilised polymers.

Both FTIR calibration curve (Section 2.5.1 page 65 and Scheme 2.1 page 72) and titration (Section 2.5.2 page66) methods were effective methods to assess MA grafting yield of maleated PP processed **with no multi-functional monomer.** Both methods are capable of assessing MA yield in both the anhydride and acid forms. The FTIR method was found very convenient and rapid for maleated PP, but for maleated EPDM and maleated PP/EPDM, titration was preferred instead, although it was time consuming and laborious. This was due to difficulty in preparing good samples for FTIR analysis.

FTIR calibration curve was however found **not to be suitable** for assessing the MA grafting yield in maleated PP processed in the presence of the multi-

functional monomer TRIS. It was found that the carbonyl absorption peak of TRIS overlapped with the acid peak of the anhydride moiety, necessitating the use of titration instead of IR in this case.

6.1.7 Two routes were used to synthesis PP/EPDM copolymers for use as compatibilisers (or solid phase dispersant) in PP/EPDM blends. Firstly, copolymers were synthesised from maleated-PP and maleated-EPDM in the presence of an interlinking agent such as hexadiamine monomer (HEMDA) via two step-route (Scheme 4.1 page 155). Addition of such copolymers into PP/EPDM blends caused premature failure during tensile testing (see Section 4.2.1.1 and Table 4.1 page157). This could be attributed to high gel content in maleated-EPDM due to extensive crosslinking during the MA functionalisation step (see Table 3.6 page115).

In the second route, copolymers were synthesised in a 'one-step continuous reaction', (see Section 4.2.1.2 and Scheme 4.2 page156). PP/EPDM blends were first functionalised with MA in the presence of TRIS and trace amount of FRI for 10 minutes. This was followed by the amidisation reaction where a small amount of the diamine monomer HEMDA was added in order to achieve an interlinking reaction between the MA-functionalised PP and MA-functionalised EPDM moieties to form PP/EPDM copolymers in one step . Tensile test data indicated that the PP/EPDM copolymers synthesised by this method showed better tensile strength and stiffness when compared to that of pure PP/EPDM blends but

generally suffered from lower elongation at break and toughness factor (see Table 4.3 and Fig 4.1 page 161).

6.1.8 It was observed that the addition of EPDM (25 w/w%) to PP (75 w/w%) resulted in a drastically reduction of the mechanical properties of PP (e.g. strength and stiffness), but led to improvement in elongation at break and the toughness factor of the PP (Fig. 5.1 page 191). The binary blends showed a two-phase system (from SEM micrograph Fig. 5.8 page 203) with small size rubber particles distributed homogeneously within the continuos PP matrix. The morphology indicated that the two phases had very poorly adhesion.

6.1.9 MA functionalised and imidised PP/EPDM copolymers synthesised via the 'one-step continuous reaction' were used for compatibilisation of PP/EPDM 75/25 blends (Chapter 5). Formation of fabrils and dislocation glides observed in the SEM micrographs as shown in Figures. 5.9a and 5.10a, and Figures. 5.9b and 5.10b (pages 204 and 205), respectively, indicate that these PP/EPDM copolymers are effective compatibilisers for PP/EPDM blends and give rise to significant improvement of the adhesion between the PP and EPDM phases.

All the compatibilised blends showed excellent improvement in the tensile strength and Young's modulus when compared to that of a binary blend (Figures 5.3 A and B, and 5.4 A and B page 195 to 198). However all blends compatibilised with PP/EPDM60/40 copolymer, except CPB141 (see Table 5.3

216

page189) suffer low elongation at break and toughness factor compared to the binary blends (Figures 5.3 C and D page196). PP/EPDM blends containing more than 3 phr PP/EPDM 75/25 copolymers show similar trend, but blends compatibilised by up to 3 phr PP/EPDM75/25 copolymers exhibited excellent elongation at break and toughness factor when compared to the binary blends (Figures 5.4 C and D, and 5.12 page 207). The results indicate that PP/EPDM75/25 copolymers are more effective compatibilisers for PP/EPDM blends than PP/EPDM60/40 copolymers. PP/EPDM blend (sample no. CPB179) compatibilised with 1 phr copolymer synthesised from MB65 (PP/EPDM75/25 + 6phr MA + 4phr TRIS + 0.002 m.r.) and imidised with 10phr HEMDA exhibits overall excellent tensile properties compared to that of the corresponding binary blend (Table 5.4 and Fig.5.12 page189 and 207, respectively). The excellent properties of these compatibilised blends over the binary blend can be explained by the capabilities of the PP/EPDM75/25 copolymers to play an important role as efficient compatibiliser. The two parts of PP/EPDM copolymer (the compatibiliser) should penetrate preferentially into their respective polymer phases hence reducing the interfacial tension, strengthening the adhesion at the phase boundaries, and stabilising the morphology of the blends.

6.1.10 Results from this study - optimum MA functionalised PP, EPDM and PP/EPDM blends, and synthesised copolymers and compatibilised blends having overall best tensile performance - are summarised in Table 6.1 and Table 6.2, respectively.

Table 6.1: Optimum samples of MA functionalised PP, EPDM
and PP/EPDM blends.

Optimum samples	MA grafted		MFI	% Gel content	Ref.
	phr	of initial MA %			
1. Functionalisation of PP with MA alone					
1.1 PMA2 (6phr MA + 0.002 m.r FRI)	0.4	6	2.1	5	Tab3.4
1.2 PMA3 (6phr MA + 0.005 m.r FRI)	0.5	11	4.0	6	Fig3.6
2. Functionalisation of PP with MA and TRIS					
2.1 PMA 52 (6phrMA + 4phrTRIS + 0.002m.r T101)	2.6	43	1.3	9	Tab3.5
2.2 PMA50 (10phrMA + 2.4phrTRIS + 0.002m. T101)	2.7	27	0.85	5	Fig3.20
3. Functionalisation of EPDM					
3.1 MAT 12 (8phrMA + 2phrTRIS + 0.005 m.r T101)	3.4	44	n/a	26	Tab3.6 Fig3.27
4. Functionalisation of PP/EPDM (75/25)					
4.1 MB73 (6phrMA + 4phrTRIS + 0.001m.r T101)	1.5	25	n/a	n/a	Tab3.7
4.2 MB65 (6phrMA + 4phrTRIS +0.002 mr T101)	1.7	28			Fig3.3
4.3 MB77 (6phrMA + 4phrTRIS +0.005 mr T101)	2.0	33			
5. Functionalisation of PP/EPDM (60/40)					
5.1 MB94 (6phrMA + 4phrTRIS + 0.005m.r T101)	2.5	42	n/a	n/a	Tab3.8

Table 6.2 : Optimum samples of synthesised PP/EPDM copolymers, and compatibilised PP/EPDM blends.

Item	Optimum sample	Chemical composition		Note	Ref.
1. PP/EPDM 75/25 copolymer (SPD)	SPD80	MB65 + 5phr HEMDA		better TS & YM but poor Eb and TF than binary blend [1].	Tab4.5
2. PP/EPDM 60/40 copolymer (SPD)	SPD104	MB94 + 5phr HEMDA		better TS,YM and TF but poor Eb than binary blend.	Tab4.5
3. Compatibilised blends (CPB) (PP/EPDM 75/25)		X phr	SPD phr		
3.1 Compatibilised by MB65 (PP/EPDM75/25) + X phr HEMDA	CPB179	10	1		Tab5.4 Fig5.12 Fig5.13
	CPB178	3	1		
	CPB185	10	3		
	CPB180	15	1		
	CPB184	3	3	all these compatibilised blends have better tensile properties than binary PP/EPDM blends. Optimum blend : CPB179	
	CPB173	5	1		
	CPB186	15	1		
3.2 Compatibilised by MB94 (PP/EPDM60/40) + X HEMDA	CPB141	3	1		Tab5.3

Note: 1. TS, YM, Eb and TF are tensile strength, Young's modulus, Elongation at break and Toughness factor, respectively

6.2 RECOMMENDATIONS FOR FURTHER WORK

6.2.1 Efficiency of MA grafting reaction, structures of the MA-functionalised polymers and synthesised PP/EPDM copolymers are not been fully studied and understood. To further investigate, high sensitive analytical techniques, such as solid state NMR which can identify the change of chain sequence of polymer backbone and distinguish various configurations of carbon atoms in the polymer, are recommended for analysis of the maleated-polymers. Furthermore, this technique could be very useful to study the role of tri-functional coagent TRIS in enhancing the MA grafting level.

6.2.2 Results from this work has shown that addition of tri-functional coagent TRIS during reactive processing of MA with polymer melt in an internal mixer, in the presence of low concentration of free radical initiator has significantly enhanced the MA grafting level from about 16 % to about 40 % of initial MA added. However from the economic and environmental point of views, a near 100% grafting efficiency is more desirable which then will omit 'washing- step' to purify maleated-polymer from impurity of non-grafted MA. To improve the efficiency of a functionalisation reaction, a better design of processing operation is necessary. A continuos processing machine with many inlets at different positions and possibility of resident time variations may suitable. Therefore, in a reactive processing, reactive agents could be added separately from different

inlet as needed. Furthermore the production capacity of maleated-polymer could be multiplied.

6.2.3   In this study only one particular grade of EPDM and PP was used. Comparison of the effectiveness of MA functionalisation onto a range of inert polymers by the methodology detailed in the present work may further indicate the effectiveness of using tri-functional acrylate monomer TRIS in enhancing the MA grafting efficiency.

6.2.4   Results in Chapter 5 shows that PP/EPDM 75/25 copolymers were better compatibilisers for PP/EPDM 75/25 blends than PP/EPDM 60/40 copolymers. Further work is necessary to justify PP/EPDM 75/25 copolymers will show similar performance when applied to different ratio of PP/EPDM blends.

References

1.   Van de Grampel H.T., *Blends and Alloys of Engineering Thermoplastics*, RAPRA REVIEW Report 49, Pergamon Press, Oxford, **5(1)** , 2, (1991)

2.   Jo W.H., Park C.D., and Lee M.S., *Preparation of Functionalised PS by Reactive Extrusion and its Blend with Polyamide 6*, Polymer, **37**, 1709, (1996)

3.   Lohse D.J., Datta S., and Krege E.N., *Graft Copolymer Compatibilisers for Blends of PP and EPR copolymer*, Macromolecules, **24**, 561-566, (1991)

4.   Tzoganakis C., and Shearer G., *Radically Induced Hydrosilylation of PP through Reactive Extrusion*, ANTEC 97, Annu. Tech. Conf. Soc Plast. Eng., 43   (1997)

5.   Allan J.R., Bonner J.G., and Gerrard D.L., *Preparation and Characterisation of Metal Acrylate Grafted PP*, Plastics, Rubber and Composites Processing and Application, **24**, 43-46, (1995).

6.   Miller M.M., Cowie J.M.G., and Mather R.R., *Fibres from PP and Liquid Crystal Polymer Blends using Compatibilising Agents: 3. Assessment of Graft Side Chain Liquid Crystalline Compatibilisers based upon Acrylic Acid-Functionalised PP*, Polymer, **38(7)** , 1565, (1997).

7.   Mehta I.K., Misra B.N., and Chauhan G.S., *Behaviour of Isotactic PP Fiber Graft Copolymerised with Acrylic Monomers Using Preirradiation Method*, J. Appl. Polym. Sci., **21(8)** , 1171, (1994).

8.   Utracki L.A., *Introduction to Polymer Alloys and Blends*, in Polymer Alloys and Blends: Thermodynamic and Rheology, Hanser Publishers, N.Y., Part 1, (1989).

9.   Utracki L.A., Abdellah Ajji, *Interphase and Compatibilisation of Polymer Blends*, Polym. Eng. Sci., **36(12)**, 1574, 1996.

10.   Martuscelli E., *Rubber Modification of Polymers: phase structure, crystallisation, processing and properties*, in Thermoplastic Elastomers From Rubber-Plastic Blends, De S. K., Ellis Horwood, London, Chap.2, (1990)

11.   Cowie J.M.G., *Miscibility*, in Encylopedia of Polymer Science and Engineering, Mark H.F., Bikales N.M., Overberger C.G., Menges G., and Kroschwitz J.I. (Ed.), John Wiley, N.Y., 2nd. Edition, **Supplement** , 455-480, (1989)

12.   Paul D.R., and Barlow J.W., *Polymer Blends (or Alloys)* , J. Macrmol. Sci.-Rev.Macromol. Chem., **C18(1)**, 109-168, (1980).

13.   Utracki L.A., *Polymer/Polymer Miscibility*, in Polymer Alloys and Blends: Thermodynamic and Rheology, Hanser Publishers, N.Y., Part 2, 124, (1989).

14. Gaylord N.G., *Compatibilisation Concepts in Polymer Applications*, Adv. In Chemistry, Gould R.F. (Ed.), **Series 142**, Chap.7, 76-84, (1975).

15. Paul D.R., *Interfacial Agents ("Compatibilisers") for Polymer Blends*, in Polymer Blends, Paul D.R., and Newman S. (Ed.), Acad. Press., N.Y., **Chap. 12**, (1978).

16. Liu N.C., and Baker W. E., *Reactive Polymers for Blends Compatibilisation*, Adv. Polym. Tech., **11(4)**, 249-262, (1992)

17. Xanthos M. and Dagli S.S., *Compatibilisation of Polymer Blends by Reactive Processing*, Polym. Eng. Sci., **31(13)** , 929, (1991)

18. Xanthos M., *Interfacial Agents for Multiphase Polymer Systems: Recent Advances*, Polym. Eng. Sci., **28(21)**, 1392, (1988)

19. Fayt R., Jerome R., and Teyssie P., *Molecular Design of Multicomponent Polymer Systems XIV: Control of Mechanical Properties of PE-PS Blends by Block Copolymers*, J. Polym. Sci., Pt. B - Polym. Phy., **27**, 775, (1989).

20. Gaylord N.G., *Use Surfactants to Blend Polymers*, Chemtech, **July**, 435, (1989)

21. Duvall J., Sellitti C., Myers C., Hiltner A., and Baer E., *Effect of Compatibilisation on the Properties of PP/PA-66 Blends*, J. Appl. Polym. Sci., **52**, 195-206, 1994

22. Lie N.C., Xie H.Q., and Baker W.E., *Comparision of the Effectiveness of Different Basic Functional Groups for the Reactive Compatibilisation of Polymer Blends*, Polymer, **34(22)**, 4680, 1993.

23. Tzoganakis C., *Reactive Extrusion of Polymer : A Review*, Adv. Polym. Tech., **9(4)**, 321-330 (1989).

24. Kim K.J., OK Y.S. and Kim B.K., *Crosslinking of Polyethylene with Peroxide and Multifunctional Monomers during Extrusion*, J. Eur. Polym., **28(12)**, 1487 (1992)

25. Kim B.K., and Kim K.J., Cross-linking of Polypropylene by Peroxide *and Multifunctional Monomers during Extrusion*, Adv. Polym. Tech., **12(3)**, 263-269 (1993).

26. Coran A.Y., and Patel R.P., *Thermoplastic Elastomers by Blending and Dynamic Vulcanisation*, Chapter 6, Vol.2, in Polypropylene - Structure, Blends and Composites, J. Karger-Kocsis, (Ed.), Chapman & Hall, (1995).

27. Brown S.B., and Orlando C.M., *Reactive Extrusion*, in Encyclopaedia of Polymer Sci. Eng., Mark, Bikales, Over Berger and Menges, 2nd. Edition, **14**, 169, 1989.

28.   Coates P.D., Brown M.W.R., Fleming D.J., Johnson A.F., and Tsui S.W., *Reactive Extrusion of Polyolefins: In-Process Measurements*, ANTEC '95, Annu. Tech. Conf. Soc. Plast. Eng., **41**, 1620-1624, (1995).

29.   Sakai T., *Report on the State of the Art: Reactive Processing Using Twin-Screw Extruders*, Adv. Polym. Tech., **11(2)**, 99-108 (1991/1992)

30.   Kelleher P.G., *Report on the State of Art: Injection Molding of Fiber Reinforced Thermoplastics. Pt. 1. Materials and Processes*, Adv. Polym. Tech., **10(3)**, 219-230 (1990)

31.   Biesenberger J.A., *Principles of reaction engineering*, in Reactive Extrusion: Principles and Practice, M. Xanthos (Ed.), Hanser, N.Y., **Chap. 6**, (1992).

32.   Coates P.D., Davies G.R., and Duckett R.A., Johnson A.F., and Ward I.M., *Some Routes for Tailoring of Polymer Properties Through Reactive Processing*, Trans IChemE, **73(A)**, 753-770, 1995.

33.   Jakopin S., *Practical Aspects of Reactive Compounding in a Continuous Kneader*, Adv. Polym. Tech., **11(4)**, 287-294, (1992)

34.   Brown S.B., Reactive Extrusion: *A Survey of Chemical Reactions of Monomers and Polymers during Extrusion Processing*, in Reactive Extrusion: Principles and Practice, M. Xanthos (Ed.), Hanser, N.Y., **Chap. 4**, (1992).

35.   Kowalski R.C., *Fit the Reactor to the Chemistry: Case Histories of Industrial Studies of Extruder Reactions*, in Reactive Extrusion: Principles and Practice, M. Xanthos (Ed.), Hanser, N.Y., **Chap. 1**, (1992).

36.   Todd D.V., Features of Extruder Reactors, in Reactive Extrusion: Principles and Practice, M. Xanthos (Ed.), Hanser, N.Y., **Chap. 5**, (1992).

37.   Al-Malaika S., *Reactive Modifiers for Polymers*, Blackie Acad. & Professional, Lon. (1997)

38.   Ratzsch M., *New Results and Prospects in Radical Polymerisation: Modification and Reactive Blending*, Prog. Polym. Sci., **19**, 1011 - 1029, (1994).

39.   Singh R.P., *Surface Grafting onto PP - a Survey of Recent Developments*, Prog. Polym. Sci., **17**, 251-281, (1992).

40.   Jagur-Grodzinski J., *Modification of Polymers Under Heterogeneous Conditions*, Prog. Polym. Sci., **17**, 361-415, (1992).

41.   Lambla M., Hu G.H., and Flatt J.J., *Free-radical Grafting of Monomers onto Polymers by Reactive Extrusion: Principle and Application, in Reactive Modifier for Polymer*, Al-Malaika S., (Ed.), Blackie Acad. & Professional, **Chap. 1**, (1997).

42.   Hudec I., Sain M.M., and Sunova V., *Improved Interaction Effected by Maleic Anhydride Grafted PP in PRT Triblock Polymer - EVA Blend.* J. Appl. Polym. Sci., **49**, 425, (1993)

43.   Marciniec B., Urbaniak W., and Maciejewski H., *Silane Coupling Agents Pt.3. 3-Methacryloxypropyl trialkoxy silanes*, Int. Polym. Sci. Tech., **20(6)** , T/53, (1993)

44.   Si K., and Qiu K.Y., *Grafting Reaction of Macromolecules with Pendant Amino Groups via Photoinitiation with Benzophenone*, Macromol. Chem. Phys., **197**, 2403, (1996)

45.   Tommi V., Hu G.H., Lambla M., and Sepalla J.V., *Functionalised PP prepared by Melt Free Radical Grafting of Low Volatile Oxazoline and Its Potential in Compatibilisation of PP/PBT Blends*, J. Appl. Polym. Sci., **61**, 843-852, (1996).

46.   Trivolli and Robinson, *Introduction, Chapter 1 in Maleic Anhydride*, Plenum, N,Y., (1982)

47.   Gaylord N.G., Reactive extrusion in the preparation of carbonyl-containing polymers and their utilisation as compatibilising agents, in Reactive Extrusion: Principles and Practice, M. Xanthos (Ed.), Hanser, N.Y., **Chap. 3** , (1992).

48.   Hogt A., *Modification of PP with Maleic Anhydride*, ANTEC '88, Annu. Tech. Conf. Soc. Plast. Eng., **34**, 1478, (1988).

49.   Gaylord N.G., and Mehta M., *Role of Homopolymerisation in the Peroxide Catalyst Reaction of MA and PE in the Absent of Solvent*, J. Polym. Sci.: Polym. Lett. Ed., **19**, 107 -112, (1981)

50.   Wu C.J., Chen C.Y., Woo E., and Kuo J.F., *A Kinetic Study on Grafting of MA onto a Thermoplastic Elastomer*, J. Polym. Sci. Pt.A: Polym. Chem., 31, 3405 - 3415, (1995)

51.   Minoura Y., Ueda M., Mizunuma S., and Obe M., *The reaction of PP with MA.*, J. Appl. Polym. Sci., **13**, 1625 - 1640, (1960)

52.   Sun Y.J., Hu G.H., and Lambda M., *Free Radical Grafting of Glycidal Methacrylate onto Polypropylene in a Co-Rotating Twin Screw Extruder*, J. Appl. Polym. Sci., **57**, 1043-1054, (1995)

53.   Jo W.H., Park C.D., and Lee M.S., *Preparation of Functionalised Polystyrene by Reactive Extrusion and its Blend with Polyamide-6*, Polym. **37/9**, 1709-1714, (1996).

54.   Carrot C., Jaziri M., Guillet J., and May J.F., *Grafting of Maleic Anhydride on ABS in the molten state*, Plast. And Rub. Process. And Appl., **1414**, 245-248, (1990).

55.   Sachin N.S., Srinivasa G.S., and Surekha D., *Grafting of MA onto PP: Synthesis and Characterisation*, J. Appl. Polym. Sci., **53**, 239 - 245, (1994).

56.   Sipos A., McCarthy J., and Russel K.E., *Kinetic Studies of Grafting of MA to Hydrocarbon Substrate*, J. Polym. Sci. Pt.A: Polym. Chem., **27**, 3353 - 3362, (1989)

57.   Gaylord N.G., and Maiti S., *Participation of Excited Species in Radical Catalyst Homopolymerisation*, J. Polym. Sci. Polym. Lett. Ed., **11**, 253 - 256, (1973)

58.   Gaylord N.G., Nagler M., and Watterson A.C., *Structure of alternating cis- and trans-piperlene-maleic anhydride copolymer by* ^{13}*C-NMR analysis*, J. Eur. Polym., **19 (10/11)** , 877 -879, (1983)

59.   Gaylord N.G., and Koo j.Y., *Participation of Cationic Intermediates in Radical-Induced Homopolymerisation of MA*, J. Polym. Sci. Polym. Lett. Ed., **19**, 107 - 112, (1981)

60.   Gaylord N.G., and Munmaya R., Nondegradative reaction of MA on Molten PP in the Presence of Peroxides., J. Polym. Sci. Polym. Lett. Ed., 21, 23 - 30, (1983)

61.   Gaylord N.G., Mehta M., and Kumar V., *Graft Copolymerisation of MA onto PE*, Polym. Sci. Tech.: Modification of Polymer, Charles Jr. and James A.M., (Ed.), **21**, 171 (19)

62.   Gaylord N.G., and Elayaperumal P., *Dicumyl peroxide - catalysed degradation of PS in the presence of MA.*, Polym., **35**, 5693, (1994)

63.   Heinen W., Rosenmoller C.H., Wenzel C.B., de Groot H. J. M., Lugtenburg J., and van Dein M., ^{13}*C NMR study on the grafting of maleic anhydride onto polyethene, polypropene, and ethylene-propene copolymers*, Macromol. **29**, 1151-1157, (1996).

64.   Thomas R., Stefan Z. and Hartmut K., *Grafting of maleic anhydride onto poly(tetrahydrofuran)*, Macromol. Chem. Phys., **197**, 991-1005, (1996).

65.   Russell K.E., Sipos A., and McCarthy J., *Kinetic studies of grafting of maleic anhydride to hydrocarbon substrates*, J. Polym. Sci.: Pt.A: Polym. Chem., **27**, 3353-3362 (1989).

66.   Lang J.L., Pavelich W.A., and Clarey H.D., *Homopolymerisation of MA: 1. Preparation of the Polymer*, J. Polym. Sci., **A1**. 1123 - 1136 (1963)

67.   Gaylord N.G., *Poly(maleic anhydride)*, in Review in Macromol. Chem., Butler G.B., O'Driscoll K.F., and Mitchel Shen (Eds.) **14A** , 235 - 258, (1976).

68. Joshi R.M., *The Free Radical Polymerisation of Maleic Anhydride*, Macromol. Chem., **53**, 33, (1962)

69. Seghir M.K., and Jenner G., *Homopolymerisation Radicalaire de L' Anhydride Maleique,* J. Eur. Polym., **12**, 883 - 887, (1976)

70. Hamann S.D., *Polymerisation of Maleic Anhydride by an Intensive Shock Wave*, J. Polym. Sci., **5**, 2939 - 2941, (1967)

71. Roover B.D., Sclavons M., Carlier V., devaux J., Legras R., and Momtaz A., *Molecular Characterisation of Maleic Anhydride onto PP: Synthesis and Characterisation*, J. Appl. Polym. Sci., **53** , 239 - 245, (1994)

72. Russell K.E., *Grafting of Maleic Anhydride to n-Eicosane*, J. Polym. Sci. Pt.A: Polym. Chem., **26**, 2273 - 2280, (1980)

73. Russell K.E., *Grafting of Maleic Anhydride to Hydrocarbons Below the Ceiling Temperature,* , J. Polym. Sci. Pt.A: Polym. Chem., **33**, 555 - 561, (1995)

74. Tzoganakis C., Vlachopoulos J., and Hamielec A., *Production of Controlled - Rheology PP Resins by Peroxide Promoted Degradation During Extrusion*, Polym. Eng. Sci., **28(3)** , 170-180, (1988).

75. Hogt. A.H., Meijer J., and Jelenic J., *Modification of polypropylene by organic peroxide*, Al-Malaika S., (Ed.), Blackie Acad. & Professional, **Chap. 1**, (1997).

76. S. Al-Malaika, *Reactive modifiers for polymers,* in Chemical Reactions on Polymers, ACS Symp. Ser., Washington, **364**, 409-425 (1988).

77. Lin Q., Talukder M., Pittman C.U., *Styrene-maleic anhydride copolymerisation through polar transition states in polar solvents*, J. Polym. Sci., Pt.A: Polym. Chem., **33**, 2375-2383 (1995)

78. Manfred R., and Vogl O., *Radical Copolymerisation of Donor/Acceptor Monomers*, Prog. Polym. Sci., **16**, 279-301, (1991).

79. Mattiussi A., and Forcucci F., Polyolefinic Blends: Recent Applications and Developments, in Polymer Blends : Processing, Morphology and Properties, Martuscelli E., Rosario P., and Kryszewski M. (Eds.), Plenum Press, Lon., 469-484, (1990).

80. Rader C.P., and Stemper J., *Thermoplastic Elastomer - A Major Innovation in Rubber*, Prog. In Rubb. And Plast. Tech., **6(1)**, 50-99, (1990).

81. Kresge E.N., *Elastomeric Blends*, J. Appl. Polym. Sci. : Appl. Polym. Symp., **39**, 37-57, (1984)

82.   Blom H.P., Teh J.W., Rudin A., *Effect of Addition of HDPE to PP*, J. Appl., Polym. Sci., 58, 995, (1995).

83.   Platt A.E., *Rubber Modification of Plastics*, in Comprehensive Polym. Sci., Allen G., and Bevington J, (Eds.) Pergamon Press, Lon., **Vol. 2**, 437, (1989).

84.   Dunn J.R., Blends of Elastomers and Thermoplastics - a review, Rubb. Chem. Technol., 49(4) , 978-991, (1976).

85.   Dennis J.S., Deniel F.S., and Emmanuael G.K., *EPDM-Polypropylene Blends, in: Thermoplastic Elastomers from Rubber-Plastic Blends*, De S.K., and Bhomick A.K. (ed.), Ellis Horwood, England, (1990).

86.   Utracki L.A., and Dumoulin M.M., *Polypropylene Alloys and Blends with Thermoplastics, in: Propylene- Structure, Blends and Composite,* , J. Karger-Kocsis (ed.), Chapman & Hall, **Vol. 2**, 1995.

87.   Kryszewski M., *Recent Progress in the Studies on the preparation and properties of polymer blends*, in Polymer Blends : Processing, Morphology and Properties, Martuscelli E., Rosario P., and Kryszewski M. (Eds.), Plenum Press, Lon., (1990).

88.   Rader C.P., Abdou-Sabet, S., *Two-phase elatomeric alloys*, in Thermoplastic Elastomers From Rubber-Plastic Blends, De S. K., and Anil K.B.,(eds), Ellis Horwood, London, **Chap.6**, (1990)

89.   Lohse D.J., *The melt compatibility of blends PP and EPR copolymer*, J. Polym.Eng. Sci., **21** , 1500 (1986).

90.   Elliot D.J., *Natural rubber - polypropylene blends*, in Thermoplastic Elastomers From Rubber-Plastic Blends, De S. K., and Anil K.B.,(eds), Ellis Horwood, London, **Chap.4**, (1990)

91.   Dao K.C., *Mechanical properties of PP/crosslinked rubber blends*, J. Appl. Polym. Sci., **27**, 4799, (1982).

92.   Chang S.H., *Tensile properties and morphology of the dynamically cured EPDM and PP/HDPE ternary blends*, J. Appl. Polym. Sci., **37**, 317-334 (1989).

93.   Meredith C.L., *EPDM elastomers in rubber modified plastics*, Rubb. Chem. Tech., **44** , 1130 (1971).

94.   Kresge E.N., *Polyolefins thermoplastic elastomer blends*, Rubb. Chem. Tech., **64(3)**, 469-470 (1991).

95.   Paul D.R., Barlow J.W., and Keskula H., *Polymer blends* , in Encylopedia of Polymer Science and Engineering, Mark H.F., Bikales N.M., Overberger C.G., Menges G., and Kroschwitz J.I. (Ed.), John Wiley, N.Y., 2nd. Edition, **12**, (1989)

96.   Ranali R., *Ethylene-propylene rubber-propylene blends* , in Dev. In Rubb. Tech., Whelan A., and Lee S.K., (eds.), **3** , Chap. 2, (1982).

97.   Lohse D.J., and Datta S., *Graft Copolymer Compatibilisers for Blends of PP and EPR copolymer*, ANTEC '92 Annu. Tech. Conf. Soc. Plast. Eng., **38**, 1036 (1992).

98.   Lohse D.J., and Datta S., *Graft Copolymer Compatibilisers for Blends of isotactic PP and ethene-propene copolymer: 2 Functional polymer approach,* Macromol., **26** , 2064 - 2076 (1993).

99.   Ide F., and Hasegawa A., *Studies on polymer blend of nylon 6 and PP or nylon 6 and Ps using the reaction of polymer*, J. Appl. Polym. Sci., **18**, 963 (1974)

100.   We J.Y., Lee W.C., Kuo W.F, Kao H.C., Lee M.S., and Lin J.L., *Effect of molecular weights and compatibilising agents on the morphology and properties of blends containing PP and nylon-6,* Adv. In Polym. Tech., **14**, 47-58, (1995).

101.   Barlow J.M., and Paul R.B., *In-situ reactive compatibilisation of nylon-6/PS blends using anhydride functionalised PS*, J. Polym. Sci., Pt.B : Polym. Phy., **30(9)**, 1021 -1033 (1992).

102.   Paul D.R., *Reactive compatibilisation pf blends of nylon-6 and ABS*, Polymer, **32(8)**, 531 -551, (1992)

103.   Cimmino S., D'orazio L., Greco R., Maglo G., Malinconico M., Mancarella C., Martuscelli E., Palumbo R., and Ragosta G., *Morphology - properties relatioships in binary PA-6/rubber blends : Influence of the addition of a functionalised rubber*, Polym. Eng. Sci., **24(1)**, 48 (1984).

104.   Park I., Barlow J.W., and Paul D.R., *The in situ reactive compatibilisation of nylon-6/polystyrene blends using anhydride functionalised polystyrenes*, J. Polym. Sci.: Pt.B: Polym. Phys., **30**, 1021-1033, (1992).

105.   Kim B.Y., Park S.Y., and Park S.J., *Morphology, thermal and rheological properties of blends: PE/nylon-6, PE/nylon-6/(MA-g-PE) and (MA-g-PE)/nylon-6,* J. Eur. Polym., **27(4/5)**, 349, (1991).

106.   Jo W.H., Park C.D., and Lee M.S., *Preparation of functionalised PS by reactive extrusion and its blend with polyamide-6,* Polymer, **37(9)** , 1709 , (1996).

107a.   Al-Malaika S., and Scott G., *Modified Polymers*, US Patent, 5,382,633 (1995).

107b.   Al-Malaika S., S.H.H. Sheena and Scott G., *Graft Copolymer and their Production*, Patent Int. Application No. PCT/GB96/01380 (1996)

108.   Inoue T., Hattori M., Hayama K., and Maruta R., *Process of purifying MA-modified polyolefin*, US Patent 4,698,395, (1987)

109. Kozel T.H., and Kazmierczak R.T., A rapid Fourier Transform Infrared (FTIR) method for determination of grafted maleate on polyolefins, ANTEC '91, Annu. Tech. Conf. Soc. Plast. Eng., **37**, 1570 (1991).

110. Gaylord N.G., Mehta M., and Mehta R., *Maleation of ethylene-polar monomer copolymers by reactive processing with maleic anhydride-peroxide*, ANTEC '95, Annu. Tech. Conf. Soc. Plast. Eng., **41**, 1635 (1995).

111 Petruj J., and Kolar P., *Controlled degradation of PP in presence of maleic anhydride*, unpublished work

112. Shiah C.M., and Chen I.M., *Grafting of maleic anhydride onto thermoplastic elastomers by melt blending*, ANTEC 89, Annu. Tech. Conf. Soc. Plast. Eng., **35**, 1398 (1989).

113 ASTM D 882 - *83 Standard Test Methods for Tensile Properties of Thin Plastic Sheeting*

114. Fernanda M.B.C., and Ferreira M.I., *Optimisation of reaction conditions of bulk functionalisation of EPDM rubbers with maleic anhydride*, Eur. Polym. J., **30** , 911-918, (1994)

115. Rische T., Zschoche S., and Komber H., *Grafting of maleic anhydride onto poly(tetrahydrofuran)*, Macromol. Chem. Phys., **197**, 991-1005 (1996).

116. Al Malaika S., *Modifications of polyolefins in-situ: reactive processing in mixtures and extruders*, Polymer Preprints, 29(1), 555 - 556 (1988).

117. Coutinho F.M.B., and Ferreira M.I.P., *Characterisation of EPDM rubber modified with maleic anhydride by diffuse reflectance FTIR (DRIFT)*, Polym. Testing, **13**, 25-34 (1995)

118. Thames S.F., Rahman A., and Poole P.W., *The maleinization of low molecular weight guayule rubber*, J. Appl. Polym. Sci., **49**, 1963 - 1969 (1993)

119. Saier E.L., Petrakis L., and Causins L.R., Infrared and nuclear magnetic resonance of maleic anhydride copolymers and their half esters, J. Appl. Polym. Sci., 12, 2191 - 2200 (1968).

120. Huang N.J., and Sunberg D.C., *A GPC method to determine grafting efficiency during graft copolymerisation*, Polym., **35**, 5693, (1994)

121. Lee W., *Studies of graft copolymerisation of glycidyl methacrylate onto PVC and curing behaviour of its grafted copolymer*, J. Appl. Polym. Sci., **55**, 1197, (1995).

230

122. Li N., and Narayanan R., *Upper limit of grafting conversion and phase homogeneity: cellulose acetate/poly(styrene-co-maleic anhydride) grafting reaction system*, Polymer, **35(20)**, 4335, (1995).

123. Ruggeri G., Aglietto M., Petragnani A., and Ciardelli F., *Some aspects of PP functionalisation by free radical reactions*, J. Eur. Polym. Chem., **33**, 829-842, (1995).

124. Achmad S., Isminingsih G., Watanabe Y., and Hatakeyama T., *Adhesive properties of PP modified with maleic anhydride by extrusion molding*, J. Appl. Polym. Sci., **37**, 1141-1145, (1989)

125. Baker W.E., Xie H., Seay M., and Oliphant K., *Search for nonoxidative, hydrogen-abstracting initiators useful for melt grafting processes*, J. Appl. Polym. Sci., **48**, 1199-1208 (1993)

126. Karychev I.A., Bratchikov A.V., and Budnitskii Y.M., *Modification of polypropylene during processing*, International Polym. Sci. and Tech., **20(4)**, 42-45, 1993)

127. Al-Malaika S., *Reactive processing and polymer performance*, Polym. Plast Technol. Eng., **29(1&2)**, 73-86, (1990).

128. Yamaguchi K., and Okumura J., *Modification of rubbers with macromonomers*, International Polym. Sci. and Tech., **20(1)**, 44-51, (1993)

129. Yahya I.B., *Functionalisation of PS and EPDM with acrylic acid by reactive processing and physical properties characterisation*, in Compatibilisation of heterogeneous polymer blends by reactive processing, PhD Thesis, PPP Group, Aston Univ., Birmingham, U.K., **Chap. 4**, (1994)

130a. Artun K.J., *The chemical modification of polymer blends by reactive processing*, PhD Thesis, PPP Group, Aston University, Birmingham, U.K., (1994)

130b Al-Malaika S., and Artus K.J., J. App. Polym. Sci., in Press.

131. Suharty N.S., *Reactive processing of polyolefins using antioxidants system*, PhD Thesis, PPP Group, Aston University, Birmingham, U.K., (1993)

132. Zhu S., *Effect of polyradical on gel formation in free radical polymer modification*, J. Polym. Sci. Pt.B : Polym. Phy., **34**, 505-516, (1996)

133. Bonner J.G., and Hope P.S., *Compatibilisation and reactive blending, in Polymer Blends and Alloys*, Folkes M.J., and Hope P.S.,(eds.), Blackie Acad. 7 Professional, **Chapter 3**, (1993)

134. Padwa A.R., Sasaki Y., Wolske K.A., and Macosko C.W., *Kinetics of amine-cyclic anhydride reactions in moderately polar solutions*, J. Polym. Sci. Pt.A : Polym. Chem., **33**, 2165, (1995)

135. Chen H., *Synthesis of a PE-g-PS copolymer and its compatibilisation for linear low density polyethylene/poly(phenylene oxide) blends*, Macromol. Chem. Phys., **196**, 2173-2182, (1995).

136. Aaltonen P., Fink G., Lofgren B., and Seppala J., *Synthesis of hydroxyl group containing polyolefins with metallocene/methylaluminoxane*, Macromol., **29**, 5255-5260, (1996).

137. Tritto I., Fan Z-Q., Locatelli P., and Sacchi M.C., ^{13}C *NMR studies of ethylene-propylene prepared with homogeneous metallocene-based Ziegler-Natta catalysts*, Macromol., **28**, 3342-3350, (1995).

138. Roover D., Devaux J., and Legras R., *Maleic anhydride homopolymerisation during melt functionalisation of isotactic polypropylene*, J. Appl. Polym. Sci. : Pt.A :Polym. Chem., **34**, 1195 - 1202, (1996)

139. Song Z., and Baker W.E., *Chemical reactions and reactivity of primary, secondary, and tertiary diamines with acid functionalised polymers*, J. Appl. Polym. Sci. : Pt.A :Polym. Chem., **30**, 1589-1600, (1992).

140. Marechal P., Coppens G., Legras R., and Dekoninck J-M., *Amine/anhydride reaction versus amide/anhydride reaction in polyamide/anhydride carriers*, J. Appl. Polym. Sci. : Pt.A :Polym. Chem., **33**, 757-766, (1995).

141. Wingrove A.S., and Caret R.C., *Organic Chemistry*, Harper & Row, Lon. 993, (1981)

142. Bucknall C.B., *Mechanisms of rubber toughening*, in Toughened Plastics, Appl. Sci. Publ., Lond., **Chap. 7**, (1977)

143. Gaylord N.G., Compatibilising agents: Structure and function in polyblends, J. Macromol. Sci.: Chem., A26(8), 1211 -1229 (1989)

144. Rudin A., Copolymer in Polymer blends, J. Macromol. Sci. Rev. Macromol. Chem., C19(2), 267-292, (1980)

APPENDICES

Appendix 1 (data in connection with Table 4.1, page 157)

Sample code	Tensile strength, MPa	Young's modulus, MPa	Elongation at break, %	Toughness Factor, MPa
	19.6	450	33	13.0
	18.1	432	35	12.9
CPB12	18.8	440	32	13.5
	18.5	430	37	13.9
	17.9	417	38	14.3
average	**18.6 ± 0.9**	**434 ± 17**	**35 ± 3**	**13.5 ± 0.8**
	17.9	465	45	14.1
	19.3	500	50	15.5
CPB13	18.5	480	48	15.0
	19.4	510	51	15.8
	18.1	480	46	14.0
average	**18.6 ± 0.8**	**487 ± 23**	**48 ± 3**	**14.9 ± 0.9**
	17.3	458	64	17.9
	16.6	433	58	16.0
CPB19	17.7	470	64	18.1
	17.0	455	60	17.7
	16.4	435	56	16.1
average	**17.0 ± 0.7**	**450**	**60**	**17.1**
	17.5	483	52	18.0
	18.5	500	54	19.5
CPB20	18.9	515	58	20.0
	17.8	498	51	17.5
	18.0	505	55	19.0
average	**18.0**	**500**	**54**	**19.0**
	17.0	380	23	11.7
	17.1	385	24	11.5
CPB21	18.0	408	26	12.2
	18.4	410	26	12.8
	17.9	394	25	12.0
average	**17.7**	**395**	**25**	**12.0**
	20.0	430	23	11.7
	19.5	410	24	11.5
CPB22	20.0	445	26	12.2
	19.0	410	26	12.8
	18.6	394	25	12.0
average	**19.4**	**395**	**25**	**12.0**

Appendix 1 (cont.)

Sample code	Tensile strength, MPa	Young's modulus, MPa	Elongation at break, %	Toughness Factor, MPa
CPB23	17.6	485	41	14.6
	19.0	510	48	16.0
	19.0	507	48	15.8
	17.4	443	42	14.2
	18.0	480	46	15.0
average	**18.2**	**485**	**45**	**15.1**
CPB24	17.8	485	49	17.9
	18.0	490	51	18.8
	19.1	510	55	19.8
	19.0	503	55	19.4
	17.6	462	50	17.5
average	**18.3**	**490**	**52**	**18.6**
8020	22.2	560	501	75
	20.8	543	450	67
	21.7	550	475	72
	22.0	572	500	70
	20.8	525	445	68
average	**21.5**	**550**	**474**	**70.4**

Appendix 2 (data in connection with Table 4.3, page 158)

Sample code	Tensile strength, MPa	Young's modulus, MPa	Elongation at break, %	Toughness Factor, MPa
CPB131	20.2	722	269	47.7
	18.8	670	253	45.0
	19.6	700	262	45.8
	18.9	663	248	46.2
	20.0	725	273	47.3
average	**19.5 ± 0.9**	**696 ± 33**	**261 ± 13**	**46.4 ± 1.3**
CPB125	18.7	525	215	39.0
	19.6	530	220	43.0
	20.3	572	236	43.6
	19.0	540	222	39.7
	19.9	568	232	42.2
average	**19.5 ± 0.8**	**547 ± 25**	**225 ± 11**	**41.5 ± 2.5**
CPB133	18.9	575	280	49.2
	19.5	585	290	50.0
	19.8	600	295	53.0
	20.2	620	300	54.1
	20.6	630	305	55.7
average	**19.8 ± 0.9**	**602 ± 28**	**294 ± 14**	**52.4 ± 3.3**

Appendix 2 (cont.)

Sample code	Tensile strength, MPa	Young's modulus, MPa	Elongation at break, %	Toughness Factor, MPa
	17.8	400	428	69.0
	18.1	397	457	72.5
7525	17.7	385	450	70.0
	16.8	373	420	67.2
	17.1	380	445	68.8
average	**17.5 ± 1.0**	**387 ± 14**	**440 ± 20**	**69.4 ± 2.6**

Appendix 3 (data in connection with Table 4.4, page 158)

Sample code	Tensile strength, MPa	Young's modulus, MPa	Elongation at break, %	Toughness Factor, MPa
	19.3	450	130	23.8
	19.1	447	130	23.3
119	20.0	465	128	24.5
	18.4	423	122	21.6
	18.6	430	125	21.8
average	**19.1 ± 0.9**	**443 ± 22**	**127 ± 5**	**23.0 ± 1.5**
	18.8	527	108	21.4
	20.0	550	113	23.4
120	19.7	545	108	22.6
	18.6	516	105	21.1
	20.4	567	115	23.5
average	**19.5 ± 0.9**	**541 ± 26**	**110 ± 5**	**22.4 ± 1.3**
	20.1	496	97	20.8
	21.5	538	106	21.1
121	22.0	545	109	22.6
	20.2	499	100	20.8
	21.2	532	103	21.7
average	**21.0 ± 1.0**	**522 ± 26**	**103 ± 6**	**21.4 ± 1.2**
	22.9	534	128	30.0
	24.3	575	140	32.5
80	23.9	560	137	32.2
	23.7	551	134	31.1
	25.2	590	146	34.2
average	**24.0 ± 1.2**	**562 ± 28**	**137 ± 9**	**32.0 ± 2.2**
	20.8	500	121	22.7
	21.1	513	122	24.4
124	20.0	490	116	23.2
	19.8	475	112	23.0
	19.3	467	109	21.7
average	**20.2 ± 0.9**	**489 ± 24**	**116 ± 6**	**23.0**

Appendix 3 (cont.)

Sample code	Tensile strength, MPa	Young's modulus, MPa	Elongation at break, %	Toughness Factor, MPa
	20.3	478	115	26.2
	20.7	489	119	27.2
123	21.0	495	119	27.8
	21.8	510	125	28.5
	22.2	523	127	29.3
average	**21.2 ± 1.0**	**499 ± 24**	**121 ± 6**	**27.8 ± 1.6**
	22.3	541	129	31.4
	20.6	505	121	29.7
122	20.4	493	116	28.5
	22.1	520	123	29.9
	21.6	531	126	30.5
average	**21.4 ± 1.0**	**518 ± 25**	**123 ± 7**	**30.0 ± 1.5**
	17.1	381	105	18.8
	18.4	409	111	20.0
204	17.9	395	110	20.3
	17.6	395	109	19.7
	18.7	420	115	21.2
average	**17.9 ± 0.8**	**400 ± 20**	**110 ± 5**	**20.0 ± 1.2**

Appendix 4 (data in connection with Table 4.5, page 159)

Sample code	Tensile strength, MPa	Young's modulus, MPa	Elongation at break, %	Toughness Factor, MPa
	20.5	466	109	22.5
	20.9	473	111	23.0
78	21.7	492	114	24.0
	22.5	513	120	25.5
	21.9	501	116	25.0
average	**21.5 ± 1.0**	**489 ± 24**	**114 ± 6**	**24.0 ± 1.5**
	22.9	534	128	30.0
	24.3	575	140	32.5
80	23.9	560	137	32.2
	23.7	551	134	31.1
	25.2	590	146	34.2
average	**24.0 ± 1.2**	**562 ± 28**	**137 ± 9**	**32.0 ± 2.2**
	23.0	410	78	17.1
	23.3	417	80	17.6
82	24.0	431	83	18.0
	25.3	452	86	18.9
	24.9	445	83	18.4
average	**24.1 ± 1.2**	**431 ± 21**	**82 ± 4**	**18.0 ± 0.9**

Appendix 4 (cont.)

Sample code	Tensile strength, MPa	Young's modulus, MPa	Elongation at break, %	Toughness Factor, MPa
	13.2	241	192	21.0
	12.3	227	177	19.2
106	12.0	219	174	19.0
	12.5	228	183	20.3
	13.0	235	189	19.7
average	12.6 ± 0.6	230 ± 11	183 ± 9	20.0 ± 1.0
	16.2	258	232	30.7
	15.0	239	215	28.0
107	14.7	233	206	27.8
	15.9	256	222	30.9
	15.2	244	220	29.1
average	15.4 ± 0.7	246 ± 12	219 ± 13	29.3 ± 1.5
	17.1	278	206	33.4
	17.8	295	219	34.6
108	18.7	307	235	37.0
	18.4	300	230	36.5
	17.5	280	215	33.5
average	17.9 ± 0.9	292 ± 15	221 ± 15	35.0 ± 2.0
	17.7	280	110	13.8
	17.1	272	103	13.2
109	18.2	285	108	14.3
	18.1	293	112	14.0
	18.9	300	117	14.7
average	18.0 ± 0.9	286 ± 14	110 ± 7	14.0 ± 0.8
	14.7	270	180	21.3
	14.5	262	195	21.3
102	15.5	283	190	23.5
	15.0	278	177	22.9
	14.3	257	168	21.0
average	14.8 ± 0.7	270 ± 13	178 ± 12	22.0 ± 1.5
	17.0	281	207	32.0
	17.6	290	211	32.8
103	18.6	309	227	36.0
	18.1	302	221	35.0
	17.7	293	214	34.2
average	17.8 ± 0.8	295 ± 14	216 ± 11	34.0 ± 2.0
	19.1	330	224	35.0
	20.5	357	256	39.2
104	18.9	323	215	33.3
	19.2	340	236	35.9
	19.8	350	349	38.1
average	19.5 ± 1.0	340 ± 17	234 ± 22	36.3 ± 3.0

Appendix 4 (cont.)

Sample code	Tensile strength, MPa	Young's modulus, MPa	Elongation at break, %	Toughness Factor, MPa
	20.2	295	116	20.2
	19.7	287	108	19.5
105	20.3	305	115	20.8
	21.5	318	124	22.5
	20.8	310	117	22.0
average	20.5 ± 1.0	303 ± 15	116 ± 8	21.1 ± 1.5
	11.8	291	325	33.0
	12.0	306	332	33.0
6040	12.4	313	345	34.8
	11.9	300	328	33.2
	11.4	285	309	31.0
average	11.9 ± 0.5	299 ± 14	328 ± 19	33.0 ± 2.0

Appendix 5 (data in connection with Table 4.6, page 160)

Sample code	Tensile strength, MPa	Young's modulus, MPa	Elongation at break, %	Toughness Factor, MPa
	17.7	495	75	12.0
	18.2	501	77	12.3
98	18.7	521	78	12.7
	17.5	493	71	11.8
	16.9	475	69	11.3
average	17.8 ± 0.9	497 ± 24	74 ± 5	12.0 ± 0.7
	20.5	466	109	22.5
	20.9	473	111	23.0
78	21.7	492	114	24.0
	22.5	513	120	25.5
	21.9	501	116	25.0
average	21.5 ± 1.0	489 ± 24	114 ± 6	24.0 ± 1.5
	21.1	562	115	21.0
	20.6	545	111	20.4
79	20.5	540	110	20.3
	19.6	523	103	19.2
	19.2	510	101	19.1
average	20.2 ± 1.0	536 ± 26	108 ± 7	20.0 ± 1.0
	17.1	359	129	21.7
	18.1	388	142	23.4
84	18.7	395	147	24.2
	17.6	366	132	22.4
	18.0	377	140	23.0
average	17.9 ± 0.8	377 ± 18	138 ± 9	23.0 ± 1.2

Appendix   5 (cont.)

Sample code	Tensile strength, MPa	Young's modulus, MPa	Elongation at break, %	Toughness Factor, MPa
	19.7	461	78	12.7
	20.0	470	79	13.0
99	19.0	449	74	12.1
	21.0	494	84	13.9
	20.3	486	80	13.3
average	**20.0 ± 1.0**	**472 ± 23**	**79 ± 5**	**13.0 ± 0.9**
	22.9	534	128	30.0
	24.3	575	140	32.5
80	23.9	560	137	32.2
	23.7	551	134	31.1
	25.2	590	146	34.2
average	**24.0 ± 1.2**	**562 ± 28**	**137 ± 9**	**32.0 ± 2.2**
	21.8	451	125	26.0
	21.3	447	126	25.5
81	23.3	492	142	28.8
	22.3	473	135	27.1
	22.8	487	137	27.6
average	**22.3 ± 1.0**	**470 ± 23**	**133 ± 9**	**27.0 ± 1.8**
Sample code	Tensile strengt, MPa	Young's modulus, MPa	Elongation at break, %	Toughness Factor, MPa
	18.6	360	123	19.6
	19.2	366	129	19.9
85	20.3	397	140	22.4
	20.0	392	138	21.9
	19.4	380	130	21.2
average	**19.5 ± 0.9**	**379 ± 18**	**132 ± 9**	**21.0 ± 1.4**
	22.3	515	68	13.3
	22.7	528	71	13.6
100	21.8	500	66	12.8
	20.9	480	61	12.6
	21.8	492	64	12.7
average	**21.9 ± 1.0**	**503 ± 25**	**66 ± 5**	**13.0 ± 0.6**
	23.0	410	78	17.1
	23.3	417	80	17.6
82	24.0	431	83	18.0
	25.3	452	86	18.9
	24.9	445	83	18.4
average	**24.1 ± 1.2**	**431 ± 21**	**82 ± 4**	**18.0 ± 0.9**

Sample code	Tensile strength, MPa	Young's modulus, MPa	Elongation at break, %	Toughness Factor, MPa
83	24.7	451	80	17.4
	25.3	460	83	17.8
	24.1	440	78	17.2
	22.9	419	73	16.2
	23.5	425	76	16.4
average	24.1 ± 1.2	439 ± 22	78 ± 5	17.0 ± 0.8
86	17.8	305	69	10.6
	18.6	327	73	11.3
	18.2	316	71	11.1
	19.1	332	76	11.7
	17.3	300	66	10.3
average	18.2 ± 0.9	316 ± 16	71 ± 5	11.0 ± 0.7
88	18.1	492	184	29.5
	16.8	451	169	26.1
	17.7	475	177	28.2
	16.9	455	170	26.3
	18.5	497	185	29.9
average	17.6 ± 0.9	474 ± 23	177 ± 8	28.0 ± 1.9
204	17.1	381	105	18.8
	18.4	409	111	20.0
	17.9	395	110	20.3
	17.6	395	109	19.7
	18.7	420	115	21.2
average	17.9 ± 0.8	400 ± 20	110 ± 5	20.0 ± 1.2

Appendix 6 (data in connection with Table 4.7, page 160)

Sample code	Tensile strengt, MPa	Young's modulus, MPa	Elongation at break, %	Toughness Factor, MPa
80	22.9	534	128	30.0
	24.3	575	140	32.5
	23.9	560	137	32.2
	23.7	551	134	31.1
	25.2	590	146	34.2
average	24.0 ± 1.2	562 ± 28	137 ± 9	32.0 ± 2.2
88	18.1	492	184	29.5
	16.8	451	169	26.1
	17.7	475	177	28.2
	16.9	455	170	26.3
	18.5	497	185	29.9
average	17.6 ± 0.9	474 ± 23	177 ± 8	28.0 ± 1.9
65	16.5	468	50	7.7
	17.2	482	52	8.2
	15.8	473	46	7.2
	16.1	448	47	7.6
	16.4	460	50	7.8
average	16.4 ± 0.8	459 ± 23	49 ± 3	7.7 ± 0.5
204	17.1	381	105	18.8
	18.4	409	111	20.0
	17.9	395	110	20.3
	17.6	395	109	19.7
	18.7	420	115	21.2
average	17.9 ± 0.8	400 ± 20	110 ± 5	20.0 ± 1.2
7525	17.8	400	428	69.0
	18.1	397	457	72.5
	17.7	385	450	70.0
	16.8	373	420	67.2
	17.1	380	445	68.8
average	17.5 ± 1.0	387 ± 14	440 ± 20	69.4 ± 2.6

Appendix 7 (data in connection with Table 5.1 page 188)

Sample code	Tensile strength, MPa	Young's modulus, MPa	Elongation at break, %	Toughness Factor, MPa
6040	11.8	291	325	33.0
	12.0	306	332	33.0
	12.4	313	345	34.8
	11.9	300	328	33.2
	11.4	285	309	31.0
	11.9 ± 0.5	**299 ± 14**	**328 ± 19**	**33.0 ± 2.0**
7525	17.8	400	428	69.0
	18.1	397	457	72.5
	17.7	385	450	70.0
	16.8	373	420	67.2
	17.1	380	445	68.8
average	**17.5 ± 1.0**	**387 ± 14**	**440 ± 20**	**69.4 ± 2.6**
8020	22.2	560	501	75
	20.8	543	450	67
	21.7	550	475	72
	22.0	572	500	70
	20.8	525	445	68
average	**21.5**	**550**	**474**	**70.4**
PP	37.9	938	16	4.5
	36.9	921	15	4.1
	36.0	896	15	4.3
	35.2	873	15	4.1
	34.5	852	14	4.0
	36.1 ± 1.8	**896 ± 44**	**15 ± 1**	**4.2 ± 0.3**

Appendix 8 (data in connection with Table 5.2 page 188)

Sample code	Tensile strength, MPa	Young's modulus, MPa	Elongation at break, %	Toughness Factor, MPa
165	20.9	627	280	50.3
	21.3	640	292	51.4
	20.4	615	273	48.0
	19.3	583	254	44.8
	19.6	600	266	46.0
average	20.3 ± 1.0	613 ± 30	273 ± 19	48.1 ± 3.3
166	21.2	619	272	52.6
	19.8	583	244	47.0
	20.5	590	257	49.8
	21.1	593	264	52.4
	19.4	565	238	46.7
average	20.4 ± 1.0	590 ± 29	255 ± 17	49.7 ± 3.0
167	18.7	547	200	36.0
	19.6	572	213	38.0
	17.8	518	190	33.5
	18.4	525	201	35.1
	19.0	563	211	37.4
	18.7 ± 0.9	545 ± 27	203 ± 10	36.0 ± 2.5
162	17.4	573	274	42.3
	17.7	585	288	44.0
	19.2	630	312	48.3
	18.9	616	301	46.6
	18.3	596	295	45.3
average	18.3 ± 0.9	600 ± 30	294 ± 20	45.3 ± 3.0
163	18.1	544	276	50.6
	18.5	555	280	53.2
	19.2	575	300	55.0
	19.4	586	308	55.6
	19.8	600	316	58.6
average	19.0 ± 0.9	572 ± 28	296 ± 20	54.6 ± 4.0
164	17.5	467	281	47.0
	18.6	506	311	50.7
	17.8	482	290	47.4
	18.1	497	300	49.0
	17.0	458	273	44.4
average	17.8 ± 0.8	482 ± 24	291 ± 20	47.7 ± 3.3
141	21.1	650	470	96.2
	20.5	628	445	91.8
	21.5	661	477	98.0
	22.5	694	508	105.8
	21.9	672	475	102.2
average	21.5 ± 1.0	661 ± 33	475 ± 33	98.8 ± 7.0

Sample code	Tensile strength, MPa	Young's modulus, MPa	Elongation at break, %	Toughness Factor, MPa
128	22.0	630	358	65.7
	21.4	623	348	64.0
	20.8	600	345	62.0
	20.5	577	330	61.8
	20.3	570	324	60.0
average	**21.0 ± 1.0**	**600 ± 30**	**341 ± 17**	**62.7 ± 3.0**
129	19.1	533	245	44.1
	20.2	565	266	48.0
	19.8	560	260	47.0
	21.0	589	281	50.7
	19.9	558	263	47.2
average	**20.0 ± 1.0**	**561 ± 28**	**263 ± 18**	**47.4 ± 3.3**
169	18.0	562	285	51.3
	17.8	550	280	49.7
	18.9	588	304	54.5
	18.1	567	290	52.0
	17.2	533	266	47.5
average	**18.0 ±0.9**	**560 ± 28**	**285 ± 19**	**51.0 ± 3.5**
170	19.2	575	287	58.8
	18.0	545	265	54.1
	18.8	555	271	56.1
	17.9	540	262	54.0
	17.6	525	260	52.0
average	**18.3 ± 0.9**	**548 ± 27**	**269 ± 18**	**55.0 ± 3.8**
171	18.1	495	251	49.5
	16.5	450	219	43.4
	17.0	466	224	44.1
	17.6	481	246	48.5
	17.3	473	235	46.0
average	**17.3 ± 0.8**	**473 ± 23**	**235 ± 16**	**46.3 ± 3.2**
7525	17.8	400	428	69.0
	18.1	397	457	72.5
	17.7	385	450	70.0
	16.8	373	420	67.2
	17.1	380	445	68.8
average	**17.5 ± 1.0**	**387 ± 14**	**440 ± 20**	**69.4 ± 2.6**
PP	37.9	938	16	4.5
	36.9	921	15	4.1
	36.0	896	15	4.3
	35.2	873	15	4.1
	34.5	852	14	4.0
	36.1 ± 1.8	**896 ± 44**	**15 ± 1**	**4.2 ± 0.3**

Appendix 9 (data in connection with Table 5.3 page 189)

Sample code	Tensile strength, MPa	Young's modulus, MPa	Elongation at break, %	Toughness Factor, MPa
141	21.1	650	470	96.2
	20.5	628	445	91.8
	21.5	661	477	98.0
	22.5	694	508	105.8
	21.9	672	475	102.2
average	21.5 ± 1.0	661 ± 33	475 ± 33	98.8 ± 7.0
128	22.0	630	358	65.7
	21.4	623	348	64.0
	20.8	600	345	62.0
	20.5	577	330	61.8
	20.3	570	324	60.0
average	21.0 ± 1.0	600 ± 30	341 ± 17	62.7 ± 3.0
129	19.1	533	245	44.1
	20.2	565	266	48.0
	19.8	560	260	47.0
	21.0	589	281	50.7
	19.9	558	263	47.2
average	20.0 ± 1.0	561 ± 28	263 ± 18	47.4 ± 3.3
143	18.9	604	251	41.4
	18.6	595	240	43.0
	19.5	628	264	47.3
	17.9	570	230	40.3
	19.9	598	250	44.5
average	18.8 ± 0.9	599 ± 29	247 ± 17	43.3 ± 3.0
130	18.0	500	265	40.2
	17.4	483	244	38.0
	17.0	480	248	37.6
	16.6	457	233	35.0
	17.0	485	250	37.2
average	17.2 ± 0.8	481 ± 24	248 ± 17	37.6 ± 2.6
7525	17.8	400	428	69.0
	18.1	397	457	72.5
	17.7	385	450	70.0
	16.8	373	420	67.2
	17.1	380	445	68.8
average	17.5 ± 1.0	387 ± 14	440 ± 20	69.4 ± 2.6

Appendix 10 (data in connection with Table 5.4 page 189)

Sample code	Tensile strength, MPa	Young's modulus, MPa	Elongation at break, %	Toughness Factor, MPa
178	19.7	502	575	114.2
	19.2	492	560	107.0
	20.3	519	605	116.0
	18.6	472	527	102.0
	19.2	490	563	105.8
average	19.4 ± 0.9	495 ± 24	566 ± 39	109.0 ± 7.0
184	18.9	523	472	88.2
	20.1	569	510	96.1
	20.5	573	540	100.0
	19.6	535	500	92.2
	19.9	550	503	94.0
average	19.8 ± 0.9	550 ± 27	505 ± 35	94.1 ± 6.0
187	19.0	571	367	62.9
	17.9	529	330	56.0
	17.4	519	322	54.6
	18.5	550	350	58.8
	18.7	561	361	61.7
average	18.3 ± 0.9	546 ± 27	346 ± 24	58.8 ± 4.1
190	17.9	560	395	65.0
	16.5	520	346	57.1
	17.0	540	370	60.9
	17.7	554	394	64.8
	16.4	511	345	56.7
average	17.1 ± 0.8	537 ± 26	370 ± 25	60.9 ± 4.2
173	18.0	530	444	85.0
	18.8	551	475	90.7
	19.4	561	486	94.7
	19.7	581	510	97.7
	18.6	547	470	88.4
average	18.9 ± 0.9	554 ± 27	477 ± 33	91.3 ± 6.4
125	20.8	605	441	68.5
	21.9	630	475	73.2
	23.0	663	506	78.2
	21.4	615	460	71.1
	22.4	647	483	75.0
average	21.9 ± 1.1	632 ± 31	473 ± 33	73.2 ± 5.0
126	19.2	560	249	48.4
	20.0	584	267	51.9
	20.1	590	267	52.4
	20.7	585	267	52.2
	21.0	616	285	55.1
average	20.2 ± 1.0	587 ± 29	267 ± 18	52.0 ± 3.6

Appendix 10 (cont.)

Sample code	Tensile strength, MPa	Young's modulus, MPa	Elongation at break, %	Toughness Factor, MPa
179	22.0	563	605	116.9
	21.4	560	594	115.4
	20.8	528	560	110.8
	20.2	515	530	105.9
	20.6	519	541	108.0
average	**21.0 ± 1.0**	**537 ± 26**	**566 ± 39**	**111.4 ± 5.5**
185	19.9	603	628	106.0
	18.3	554	558	94.9
	19.2	580	590	100.4
	19.5	589	613	104.0
	18.1	549	546	92.7
average	**19.0 ± 0.9**	**575 ± 28**	**587 ± 41**	**99.6 ± 6.9**
188	18.3	526	527	77.1
	17.0	477	463	69.9
	17.7	520	522	76.5
	17.5	506	493	73.5
	17.0	476	460	70.5
average	**17.5 ± 0.8**	**501 ± 25**	**493 ± 34**	**73.5 ± 3.6**
191	19.3	539	340	64.0
	18.0	496	310	58.2
	18.2	510	315	59.0
	17.7	490	297	56.1
	18.8	535	333	62.2
average	**18.4 ± 0.9**	**514 ± 25**	**319 ± 22**	**59.9 ± 4.1**
180	20.1	575	560	104.0
	18.5	522	511	91.1
	19.0	544	530	97.1
	19.7	569	558	101.7
	18.7	530	526	92.1
average	**19.2 ± 0.9**	**548 ± 27**	**537 ± 26**	**97.2 ± 6.8**
186	19.9	606	475	88.2
	18.7	573	440	82.0
	19.5	601	470	87.5
	20.3	635	505	94.1
	19.6	600	470	88.2
average	**19.6 ± 0.9**	**603 ± 30**	**472 ± 33**	**88.0 ± 6.1**
189	19.6	607	372	74.2
	19.3	589	369	72.1
	19.0	586	333	67.1
	18.0	552	326	64.6
	18.6	577	350	69.0
	18.9 ± 0.9	**581 ± 29**	**350 ± 24**	**69.4 ± 4.8**

Appendix 11 (data in connection with Table 5.5, page 190)

Sample code	Tensile strength, MPa	Young's modulus, MPa	Elongation at break, %	Toughness Factor, MPa
1471	20.5	588	198	34.6
	19.7	565	174	32.2
	20.6	590	185	34.6
	21.7	620	200	36.9
	21.0	602	178	34.2
average	**20.7 ± 1.0**	**593 ± 29**	**187 ± 13**	**34.5 ± 2.4**
1473	20.4	616	173	29.6
	19.5	588	162	27.0
	19.9	606	169	29.1
	18.9	565	155	27.0
	18.8	560	151	25.8
average	**19.5 ± 0.9**	**587 ± 29**	**162 ± 11**	**27.7 ± 1.9**
1475	20.0	593	120	19.7
	19.0	564	114	18.6
	18.7	541	110	17.8
	19.6	588	116	19.1
	18.2	539	110	17.3
average	**19.1 ± 0.9**	**565 ± 28**	**114 ± 7**	**18.5 ± 1.2**
1481	18.9	534	255	37.9
	19.7	555	267	39.0
	18.7	528	250	36.2
	20.2	576	278	40.4
	20.5	582	285	41.0
average	**19.6 ± 0.9**	**555 ± 27**	**267 ± 18**	**38.9 ± 2.7**
1483	20.1	656	235	38.9
	19.0	620	223	35.8
	18.9	607	216	35.2
	19.5	642	229	38.0
	18.5	600	207	34.1
average	**19.2 ± 0.9**	**625 ± 31**	**222 ± 15**	**36.4 ± 2.5**
1485	18.7	615	217	31.5
	18.0	584	201	30.3
	17.6	580	198	29.4
	18.9	631	221	33.0
	19.3	640	223	33.8
average	**18.5 ± 0.9**	**610 ± 30**	**212 ± 14**	**31.6 ± 2.2**
1491	19.8	644	260	40.4
	19.3	631	255	38.2
	18.1	584	232	35.5
	19.1	614	250	38.0
	18.7	597	248	36.9
average	**19.0 ± 0.9**	**614 ± 30**	**249 ± 17**	**37.8 ± 2.6**

Appendix 11 (cont.)

Sample code	Tensile strength, MPa	Young's modulus, MPa	Elongation at break, %	Toughness Factor, MPa
1491	19.8	644	260	40.4
	19.3	631	255	38.2
	18.1	584	232	35.5
	19.1	614	250	38.0
	18.7	597	248	36.9
average	19.0 ± 0.9	614 ± 30	249 ± 17	37.8 ± 2.6
1493	18.9	630	179	27.3
	17.3	572	160	24.1
	18.2	610	171	26.0
	17.7	592	162	25.1
	17.9	606	168	25.5
average	18.0 ± 0.9	602 ± 30	168 ± 11	25.6 ± 1.7